# GEOPHYSICAL INVESTIGATIONS OF THE DEEP GEOLOGY OF THE EAST MIDLANDS

A Thesis

Submitted for the degree of

DOCTOR OF PHILOSOPHY

In the

FACULTY OF SCIENCE OF THE UNIVERSITY OF LEICESTER

by

GRAHAM ARTER

B.Sc. (London)

November 1982





ProQuest LLC
789 East Eisenhower Parkway
P.O. Box 1346
Ann Arbor, MI 48106-1346

GEOPHYSICAL INVESTIGATIONS OF THE DEEP GEOLOGY OF THE EAST MIDLANDS. Graham Arter. 1982.

Late Precambrian meta-sediments and Caledonian granitic intrusions are exposed in Leicestershire. Similar rocks are found at shallow depth in boreholes from Leicester to East Anglia.

Two seismic refraction experiments, each comprising two 10-30 km. profiles, have been carried out over potential field anomalies in the East Midlands.

The Melton Mowbray experiment, located to the east of the Charnian Inlier, defined the top surface of the Melton Mowbray granitic intrusion at less than 0.5 km. depth, and the southern margin of the Carboniferous Widmerpool Gulf. The Melton intrusion was found to have a similar p-wave velocity (c. 5.7 $km.s^{-1}$) to the surrounding Precambrian basement. The refraction interpretations, together with some seismic reflection data, are used to constrain 3-dimensional modelling of the aeromagnetic anomalies in this area.

The Peterborough experiment was located over a negative Bouguer gravity anomaly to the north of Peterborough. Refractor velocities typical of late Precambrian basement were detected at shallow depth (0.5 km.) across the gravity anomaly. The gravity data is modelled as a intra-basement intrusion.

Measurements have been made of physical properties of samples of basement rocks from outcrop and from boreholes within the area. These are used in the interpretation of the potential field data.

A pre-Carboniferous palaeogeological map has been compiled from borehole and geophysical data. A compilation of non-confidential borehole data is included as an appendix.

The potential field and seismic studies show that two groups of granitic intrusions can be recognised, one group is more basic than the other.

ACKNOWLEDGEMENTS

I would like to thank the following:

Drs. Ian Hill and Peter Maguire for supervising this work and for help in the writing of this thesis.

The staff of the geology department for helpful discussions about local geology.

The large numbers of people who have participated in the seismic refraction experiments, in particular the technical staff of the Geology Department.

My fellow research students for interesting discussions, occasionally of a geological nature.

Mrs. J. Allsop of the Deep Geology Unit IGS for supplying borehole logs and other information.

The geology departments of The Universities of Birmingham, Durham, East Anglia and Reading and the NERC seismic equipment pool, for the loan of equipment.

NERC for providing a research studentship and Leicester University Geology Department for financing the fieldwork.

TABLE OF CONTENTS

## LIST OF TABLES

## LIST OF FIGURES

Figures 1.1, 1.2, 3.1, 5.1, 5.2, 5.3, 6.1, 6.2, 6.3, 7.3, 7.4 and 7.6 are based, in whole or in part, on publications of the Institute of Geological Sciences.

# CHAPTER ONE

# INTRODUCTION TO THE AREA

## 1.1 GENERAL INTRODUCTION

The geophysical investigations described in this thesis are concerned with the pre-Carboniferous basement of an area extending east and south from the Precambrian inlier of Charnwood Forest.

The work described here is a continuation of previous seismic, magnetic and gravity work carried out in the East Midlands by Arab (1972), Maroof (1973), Whitcombe (1979) and El-Nikhely (1980).

The seismic experiments and potential field interpretations described here are all concerned with investigating the distribution of (Caledonian) granitic intrusions within the upper crust of the East Midlands.

Melton Mowbray seismic refraction profiles: this experiment was intended to investigate the Melton Mowbray granitic intrusion and its relationship to the Mountsorrel granodiorite. Recorded in August-September 1980, the survey consisted of two profiles 20 and 30 kilometres long. The experiment is described in chapter 5, a small refraction survey connected with the main experiment is described in chapter 3B.

National Coal Board seismic reflection surveys: 60 line kilometres of commercial shallow seismic reflection data, and a number of borehole sonic logs, from the Melton Mowbray

area have been interpreted. These interpretations provide velocity and depth data for the Melton refraction experiment and also help to define the top surface of the Melton granitic intrusion for magnetic modelling. The reflection interpretation is described in chapter 4.

Peterborough seismic refraction profiles: this experiment was carried out in September 1981 to determine the depth to basement over a negative gravity anomaly to the north of Peterborough. The experiment consisited of two profiles 18 and 11 kilometres long and is described in chapter 6.

Countesthorpe survey: this survey consisted of a two kilometre seismic refraction profile and a small gravity survey. The survey was carried out to investigate the lateral extent of the South Leicestershire Diorites and is described in chapter 3A.

Potential field interpretations: aeromagnetic data from the Melton area and gravity data from Peterborough have been interpreted using 3-dimensional techniques. Saturated densities have been measured on about 40 samples from boreholes and from outcrop. The results of the potential field studies are presented in chapters 7 and 8.

A pre-Carboniferous palaeogeological map based on borehole and geophysical evidence is presented and described in chapter 9, together with location maps for the boreholes. Lees and Taitt (1946), Falcon and Kent (1960) and Le Bas (1968) have published details of boreholes which encounter pre-Carboniferous formations in the East Midlands. There is not, however, a compilation for the more recent boreholes or for the whole of the East Midlands area. For this reason, brief details of all the boreholes that prove pre-

Carboniferous formations within the study area have been compiled and are included as appendix 1.1. A less complete compilation for the Carboniferous and younger formations, based mainly on unpublished data, is given in appendix 1.2.

A summary of the geology of the study area, together with some of the previous geophysical work is given below. The detailed geology of the individual survey areas will be described, as necessary, in the relevant chapters.

### 1.1.1 The Caledonian orogeny

The late Precambrian and Lower Palaeozoic geology of Central England is linked with the evolution of the Caledonian orogen. The plate tectonic model for the Caledonides, as proposed by Dewey (1969) and McKerrow and Ziegler (1972) suggests a cycle of ocean development and closure. This cycle began in the late Precambrian with the opening of the Iapetus Ocean. The ocean continued to open throughout the Cambrian and probably reached its maximum extent in the Lower Ordovician. There then followed a period of ocean closure, with subduction probably occurring along both margins. The Iapetus closed in the late Ordovician to Silurian, with the continental collision occurring progressively later towards the southwest. The present day position of the Iapetus suture is probably in a line trending southwest to northeast along the Solway Firth (Phillips et.al. 1976).

The various hypotheses for the late Precambrian and Lower Palaeozoic evolution of the southern margin of the Iapetus are discussed in Anderton et.al. (1979). In the late

Precambrian the Midlands experienced considerable subsidence together with associated volcanic and plutonic igneous activity. The igneous material was probably derived from a downgoing slab of ocean crust, but whether this represented a southeastward subduction of the Iapetus under Anglesey or the northward subduction of the Cadomian Ocean, or both, remains open to speculation.

By the Cambrian the Midlands of England formed a more stable platform and represented a foreland to the orogenic belt and the developing Welsh basin, which were located to the northwest. Normal shelf sedimentation appears to have proceeded with the deposition of carbonates in Shropshire and sands and muds in the Malverns and Warwickshire.

The Lower Palaeozoic calc-alkaline igneous activity, which was widespread, was probably related to the development of island arcs and marginal basins across the southern continent (LeBas 1981, Harris et.al. 1981).

There is no evidence for ancient continental crust, equivalent to the Lewisian of northern Scotland, under southern Britain. U-Pb isotopes from zircons in Caledonian granites (Pidgeon and Aftalion 1978) show no evidence of an inherited component of older zircon. This is in contrast to the granites of northern Scotland, where there is a significant component of c.1600 m.yr. zircon. This suggests that the source of the Caledonian magmas was either young Precambrian crust (S type) or the mantle (I type).

The LISPB experiment (Bamford et.al. 1978) indicated a crustal thickness of about 30 kilometres in northern England.

The Lower Palaeozoic and Precambrian rocks found at

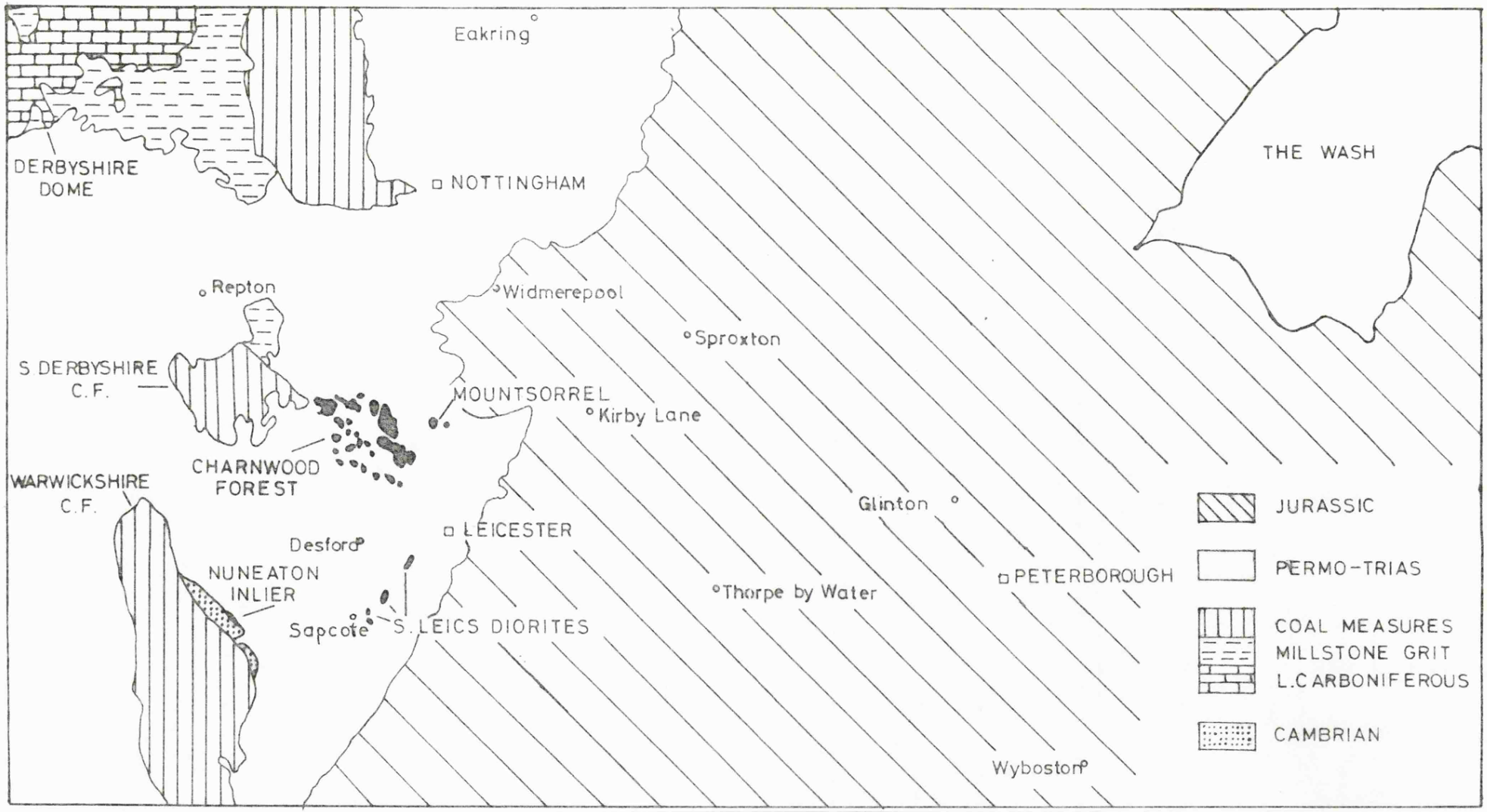


Figure 1.1 : The surface geology of the East Midlands.

outcrop, and in boreholes, in the East Midlands show low metamorphic grades which indicates that these rocks have never been subjected to deep burial. Heat flow measurements in the area (Richardson and Oxburgh 1978) give values that are close to the 1.4 hfu average value for England and Wales. Clearly this does not support the concept of the Midlands being a site of major Caledonian plutonism. Heat flow measurements at Croft Quarry, in the South Leicestershire Diorites, indicated a very low heat flow of Ø.88 hfu (Richardson and Oxburgh 1978). This may be because the intrusion was emplaced at a high level within cool country rocks therby limiting the time available for the fractionation of heat producing elements. Such an explanation is acceptable for small intrusive cupolás but is unlikely to be valid for large intrusions within the upper crust, if these can be shown to exist.

## 1.2 THE GEOLOGY OF THE AREA

### 1.2.1 The Precambrian

The Precambrian geology of the area is confined to the outcrops of Charnwood Forest and the Nuneaton Inlier together with a few borehole samples of probable Precambrian age.

The late Precambrian rocks of Charnwood Forest (The Charnian) are described in detail by Watts (1947) and Evans (1968). The stratigraphic succession and thicknesses, as worked out by Watts, are as follows:

| | |
|---|---|
| BRAND SERIES | Swithland slate |
| (Ø.3 km. thick) | Trachose grit & quartzite |
| | Hanging rocks conglomerate |
| MAPLEWELL SERIES | Woodhouse and Bradgate beds |
| (1.4 km. thick) | Slate agglomerate |
| | Beacon Hill beds |
| | Felsitic agglomerate |
| BLACKBROOK SERIES | Blackbrook beds |
| (Ø.9 km. thick) | |

The Brand Series is dominantly epiclastic whilst the Maplewell and Blackbrook are dominantly pyroclastic. The pyroclastic rocks comprise tuffs and volcanic agglomerates and have a predominantly acid volcanic and andesitic composition. The Brand series fines upward from basal rhyolitic and trachytic conglomerates, through coarse grits and quartzites to mudrocks.

Charnian igneous rocks. Two suites of igneous rocks are found in the Charnian, these are the porphyroids and the diorites. The porphyroids are of acid to intermediate composition and are intrusive at some localities. Blocks of probable porphyroid occur in some of the volcanic breccias and agglomerates which suggests that these rocks represent penecontemporaneous volcanic and shallow intrusive igneous activity. K-Ar dating gives a minimum age of 684±29 m.yr. for the porphyroids (Meneisy and Miller 1963).

The diorites can be sub-divided into two groups, the northern and the southern. The southern diorites, which take

the local name of Markfieldites, occur as massive bodies intruded at various levels near to the junction of the Brand and Maplewell Series. Cribb (1975) obtained an Rb-Sr date of 552±58 m.yr. for the southern diorites, this is in agreement with the K-Ar date of 547±24 m.yr. of Meneisy and Miller (1963). The northern diorites are less abundant in occurrence, and more basic in composition, than the southern.

The geochemistry of the Charnian was studied by Thorpe (1972) and is reviewed by Le Bas (1981) who describes the intrusive and extrusive rocks as having calc-alkaline affinities. The Charnian extrusives show similar fractionation trends to the Uriconian volcanics of Shropshire but are distinct from the tholeiitic Warren House Lavas of the Malvern Hills.

The principal structure of the Charnian inlier is that of an anticlinal fold with an axial plunge to the southeast. In the southeast of the inlier this trend swings around to the east. Sedimentary structures indicate that no inversion has occurred. The Charnian rocks have a pervasive cleavage which strikes 280°. The cleavage follows a sinuous path across the fold axis suggesting that it is superimposed. The Charnian inlier is truncated to the west by a major Hercynian reverse fault, the Thringston Fault. This fault throws the Coal Measures of the Leicestershire Coalfield against the Charnian.

The Nuneaton Inlier. The Nuneaton Inlier contains a small exposure of Precambrian rocks. The lithologies resemble those of Charnwood Forest being largely pyroclastic deposits (The Caldecote Volcanic Series) with dioritic intrusions (The Blue Hole Intrusive Series). The inlier is

truncated to the northeast by the Eastern Boundary Fault of the Warwickshire Coalfield.

Precambrian in boreholes. A number of boreholes to the south and east of Leicester (eg. at Great Oxendon, Orton, Glinton, Wittering, Sproxton, Wiggenhall and North Creake) have found volcanic tuffs and agglomerates of probable Charnian affinity (figure1.1). Kent (1968) suggested that a ridge of Precambrian basement extended eastwards from the Charnian Inlier to the North Creake borehole in Norfolk. More recent boreholes and seismic refraction surveys have, in general, supported this idea, although the extent of Caledonian igneous intrusions within the basement ridge is now known to be far greater than was previously thought.

### 1.2.2 Lower Palaeozoic

The only exposure of Lower Palaeozoic rocks in the East Midlands is in the Nuneaton Inlier. Here the Lower Cambrian is represented by the 275 metre thick Hartshill Quartzite. The quartzite contains boulders of the Blue Hole Intrusive Series and lies unconformably on the Caldecote Volcanics. The Hartshill Quartzite is overlain by about 800 metres of Lower Cambrian to Tremadocian shales, known collectively as the Stockingford Shales. The Tremadocian is overlain by Middle Coal Measures.

The Hartshill Quartzite is interpreted by Allen (1968) as a shallow water deposit, with some units possibly intertidal in origin. The Stockingford Shales show a general trend towards deeper water shelf sedimentation, although there is evidence for occasional shoaling. At the top of the Stockingford Shales are the Merevale Shales which have a

good graptolitic and trilobitic fauna of Tremadocian age.

Shales with a Cambrian to Tremadocian fauna, similar to the Stockingford Shales, have been identified in borings around Leicester (Leicester Forest East, Evington, Aston Flamville, Dadlington, Merry Lees) and further afield at Towcester and Deanshanger. In addition several boreholes have encountered unfossiliferous shales, mudstones and quartzites of probable Lower Palaeozoic age (e.g. Nocton, Eakring, Spalding, Thorpe-by-Water, Stixwould). An Rb-Sr whole rock isochron of 470 m.yr. was obtained for the Thorpe by Water siltstone (Bath, vide Richardson and Oxburgh 1978).

Ordovician shales have been found in the Great Paxton borehole and the Gas Council GH 5, both located near to Huntingdon, and in an offshore well to the north of Norfolk. The Lower Palaeozoic rocks are widespread in the sub-surface, dips of 40° to 80° are common but the metamorphic grade is low. Bullerwell (1967) commented on the association of steeply dipping mudstones in the Great Paxton and Deanshanger boreholes with low seismic velocities (3.4 to 3.5 $km.s^{-1}$), and suggested that the dips might be due to faulting rather than to a regional deformation.

Bullard et.al (1946) carried out a number of seismic refraction experiments in the vicinity of Cambridge. Surveys at Laxton, Corby and Benefield all gave refractor velocities indicative of Precambrian basement at depths of about 100 metres deeper than the siltstone in the nearby Thorpe-by-Water borehole. This suggests that the Lower Palaeozoic siltstones are thin.

The available evidence suggests that the Lower Palaeozoic in the East Midlands forms a thin veneer to the

Precambrian basement and does not attain geosynclinal thicknesses.

### 1.2.3 Caledonian igneous intrusions

Two Caledonian igneous intrusions are exposed in Leicestershire, these are the South Leicestershire Diorites and the Mountsorrel Granodiorite. Two other granitic to dioritic intrusions have been proved by boreholes at Melton Mowbray, east of Mountsorrel, and at Warboys in Cambridgeshire.

The Mountsorrel granodiorite. The Mountsorrel intrusion is exposed over an area of about 6 square kilometres to the east of Charnwood Forest. The intrusion is composed of pink and white granodiorite with less abundant basic diorite and gabbro (Le Bas 1968). Pidgeon and Aftalion give a U-Pb date of 452±8 m.yr. for the granodiorite. This age is consistent with an earlier Rb-Sr date of 433±17 m.yr. (Cribb 1975) and the K-Ar minimum age of 405±17 m.yr. (Miller and Podmore 1961).

On the western edge of the intrusion there is a contact between a diorite and a micaceous hornfelsed shale. The age of this shale is not known but Lowe (1926) commented on the possibility that it was eqivalent to the Stockingford Shales. Le Bas (1968) believed that the shale was petrographically similar to hornfelsed Stockingford Shale at Nuneaton and unlike any equivalently metamorphosed Charnian slate.

Lowe (1926) suggested that the outcrop of the granodiorite was truncated to the northeast by a fault running along the Soar Valley. Davies and Matthews (1966) carried

out a gravity traverse across the line of the projected fault. The interpretation of this survey was consistent with a fault downthrown to the northeast by up to 70 metres.

The aeromagnetic map of the area (see chapter 8) shows that the positive anomaly associated with the Mountsorrel granodiorite is only a small southern extension of a larger anomaly. It has been suggested that this anomaly is due to a much larger buried intrusion. Previous seismic work in this area is reviewed below.

The South Leicestershire Diorites. These are a group of diorites, microdiorites and tonalites which are exposed in a group of quarries 10 to 15 kilometres southwest of Leicester. LeBas (1972) suggested that the outcrops were part of a larger, zoned, intrusion ten kilometres in diameter. The Countesthorpe and Desford boreholes encountered similar rocks to those exposed in the quarries. Sills of a similar composition to the diorites intrude the Stockingford Shales in the Merry Lees drift mine (Le Bas 1968).

U-Pb dating of zircon from the Enderby tonalite (Pidgeon and Aftalion 1978) gave an age of 452+8/-5 m.yr. This invalidates the earlier Rb-Sr date of 546±22 m.yr. of Cribb (1975). The only known exposure of a country rock in contact with the intrusion was in the now infilled Coal Pit Lane Quarry at Enderby. The contact is described by Hill and Bonney (1878), Harrison (1884), Bonney (1895) and Lowe (1928). All the reports describe a wedge like mass of grey green altered (hornfelsed) shale or slate which was somewhat fissile away from the contact and weathered fairly easily. After some debate all those who saw the shale came around to the opinion that it was too soft to be Charnian and was

probably related to the Stockingford Shales at Nuneaton. Bonney compared the shale with the Brazil Wood slates whilst Harrison related it to the slatey rock in the nearby Sapcote Freeholt borehole (now shown by the NCB Aston Flamville borehole to have been Cambrian).

The aeromagnetic anomaly map for the area, together with the absence of diorite in the Sapcote borehole (two kilometres west of the exposed diorites) suggest that the intrusion is truncated to the west of the exposed diorites by a southward extension of the Thringston Fault. However NCB seismic reflection surveys have indicated a possible igneous boss at very shallow depth beneath the Trias in the Hinckley area (Allsop pers. comm.). It is hoped that these data will be released shortly.

Melton Mowbray granite. The NCB Kirby lane borehole confirmed the presence of this intrusion, as deduced from aeromagnetic evidence, at a depth of 402 metres. The core recovered is strongly weathered but has been described by Le Bas (1981) as a biotite granite with a similar calc-alkaline major element geochemistry to the other Leicestershire intrusions.

Warboys diorite. Le Bas (1972) described specimens from the Warboys borehole as diorites with increasing hydrothermal alteration with depth. This, together with a K-Ar age of 305±10 m.yr. is consistent with the intrusion being Caledonian with subsequent alteration by Hercynian mineralisation. The Warboys borehole was located on the western spur of a 50 nT positive aeromagnetic anomaly. The extent of this anomaly suggests that the intrusion might be of comparable size to the South Leicestershire Diorites.

From the isotopic ages available the Leicestershire intrusions are post-tectonic, in that they are later than the main Grampian metamorphism in Scotland, but they pre-date the "newer granites" of the Southern Uplands and Northern England.

## 1.2.4 THE UPPER PALAEOZOIC

Old Red Sandstone. The post orogenic Old Red Sandstone attains its maximum thickness in the West Midlands, Welsh Borders and Brecon Beacons. In the East Midlands its occurrence is restricted to a small inlier near Nuneaton and to a few boreholes. At Dukes Wood (Eakring) there are about 75 metres of conglomerates between the Carboniferous and the Cambrian. At the Wyboston borehole the ORS and Devonian were 115 metres thick and overlay the Cambrian. Boreholes at Gayton (Northamptonshire) and around Huntingdon (Gas Council G H series) have bottomed in ORS conglomerates.

The Carboniferous. The dominant palaeogeographic feature in Central England during the Carboniferous was the landmass of St. Georges Land and its eastward extension, the Mercian Highlands (essentially the basement ridge of Kent 1968).

The Carboniferous Limestone was deposited as a massif and a basin facies. The massif facies was characterised by slow deposition in stable environments, resulting in relatively pure, well bedded, limestones. The exposed Lower Carboniferous in the Midlands is mainly of the massif (or block) facies, as represented by the Derbyshire Dome and the limestone inliers in South Derbyshire and at Grace Dieu to

the north of Charnwood Forest. The basin facies consists of dark, impure and shaley, limestones with a poor fauna. This facies occurs in an inlier to the south of the Derbyshire Dome, and has been proved by boreholes at Widmerpool and Long Clawson to the northeast of Leicester and at Repton and Mickleover between Charnwood Forest and the Derbyshire Dome.

Falcon and Kent (1960) proposed that the Staffordshire Gulf extended eastwards to the north and northeast of Charnwood Forest as the Widmerpool Gulf (figure 1.2). There are over 500 metres of Lower Carboniferous in the Widmerpool borehole, down to a TD at 1890 metres. The Lower Carboniferous thins against the Mercian Highlands and is only 8.3 metres thick in the Desford borehole whilst it is absent at Kirby Lane. To the south of the Mercian Highlands borings in Northamptonshire (Gayton and Kettering Road) and at Cambridge have proved Carboniferous Limestone.

The Millstone Grit was deposited in a series of deltas to the north of the Mercian Highlands. The greatest thicknesses (1200 metres) occur in North Staffordshire. The Widmerpool and Long Clawson boreholes have 730 and 480 metres of Millstone Grit respectively. The Millstone Grit also thins against the ancient landmass with 4 metres at Desford and 22 metres at Kirby Lane. Further east at Sproxton there are 75 metres of Millstone Grit lying on probable Precambrian basement.

The Lower and Middle Coal Measures were deposited on the extensive deltas initiated in the Namurian. The Upper Coal Measures are largely unproductive "red bed" facies. The Leicestershire coalfield lies beneath the Triassic cover to the west of the Charnian Inlier. The Coal Measures thin to

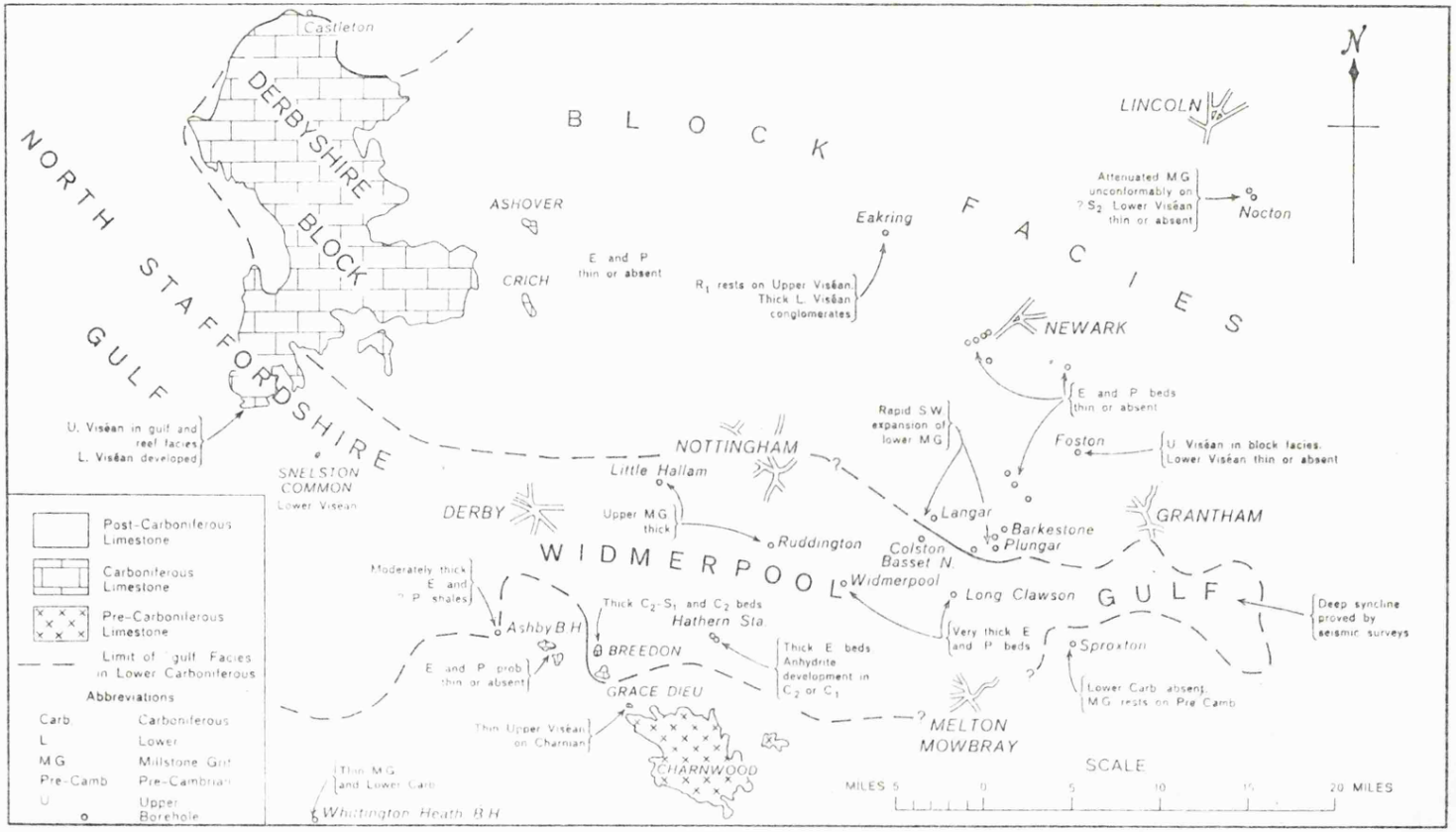


*Limits of the Widmerpool Lower Carboniferous gulf. $C_1$, $C_2$, $S_1$, $S_2$, P, E and $R_1$ are the initial letters of Zones and Stages within the Carboniferous Limestone Series and Millstone Grit Series* (from Falcon and Kent 1960, *Mem. Geol. Soc.* No. 2)

Figure 1.2 : The Widmerpool Gulf (from Hains and Horton 1969).

the west and are truncated to the east by the Thringston Fault. Both the Leicestershire and South Derbyshire coalfields are faulted along a northwest to southeast "Charnoid" trend (Spink and Ford 1968). The Derbyshire coalfield is folded into a syncline with a Caledonide trend.

The North East Leicestershire coalfield is as yet undeveloped. The structure is basinal with the Coal Measures truncated by subcropping at the Permo-Trias unconformity and thinning to the south against the basement ridge (Jones 1981).

There was considerable igneous activity during, or shortly after, the Carboniferous. Many of the boreholes in the Widmerpool Gulf show intrusions of dolerite which intrude the Coal Measures but pre-date the overlying Triassic sediments.

### 1.2.5 Post Carboniferous

Permian rocks are not exposed in the East Midlands south of Nottingham, although they may be present above the Coal Measures in the Long Clawson borehole.

Most boreholes from the basement ridge southwards show the pre-Carboniferous basement overlain by Bunter pebble beds or by Keuper sandstones. By the Keuper times the Hercynian highlands had been eroded and deposition was in a series of subsiding non-marine basins. The Keuper fines upwards to the Keuper Marl which is exposed extensively to the west of Leicester.

Moving eastwards from Leicester to East Anglia there is a complete Mesozoic succession. The Jurassic has an easterly dip of one degree or less.

Pleistocene and Recent deposits, mainly Boulder Clay but with some sands and gravels, are widespread in the area. These deposits are significant only in that the clays provide a good medium for the drilling of seismic shot holes. The thickness of these deposits rarely exceeds 20 metres.

## 1.3 PREVIOUS SEISMIC WORK IN THE EAST MIDLANDS.

The geologic interpretation of the results of seismic refraction surveys is largely dependent on the interpretation of the various refractor velocities as being characteristic of a particular rock type or formation. Information on refractor velocities comes from five principal sources:

1. Refraction surveys over outcropping rocks.
2. Refraction surveys near boreholes where the depth control is well established.
3. Measurement of velocities in a borehole by seismic logging, or preferably, a velocity survey.
4. Laboratory measurements.
5. Comparison with previous surveys and their interpretation. (Such second hand evidence is both the least reliable and the most commonly available.)

This discussion is concerned with the velocities obtained for the basement refractor in the East Midlands and the types of basement interpreted for these velocities.

1.3.1 Surveys over outcropping basement.

Whitcombe and Maguire (1980) analysed first arrival travel times for quarry blasts located in and around the Charnian inlier into a 5 kilometre aperture seismic array located on the Charnian inlier. They concluded that the region where the Maplewell Series rocks are exposed corresponded to a p-wave velocity of 5.65 $km.s^{-1}$. A lower p-wave velocity, about 5.4 $km.s^{-1}$ was found to correspond with the older Blackbrook Series rocks.

The same study detected a basement refractor beneath the Charnian at a depth of over 2 kilometres. This refractor had a velocity of about 6.4 $km.s^{-1}$.

1.3.2 Surveys tied to boreholes.

Chroston and Sola (1982) report the results of a number of refraction surveys in East Anglia. Lines in North Norfolk close to the North Creake and Wiggenhole boreholes,which prove low grade metamorphic basement of probable Precambrian age, show velocities for the basement refractor in the range 5.6-6.0 $km.s^{-1}$.

Bullard et al (1946) carried out seismic refraction surveys around Cambridge. A survey near the Great Oxendon borehole (presumed Precambrian quartz felsite at 118 metres below OD) gave a refractor velocity of 5.17 $\pm$ .15 $km.s^{-1}$ at 107 metres below OD.

1.3.3 Borehole and Laboratory Measurements.

Chroston and Sola (1982) have examined sonic logs for the Somerton, East Rushton and Saxthorpe boreholes in Norfolk. All the boreholes contain Lower Palaeozoic shales

and siltstones, the velocities from the sonic logs are in the range 5.1-5.5 $km.s^{-1}$. The South Creake borehole, with Precambrian shales and quartzites gives variable velocities up to 5.5 $km.s^{-1}$.

Bullerwell (1967) reports the results of borehole sonic logging at four boreholes:

| | |
|---|---|
| Upwood (Precambrian tuffaceous agglomerate) | 4.57 $km.s^{-1}$ |
| Warboys (diorite) | 5.94 $km.s^{-1}$ |
| Great Paxton (Ordovician mudstone) | 3.41 $km.s^{-1}$ |
| Deanshanger (Tremadocian mudstone) | 3.47 $km.s^{-1}$ |

The velocity at Upwood is significantly lower than the typical Precambrian velocities noted above.

Wyrobek (1959) analysed well velocity data for a number of boreholes in Eastern England and in Lancashire. The results of this study indicate the problems of trying to produce typical velocities for any formation and underline the value of local velocity data in the interpretation of refraction data. Wyrobek fitted functions of the form $V_H = V_0 . H^{\frac{1}{N}}$ to the interval velocity and depth data, where V is the interval velocity at a depth H. Wyrobek's curve for the Keuper is shown in figure 1.3. Whilst there is a trend for increasing velocity with depth there is a very large scatter of velocities at shallow depths.

Solutions to refraction travel time data frequently use solutions in which the velocity increases with depth. As can be seen from the data of Wyrobek and others this is geologically acceptable in large thicknesses of sedimentary rocks since it allows for compaction and burial diagenesis.

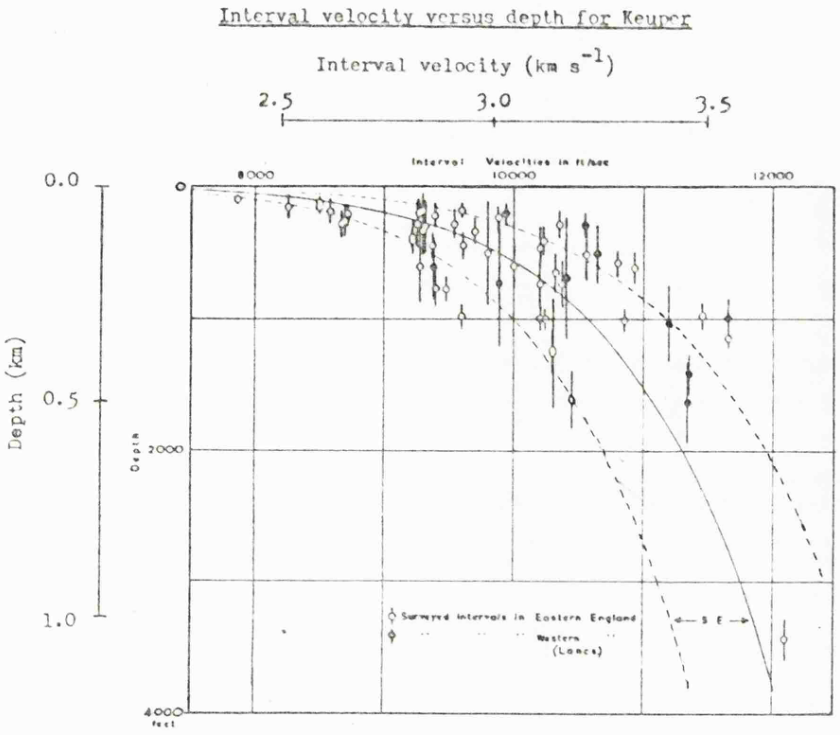


Figure 1.3 : Borehole interval velocity measurements for the Keuper (from Wyrobek 1959).

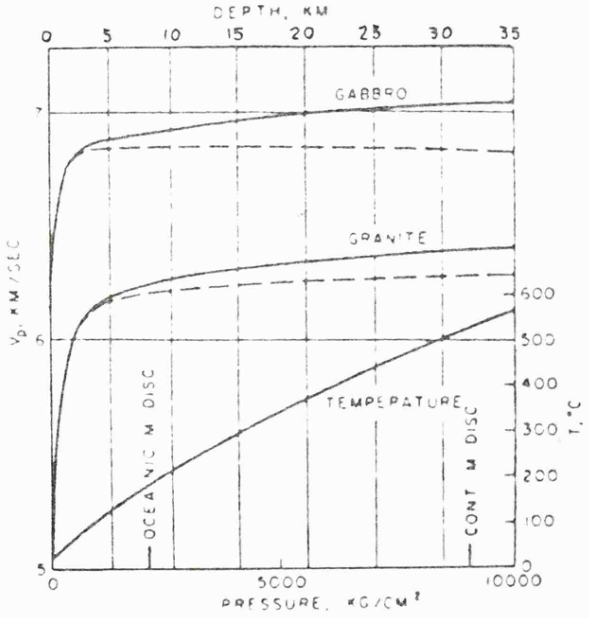


Figure 1.4 : P-wave velocity variations with depth. The dashed line includes the effects of pressure as well as temperature (from Birch 1958).

In crystalline rocks increasing pressure causes fractures to close and hence causes an increase in p-wave velocity. Figure 1.4 is taken from Birch (1958) and dramatically illustrates the relationship between pressure and velocity in the first 5 kilometres of burial.

1.3.4 Other refraction experiments in the area.

The refractor velocities determined by Bullard et.al. (1946) (see 1.2.2) were 5.43 $km.s^{-1}$ at Laxton, 5.69 $km.s^{-1}$ at Corby and 5.5 $km.s^{-1}$ at Benefield.

Davies and Matthews (1966) carried out geophysical surveys in the area between the exposed Mountsorrel granodiorite and the Charnian inlier at Woodhouse Eaves. Two distinct groups of basement velocities were determined from the eight refraction profiles (each 600 metres long). The three profiles closest to the granodiorite at Buddon Wood and Swithland reservoir gave velocities of 4.8-5.0 $km.s^{-1}$, the other profiles gave velocities of 3.7-4.4 $km.s^{-1}$. The authors interpreted these velocities as being due to an eastward continuation of the Charnian slates which are exposed at Woodhouse Eaves. The higher velocities near the granite were interpreted as a compositional change within the slates near the granite contact. A magnetic survey of the same area indicated a rapid westward fall-off of the magnetic anomaly at the edge of the granite, suggesting a near vertical western margin to the intrusion.

In the light of the reinterpretation of the contact rocks in Brazil Wood as Lower Palaeozoic it seems likely that the lower group of velocities recorded by Davies and Matthews (1966) are due to Lower Palaeozoic shales.

Velocities of about 3.5 to 4.0 $km.s^{-1}$ are typical of these rocks in the East Midlands. The Charnian velocities of Whitcombe and Maguire (1980) suggest that velocities of 3.7 to 5.0 $km.s^{-1}$ are too low to be Charnian. The Swithland Slate was not included in their study, due to its restricted outcrop, but it does have a similar density to the other Charnian rocks (see chapter 7).

The increase in velocities reported by Davies and Matthews (1966) is probably due to alteration of the shales near to the contact. Only one of the profiles was sufficiently close to the margin of the intrusion for a sideswipe refraction to be a possibility.

Maroof (1973) carried out a refraction survey on Prestwold airfield. The line was 2200 metres long and was orientated west to east on the 250 nT aeromagnetic anomaly which is presumed to represent a northern extension of the Mountsorrel granodiorite. The survey indicated a refractor of velocity of about 4.84 $km.s^{-1}$ at about 450 metre depth which was interpreted as the top of the buried extension of the Mountsorrel granodiorite. This velocity was subsequently used as evidence for low velocities being associated with shallow igneous basement (Whitcombe & Maguire 1981a).

El-Nikhely (1980) however, has presented two-way time and depth maps for the NCB seismic reflection survey to the east of Loughborough. Line 74-46 of the Loughborough survey passed about 2 kilometres north of Maroof's refraction line. El-Nikhely's interpretations put the base of the Carboniferous Limestone at 1250 metres with about 300 metres of pre-Carboniferous overlying a possible basement reflector at about 1550 metres.

Jones (1981) concurs with this interpretation by describing structures seen on seismic sections at below 800 metres as probably occurring within basinal facies Lower Carboniferous. Clearly this difference in depths between the refraction and reflection interpretations will have considerable significance in the interpretation of the aeromagnetic anomaly due to the intrusion (see chapter 8A). The 4.85 $km.s^{-1}$ velocity at 450 metres obtained by Maroof is, by analogy with the reflection data, a sill within the Coal Measures or Millstone Grit.

In addition to the Charnwood array Whitcombe (1979) carried out three refraction profiles. These profiles are reported in Whitcombe and Maguire (1981a,b) and the results are shown in figure 1.5. The profiles radiated out from the Charnian Inlier to Holwell in the Widmerpool Gulf; to Mancetter in the Nuneaton Inlier and to Ballidon in the Derbyshire Dome.

Bardon to Holwell line: this line showed a basement refractor of velocity 5.64 $km.s^{-1}$ dipping away from Charnwood Forest into the Widmerpool Gulf. By analogy with the Charnwood array data this refractor was interpreted as Precambrian. The profile also detected a low velocity region within the basement refractor with a velocity of 5.0 $km.s^{-1}$, or $4.8 \pm 0.7z$ $km.s^{-1}$ if an increasing velocity with depth was used in the time term solution. The low velocity region correlated with the northern extension of the Mountsorrel magnetic anomaly, the line passed to the southeast of the peak of the anomaly at the 100-150 nT contours. Even if the refractor detected by Maroof (1973) at Prestwold (see above)

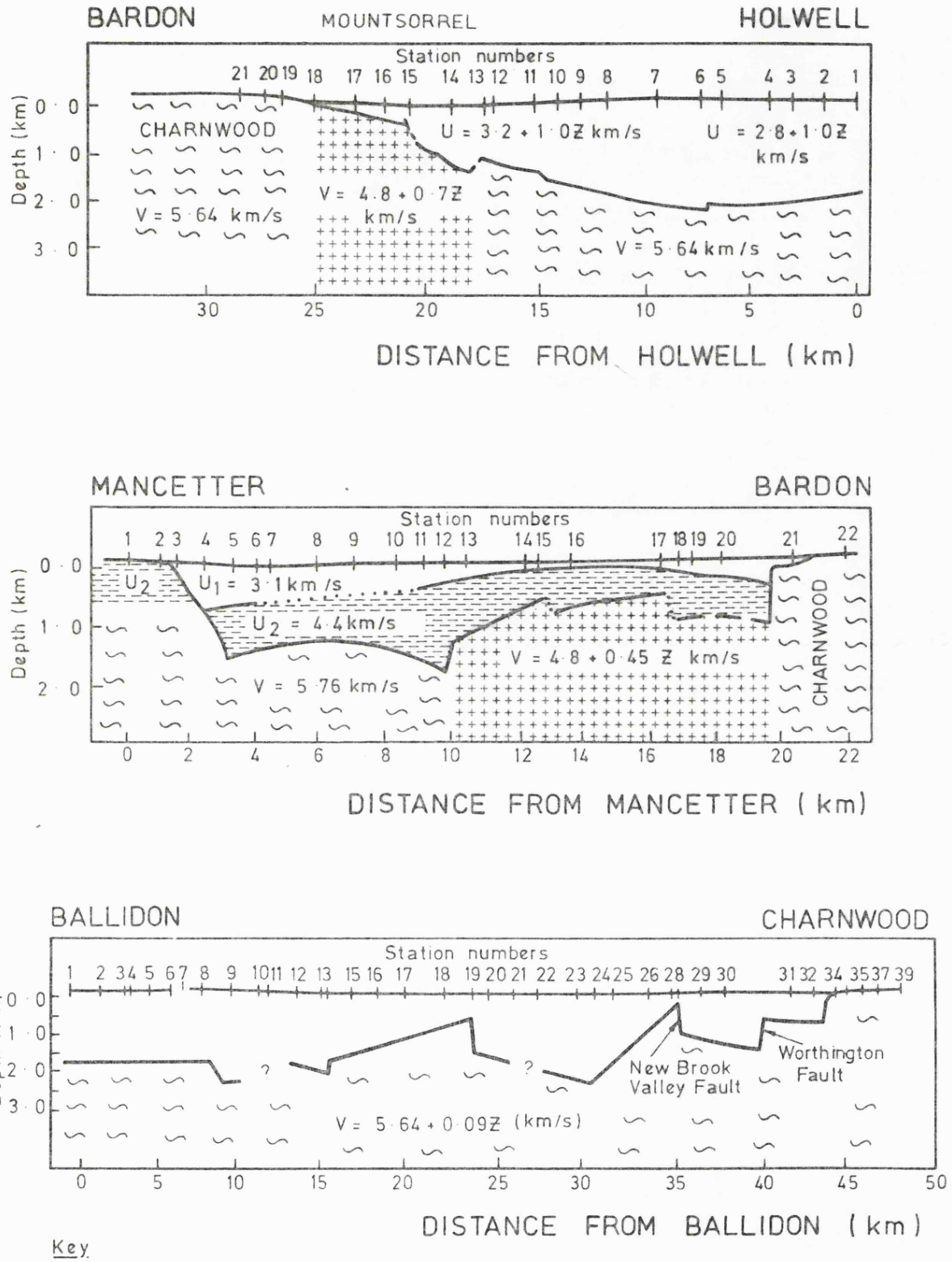


Figure 1.5 : Results of previous seismic refraction profiles (from Whitcombe and Maguire 1981a,b).

was not due to the intrusion the correlation of the low velocity region and the aeromagnetic anomaly indicate that this region is a northern extension of the Mountsorrel intrusion. A fault near station 15 (see fig. 1.5) was interpreted as Lowe's (1926) "Soar Valley Fault". For this to be possible the fault, as detected to the north of Buddon Wood by Davies and Matthews (1966), would have to swing north from the line that Lowe suggested. A second explanation is that there are at least two faults present; step faulting is observed on the northern margin of the Melton intrusion to the east of Mountsorrel (see chapter 4). The position of the fault on the seismic line agrees well with the northward extension of the Sileby fault (IGS sheet 142, figures 5.1, 5.5). Seismic reflection work in progress at Leicester should resolve this question as well as providing more information about the margins of the intrusion.

The Bardon to Mancetter line : this line also detected a low velocity region ($4.8 \pm 0.45z$ km.s$^{-1}$) and a presumed Precambrian refractor (velocity 5.67 km.s$^{-1}$) underlying the Nuneaton basin. The displacement of the basement at the Thringston Fault was shown to be 500 metres. The low velocity basement in this case most probably represents a westward extension of the South Charnwood Diorites.

The Charnwood to Ballidon line: the southern part of this line ran along the postulated Derby to Melbourne causeway, a ridge of positive gravity anomalies linking Charnwood Forest to the Derbyshire Dome. The velocity of the basement refractor along this profile was determined as $5.64 \pm 0.09z$ km.s$^{-1}$. The refractor showed considerable topography (fig.1.5) especially at its southern end where Hercynian

faulting was detected in the basement surface. Basement depths of up to 1.8 kilometres are indicated for the western extension of the Widmerpool Gulf.

### 1.3.5 The crustal structure of Northern Britain

The LISPB experiment (Bamford et.al. 1977,1978) defined three layers in the upper crust of Northern England extending as far south as the end of the northern profile at Buxton in Derbyshire. The uppermost layer "$a_s$" had a veocity of 4.Ø to 5.Ø km.s$^{-1}$ and was correlated with Upper Palaeozoic sediments. The base of this layer was about two kilometres deep at Buxton. Beneath this layer was the "$a_0$" refractor with a velocity of 5.6 to 5.8 km.s$^{-1}$. The data was found to be best fitted by models in which the velocity of this layer was allowed to increase to about 6.Ø km.s$^{-1}$ at its base. The base of this layer was about 14 kilometres deep in Northern England and about 9 kilometres deep at Buxton. This layer was interpreted as Lower Palaeozoic basement. The underlying "$a_1$" layer had a velocity of about 6.25 km.s$^{-1}$ and was interpreted as pre-Caledonian basement. The structure of the lower crust and uppermost mantle on the southern (gamma) section of the profile was not well defined.

From the results of the Charnwood array and the Charnwood to Ballidon profile described above it is probable that the LISPB "$a_0$" refractor is in fact equivalent to the presumed Charnian basement detected at a depth of 1.8 kilometres at Ballidon (Whitcombe and Maguire 198Ø and 1981b). The "$a_1$" layer can be tentatively correlated with the 6.4 km.s$^{-1}$ refractor detected at between 2 and 4 kilometres beneath the Charnwood array. High velocity

refractors were also detected beneath the Charnian type basement on the Holwell and Ballidon profiles.

## 1.4 SUMMARY

The Midlands platform has remained a stable feature since the Cambrian. There is increasing evidence for a Caledonian calc-alkaline igneous province within the upper crust in this area. The absence of any medium or high metamorphic grades within the Precambrian basement indicates that deep burial has not occurred. Clearly granitic intrusions, possibly following older, Charnian type, structural trends, could have been important in maintaining the stability of the Midland platform.

Geophysically it seems possible to discriminate between Precambrian ("Charnian") basement and igneous intrusions by the lower p-wave velocities of the latter. The boreholes which reach basement in the East Midlands indicate a level platform at depths of up to 500 metres below OD. This suggests that some of the anomalies observed on the Bouguer gravity maps (see chapter 7) cannot be explained by sediment accumulations and must be intra-basement in origin.

# CHAPTER TWO

# SEISMIC REFRACTION SURVEYING

## 2.1 INTRODUCTION

Sections 2.2 and 2.3 of this chapter contain details of the techniques used to analyse the seismic refraction data from the various experiments. The time term method, in particular, is described.

Section 2.4 describes the experimental procedure followed for the Melton and Peterborough experiments. This includes the recording of both quarry blasts and controlled shots and the location of the recording sites. The recording equipment used is described briefly in 2.5.

Section 2.6 contains details about the picking of first arrival travel times and the assessement of the observational errors.

## 2.2 REDUCED TRAVEL TIMES

The reduced travel time $T_R$ of an observed travel time $T^*$ is given by:

$$T_R = T^* - X/V_R \qquad (2.1)$$

where X is the shot-receiver separation and $V_R$ is the selected reducing velocity. If $d_S$ and $d_R$ are the shotpoint and recording site delay times the travel time equation for a horizontally layered constant velocity structure can be

approximated by:

$$T^{*} = d_S + d_R + X/V \qquad (2.2)$$

where V is the true refractor velocity. Combining equations 2.1 and 2.2 gives:

$$T_R = d_S + d_R + X/V - X/V_R \qquad (2.3)$$

If $V_R$ is set equal to the true refractor velocity (V) then the reduced travel time will represent the sum of the shotpoint and recording station delay times. If the reduced travel times for one shot are plotted against the receiving station position along a recording profile, the variations in reduced travel time should be indicative of changes in the recording station delay time along the profile. In the simplest case, that of a uniform velocity refractor overlain by overburden with a uniform average velocity, the reduced travel time section will show variations in refractor topography.

If the reduced travel time sections for a reversed profile are compared the delay time anomalies due to structure on the refractor will be offset, away from the shot, by a distance equal to half the critical distance. This offset allows for the separation of anomalies due to refractor topography from those due to variations such as geophone plant or a localised near surface velocity anomaly. However a velocity anomaly in the sediments immediately above the refractor would be indistinguishable from a structure on the refractor.

Reduced travel time sections therefore provide a convenient way of examining short wave-length structures before the travel time data is smeared by the summation of two, or more, delay time surfaces, as occurs in the time term method.

By comparing the reduced travel time sections for two reversed shots it is possible to estimate the reducing velocity that gives the visual best fit between the two delay time surfaces. Whitcombe and Maguire (1979) suggest that such a visually determined best fit velocity will differ from a non-iterative time term solution velocity by less than $\pm$ Ø.1 km.s$^{-1}$. If a fit cannot be determined within the limits of the observational errors it is likely that there is a lateral variation in the velocity of the refractor or the overburden.

## 2.3 TIME TERM ANALYSIS

### 2.3.1 The Method

The time term method (Willmore and Bancroft 196Ø) is a means of inverting a set of travel time observations and station separations to obtain a set of time terms(delay times) and the refractor velocity.

For a uniform velocity refractor the travel time of a refracted head wave between a shot at i and a receiver at j is given by:

$$T_{ij} = a_i + a_j + \Delta_{ij}/V \qquad (2.4)$$

where $a_i$ and $a_j$ are azimuthally independent time terms, and

$\Delta$ is as shown below.

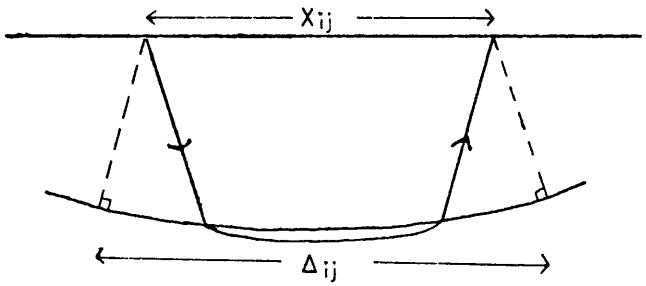


$T_{ij}$ is the true travel time, as opposed to the observed travel time $T^*_{ij}$ . There is no observational error associated with $T_{ij}$ . $\Delta_{ij}$ will be approximately equal to the station separation $X_{ij}$ , the only time the two are equal is in the case of a horizontal refractor. However $\Delta$ cannot be calculated until the depth to the refractor is known. Therefore in a first time term solution the observed travel time is given by:

$$T^*_{ij} = a_i + a_j + X_{ij}/V + e_{ij} \qquad (2.5)$$

where $e_{ij}$ is the observational error.

Each observed travel time can be represented by an equation of this form. Provided that the number of observations is greater than the number of unknowns (the time terms plus the refractor velocity) and that at least one shot point acts as a recording site for another shot, a solution is possible.

Each travel time observation in the solution will have an associated residual $r_{ij}$ :

$$T^*_{ij} = a'_i + a'_j + X_{ij}/V' + r_{ij} \qquad (2.6)$$

where a' and V' are the solution values as opposed to the

true values. The values of $r_{ij}$ are used to calculate the solution variance (see below).

The iterative approach to time term analysis (Willmore and Bancroft 1960, Bamford 1973) is based on obtaining a first solution using $T^*$ and X. The solution time terms are then converted into depths and approximate values of $\Delta$ are calculated. The solution can then be iterated until the solution variance is minimized.

## 2.3.2 Residuals and variances

The solution residuals (equation 2.6) will be dependent on:

1. the observational error $e_{ij}$
2. an increment $g_{ij}$, needed to account for the difference between X/V and $\Delta$/V.

An estimate of the solution variance for L observations and N time terms (N+1 unknowns) can be calculated:

$$\sigma_s^2 = \sum_{\ell=1}^{L} \frac{r_\ell^2}{(L-N-1)} \qquad (2.7)$$

The observational error variance is given by:

$$\sigma_e^2 = \sum_{\ell=1}^{L} \frac{e_\ell^2}{(L-1)} \qquad (2.8)$$

The values of $e_{ij}$ can be obtained by repeat picking of the same arrival. This is time consuming and, unless a number of separate people make the picks, is likely to be biased. The measurement errors associated with the pick can be accurately assessed but these are small compared with the

uncertainty of locating the first break (see below). An alternative method of assessing the errors is to estimate the range of times within which the travel time falls (the confidence limit), this technique is discussed in section 2.5.

The ratio $$\frac{\sigma_s^2}{\sigma_e^2} = F \qquad (2.9)$$

An F ratio insignificantly different to unity indicates that the chosen time term model is an adequate description of the data, but other models may be equally as good. If F is significantly greater than unity there is a source of variance other than the observational errors and the model will show a lack of fit.

If the station time terms indicate a large wavelength structure the lack of fit can be reduced by an iterative series of solutions. If the lack of fit remains the chosen time term model is inadequate.

## 2.3.3 Refractor geometry

Whitcombe and Maguire (1979) modelled the effects of refractor structure on time term solutions in order to examine the inadequacies of the method.

For a planar dipping refractor the solution velocity (v′) will always be greater than the true refractor velocity (v). The two are related by :

$$v' = v/\cos a \qquad (2.10)$$

where a is the refractor dip. Dips of up to 10° will not seriously affect the solution velocity (less than 0.1 $km.s^{-1}$ for a 6.0 $km.s^{-1}$ refractor). In the case of an anticlinal refractor the solution velocities and the radius of

curvature of the solution will be overestimated, this is because the X values used in a first solution are greater than the true ($\Delta$) distances. The converse applies to synclinal refractors where the solution velocities will be underestimates of the true velocity. In the case of long wavelength structures, such as anticlines and synclines, dips of less than $10^{\circ}$ are sufficient to seriously affect the solution velocities.

The solution for a refractor with a vertical velocity gradient will be indistinguishable from that of a synclinal refractor. This means that if a vertical velocity gradient exists but is not included in the solution synclinal structures will be exaggerated and anticlinal structures will be suppressed. The converse is also true.

Since synclinal and anticlinal structures cause opposite distortions in the time term solution serious problems can be caused if both structures are present along the profile. The solution velocity for the whole profile would be a reasonable approximation to the true velocity but a significant lack of fit would be indicated by the F ratio. If the model was split into two parts the resulting solutions would imply a lateral change in refractor velocity that did not exist but the F ratios would indicate an improved solution.

Reduced travel time plots are useful in checking the suitability of a data set for a time term solution. Plots of shots from different distances, but similar azimuths, into a recording profile can be used to detect vertical velocity gradients. Long wavelength structures can be detected and the refractor velocity estimated.

## 2.4 EXPERIMENTAL PROCEDURE

The quality of any solution depends on the quality of the recorded data and the design of the experiment. The practical limitations of the method must be remembered when the data are being interpreted.

### 2.4.1 Location of the profiles

The location of the recording profiles for the Melton and Peterborough experiments was determined by the following:

1. The geological/geophysical target under investigation (e.g. a potential field anomaly).

2. Suitable sites for shotpoints, and for the Melton experiment, quarries firing reasonable sized charges.

3. Control points such as outcropping basement rocks or boreholes.

The details of the location of the two experiments are discussed in the relevant chapters (5 and 6).

### 2.4.2 Shotpoints

The controlled shots were drilled by the geology department's trailer mounted three inch auger drill, which is capable of drilling to a depth of 19 metres. In the areas where the experiments were carried out, the near surface deposits were mostly clays which could be drilled fairly easily, at a rate of one or two holes a day. Because the holes were left standing for some time between drilling and firing they were cased with PVC pipe.

The explosive used was Nobel's Special Gelatine (80%

strength) with seismic electric detonators (delay less than Ø.ØØ1 sec.). Charges of up to 25 kilogrammes could be placed in a single drill hole 19 metres deep leaving about 1Ø metres for stemming, this was sufficient to prevent the hole blowing out.

Clay, especially if it is water saturated, provides the best medium for shotfiring since it gives maximum coupling between the charge and the ground. Firing in rock causes a lot of the energy to be wasted in fracturing the rock, this can result in a reduction in signal strength by as much as a factor of five.

Extensive use was made of quarry blasts during the Melton experiment. All three quarries at which blasts were timed were in residential areas and therefore were careful to minimize the vibrations caused by their blasts. The ripple firing technique was used at all three quarries with a Ø.Ø25 second delay between the charges. The charge used on the zero delay varied between 1ØØ and 25Ø kilogrammes, this is probably the best measure of the effective charge that produces the first arrival energy. However this charge is fired into a free face in hard rock, therefore much of the energy is lost in fracturing and knocking down the rock. In addition the explosives used were not always gelignite, part of the charge was often a slurry such as "Ampho" which, weight for weight, has a smaller explosive power than gelignite.

For a ripple delay of Ø.Ø25 seconds and a rock velocity in excess of 5.Ø $km.s^{-1}$ the initial p-wave energy will have travelled over 125 metres before the second charge is detonated. The orientation of the ripple should therefore

have no effect on the seismic energy propagated along the profile.

Burkhardt and Rees (1976) carried out a detailed study of the source characteristics of Eschenlohe quarry in West Germany. A number of charges of 6 to 22 tonnes were monitored both within the quarry and at a distance from it. Burkhardt and Rees conclude that the received seismic signal was largely independent of the position of the charge within the quarry and that the quarry blasts could therefore be considered as reproducible seismic sources. Furthermore they suggest that the radiated signal is not directly dependent on the primary pulse but on secondary effects within the quarry, possibly a natural vibration of the rock body.

### 2.4.3 Recording sites

The recording sites were distributed as evenly as possible along the profiles, typically at intervals of one to two kilometres. The sites were located away from sources of noise, pincipally roads, but with reasonable access, according to the type of equipment used at the site.

For the Melton experiment the Geostore recorders used were sited where they were in line of sight with the telemetered outstations. Because of a shortage of UHF radio links some stations were linked to Geostores by landlines.

Seismometers were placed in pits 0.5 metres deep and then covered with a lid. The Geostore stations on the Melton experiment were lined with a pipe set in a cement base to ensure that the seismometer remained vertical for several weeks and to improve the ground coupling.

The recording sites and borehole shotpoints were

located on 1:10,000 Ordnance Survey maps by measurement from marked features. Grid references were determined to ± 10 metres which is equivalent to a travel time error of less than 0.002 seconds for a refractor velocity greater than 5.0 $km.s^{-1}$. Elevations were estimated from topographic maps with an accuracy of about ± 5 metres. The location of the quarry blasts used in the Melton experiment is described in chapter 5.

## 2.5 RECORDING EQUIPMENT

The four types of recording equipment are described briefly.

Geostore system: this system is described in full by Whitcombe (1979). It comprises a 14 track analogue magnetic tape recorder which records on 1/2 inch tape at speeds of 15/640, 15/320, 15/160 ips. There is a 32 Hz. upper limit to the frequency of the recorded signal at 15/160 ips. The recorder can be set to run in uni or bi-directional mode. In bi-directional mode two tracks are used for flutter compensation and internal clock leaving 5 for data (four seismic and an external clock such as MSF). In uni-directional mode there are 11 data channels but it is advisable to record the external clock on two tracks since two different recording heads are used to record two sets of seven tracks. At 15/160 ips one pass of a standard 2400' tape takes about 3.5 days. The seismometer (Willmore III or HS 10) output is fed to an amplifier modulator where it is frequency modulated at 676 Hz. ± 40%. The modulated output is sent to the recorder either by cable or via a UHF radio

link. The radio links have a line of sight range of about 30 kilometres.

MARS system: this is a portable recording system designed for use with explosive sources, it is described briefly by Berchemer (1976) and can be summarised:

Recorder: Uher 1/4" reel to reel tape with speeds of 2.4, 4.7, 9.5, 19.0 $cm.s^{-1}$.

Amplifier: Lennartz, 0.2-200 Hz. (optional 20 Hz. low pass for high noise conditions)

Modulator: 6.4 kHz. flutter control.
9.6 kHz. $\pm$ 15% for time code recording.
4.2,2.4.0.86 kHz. $\pm$ 15% for seismic data.

Reading University cassette recorders: these single channel recorders were designed by Dr. D.T. Hopkins or Reading University. They use a mono audio cassette recorder modified to record on both tracks:

1: Frequency modulated seismic signal.

2: Time code (MSF).

3: 400 Hz. reference signal

The recorders have an electronic timer which can be preset by up to 24 hours for unmanned recording. The record time is then 45 minutes (one pass of a cassette tape).

Durham University recorders: these recorders were used during the Peterborough experiment. There are three different types of recorder.

Type 1. Amplifier: 0.005 to 40 Hz.
Modulator: 415 Hz. ± 15% frequency modulation
Time code: Recorded at fm saturation frequencies (290 & 530 Hz.)

Type 2. Tape speed: 12/160 ips.
Amplifier: has a 6db point at 20 Hz.
Modulator: 71 Hz. ± 30% frequency modulation.
Time code: switched between 50 and 100 Hz.

Type 3. Amplifier: high cut greater than 40 Hz.
Modulator: 800 Hz. ± 30% frequency modulation.
Time code: recorded direct.

The type 1 and 2 use Willmore III seismometers, the type 3 use Willmore II; all with a 2 Hz. resonant frequency. An early version of the type 1 recorders is described by Long (1974). The low modulator frequency of the type 2 recorders and the direct time code recording of the type 3 both caused some problems with the data recorded (see chapter 6).

## 2.6 TRAVEL TIME ERRORS

The assessement of the errors associated with the travel time observations is important if the F ratio is to be used to compare time term solutions.

### 2.6.1 Sources of error

Rounding of the seismic signal: preferential attenuation of high frequencies in the signal will cause a rounding of the first break, this will increase with distance from the

source. Typical p-wave signals from explosive sources at ranges of up to 30 km. have dominant frequencies of 10-20 Hz. The onset time of such a signal can be picked to better than 0.010 sec. Errors due to rounding are likely to be smaller than those due to noise for all but the highest signal to noise ratios (ie. greater than ten to one).

Seismic noise: the accuracy with which a first arrival can be picked depends largely on the signal to noise ratio and the relative frequency content of the signal and noise. Noise is usually of similar frequencies to the seismic signal. High frequency noise is usually generated within the recording system, low frequencies (<5 Hz.) are not a serious problem in picking the first break.

At signal to noise ratios above about three the first cycle will be easily identifiable. In such cases the first arrival can be picked with an accuracy better than the time to the first peak/trough; for a 10-20 Hz. signal this will be 0.025 to 0.013 seconds. In practice the onset can probably be located to within 0.005-0.010 seconds.

Lower signal to noise events can present a problem in identifying the correct cycle. These events are best picked by correlation with the better quality events. Using a correlation can carry a systematic error along the recording profile but prevents the individual travel times from being in error by a complete cycle. Events picked in this way are usually located to 0.020 seconds.

Measuring the onset time: The accuracy with which an onset time can be measured depends on the length of paper playout occupied by one second of the data. The equipment available for the replay of Geostore tapes gave a maximum replay scale

of 50 $mm.s^{-1}$ for tapes recorded at 15/160 ips. All the other recordings were replayed at 100 $mm.s^{-1}$ . Provided that the MSF time signal was recorded as a clean square wave with no rounding of the pulses it was possible to measure the traces to 0.25 mm. This is equivalent to an accuracy of 0.005 sec. for the Geostore data and 0.0025 sec. for the other data.

Timing the shot instant: The borehole shots and quarry blasts were timed by means of an uphole geophone (HS 10) and a single channel MARS recorder. Because of the very large signal strength of the first break the only error in the shot time is the 0.0025 sec. due to measurement. During the Peterborough experiment accurate uphole times were obtained for some of the shots by using an automatic blaster triggered by the MSF time code, or else by using a Nimbus recorder triggered by the Beethoven blaster. Where uphole times were not available they were calculated from the depth to the charge, the offset of the geophone from the hole and the near surface velocity. For a geophone 15 metres from the charge an error of 25% in the estimate of near surface velocity would cause a timing error of less than 0.002 sec.

### 2.6.2 Error assessment

When picking the first arrivals an estimate was made of the maximum range of arrival times within which the arrival could occur. It was assumed that the correct cycle was being picked and that any gross errors would be revealed by the reduced travel time plots. Repeated picking and measurement of selected events was carried out to check that all the travel times fell within the estimated maximum error.

As discussed above the observational error variance can

be calculated and used to find the solution F ratio. If the estimated maximum errors are used then, for L observations:

$$\sigma_e^2(\text{est}) = \sum_{\ell=1}^{L} \frac{(n_\ell \cdot em_\ell)}{L} \qquad (2.11)$$

Where $n_\ell$ is a uniformly distributed random number between -1.0 and +1.0 and $em_\ell$ is the estimated maximum error associated with the $\ell$ th. observation. The use of a random distribution between set limits is an oversimplification, the errors will probably have some form of skewed distribution but it is impossible to assess the shape of this distribution.

This value will not be as accurate as estimates of $\sigma_e^2$ obtained from equation (2.8) if the errors are not uniformly distributed within the estimated range. A systematic overestimate of em by a factor of 2 will cause $\sigma_e^2$ (est) to be overestimated by a factor of 4.

Such considerations give an indication of the limitations of the F ratio in assessing a time term solution.

# CHAPTER THREE

## A. COUNTESTHORPE SEISMIC REFRACTION PROFILE

### 3A.1 INTRODUCTION

The purpose of this experiment was twofold:

1. To invesigate the lateral extent of the dioritic intrusions seen in the Countesthorpe borehole and exposed in quarries around Croft, some seven kilometres to the west of Countesthorpe.

2. To develop the ability to carry out small scale (one to two kilometre) refraction profiles using a 12 channel "Nimbus" seismograph and the department's trailer mounted auger drill.

Figure 3.1 shows the surface geology together with the Bouguer gravity and aeromagnetic anomalies around the profile. As was discussed in chapter one the South Leicestershire Diorites are Caledonian in origin and have been described by Le Bas (1972,1981) as forming part of the "Leicestershire Pluton". The Countesthorpe Borehole proved a microtonalite at a depth of 193 metres. The aeromagnetic anomaly map suggests that the South Leicestershire intrusion is over 10 kilometres in diameter with the peak of the anomaly to the east of the exposed diorites.

The surface geology consisted of Lower Jurassic and Triassic sediments overlain by Boulder Clay; the strike of the Jurassic was approximately parallel to the seismic profile. As discussed in chapter 1 no formations older than

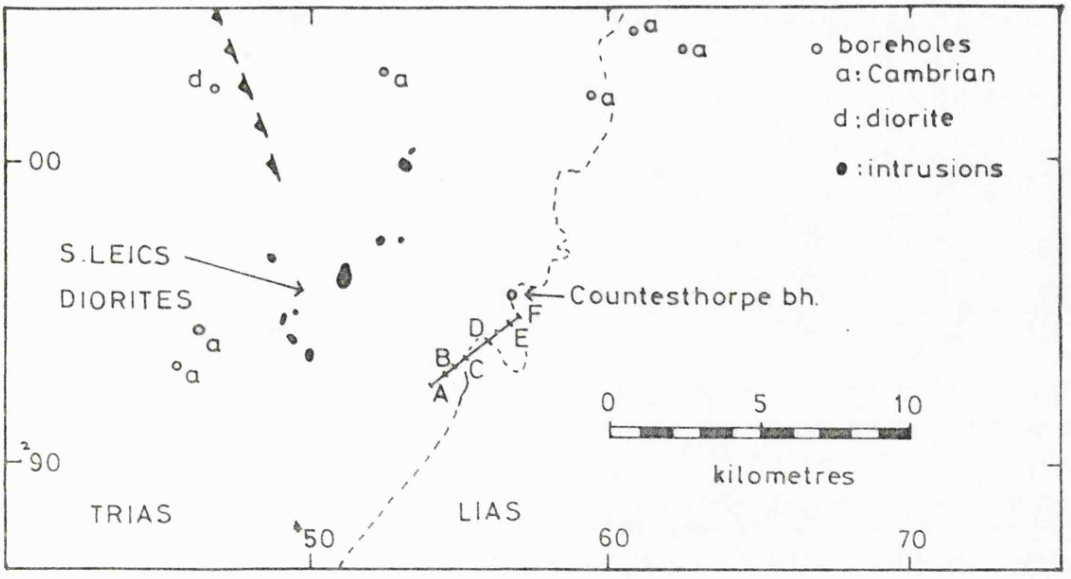


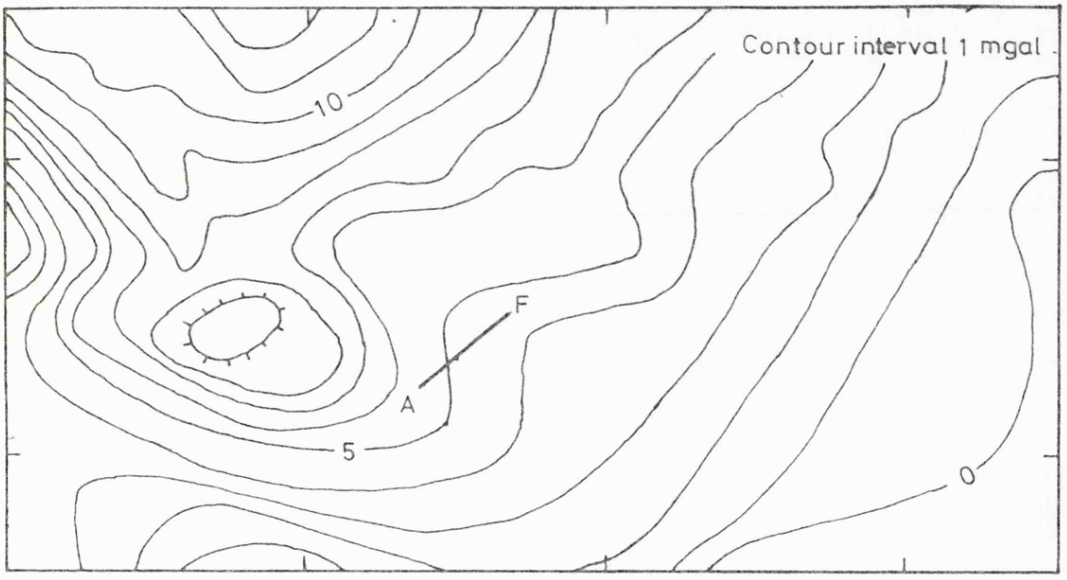


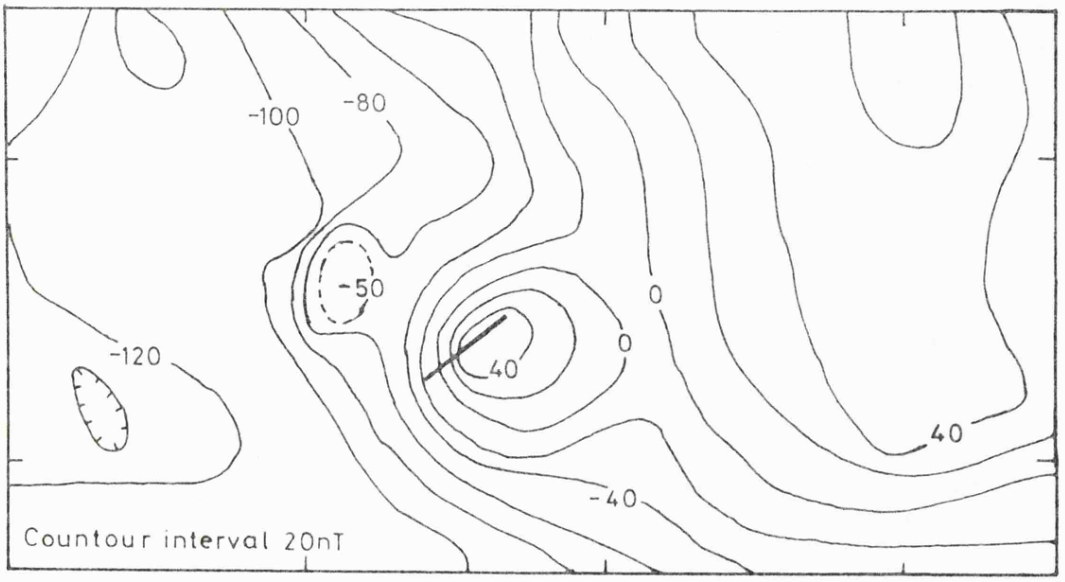


Figure 3.1 : Surface geology, gravity and aeromagnetic maps.
A-F are seismic shotpoints.

the Keuper are known to be in contact with the diorites but there is some evidence for the presence of Cambrian shales in contact with the diorites at Enderby. These shales are known, from NCB boreholes, to have a velocity of about 4.0 $km.s^{-1}$. It was therefore possible that such a refractor would be detected beneath the Keuper. Figure 3.1 also shows the location of the boreholes in the area which found shales of probable Cambrian to Tremadocian age.

## 3A.2 THE EXPERIMENT

The recording profile was located on a disused railway line that ran southwest from Countesthorpe across the margin of the aeromagnetic anomaly. Because of problems with access to the land the profile could not be extended far enough to the southwest to fully cross the margin of the magnetic anomaly. A further problem was caused by the M1 motorway, which bisected the railway line, so that the profile was recorded as two geophone spreads separated by about 900 metres.

In addition to the Nimbus recorder a Trio 12 channel seismograph belonging to Birmingham University was used. Geophone spacings were 40 metres for the Nimbus and 35 metres for the Trio enabling a total line length of 825 metres to be recorded at one time. A total of six shotpoints (A-F) was used with shotpoint A at the southwestern end of the line and shotpoint F at the northeastern end. Geophone spreads were laid out between B-C and D-E. Shots A1-F1 were fired into spread D-E and shots A2-D2,F2 into spread B-C. The positions of the shotpoints and recording spreads are

shown in figure 3.2, the maximum shot to geophone separations obtained were 3.215 kilometres into spread D-E and 2.855 kilometres into spread B-C.

3A.2.1 The data

The seismic records were recovered in the field as analogue traces on ultra-violet sensitive paper. The traces were replayed at speeds of 100 $cm.s^{-1}$ for the Trio recorder and 50 $cm.s^{-1}$ for the Nimbus. The signal to noise ratios were generally greater than three to one and the first arrival times could be picked with an accuracy of $\pm$ 0.002 seconds on most of the records and 0.004 seconds on the poorer quality data (S/N less than three). Low gain settings on the Nimbus record for shot F1 and the Trio records for B1 and F1 caused an attenuation of the first arrivals and tracing paper correlations had to be used to pick these arrivals.

No Nimbus records were recovered for shots A1 and F2 as the recorder failed to trigger. No shot instant mark was recorded for the Trio records for shots A1 and C1. A geophone position common to both recorders was used to calculate the travel times for shot C1 but the arrivals for shot A1 could only be used to determine the refractor velocity.

The problems with the triggering and shot instants were probably due to the large distances (two to three kilometres) between the shotpoints and the recording equipment and hence the impedance of the cable used to transmit the shot instant signal from the blaster. Subsequent modifications to the system eliminated this problem.

For a total of eleven shots into 46 recording positions

77% of the records were recovered with good quality data, 14% with weak or untimed arrivals and 9% were lost.

After calculation of the velocities, the travel times were corrected for the offset of the shotpoint from the reference points A-F, the greatest offset being 10 metres. This represents corrections of 0.003 and 0.002 seconds for refractions from layers 2 and 3 respectively (see below).

## 3A.3 INTERPRETATION

### 3A.3.1 Apparent velocities

All the first arrival data are shown on the time distance graphs in figure 3.2, the velocities of the various segments were determined by linear regression with the breaks chosen so as to maximize the correlation coefficients. Three layers can be distinguished by their apparent velocities.

LAYER 1: The velocity of this layer was measured from two or three arrivals at shotpoints B,C,D,E and varied from 0.95 to 1.93 $km.s^{-1}$. This variation was to be expected given that the ground along the profile varied from a seven metre high embankment to an eight metre deep cutting.

LAYER 2: Arrivals from this layer were recorded for the four on-end shots (D1,E1,B2,C2) and for F1. The apparent velocities varied from 3.21 to 3.61 $km.s^{-1}$ for these arrivals. Shots D1,E1,B2, indicated slighty lower velocities for arrivals within about 200 metres of the shotpoints. These apparent velocities ranged from 2.87 to 3.07 $km.s^{-1}$. Since the lower velocity arrivals were not reversed they were used with the other arrivals for this layer in the interpretations below. A simple horizontal layer interpretation for

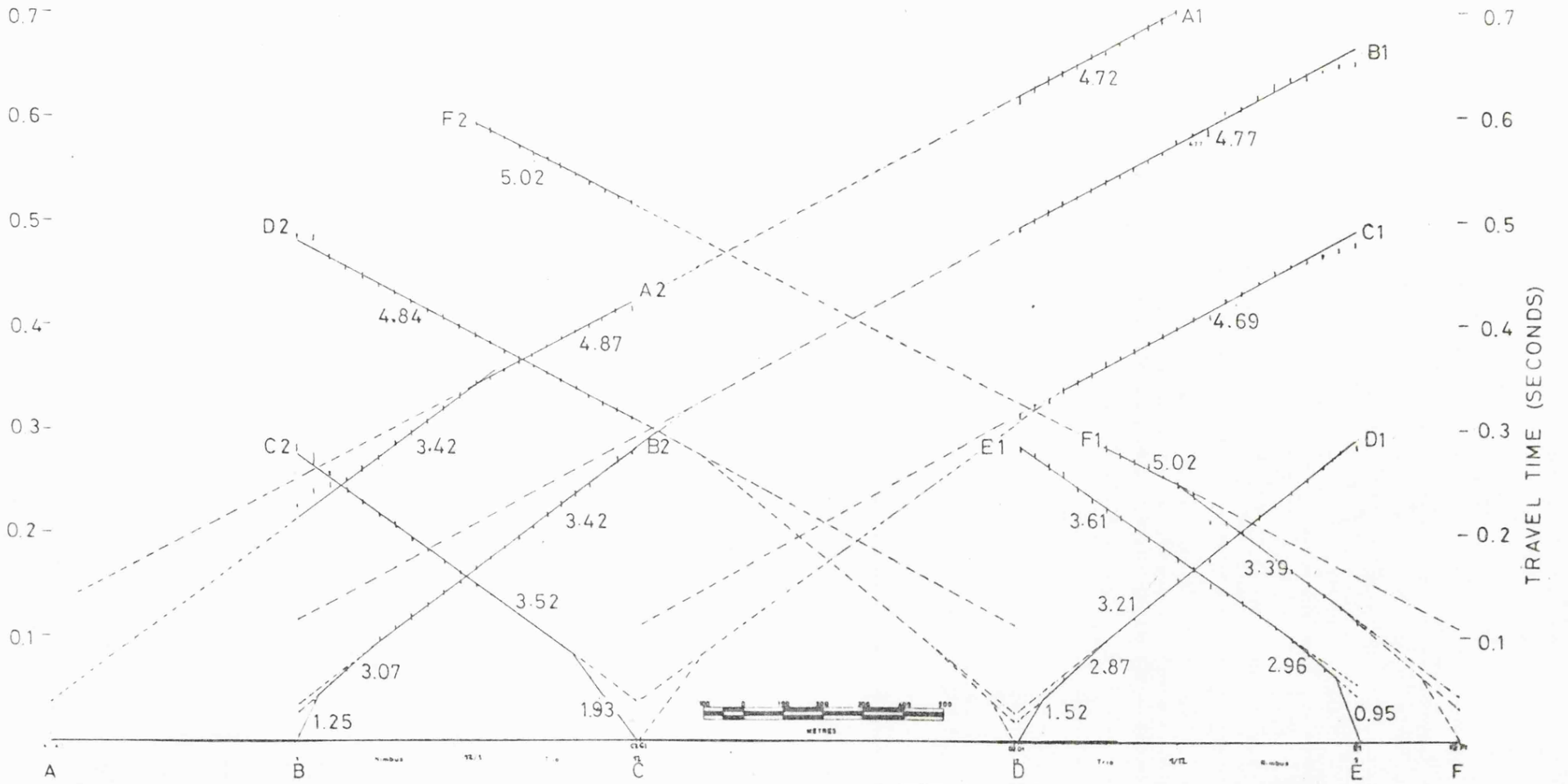


Figure 3.2 : Time-distance graph for the Countesthorpe survey.

the lower velocity segments indicated a thickness of about 20 metres for this layer.

Shots C2 and A2 indicated a localised low velocity zone in the vicinity of shotpoint B since the arrivals from both refractors were delayed by about 0.010 seconds.

LAYER 3: Arrivals from this layer had apparent velocities in the range 4.6 to 5.1 $km.s^{-1}$. Shots B1 and C1 indicated a marked increase in apparent velocity near shotpoint E. This section was not reversed but the velocities observed were too large (>8.0 $km.s^{-1}$) to be considered realistic and must have been due to refractor dip.

There was no indication of a 4.0 $km.s^{-1}$ layer, the detection limit for such a layer would be about 70 metres. If the Cambrian shales had a velocity of 3.5 $km.s^{-1}$, as observed in the Deanshanger borehole, they would not have been detected.

### 3A.3.2 Plus-minus interpretation

A plus-minus interpretation (Hagedoorn 1959) was applied to the refracted arrivals from layers 2 and 3. Delay times (TG) at each geophone location were calculated:

$$TG = 1/2(T+ - Tab)$$

where: T+ is the plus time

Tab is the end to end time

The end to end times for the various pairs of shots were determined from the t:x graphs. For the unreversed arrivals the delay times were extrapolated using the refractor velocity obtained from linear regression of the minus times.

For the arrivals refracted from layer 2 shots D1,E1

gave a velocity of 3.36 $km.s^{-1}$ whilst shots B2,C2 gave 3.47 $km.s^{-1}$. These velocities were determined from 17 and 15 reversed arrivals respectively.

For the arrivals refracted from layer 3 shots F1,C1 and shots A2,D2 both gave velocities of 4.90 $km.s^{-1}$. These velocities were determined from 5 and 12 reversed arrivals respectively. The velocity determinations are considered accurate to $\pm$ 0.2 $km.s^{-1}$.

In order to convert the delay times to depths an average velocity of 1.75 $km.s^{-1}$ was assumed for layer 1 and 3.4 $km.s^{-1}$ for layer 2. Figure 3.3 shows the depth cross-section. The thickness of layer 1 varies from 35 to 50 metres, this probably reflects near surface velocity changes as much as changes in thickness. The depth to layer 3 ranges from 210 to 280 metres, the northeastern end of the profile shows the refractor shallowing 50 metres in about 150 metres, an apparent dip of 18 degrees.

### 3A.3.3 Interpretation of velocities

The velocity of 3.4 $km.s^{-1}$ obtained for layer 2 is consistent with the interpretation of this layer as Triassic (Keuper) as indicated by the surface geology. National Coal Board borehole logs in the Melton Mowbray area give average interval velocities of 3.2 $km.s^{-1}$ for the Triassic (chapter 4).

The 4.9 $km.s^{-1}$ refractor velocity is similar to velocities obtained from refraction surveys over the buried northern extension of the Mountsorrel granodiorite (Whitcombe 1979) and the Croft tonalite (Khan, vide Whitcombe and Maguire 1981a).

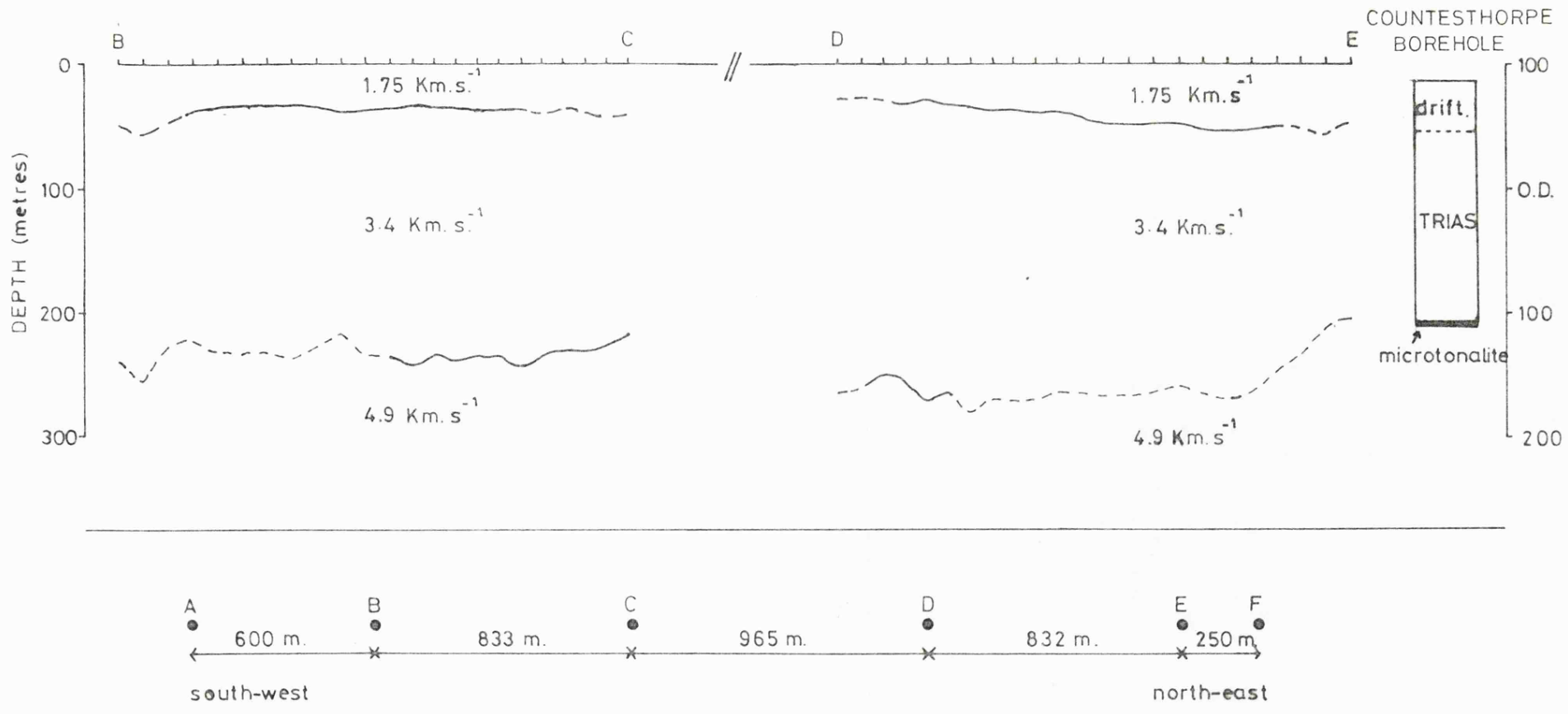


Figure 3.3 : Depth section and shotpoint plan.

### 3A.3.4 Countesthorpe borehole

The section in this borehole is described by Richardson (1931) and summarized in appendix 1A. The seismic interpretation shows a good agreement with the borehole.

| BOREHOLE | | SEISMIC LINE | | |
|---|---|---|---|---|
| Formation | Depth to base | Layer | Velocity | Depth to base |
| Drift | 26.5 | 1 | 1.75 | 20-30 |
| Trias | 193.0 | 2 | 3.4 | 220-270 |
| Microtonalite | | 3 | 4.9 | not seen |

The minimum depth to the basement refractor was observed at the northeastern end of the seismic line, 0.8 kilometres south of the borehole.

### 3A.3.5 An alternative interpretation

The lack of reversed cover for the basement refractor on spread D-E together with the weak F1 shot caused a slight problem in the interpretation. It was possible to pick the weak arrivals from F1 such that they had an apparent velocity of about 6.0 $km.s^{-1}$. When reversed against the well defined velocity of about 5.0 $km.s^{-1}$ from the A1,B1,C1 shots this indicated a refractor with a velocity of 5.5 $km.s^{-1}$ dipping from a depth of 200 metres at shotpoint D to 300 metres at shotpoint E. However on spread B-C the velocity of 5.0 $km.s^{-1}$ was well defined by shots D2 and F2 and therefore, to be compatible with the velocity on spread D-E, the refractor would have to dip in the opposite direction with depths of 300 metres at shotpoint C and 400 metres at B.

This interpretation of an anticlinal topography to the refractor did not agree with the observed depth in the

Countesthorpe borehole or the velocity measured at Croft quarry. However a margin to the intrusion near the southwestern end of the seismic line was suggested by the aeromagnetic data (figure 3.1). It was therefore decided to carry out a small gravity survey in an attempt to map the depth to the top surface of the intrusion.

## 3A.4 GRAVITY SURVEY

A simple 2 dimensional gravity model of the anticlinal structure described above (using a density contrast of 250 $kg.m^{-3}$ to represent diorite overlain by Trias) indicated an increase of 13 g.u. from shotpoint A to D and a decrease of 6 g.u. from D to F

The survey was carried out in two stages:

1. 34 stations at 50 metre intervals on the seismic line from shotpoint C to 250 metres southwest of shotpoint A. The purpose of this traverse was to check for dip on the basement refractor and to see if the edge of the intrusion could be detected.

2. 51 stations on road traverses in order to map the anomaly around the seismic lines and the borehole. (It was not possible to reoccupy the eastern section of the seismic line.

### 3A.4.1 Data reduction

For the purposes of drift and latitude corrections a site on the seismic line 400 metres southwest of shotpoint C was used as a base station (NGR 454.91 293.35)

Latitude corrections were calculated relative to the

base using the formula:

$$\Delta g_L = 8.12 \sin 2\phi \quad \text{g.u./km.}$$

where $\phi$ is the latitude (56.6 N)

The Bouguer corrections were calculated using a density of 2200 $kg.m^{-3}$ for the near surface deposits down to a datum of 75 metres above OD.

A terrain correction was calculated for the stations on the seismic line to remove the effects of the railway cutting and embankment. Measurements were made of the topography at various points along the traverse and these were used to construct two dimensional model sections perpendicular to the gravity traverse. The gravity effect of these models was then computed using a Talwani type gravity modelling program (chapter 7). This method was preferred to the use of Hammer charts because of the linear shape of the anomalous topography. No other terrain corrections were applied.

The calibration factor for gravity meter G16 was 1.05204 for the dial range 460000 to 470000. This factor was obtained from the IGS calibration line between Prees and Hatton Heath.

The accuracy of the drift corrected gravity readings was $\pm$ 0.2 g.u., elevations were determined to $\pm$ 0.05 metres and latitudes to $\pm$ 5 metres on the seismic line and $\pm$ 20 metres elsewhere.

### 3A.4.2 Interpretation

For a simple model of the diorite overlain by Triassic sediments the Bouguer anomalies shown in figure 3.4 should reflect the depth to the intrusion with the shallower depths

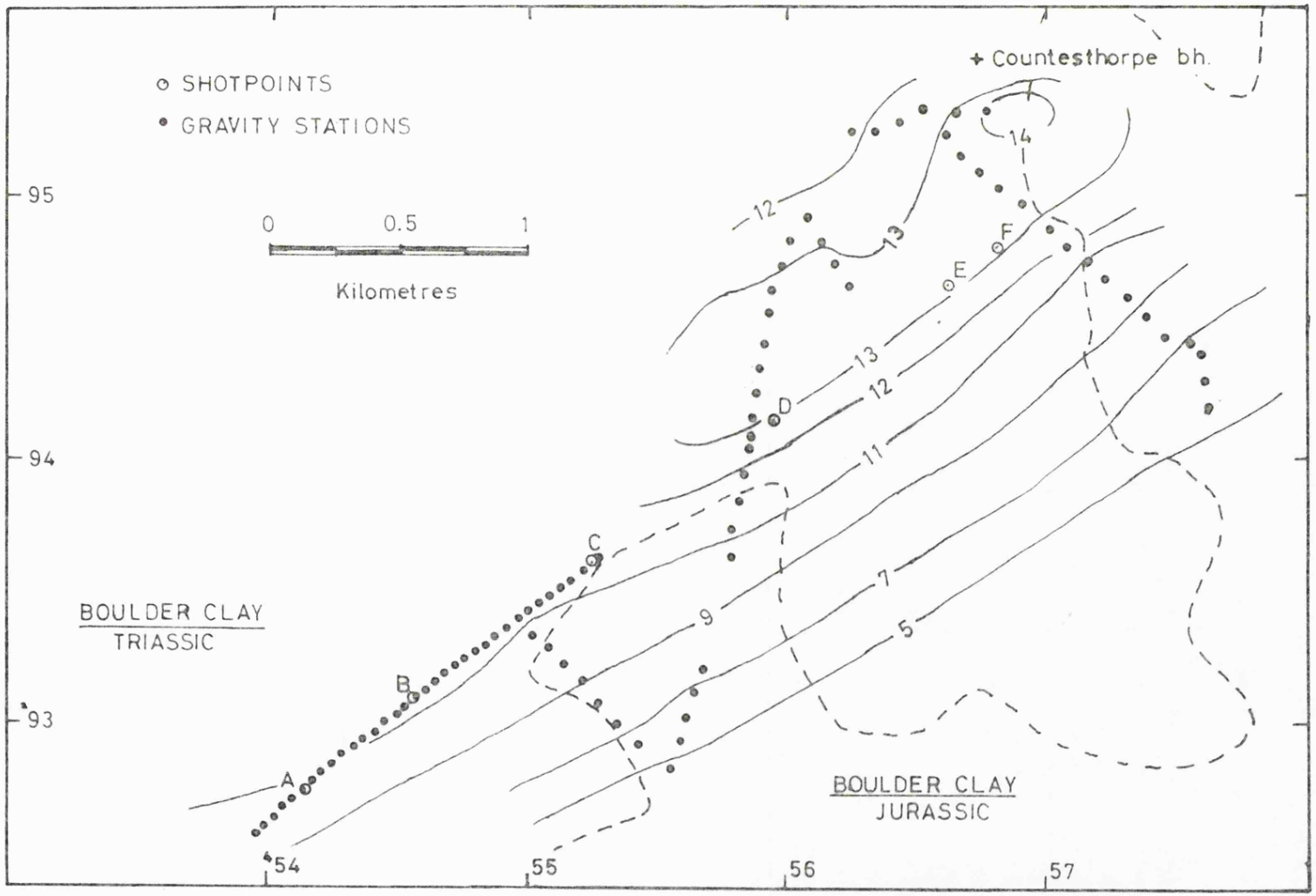


Figure 3.4 : Bouguer anomalies (in gu) for the Countesthorpe survey.

associated with the larger Bouguer anomalies. The Bouguer gravity is greatest to the north of shotpoints D,E and F and south of the borehole, this is consistent with the seismic interpretation in figure 3.3, which indicated a shallowing of the basement near shotpoint E. The gravity contours run almost parallel to the seismic line and this is consistent with the interpretation of a flat lying refractor. The map shows a decrease in Bouguer anomaly to the southeast, this is probably due to subcropping of the Lias which has a lower density than the Keuper.

Therefore there is no evidence from the gravity survey to support the anticlinal model.

## 3A.5 SUMMARY AND CONCLUSIONS

The seismic profile confirmed the presence of a large, flat topped, intrusion, at a depth of about 150 metres below OD; connecting the exposed diorites in the west with the Countesthorpe borehole in the east. The edge of the intrusion was not detected although the seismic line was located close to the southwest edge of the aeromagnetic anomaly. The basement velocity of about 5.0 $km.s^{-1}$ is consistent with the results of previous surveys over Caledonian intrusions in Leicestershire, and appears to confirm the velocity contrast between these rocks and typical Charnian type basement.

The intrusion was overlain by a refractor of velocity 3.4 $km.s^{-1}$ which, by analogy with the exposed diorites and the borehole, is interpreted as Triassic.

## 3B QUENBY SEISMIC REFRACTION SURVEY

### 3B.1 INTRODUCTION

Following the Melton Mowbray refraction experiment (chapter 5) a short seismic refraction profile was recorded on a disused railway line close to Quenby Hall (NGR 47Ø 3Ø6).

The purpose of this profile was to improve control on the near surface structure and velocity close to the Quenby shotpoint.

A southward extrapolation of the NCB seismic reflection and borehole data (see chapter 4) suggested a thickness of about 13Ø metres of Boulder Clay and Lower Jurassic overlying the Keuper. The crossover distance for basement refractions from the Quenby shotpoint was known, from the Melton refraction experiment, to be about two kilometres. This was too large a distance to be covered with the equipment available.

### 3B.2 THE EXPERIMENT

The recordings were made with a 12 channel Nimbus seismograph with single HSJ vertical geophones at 3Ø metre intervals. Two end to end spreads (B-C and C-D) were recorded giving a profile length of 66Ø metres. Shots were fired from a total of five shotpoints (A-E) located at either end of each spread and at 33Ø metres off-end in each direction.

As with the Countesthorpe survey the first arrivals were picked from the UV paper records. Because of the large charges used (table 3.1) the picking accuracy was generally ± Ø.ØØ1 seconds.

The time distance graph for the combined spread (figure 3.5) shows all the recorded data from the five shotpoints. Shotpoints C and E were not used for spread C-D due to a shortage of shotholes.

| SPREAD B-C | | | SPREAD C-D | | |
|---|---|---|---|---|---|
| SHOT | SIZE kg. | DEPTH m. | SHOT | SIZE kg. | DEPTH m. |
| A1 | 5.Ø | 12.2 | A2 | 4.Ø | 6.7 |
| B1 | 2.Ø | 6.Ø | B2 | 4.Ø | 6.Ø |
| C1 | 2.Ø | 6.2 | D2 | 2.Ø | 6.7 |
| D1 | 4.Ø,2.Ø | 6.7,5.8 | | | |
| E2 | 4.Ø | 6.2 | | | |

Table 3.1 Charge sizes and hole depths

## 3B.3 INTERPRETATION

Straight line segments were fitted to the time distance graphs by linear regression. This indicated the presence of three layers with velocities of 1.8 to 1.9, 2.45 to 2.76 and 3.Ø2 to 3.26 $km.s^{-1}$.

Having identified the arrivals from the two refractors a plus-minus interpretation (Hagedoorn 1959) was used on the reversed arrivals from each refractor in order to determine

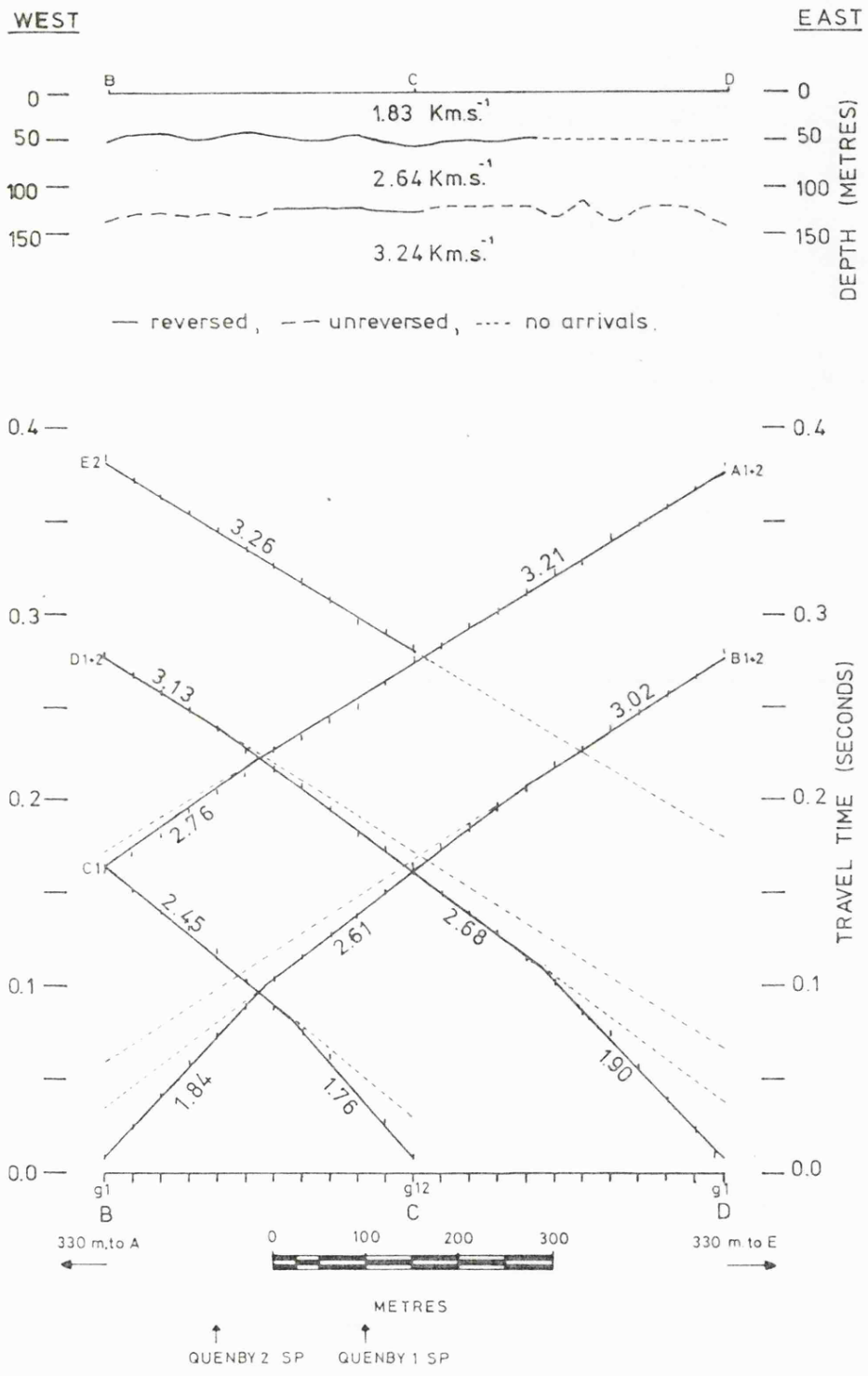


Figure 3.5 : Time-distance graphs and depth section for the Quenby Hall survey.

the refractor velocity and geophone delay times. Delay times were calculated for the unreversed arrivals by extrapolation from the reversed delay times, using the refractor velocity obtained from the minus times.

Linear regression of the minus times indicated velocities of 2.64 and 3.24 $km.s^{-1}$ for the two refractors. An average velocity of 1.83 $km.s^{-1}$ was taken for the surface layer in order to convert the delay times into depths.

The depth cross section (figure 3.5) shows that the first layer is 45 to 60 metres thick. This layer can be interpreted as Boulder Clay and weathered Lias shales. The second layer is about 70 metres thick; the velocity of 2.64 is 0.2 $km.s^{-1}$ higher than interval velocities for the Lias in NCB boreholes to the north (see chapter 4). Layer 2 is therefore interpreted as Lias shales. The velocity of layer 3, 3.24 $km.s^{-1}$, is the same as the borehole interval velocities for the Keuper.

## 3B.4 CONCLUSIONS

The near surface structure and velocities determined by the refraction profile agree with those predicted by extrapolation of the structure to the north. The velocity and depth imformation obtained will be used in the interpretation of the Melton Mowbray refraction profile (chapter 5).

# CHAPTER FOUR

# NATIONAL COAL BOARD SEISMIC REFLECTION LINES

## 4.1 INTRODUCTION

During exploration for, and subsequent evaluation of, the North East Leicestershire (Vale of Belvoir) Coalfield the NCB commissioned an extensive programme of seismic reflection lines followed up by a large number of boreholes. Some of these data were supplied by the NCB for interpretation in connection with the Melton Mowbray seismic refraction experiment (chapter 5). The purpose of the interpretation was twofold:

1: To assist with the interpretation of the refraction experiment by providing velocity and depth data for the sediments above the basement refractor.

2: To provide constraints on the basement structure, over a larger area than that covered by the refraction experiment, for subsequent modelling of the aeromagnetic data (chapter 8A).

The geology and structure of the area are described in chapter 1. Reflection data from this area have previously been interpreted by El-Nikhely (1980) who was primarily interested in the structure of the North East Leicestershire Coalfield and did not attempt to interpret the basement reflector.

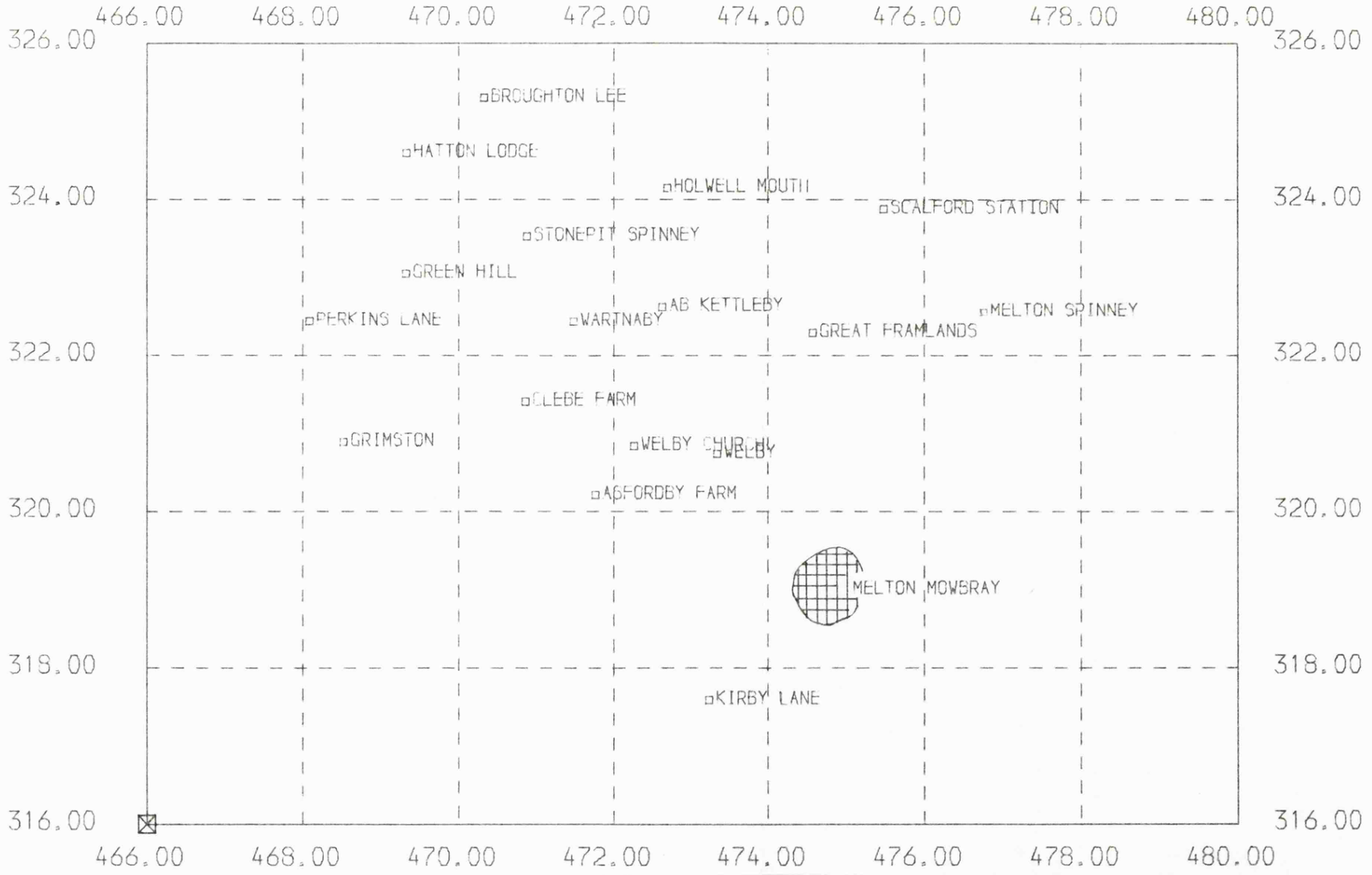


Figure 4.1 : North East Leicestershire borehole location map.

## 4.2 BOREHOLE DATA

### 4.2.1 Interval velocities

The boreholes drilled following the seismic survey (figure 4.1) were cored from the base Triassic to TD (usually in the Lower Coal Measures) and most were geophysically logged from the surface to TD.

The NCB made available lithological and integrated sonic logs for 18 boreholes in the survey area. These logs were used to determine the depth and two way travel time to various horizons in order to calculate interval velocities and to control the seismic interpretation. Table 4.1 is a compilation of the time and velocity data determined from the boreholes.

The interval velocities determined from the borehole sonic logs were measured with an accuracy of $\pm$ Ø.Ø5 km.s$^{-1}$. Details of the locations of the boreholes can be found in appendix 1.2.

Figure 4.2 shows a north-south cross section through some of the boreholes, together with the interval velocities measured for the various formations. The coal seams, because of their low velocities, are good marker horizons on the sonic logs and the section shows the subcropping of the northerly dipping Coal Measures beneath the Triassic unconformity.

Some of the boreholes drilled through a thickness of 1Ø to 3Ø metres of dolerite sills within the Coal Measures. The effect of these high velocity (4.5 to 5.5 km.s$^{-1}$) sills is included in the interval velocities for the Coal Measures given in table 4.1. For a borehole with 3Ø metres of sill in

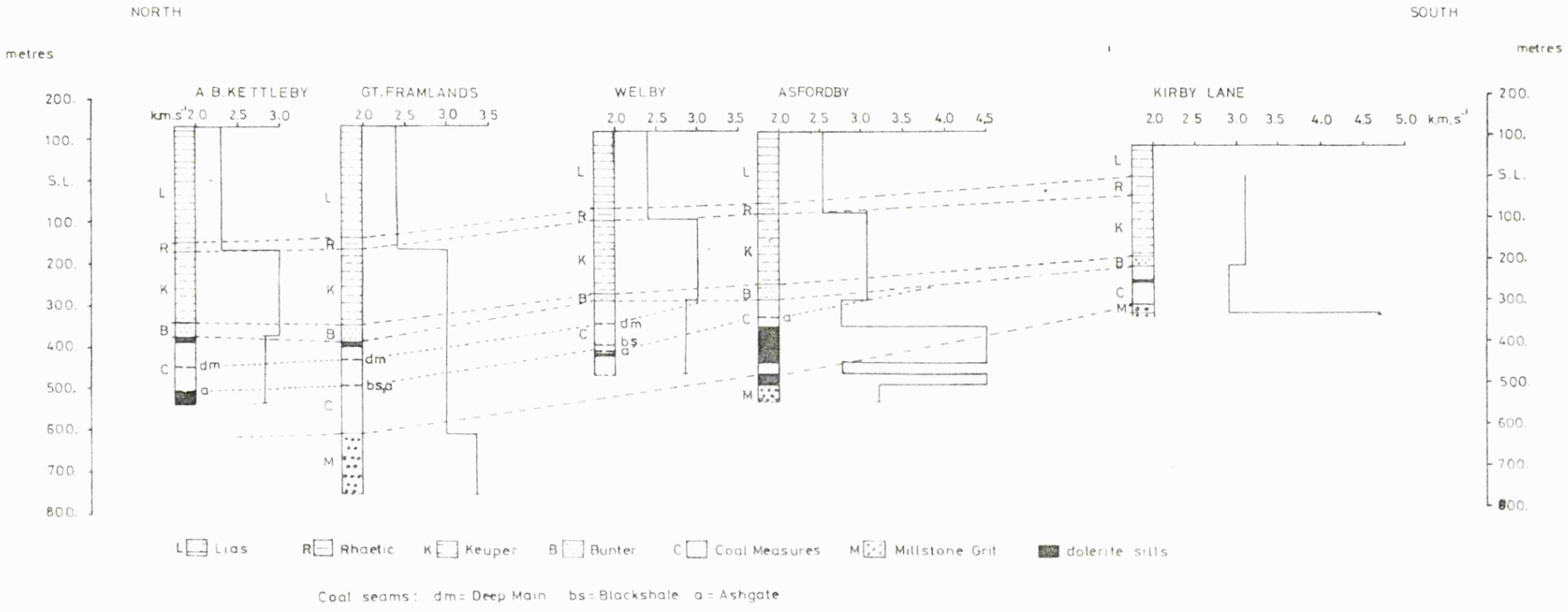


Figure 4.2 : Simplified lithologic and interval velocity logs.

| BOREHOLE | TWT(s) to TD | <------- velocity km.s$^{-1}$ -------> LIAS | TRIAS | C.MEAS | M.GRIT |
|---|---|---|---|---|---|
| 200 GRIMSTON | 0.339 | 2.39 | 3.08 | 2.73 | |
| 201 GREENNILLS | 0.364 | 2.46 | 3.28 | 2.96 | |
| 204 AB KETTLEBY | 0.359 | 2.45 | 3.23 | 2.89 | |
| 205 ASFORDBY | 0.350 | 2.52 | 3.13 | 3.30a | |
| 206 GLEBE FARM | 0.349 | 2.25 | 3.15 | 3.01 | |
| 207 GT FRAMLANDS | 0.495 | 2.57 | 3.28 | 3.01 | 3.26 |
| 210 WARTNABY | 0.353 | 2.33 | 3.12 | 2.82 | |
| 211 WELBY | 0.324 | 2.23 | 3.18 | 2.92 | |
| KIRBY LANE | 0.218b | | 3.04 | 2.90 | 3.07 |
| MEAN | | 2.41 | 3.18 | 2.92 | |
| S.D. | | 0.12 | 0.10 | 0.10 | |

Borehole numbers are used on the maps (figures 4.8 to 4.11)

Notes: a = velocity affected by sills

b = TWT to basement not TD

Table 4.1. Borehole interval velocities

a Coal Measures section of 200 metres (a typical thickness) the increase in velocity, relative to a borehole with no sills, would be about 0.1 $km.s^{-1}$.

The log for the Asfordby borehole indicates a total of 130 metres of dolerite which suggests that the borehole must have followed a dyke. The exact depth of the base of the Coal Measures in the Asfordby borehole is uncertain since the base of the dolerite is in contact with sediments of the Upper Namurian.

From the analysis of the borehole logs the following interval velocities were taken to be representative.

| | |
|---|---|
| Lias + Rhaetic | $2.4 \pm 0.2$ $km.s^{-1}$ |
| Keuper + Bunter | $3.2 \pm 0.2$ $km.s^{-1}$ |
| Coal Measures | $2.9 \pm 0.2$ $km.s^{-1}$ |
| Namurian | $3.2 \pm 0.2$ $km.s^{-1}$ |

The error limits given cover the range of values determined from the borehole logs. The velocity of the Lias and Rhaetic interval was measured from Ordnance Datum since the seismic lines were datumed to this level.

These interval velocities are the values that will be used in the conversion of the two way travel times, picked from the seismic sections, into depths.

The small variations in interval velocity between the different boreholes (table 4.1) can be accounted for by changes in the porosity and lithology of the various intervals.

### 4.2.2 Carboniferous thicknesses

The base Coal Measures horizon was not interpreted on the seismic sections and therefore it was necessary to

assume a thickness for the Coal Measures. The Kirby Lane and Great Framlands boreholes proved Coal Measures thicknesses of 94 and 223 metres respectively. The Widmerpool borehole, located 10 kilometres to the northwest of the survey area, proved 280 metres of Coal Measures and 730 metres of Namurian (Millstone Grit). At Long Clawson borehole, six kilometres north of Great Framlands, the Coal Measures thickness was 430 metres and the Millstone Grit 480 metres. It is probable, however, that the Carboniferous formations at Long Clawson have been thickened by dolerite intrusions (Lees and Taitt1946).

The seismic data did not extend north of the Great Framlands borehole and therefore the possibility that the Coal Measures thickens to the north of this borehole need not be considered. A thickness of 220 metres (equivalent to 0.150 seconds of two way time) was assumed for the Coal Measures for the area north of the east-west fault at grid line 320 (see below). To the south of this fault a thickness of 110 metres (0.075 seconds TWT) was assumed. The change in thickness was located at the fault since it represented a discontinuity in the data. As will be seen later it is possible that this fault was active during the infilling of the basin and did have some effect on sedimentation.

4.2.3 Synthetic seismograms

Velocity and density logs from the Glebe Farm borehole were processed for the NCB to produce an acoustic impedence (velocity x density) log and synthetic seismograms, these are shown in figure 4.3.

The Jurassic-Triassic boundary in the Glebe Farm

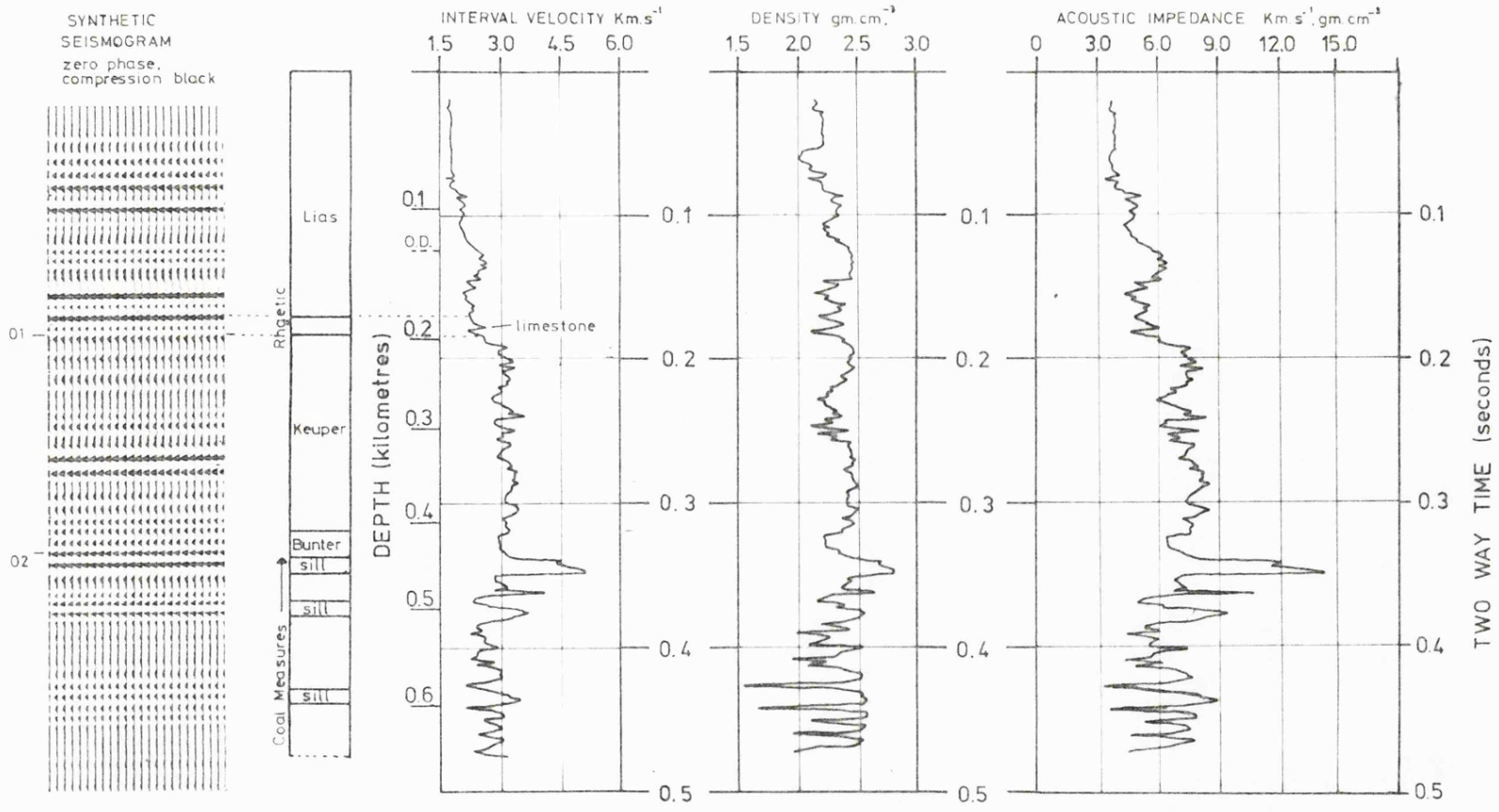


Figure 4.3 : Synthetic seismograms for the Glebe Farm borehole.

borehole is typical of most of the boreholes in the area in that it contains the sequence:

| | | |
|---|---|---|
| Lias shale | 2.4 $km.s^{-1}$ | |
| Limestone | 3.Ø-3.3 $km.s^{-1}$ | Ø.5-1.Ø metres thick |
| Shale | 2.5-2.6 $km.s^{-1}$ | 2.Ø-3.Ø metres thick |
| Keuper | 3.2 $km.s^{-1}$ | |

The thicknesses of these units are slightly exaggerated in the logs in figure 4.3.

The top of the Rhaetic limestone produces a strong compressive (black) pulse on the synthetic seismogram, as does the top of the Keuper (marked Ø1 on figure 4.3).

The base of the Triassic in this borehole is marked by a dolerite sill at the top of the Coal Measures. The sill appears on the synthetic seismogram by a compressive pulse (black) at the top and a raref~action at the base. As was shown above, and can be seen from the logs in figure 4.3, the Coal Measures have a lower velocity than the Triassic; therefore if the sill were not present the Triassic - Carboniferous boundary would be marked by a raref~action.

The interval velocity log shows that the interval velocities of the three principal formations (Lias, Trias, Coal Measures) do not increase with depth. The interval velocities for the Lias in all the boreholes were measured from Ordnance Datum and were therefore unaffected by the velocity decrease which occurs above this level.

## 4.3 THE SEISMIC REFLECTION DATA

The survey was carried out by Seismograph Services Ltd. and processed by Digital Technology Ltd. Recording and

RECORDING

| | |
|---|---|
| DATE | May/June 1975 |
| SOURCE | 1lb. (Ø.5 Kg.) dynamite at 3 metres |
| SHOT OFFSET | 3Ø metres off end |
| GROUP INTERVAL | 12 metres |
| GROUPS | 24 |
| GEOPHONE ARRAY | 12 at Ø.75 metres in line |
| RECORD TIME | 1 second |
| SAMPLE INTERVAL | 1 millisecond |
| FILTERS | LOW: out |
| | HIGH: 25Ø Hz. 72 db/octave |

PROCESSING SEQUENCE

1. BINARY GAIN RECOVERY
2. PRE FILTER 26-36 Hz. out
3. DATA DEPENDENT SCALING
4. DECONVOLUTION BEFORE STACK
5. STATIC CORRECTIONS
6. VELOCITY ANALYSIS
7. NMO CORRECTION
8. 12ØØ% CDP STACK
9. DECONVOLUTION AFTER STACK
10. TIME VARIANT BAND PASS FILTER
    - .1 8Ø-24Ø Hz. from Ø.ØØØ to Ø.15Ø seconds
    - .2 6Ø-22Ø Hz. from Ø.15Ø to Ø.3ØØ seconds
    - .3 45-2ØØ Hz. from Ø.3ØØ to Ø.45Ø seconds
    - .4 35-17Ø Hz. from Ø.45Ø to Ø.6ØØ seconds
    - .5 25-14Ø Hz. from Ø.6ØØ to 1.ØØØ seconds
11. DISPLAY positive numbers (compression) white
    vertical scale 3Ø mm = 1ØØ milliseconds
    horizontal scale 1:6ØØØ

UNMIGRATED

Table 4.2 Recording and processing parameters

processing details for the survey are given in table 4.2. The close spacing of the shotpoints and geophone groups, and the small sampling interval, reflect the requirement for high resolution at shallow depths that distinguishes coal exploration from oil exploration surveys. The shot depth of three metres is, however, very shallow and must have resulted in high frequency attenuation within the weathered layer.

The seismic reflection sections were reduced to Ordnance Datum during the static correction process, a 0.200 second bulk static was then added to preserve the shallow data. Elevations in the survey area were 100 to 150 metres above OD. Figure 4.4, which was produced by digitizing a 1:10000 shot point basemap, shows the distribution of the seismic lines.

The near surface geology in the survey area consisted of 10 to 20 metres of Boulder Clay and other Pleistocene deposits overlying Lias shales.

## 4.3.1 Interval velocities derived from stacking velocities

Stacking velocities can be converted into interval velocities using the Dix equation:

$$VI = \left( \frac{V_n^2 \cdot T_n - V_{n-1}^2 \cdot T_{n-1}}{T_n - T_{n-1}} \right)^{1/2}$$

where: VI is the Dix interval velocity, V is the stacking velocity and T is the two way time.
This relationship assumes that the stacking velocity is equivalent to the normal moveout velocity, an assumption

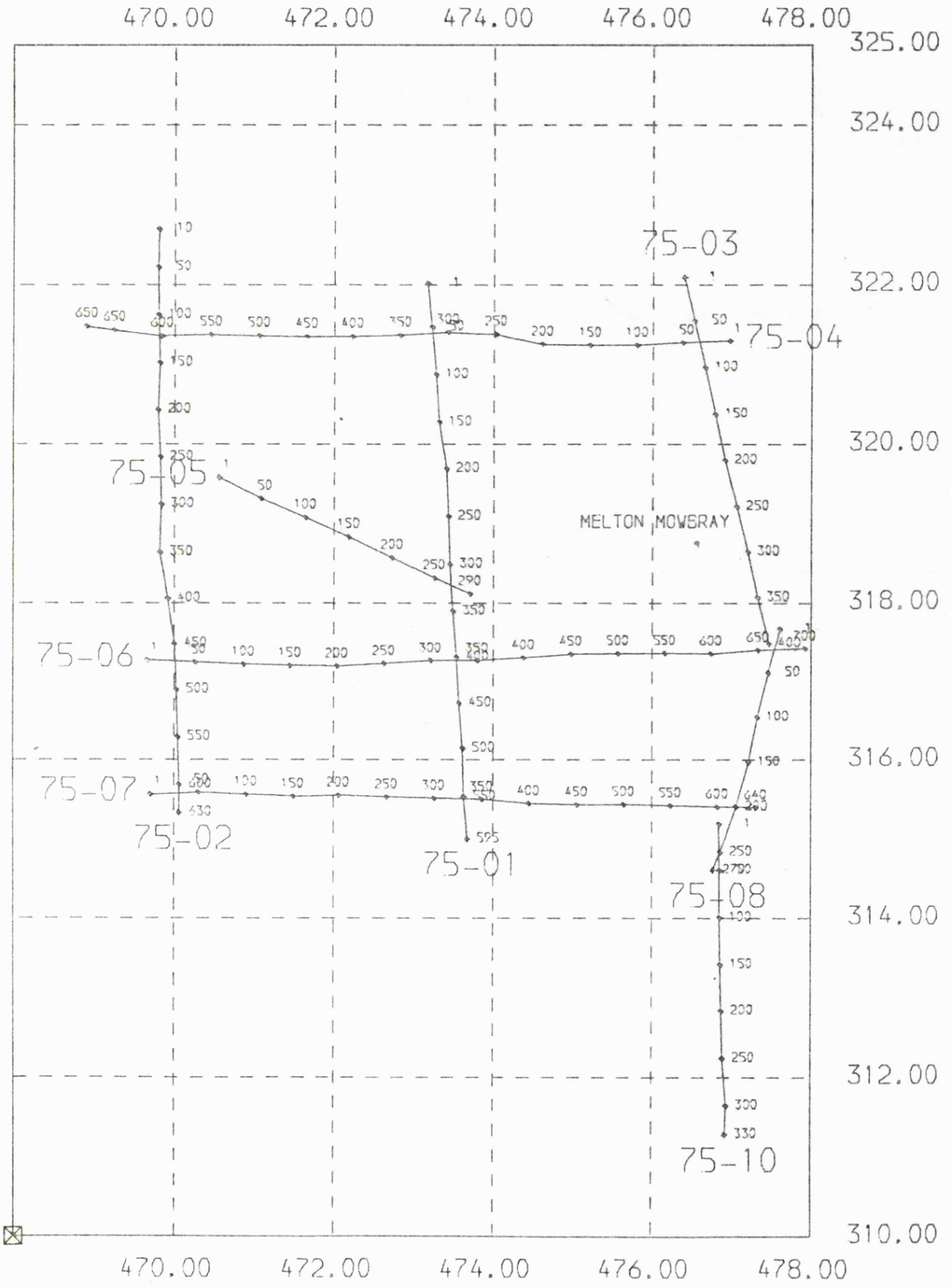


Figure 4.4 : Shotpoint basemap for the seismic survey.

which is only true for horizontal plane layering.

Figure 4.5 shows the interval velocities derived from some of the stacking velocities for line 75-Ø2, the three interpreted horizons, Ø1, Ø2, Ø3, are included for reference (the horizons are described below). The numerical data for the calculations are given in table 4.3.

To the south of SP 362, where the reflectors were relatively flat lying and parallel, there is a correlation between the breaks in the Dix interval velocities and the interpreted horizons. In particular low velocities (less than 4.Ø $km.s^{-1}$) are indicated down to the basement reflector.

To the north of SP 362 the northward dip of the reflectors results in a greater variation in Dix interval velocities and a lack of correlation with the interpreted horizons. The Ø3 horizon was not well defined on the northern part of the section. It can be seen from the interval velocity plots that a single velocity was applied to all the data below Ø.55 seconds two way time and this may explain the lack of good quality reflectors in this area.

## 4.4 SEISMIC INTERPRETATION

Following the analysis of the borehole data and an inspection of the seismic sections three horizons were selected for interpretation:

Ø1 Base Rhaetic-Top Keuper

Ø2 Base Triassic-Top Coal Measures

Ø3 "Basement" as seen in the Kiby Lane borehole

Horizon Ø1 was chosen as the base Rhaetic, rather than the

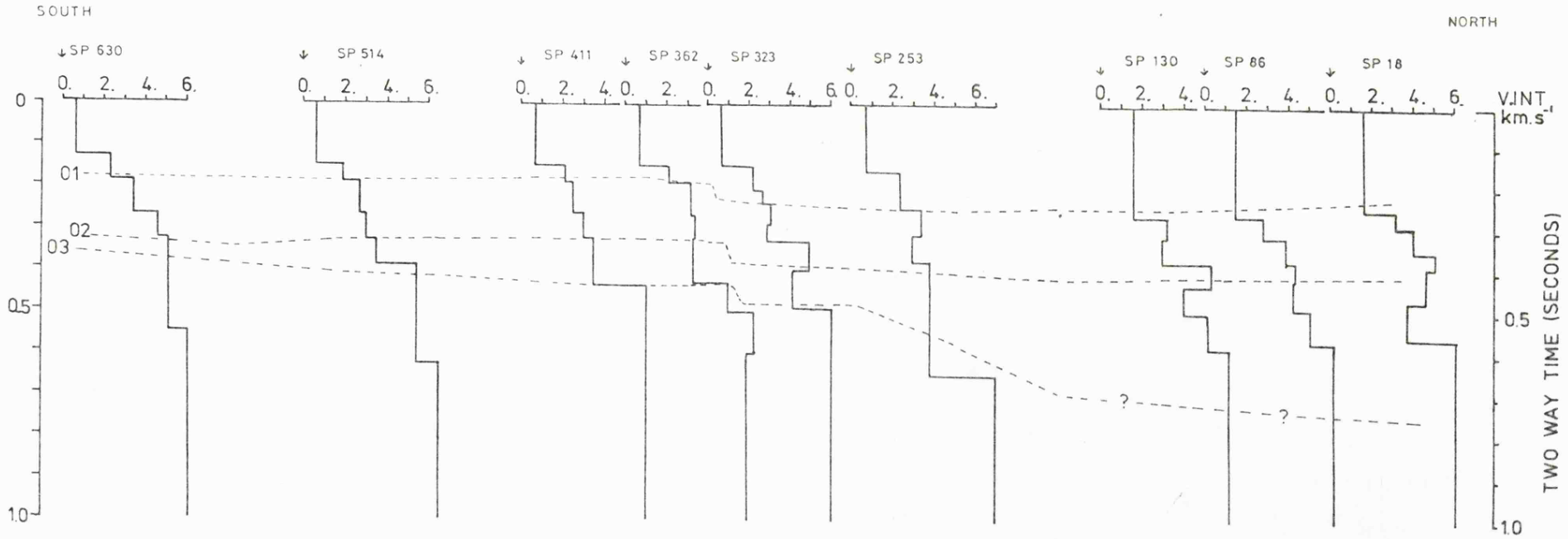


Figure 4.5 : Dix interval velocity plots for line 75-Ø2.

SHOT POINT 630

| HORIZON | TWT (S) | VNMO (M/S) | VINT (M/S) |
|---|---|---|---|
| 1 | 0.130 | 599.9 | 599.9 |
| 2 | 0.190 | 1399.7 | 2329.0 |
| 3 | 0.270 | 2199.5 | 3416.8 |
| 4 | 0.330 | 2799.3 | 4618.4 |
| 5 | 0.550 | 3899.0 | 5123.7 |
| 6 | 1.000 | 4998.8 | 6078.4 |

SHOT POINT 253

| HORIZON | TWT (S) | VNMO (M/S) | VINT (M/S) |
|---|---|---|---|
| 1 | 0.160 | 749.8 | 749.8 |
| 2 | 0.250 | 1549.6 | 2381.4 |
| 3 | 0.315 | 1999.5 | 3184.2 |
| 4 | 0.380 | 2199.5 | 2984.4 |
| 5 | 0.650 | 2999.3 | 3853.3 |
| 6 | 1.000 | 4798.8 | 7006.4 |

SHOT POINT 514

| HORIZON | TWT (S) | VNMO (M/S) | VINT (M/S) |
|---|---|---|---|
| 1 | 0.150 | 599.9 | 599.9 |
| 2 | 0.190 | 999.8 | 1843.5 |
| 3 | 0.270 | 1699.6 | 2715.7 |
| 4 | 0.330 | 1999.5 | 2998.4 |
| 5 | 0.390 | 2299.4 | 3518.4 |
| 6 | 0.625 | 3799.1 | 5441.6 |
| 7 | 1.000 | 4998.8 | 6525.3 |

SHOT POINT 130

| HORIZON | TWT (S) | VNMO (M/S) | VINT (M/S) |
|---|---|---|---|
| 1 | 0.265 | 1599.6 | 1599.6 |
| 2 | 0.320 | 1999.5 | 3306.5 |
| 3 | 0.380 | 2199.5 | 3052.1 |
| 4 | 0.435 | 2799.3 | 5343.5 |
| 5 | 0.500 | 2999.3 | 4093.3 |
| 6 | 0.585 | 3399.2 | 5158.1 |
| 7 | 1.000 | 4798.8 | 6261.3 |

SHOT POINT 411

| HORIZON | TWT (S) | VNMO (M/S) | VINT (M/S) |
|---|---|---|---|
| 1 | 0.150 | 799.8 | 799.8 |
| 2 | 0.190 | 1199.7 | 2106.6 |
| 3 | 0.265 | 1699.6 | 2561.3 |
| 4 | 0.325 | 1999.5 | 2983.0 |
| 5 | 0.440 | 2399.4 | 3275.5 |
| 6 | 0.590 | 3699.1 | 6077.3 |
| 7 | 1.000 | 4798.8 | 6039.6 |

SHOT POINT 86

| HORIZON | TWT (S) | VNMO (M/S) | VINT (M/S) |
|---|---|---|---|
| 1 | 0.265 | 1499.6 | 1499.6 |
| 2 | 0.315 | 1799.6 | 2912.5 |
| 3 | 0.375 | 2299.4 | 4005.6 |
| 4 | 0.420 | 2599.4 | 4359.0 |
| 5 | 0.490 | 2899.3 | 4278.0 |
| 6 | 0.570 | 3299.2 | 5105.6 |
| 7 | 1.000 | 4798.8 | 6255.1 |

SHOT POINT 362

| HORIZON | TWT (S) | VNMO (M/S) | VINT (M/S) |
|---|---|---|---|
| 1 | 0.150 | 799.8 | 799.8 |
| 2 | 0.190 | 1199.7 | 2106.6 |
| 3 | 0.270 | 1999.5 | 3174.1 |
| 4 | 0.325 | 2299.4 | 3408.4 |
| 5 | 0.430 | 2599.4 | 3362.2 |
| 6 | 0.500 | 3049.3 | 4990.8 |
| 7 | 0.600 | 3799.1 | 6333.1 |
| 8 | 1.000 | 4798.8 | 5993.5 |

SHOT POINT 18

| HORIZON | TWT (S) | VNMO (M/S) | VINT (M/S) |
|---|---|---|---|
| 1 | 0.250 | 1599.6 | 1599.6 |
| 2 | 0.290 | 1899.5 | 3188.7 |
| 3 | 0.350 | 2399.4 | 4017.9 |
| 4 | 0.390 | 2799.3 | 5101.7 |
| 5 | 0.470 | 3199.2 | 4682.9 |
| 6 | 0.560 | 3299.2 | 3778.6 |
| 7 | 1.000 | 4798.8 | 6203.6 |

SHOT POINT 323

| HORIZON | TWT (S) | VNMO (M/S) | VINT (M/S) |
|---|---|---|---|
| 1 | 0.150 | 649.8 | 649.8 |
| 2 | 0.210 | 1299.7 | 2203.7 |
| 3 | 0.240 | 1549.6 | 2717.8 |
| 4 | 0.290 | 1899.5 | 3066.2 |
| 5 | 0.360 | 2149.5 | 2968.6 |
| 6 | 0.400 | 2599.4 | 5097.5 |
| 7 | 0.490 | 2949.3 | 4162.6 |
| 8 | 1.000 | 4798.8 | 6066.1 |

Table 4.3 : Stacking (VNMO) and Dix interval velocities for line 75-02.

base Jurassic or the Rhaetic limestone, as the major change in interval velocity occurred at this point.

As discussed above, the base Triassic reflector was expected to vary in seismic character due to the presence of dolerite sills at the top of the Coal Measures.

The basement reflector was assumed to have a positive reflection coefficient on account of the higher velocity and density of the basement.

### 4.4.1 South from line 75-Ø6

Two of the lines (75-Ø1 and 75-Ø6) passed within Ø.3 kilometres of the Kirby Lane borehole and this was used as the starting point of the interpretation. The three horizons, together with a dolerite sill, were correlated with the borehole using the integrated sonic log. The reflectors were then carried around the grid of lines (figure 4.4) using line ties.

For the area to the south of line 75-Ø6 the spacing between line ties was two to three kilometres. In this area the three reflectors could be followed around closed loops in order to check that the correct cycle had been interpreted. The accuracy of the line ties in this area was about Ø.ØlØ seconds TWT.

HORIZON Ø1: The Jurassic strata down to this horizon were flat lying and easy to follow. The reflections had dominant frequencies of about 12Ø Hz. Surface features, such as roads, rivers and railways, caused a loss of subsurface cover which, at two way times equivalent to horizon Ø1, ammounted to about 2Ø% of the total line length. The gaps in cover were usually only 1ØØ to 2ØØ metres across and it was

possible to carry the reflector across such gaps (see figure 4.6).

HORIZON Ø2: The base Trias reflector had a short wavelength (1ØØ to 2ØØ metres) topography with an amplitude of 2Ø to 4Ø metres. The reflectors from the surface to horizon Ø2 were concordant. Figure 4.7 shows an example of the truncation of Coal Measures reflectors beneath the Triassic unconformity. Truncations such as this proved useful in the interpretation of horizon Ø2, especially over the northern part of the survey area.

HORIZON Ø3: In the area south from line 75-Ø6 the basement reflector was well defined, with the length of coherent reflections at least 5Ø% of the total line length. The horizon had a similar topography to horizon Ø2; in some areas the topography of the two reflectors was so similar that it must have been due to localised velocity changes above horizon Ø2.

On line 75-1Ø, to the south of SP 8Ø, the Triassic overstepped the Carboniferous to lie directly on the basement surface. The magnetic modelling in chapter 8A suggests that the basement in this area is not the top surface of the granite.

### 4.4.2 North of 75-Ø6

The area to the north of line 75-Ø6 was harder to interpret due to the greater spacing between the tie lines and the northward dip and downfaulting of the reflectors (see below).

The line ties for horizons Ø1 and Ø2 were accurate to better than ± Ø.Ø1Ø seconds TWT. Two boreholes provided

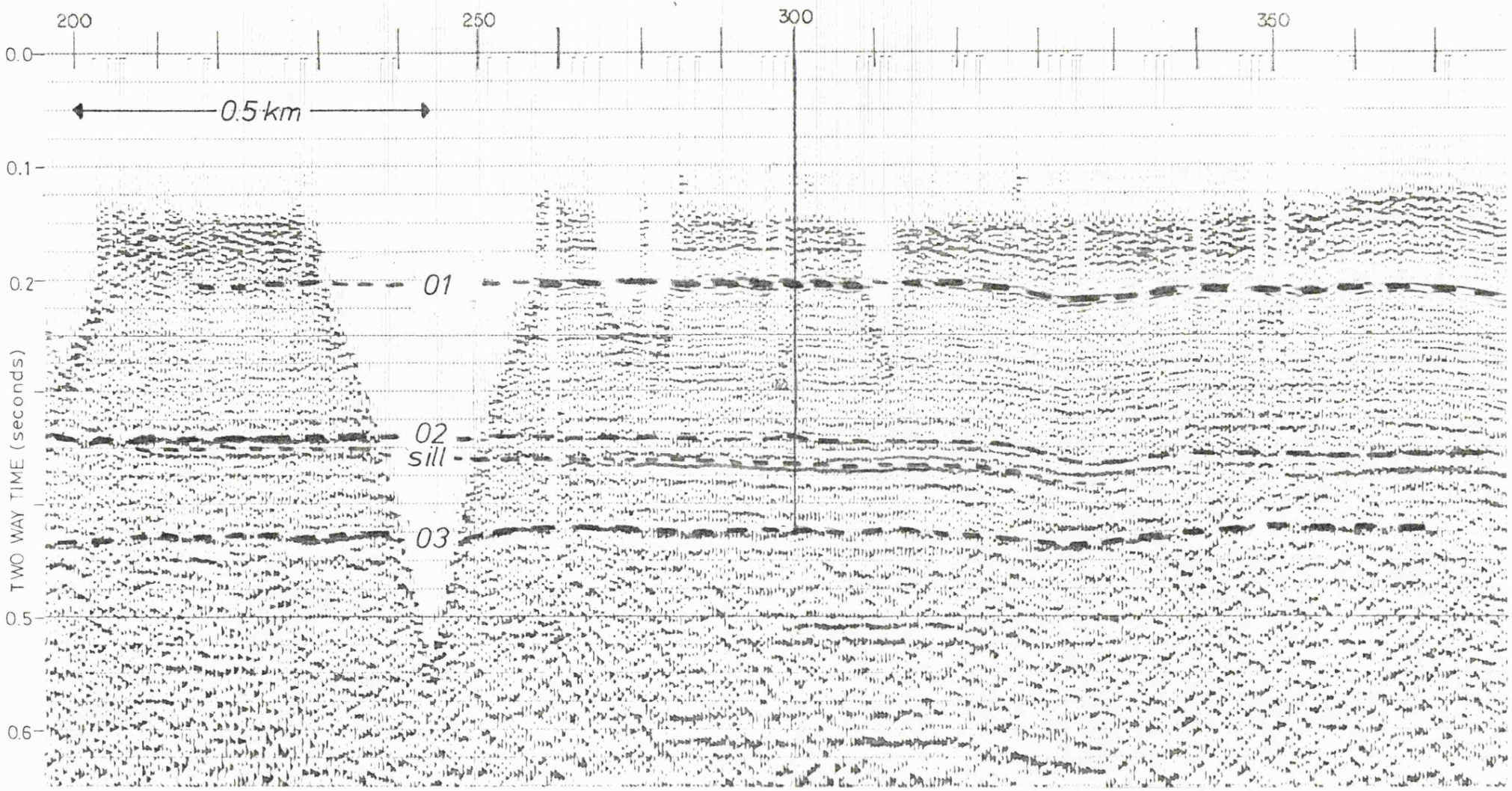


Figure 4.6 : Part of line 75-Ø6, compressions plotted as white.

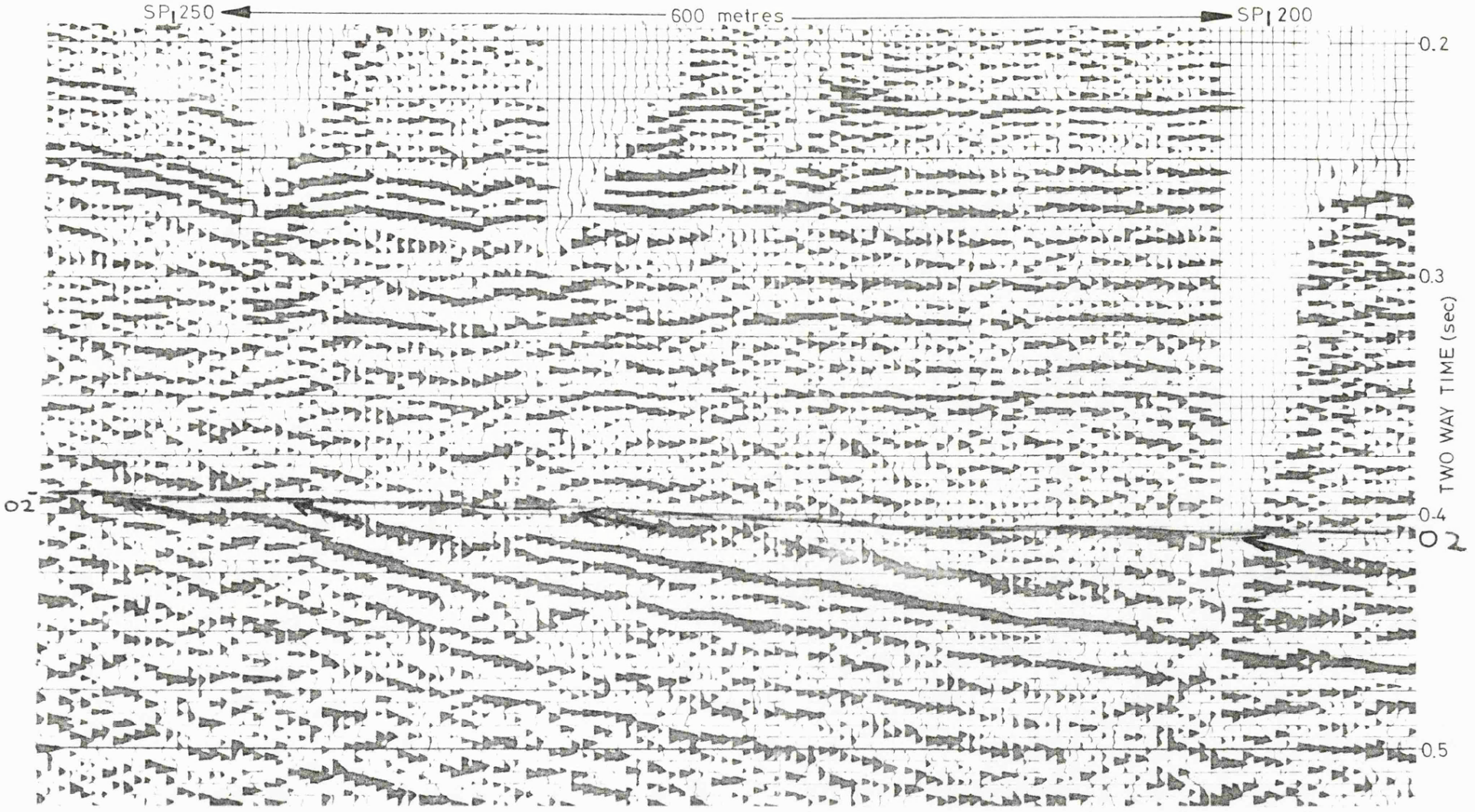


Figure 4.7 : Detail of line 75-Ø2 showing the subcrop of the Coal Measures.

control on horizons Ø1 and Ø2. The Glebe Farm borehole was adjacent to SP 52Ø on line 75-Ø4, the differences between the seismic interpretation and the travel times from the integrated sonic log were Ø.ØØ5 and Ø.Ø15 seconds TWT for horizons Ø1 and Ø2 respectively.

Line 75-Ø1 SP 11Ø was 15Ø metres west of the Welby borehole. The times to horizons Ø1 and Ø2 obtained from the borehole log were Ø.Ø64 and Ø.216 seconds TWT below OD respectively. The times from the seismic interpretation were Ø.Ø55 and Ø.2ØØ seconds below OD.

Small differences such as these can be accounted for by localised lithological variations. For example the Rhaetic in the Welby borehole was composed of eight metres of limestone. The prominent reflection would probably occur at the top of the limestone and not from the Keuper. The borehole log for Welby suggests that the basal 2Ø metres of the Bunter is a channel fill deposit with a sharp downward decrease in velocity, from 3.65 to 2.9 $km.s^{-1}$, across it's bottom surface. This change in velocity is similar to a normal Triassic - Coal Measures contact. It is possible that a channel cut into the unconformity surface would not have been resolved on the section; for a depth of 4ØØ metres and an average velocity of 2.8 $km.s^{-1}$ the first Fresnel zone of a 1ØØ Hz. wavelet would have a radius of 75 metres.

The interpretation of the basement reflector to the north of the faulting at grid line 32Ø. N was difficult due to a lack of borehole control and problems in correlating the reflector across the fault. Horizon Ø3 could not be tied between lines 75-Ø1 and 75-Ø2 because of poor data quality on the northern ends of these lines and on the tie line

(75-Ø4). This poor data quality is probably due to a combination of the small charges used and the way in which the events below Ø.5 seconds TWT were stacked.

## 4.5 FAULTING

The east-west faulting has been referred to above in connection with the choice of interval velocities and problems with the interpretation. Two faults can be traced across the survey area, both are normal faults downthrown to the north. The southern fault has a throw of 4Ø to 5Ø metres. To the west of line 75-Ø1 its trend swings south and it is probable that this fault is an extension of the Sileby fault which is mapped at the surface about 1Ø kilometres to the southwest of the survey area (see figure 5.1).

The northern fault is seen at the extreme ends of lines 75-Ø1 and 75-Ø3, the throw cannot be reliably estimated due to the lack of data on the downthrown side. The Wartnaby borehole intersected a fault in the Keuper at 2ØØ metres below OD. The throw on this fault was estimated, from the thinning of the Keuper, at about 5Ø metres.

Both the faults displace the Lias and therefore are post Lower Jurassic in age. The correlation between the southern fault and the rapid deepening of horizon Ø3 (figure 4.11) suggests that the faults were reactivated along the line of the southern boundary faults of the Widmerepool Gulf.

Arab (1972) modelled gravity data from the Widmerepool Gulf, this modelling suggested a step faulted southern

margin to the basin with throws of about Ø.5 kilometres.

## 4.6 STRUCTURE AND ISOPACH MAPS

In order to prepare these maps (figures 4.8 to 4.11) the three interpreted horizons were picked at intervals of 5Ø shotpoints (Ø.6 kilometres) with extra picks at faults and line ties. This interval was sufficiently coarse to smooth out any small scale structure on the reflectors and small enough to preserve the general trends, which was the purpose of the interpretation. The measurement accuracy was ± Ø.ØØ5 seconds TWT. The two way times were converted to depths using the velocities discussed above.

In figures 4.8 to 4.11 the numbers 2ØØ to 217 represent boreholes (see table 4.1), the sites marked A1-7 and B37-53 are refraction recording sites (see chapter 5).

HORIZON Ø1: The structure map for the base Rhaetic (figure 4.8) shows a one degree dip to the southeast for the Jurassic. To the north of the southern fault no dip direction is recognisable, the general trend is a northward increase in depth which probably reflects a greater degree of subsidence due to compaction within the basin.

HORIZON Ø2: The isopach map for the Ø1-Ø2 interval (figure 4.9) shows that this interval is typically about 25Ø metres thick. The variations in thickness are not related to the faulting.

HORIZON Ø3: The calculated Carboniferous sediment thickness (figure 4.1Ø) and the basement structure map (figure 4.11) show the thinning of the Carboniferous to the

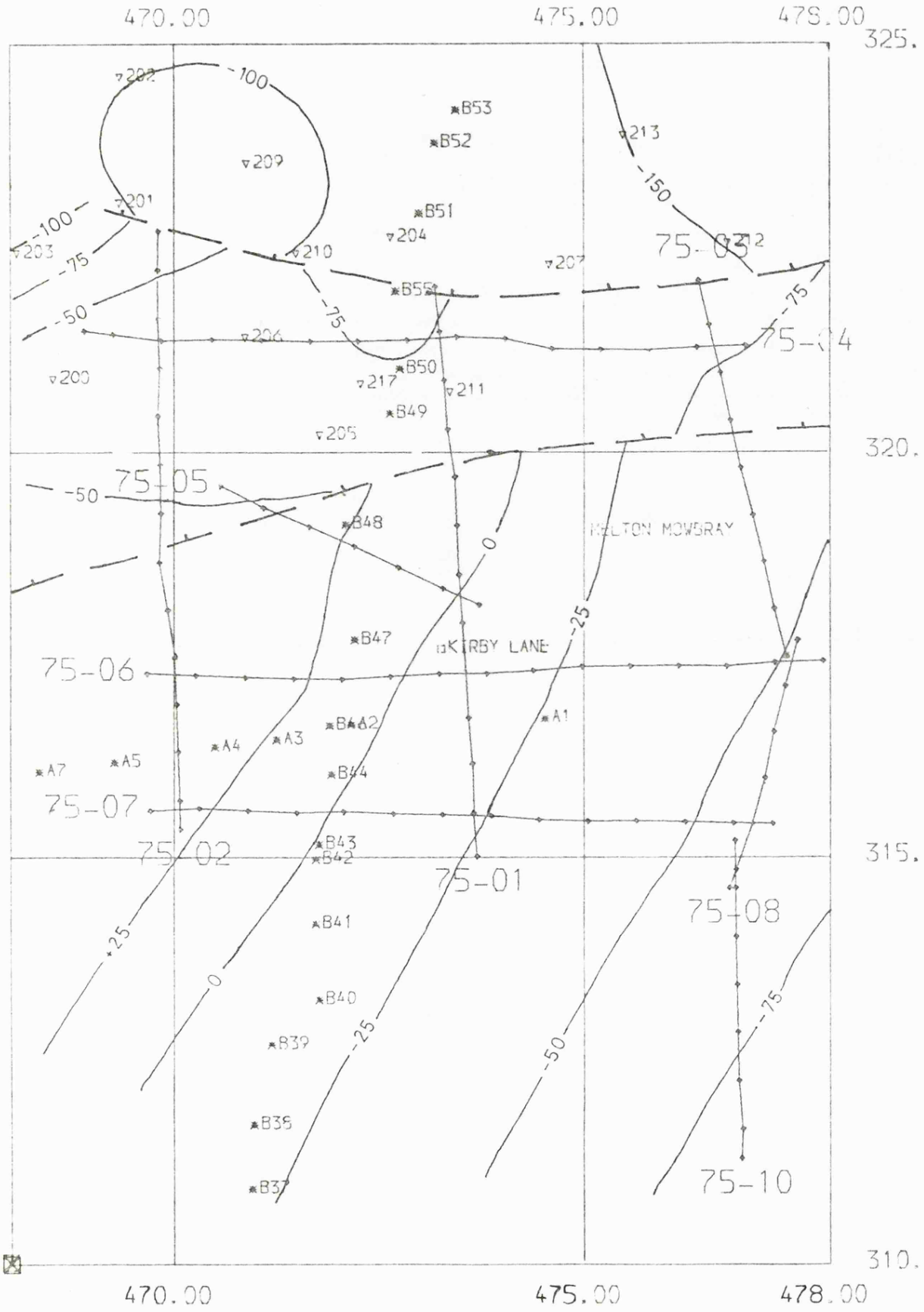


Figure 4.8 : Base Rhaetic structure map in metres above OD.

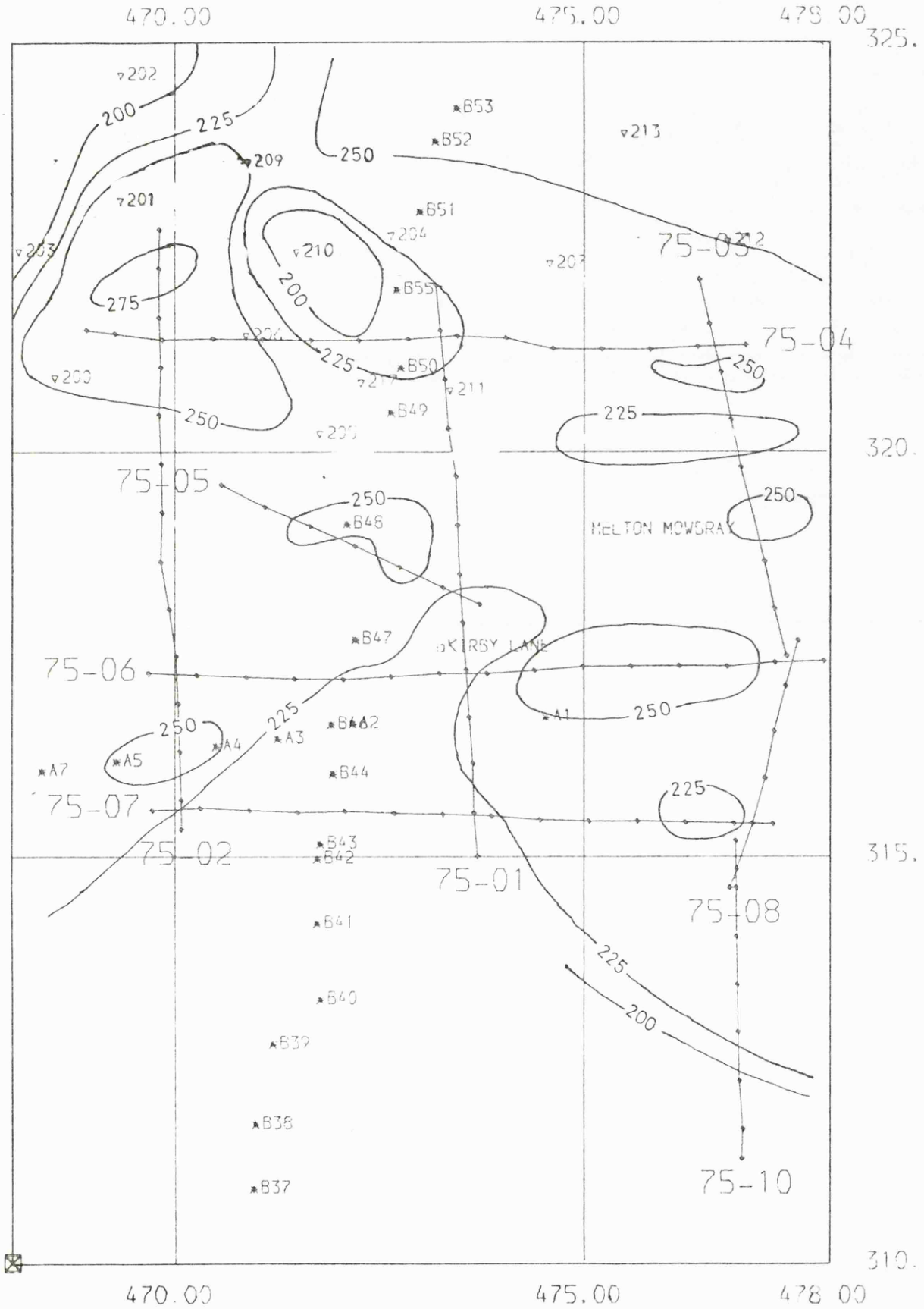


Figure 4.9 : Isopach in metres for horizons Ø1-Ø2.

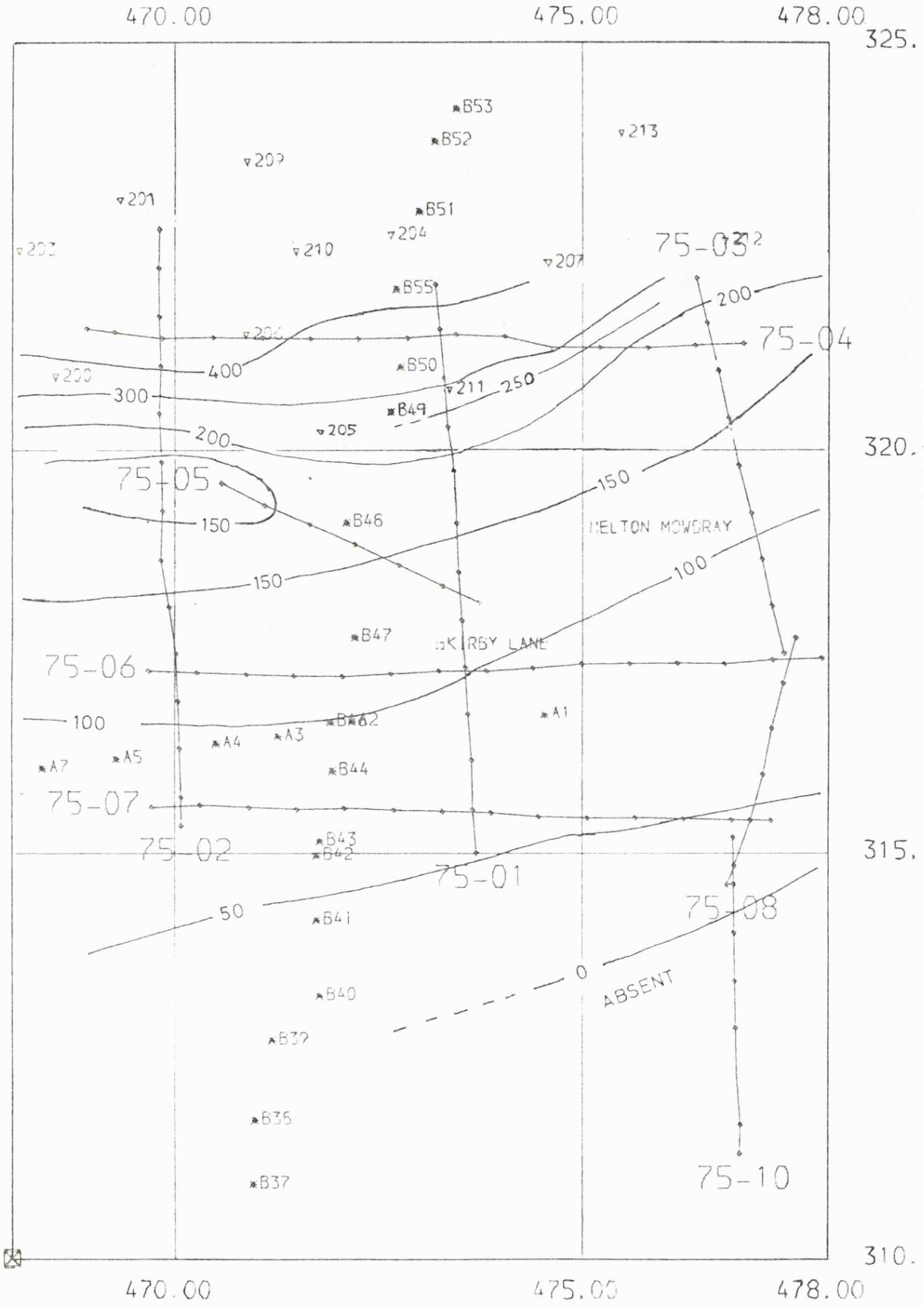


Figure 4.10 : Isopach in metres for horizons 02-03.

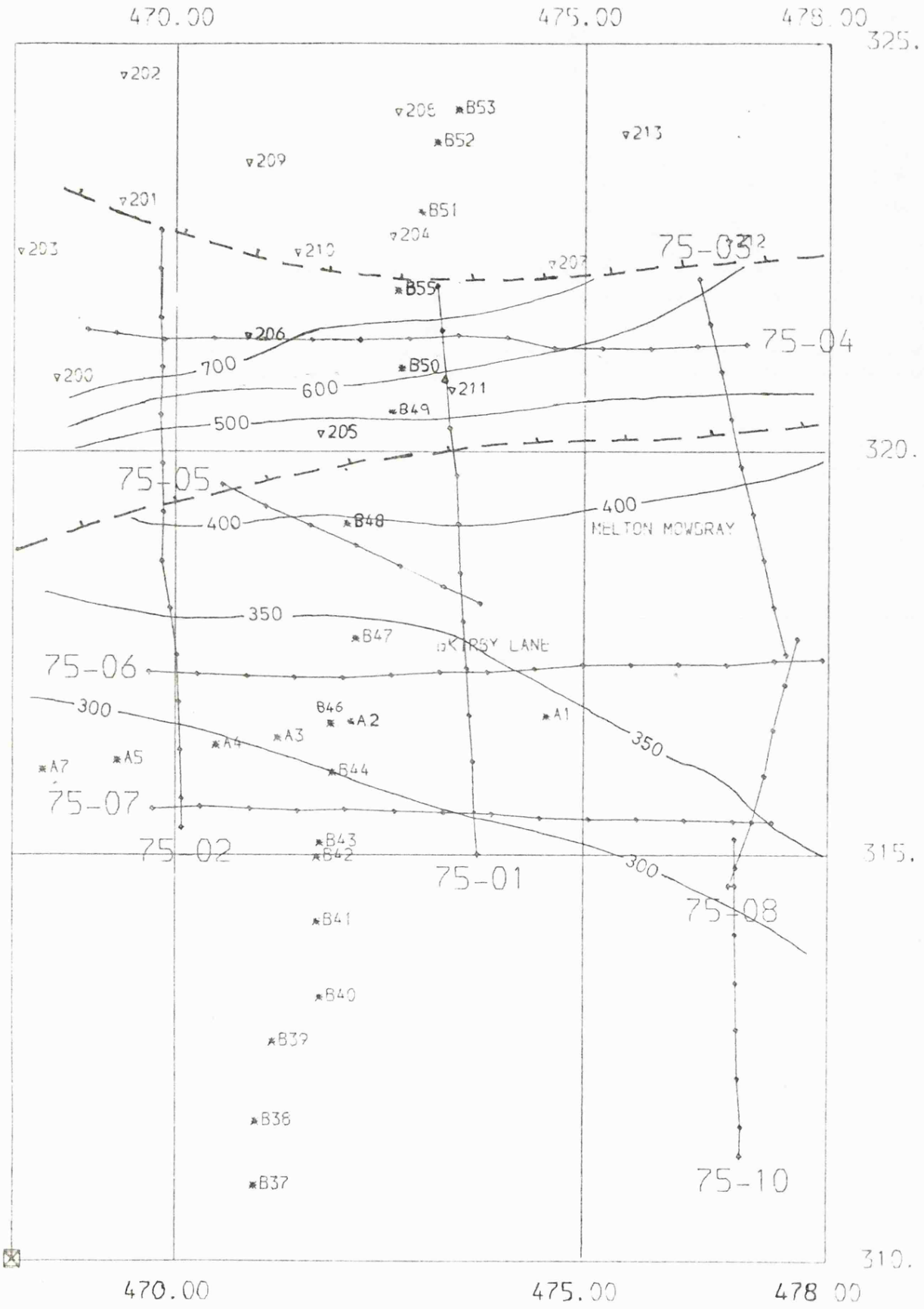


Figure 4.11 : Structure map for horizon Ø3 in metres below OD.

south where it onlaps the basement high. The thickness increases more rapidly to the north of the southern, post Lower Jurassic, fault which suggests that the basin was subsiding along a similar trend. The maximum thickness for the Ø1-Ø2 interval in the survey area is about 4ØØ metres. The Long Clawson borehole indicated 87Ø metres of Coal Measures and Millstone Grit overlying Carboniferous Limestone. This large thickness of Carboniferous sediments so close to the survey area casts doubt on the Ø3 reflector being basement in the area to the north of the southern fault. By analogy with the gravity and seismic work of Arab (1972) it is possible that the Ø3 reflector in this area is the top of the Carboniferous Limestone and the basement is downfaulted by Ø.5 kilometres or more.

The minimum depth to horizon Ø3 occurs to the southwest of the Kirby Lane borehole, as will be seen in later chapters this is the location of the peak of the aero-magnetic anomaly.

## 4.7 SUMMARY AND CONCLUSIONS

Three horizons, the base Rhaetic, base Triassic and basement (or top Carboniferous Limestone) have been interpreted to show the structure of the southern margin of the Widmerpool Gulf and the structure of the (granitic) basement around the Kirby Lane borehole.

The accuracy of the depth and thickness determinations is about $\pm$ 25 metres for the Jurassic, the Triassic and for the basement in the southern part of the survey area. This is adequate given the uses that are to be made of the

interpretations.

The thickness of the Jurassic and Triassic sediments will be used in the analysis of the seismic refraction time terms in the following chapter.

The estimates of basement depth will be used to constrain the modelling of the Melton aeromagnetic anomaly (chapter 8A). As will be seen in chapter 8A, the lines on the eastern part of the survey area have probably crossed the eastern margin of the Melton intrusion. It was not possible to detect any intra-basement structures, or changes in seismic character, on the seismic lines to support the magnetic modelling of the position of the margins.

The two faults which displace horizons Ø1 and Ø2 have small throws (< 5Ø metres) but may represent a post Lower Jurassic reactivation of the southern boundary faults of the Widmerpool Gulf, as suggested by the thickening of the Carboniferous across the southern fault. The faults may also indicate the northern margin of the granitic intrusion.

The nature of the Ø3 ("basement") reflector to the north of the southern fault is uncertain but may be resolved by the magnetic modelling (see chapter 8A).

# CHAPTER FIVE

# MELTON MOWBRAY SEISMIC REFRACTION PROFILES

## 5.1 INTRODUCTION

This seismic refraction experiment was the fourth in a series of profiles designed to map the Precambrian basement refractor surrounding the Charnian Inlier, and to investigate the relationship of this basement to the Caledonian igneous intrusions exposed in Leicestershire.

The three previous profiles are described in Whitcombe (1979) and Whitcombe and Maguire (1981a,b).

### 5.1.1 Geological setting of the experiment

The Kirby Lane borehole (figure 5.1) proved a biotite granite at a depth of 400 metres. As described in chapter 1 the geochemistry of this rock indicated that it was related to the Caledonian igneous intrusions of Mountsorrel and South Leicestershire.

The surface geology of the survey area (figure 5.1) consists of Lias shales and Keuper marls. The latter lie unconformably on the Charnian, and on the igneous intrusions. Pleistocene deposits, mostly Boulder Clay, are widespread but are usually less than 10-20 metres thick. The Sileby (Wreake Valley) fault is post-Jurassic in age. An eastward continuation of this fault is observed on NCB seismic reflection lines (chapter 4). To the west the fault can be traced at the surface into the Soar Valley where it appears

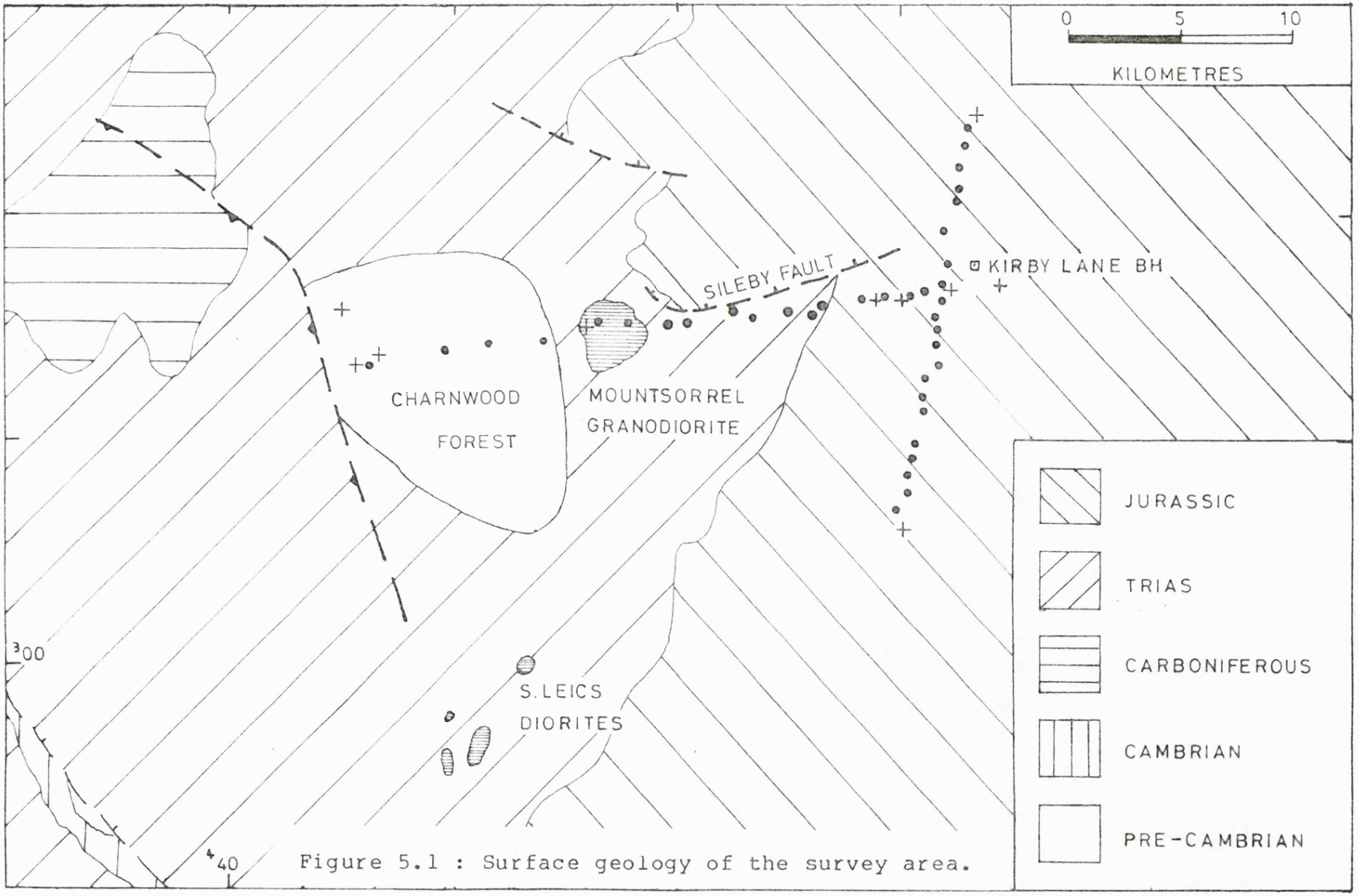


Figure 5.1 : Surface geology of the survey area.

to swing to the north (IGS sheet 142).

To the south of Mountsorrel and Melton Mowbray several boreholes prove Lower Palaeozoic or Precambrian basement at 100 to 300 metres below OD. To the north and northwest of Melton is the thick Carboniferous succession of the Widmerpool Gulf (chapters 1 and 9).

5.1.2 Geophysical background

The aeromagnetic map of the area (figure 5.2) shows the large (200-250 nT) positive anomalies associated with the Melton intrusion (A) and with the presumed northern extension (B) of the Mountsorrel granodiorite. The Melton and Mountsorrel intrusions lie in a belt of aeromagnetic anomalies that runs northwest to southeast, from north of Charnwood Forest to East Anglia (see chapter 7).

There is no discernable gravity anomaly associated with the Melton or Mountsorrel intrusions. The densities tabulated in chapter 7 suggest that the Mountsorrel granodiorite should have a lower density (c.2650 $kg.m^{-3}$) than typical Charnian rocks (c.2700-2750 $kg.m^{-3}$). However the large sedimentary thickness in the Widmerpool Gulf causes a large (100 gu.) negative gravity anomaly and this may be masking any anomaly due to the intrusions. Arab (1972) produced a gravity model for the margin of the Widmerpool Gulf to the northwest of Melton Mowbray. The model indicated a two kilometre downfaulting of the basement across the margin of the Gulf. The problem of gravity anomalies and the Leicestershire intrusions is discussed further in chapter 7.

The previous seismic work in the area has been described in chapter 1. The most useful information in the

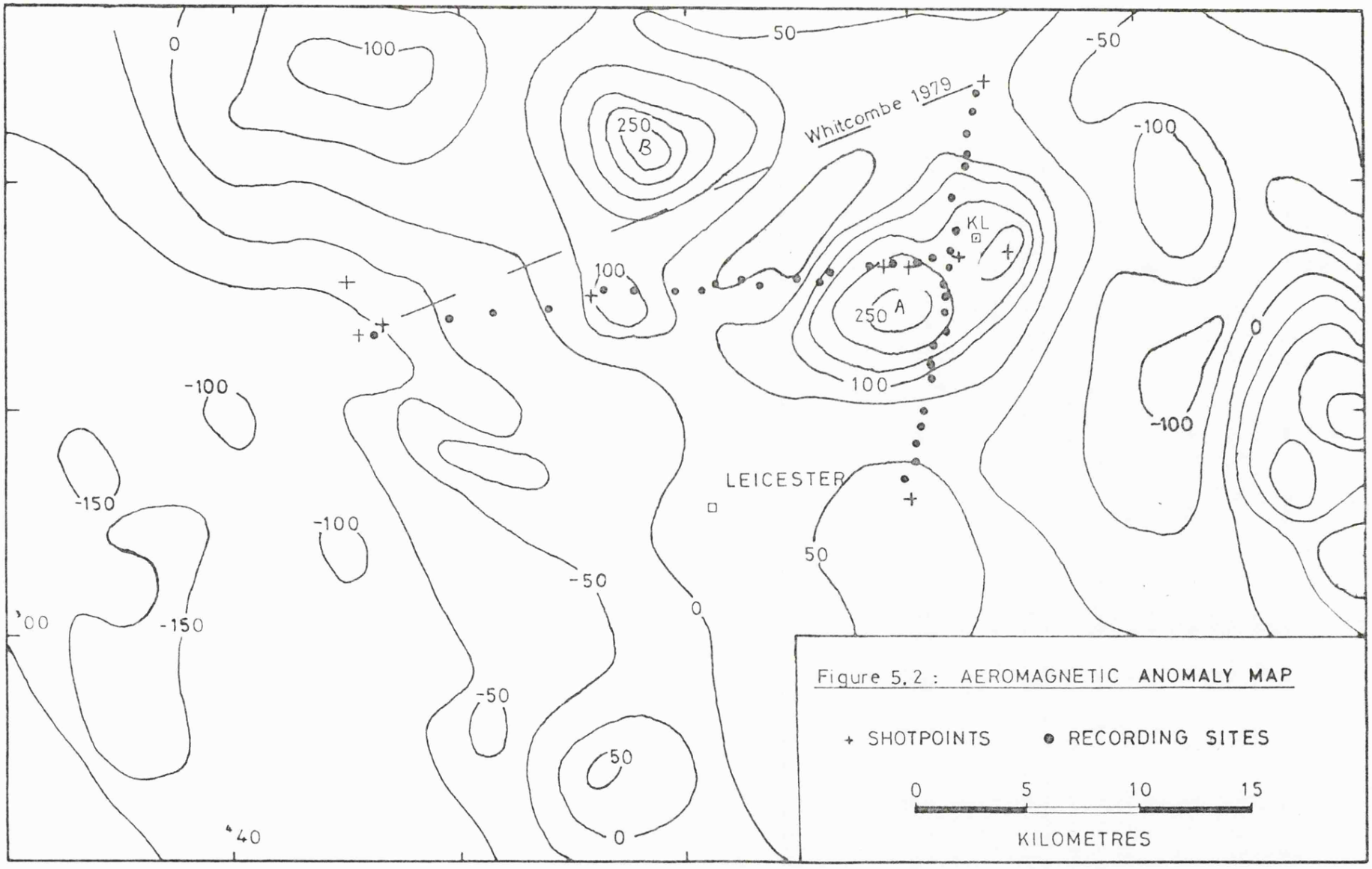
0
100
50
-50
250
B
Whitcombe 1979
-100
KL
100
250
A
100
-100
0
-100
-150
-100
LEICESTER
50
-50
-150
0
-50
50
0
Figure 5.2 : AEROMAGNETIC ANOMALY MAP
+ SHOTPOINTS
RECORDING SITES
0
5
10
15
KILOMETRES

design of the Melton experiment was the interpretation of the Bardon to Holwell line of Whitcombe (1979). This line indicated that the northern extension of the Mountsorrel aeromagnetic anomaly correlated with a low refractor velocity of 5.Ø km.s$^{-1}$ at depths of Ø.25 to 1.25 kilometres. This low velocity basement lay between the Charnian Inlier to the west, and a 1.25 to 2.Ø kilometre deep refractor, to the east, which had velocity 5.64 km.s$^{-1}$ and was interpreted as Charnian type basement. The interpretation of the Charnwood array data (Whitcombe and Maguire 198Ø and chapter 1) indicated a 6.4 km.s$^{-1}$ refractor at 2 to 4 kilometres beneath the Charnian Inlier. Stations on the Bardon to Holwell line (Whitcombe 1979), at greater than 25 kilometres from the Charnian Inlier, recorded first arrivals from a probable basement to the Charnian refractor.

### 5.1.3 The purpose of the experiment

As can be seen from figure 5.2 the aeromagnetic anomaly associated with the Melton intrusion is not contiguous with the Mountsorrel anomaly. The aim of the refraction experiment was therefore twofold:

1. To investigate the basement structure between Mountsorrel and Kirby Lane in order to see if the magnetic low was indicative of deep basement between the two intrusions (i.e. a southern extension of the Widmerpool Gulf).

2. To locate the northern and southern margins of the Melton intrusion in order to constrain subsequent modelling of the aeromagnetic data.

In order to achieve these two objectives it was necessary to record two refraction profiles. The design of

the experiment, as described below, was based on the assumption that the granitic intrusions in this area could be distinguished from Charnian type basement by their low p-wave velocities.

## 5.2 THE EXPERIMENT

### 5.2.1 Location of the profiles

The exact amount of recording equipment available was not known when the profiles were planned but the target was to achieve a mean station spacing of 1.5 kilometres.

The Bardon to Holwell profile of Whitcombe (1979) had successfully recorded arrivals from Bardon Hill and Whitwick quarries at ranges of 23 and 3Ø kilometres respectively.

Using the velocities measured from NCB borehole logs (chapter 4) the crossover distance for a 5.Ø km.s$^{-1}$ refractor at Ø.5 km depth was calculated to be about 2 kilometres. The Bardon to Holwell profile indicated a crossover distance at the Holwell shotpoint, where the refractor was about 1.8 kilometres deep, of 6 kilometres for a 5.64 km.s$^{-1}$ refractor.

The two profiles are shown in figure 5.3. Profile A was about 3Ø kilometres long and ran eastwards from the Charnian Inlier, across the exposed Mountsorrel granodiorite, to a shot point at Dalby one kilometre east of the Kirby Lane borehole. Profile B was about 2Ø kilometres long and ran north-south from a shotpoint at Holwell in the Widmerpool Gulf (used peviously by Whitcombe 1979), to a shotpoint at Quenby some 1Ø kilometres east of Leicester. The two profiles intersected in the vicinity of the Kirby Lane borehole.

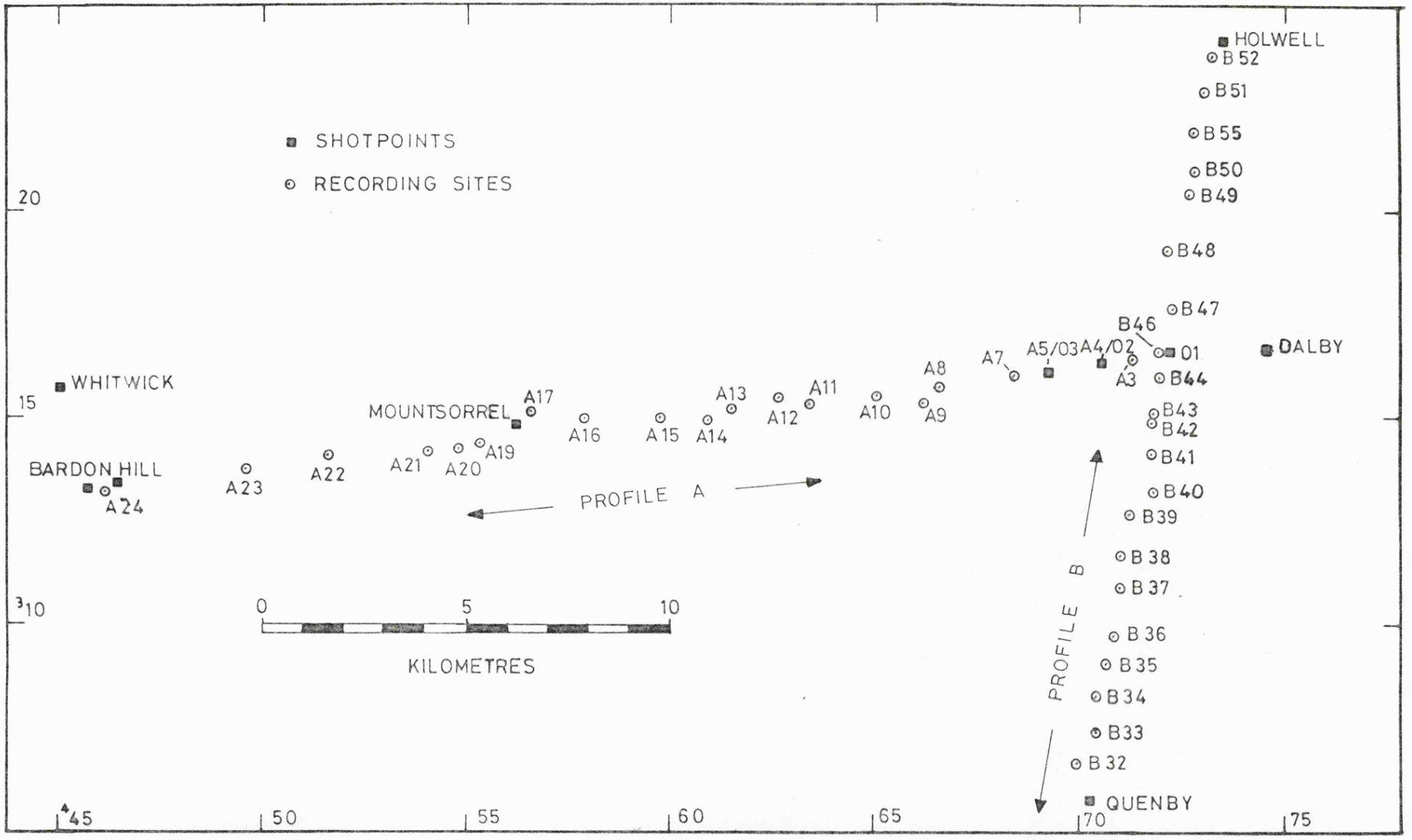


Figure 5.3 : Recording station and shotpoint locations for the Melton survey.

The constraints on the location of the recording profiles can be summarized as follows:

Profile A: 1. The profile was designed to investigate the link between the Mountsorrel and Melton intrusions. It was therefore sited to pass through Mountsorrel and close to the site of the Kirby Lane borehole.

2. The western end of the profile had to be at one of the quarries in the Charnian Inlier.

3. The maximum range of quarry blasts from Charnwood was 25 to 30 kilometres. The range of the Mountsorrel quarry blasts was probably about 20 kilometres.

4. A shotpoint had to be found at the eastern end of the profile at which to fire a 50 to 100 kg. charge.

Profile B: 1. The profile was designed to investigate the northern and southern margins of the Melton intrusion. and therefore had to be of sufficient length to give reversed cover on the refractor across the magnetic anomaly.

2. The only control point was the Kirby Lane borehole, therefore the profile should pass close to the borehole.

3. Suitable shotpoints had to be found for firing charges of up to 50 kilogrammes.

4. If, as was presumed, the Melton intrusion could be detected by a low p-wave velocity then a fan shoot from the ends of profile B into profile A would help to delineate the margins of the intrusion.

5.2.2 Shotpoints

The Holwell and Quenby shotpoints were on disused railway lines and the Dalby shotpoint on a disused airfield. In addition to these shots, three smaller charges (Ø1,Ø2,Ø3) were fired at the eastern end of profile A. These were used in connection with a seismic reflection profile which was recorded at the same time as the refraction profile (Maguire et.al. 1982). Towards the end of the experiment a controlled borehole shot was fired at Bardon Hill Quarry to supplement the quarry blast data and to improve the reversal on profile A. This shot was in a confined borehole in solid rock and not a normal quarry blast. A second shot was subsequently fired at the Quenby shotpoint to fill in some gaps on profile B. As a result a total of eight borehole shots, five timed Bardon Hill quarry blasts, three timed Whitwick quarry blasts and seven timed Mountsorrel quarry blasts were recorded. The details of the individual shots are given in table 5.1.

The locations of the quarry blasts were determined as accurately as possible from the available plans and, in the case of Bardon Hill, aerial photographs. No plans were available for Whitwick quarry and so an Ordnance Survey map was used. The Bardon and Mountsorrel quarry blasts were located to better than $\pm$ 5Ø metres. For a refractor velocity of over 5.Ø km.s$^{-1}$ this is equivalent to a travel time error of less than $\pm$ Ø.ØlØ seconds. The blasts from Whitwick quarry were located to about $\pm$ lØØ metres. This quarry was not used as a recording station and therefore any location error should appear as an anomalous time term for the shotpoint.

| BLAST | Charge | Ch Ø | BLAST | Charge | Ch Ø |
|---|---|---|---|---|---|
| MS 232 | 2125. | 25. | BH 225 | 400. | 60. |
| MS 234 | 1070. | 145. | BH 234 | 1140. | 90. |
| MS 241 | 1050. | 75. | BH 248 | 1175. | 105. |
| MS 245 | 665. | 75. | BH 262 | 1185. | 100. |
| MS 246 | 2145. | 90. | W 245 | 1450. | 255. |
| MS 247 | 1575. | 75. | W 248 | 1105. | 255. |
| MS 255 | 1040. | 125. | W 261 | 1200. | 255. |

Charge = total charge in kg, Ch Ø = charge on zero delay

| SHOT | Charge | No. holes | Hole depths |
|---|---|---|---|
| BARDON 1 | 125. | 4 | 20.0 |
| Ø1 | 9. | 1 | 19.0 |
| Ø2 | 14. | 1 | 19.0 |
| Ø3 | 20. | 1 | 19.0 |
| DALBY | 100. | 4 | 19.0 |
| HOLWELL | 35 | 2 | 16.0/12.0 |
| QUENBY 1 | 35 | 2 | 19.0/15.0 |
| QUENBY 2 | 25 | 1 | 19.0 |

Charges in kg. Hole depths in metres

| SHOT | SITE | NGR E | NGR N | ELEV |
|---|---|---|---|---|
| QUENBY 1 | B30 | 470.24 | 305.83 | 120 |
| QUENBY 2 | B31 | 470.02 | 305.82 | 120 |
| HOLWELL | B53 | 473.42 | 324.17 | 150 |
| Ø1 | A2 | 472.15 | 316.63 | 100 |
| Ø2 | A4 | 470.48 | 316.34 | 90 |
| Ø3 | A6 | 469.17 | 316.15 | 80 |
| DALBY | A1 | 474.52 | 316.71 | 110 |
| BARDON 1 | A26 | 446.47 | 313.32 | 245 |
| BH 225 | | 446.28 | 313.18 | 270 |
| BH 234 | | 445.55 | 313.03 | 220 |
| BH 248 | | 446.10 | 313.35 | 235 |
| BH 262 | A25 | 445.88 | 313.18 | 190 |
| WHITWICK | A28 | 445.00 | 315.75 | 200 |
| MS A | | 456.18 | 314.97 | 95 |
| MS B | A18 | 456.06 | 315.00 | 105 |
| MS C | | 456.05 | 315.04 | 105 |
| MS D | | 456.08 | 314.94 | 105 |

MS = Mountsorrel BH = Bardon Hill W = Whitwick
Quarry blasts numbered by Julian days (1980)
A,B,C,D = faces at Mountsorrel quarry (see text)

Table 5.1. Shotpoint data

5.2.3 Recording sites

The bulk of the data was collected on eight Geostore recorders operating in bi-directional mode at 15/160 ips. A total of 26 Willmore and HS10 seismometers of 2 Hz. resonant frequency were connected to the Geostores via UHF radio links and landlines. The longest radio link was about six kilometres, the longest landline was two kilometres. The Geostores were operated continuously for a four week period, with some interruptions due to equipment failure. For the controlled shots the number of recording stations was increased by using seven 3-component MARS recorders and up to eight single channel Reading cassette recorders (chapter 2).

The total number of recording stations successfully occupied was 21 on profile A and 24 on profile B. This gave mean station spacings of 1.4 and 0.8 kilometres for profiles A and B respectively. The recording sites were closed up over the postulated margins of the Melton intrusion and spaced out over the outcropping basement of the Charnian Inlier. As far as was possible the Geostore stations were spread evenly along the profiles and the temporary stations were used to fill in the gaps. To the east of Mountsorrel profile A crossed two small towns and so permanent sites could not be used between stations A13 and A18. The station locations and equipment types are given in table 5.2.

5.2.4 Shotpoint links

Shotpoint to shotpoint links are important for any time term solution. At least one link is necessary to invert the data, but the more links there are in a solution the better the solution will be.

| SITE | NGR E | NGR N | ELEV | Rec | Seis |
|---|---|---|---|---|---|
| A1 | 474.52 | 316.71 | 110 | M | H |
| A3 | 471.24 | 316.44 | 110 | G | W |
| A4 | 470.49 | 316.35 | 90 | c | W |
| A5 | 469.27 | 316.16 | 80 | c | W |
| A7 | 468.36 | 316.04 | 80 | t | W |
| A8 | 466.53 | 315.79 | 60 | c | W |
| A9 | 466.16 | 315.41 | 80 | G | W |
| A10 | 465.02 | 315.58 | 55 | t | W |
| A11 | 463.35 | 315.38 | 75 | t | W |
| A12 | 462.60 | 315.52 | 100 | G | W |
| A13 | 461.45 | 315.26 | 70 | t | W |
| A14 | 460.86 | 314.99 | 65 | M | H |
| A15 | 459.67 | 315.01 | 45 | M | H |
| A16 | 457.83 | 315.02 | 60 | M | H |
| A17 | 456.49 | 315.14 | 102 | t | H |
| A19 | 455.24 | 314.38 | 60 | M | H |
| A20 | 454.71 | 314.23 | 70 | R | J |
| A21 | 453.98 | 314.20 | 75 | t | W |
| A22 | 451.55 | 314.08 | 230 | G | W |
| A23 | 449.55 | 313.76 | 195 | t | H |
| A24 | 446.11 | 313.19 | 275 | t | H |

| SITE | NGR E | NGR N | ELEV | Rec | Seis |
|---|---|---|---|---|---|
| B30 | 470.19 | 305.83 | 120 | M | H |
| B32 | 469.89 | 306.69 | 155 | G | H |
| B33 | 470.38 | 307.45 | 145 | M(R) | H |
| B34 | 470.38 | 308.32 | 125 | R | J |
| B35 | 470.61 | 309.09 | 120 | R | J |
| B36 | 470.80 | 309.75 | 140 | t | W |
| B37 | 470.95 | 310.91 | 110 | (M) | (H) |
| B38 | 470.97 | 311.70 | 90 | M | H |
| B39 | 471.18 | 312.68 | 110 | R | J |
| B40 | 471.76 | 313.23 | 138 | R(R) | J(H) |
| B41 | 471.72 | 314.16 | 120 | G(R) | W(H) |
| B42 | 471.72 | 314.96 | 110 | (M) | (H) |
| B43 | 471.76 | 315.14 | 110 | t | W |
| B44 | 471.91 | 316.01 | 110 | (R) | (H) |
| B45 | 472.15 | 316.63 | 100 | (R) | (H) |
| B46 | 471.89 | 316.62 | 105 | t | H |
| B47 | 472.19 | 317.68 | 75 | M(M) | H(H) |
| B48 | 472.08 | 319.10 | 90 | G | W |
| B49 | 472.62 | 320.46 | 80 | t | W |
| B50 | 472.74 | 321.01 | 90 | t | H |
| B55 | 472.69 | 321.96 | 120 | t | H |
| B51 | 472.97 | 322.91 | 125 | t | W |
| B52 | 473.16 | 323.77 | 160 | G | H |
| B53 | 473.42 | 324.17 | 150 | M | H |

Rec = recorder: M = MARS R = Reading cassette
G = Geostore t = telemetered c = cabled outstation
Seis = seismometer: W = Willmore mk III
H = HS10 J = HSJ (14 Hz. in strings of six)
( ) : used for Quenby 2 shot

Table 5.2. Site location details

Because of a shortage of recording equipment, and the probability that they would be out of range of the quarry blasts, the Dalby, Quenby and Holwell shotpoints were not occupied by permanent recorders or outstations. They were occupied for the Ø1, Ø2, Ø3, Dalby, Quenby 1 and Holwell shots. Dalby was also occupied for the Bardon Hill borehole shot (Bardon 1). The Ø2 and Ø3 shotpoints were also Geostore outstations as were Mountsorrel and Bardon Hill quarries. The Ø1 shotpoint was a recording site for the Quenby 2 shot.

### 5.2.5 Problems during the experiment

During the course of the experiment a number of events were not recorded at certain sites. As will be seen later the areas in which the failures occurred are subject to the greatest uncertainty in the interpretations. The main problems are summarized below:

1. Mountsorrel Quarry: a telemetered outstation was installed at the quarry to record arrivals from the controlled shots and from the other quarries. A breakdown of the radio link, and subsequently the Geostore recorder, meant that this station was not operational for most of the experiment. The Bardon 1 shot was the only timed event recorded at this site.

2. Stations B41,43,46: these stations were located on the central part of profile B and were all recorded by a Geostore at B41. This Geostore failed for the week of the Quenby 1 and Holwell shots resulting in a loss of cover for the central part of profile B. The Quenby 2 shot was used to fill in for some of the missing data.

3. Shots Ø1,Ø2,Ø3,Dalby: eight Reading cassette recorders were deployed with a Ø.5 kilometre spacing at, and between, these shotpoints. The purpose of this was to obtain linking observations between the four shotpoints, as well as overburden and refractor velocities around the Kirby Lane borehole. As a result of an error in loading the tapes all the recordings were lost.

4. Quenby 2 shot: As a result of the failure of an MSF time code receiver the shot instant was not timed. However three of the recording sites for the Quenby 1 shot had been reoccupied for this shot and therefore the shot instant could be calculated from the arrival times at these sites.

## 5.3 THE DATA

### 5.3.1 Signal strengths

The signal strengths from the controlled shots were strong. Typical signal to noise ratios were between five and ten to one for many of the arrivals from the Dalby shot and about five to one for the Quenby and Holwell shots. The quarry blasts from Whitwick and Mountsorrel were strong enough to produce pickable first arrivals (s/n of two or three to one) at station A3 on profile A, but were not strong enough to give usable arrivals at the stations on profile B. The quarry blasts from Bardon Hill produced weak arrivals which were not usable to the east of Mountsorrel. The controlled shot fired at Bardon Hill was larger than the Dalby shot but was fired in solid rock rather than clay. This shot produced weak first arrivals which were only detectable above the background noise at three stations to

the east of Mountsorrel.

The quarry blasts and the Bardon shot were all fired in the daytime, usually at midday, when the cultural noise levels were high. The other controlled shots were fired in early evening when the noise levels were a factor of two lower.

With the exception of the sites to the west of Mountsorrel, the Geostore outstations were operated on high gains (7-8 for a Willmore mk III) in order to record the quarry blasts. Because of the large number of sites involved it was not possible to change the gain settings before and after the controlled shots. The Dalby shot produced overloaded arrivals at the eastern end of profile A and on the central part of profile B. The shots were fired in pairs (Ø1-Ø2, Dalby-Ø3, Quenby-Holwell) to enable portable recorders to be used to fill in gaps in the recording profiles. In the case of profile B this meant that the Geostore stations at either end of the profile were overloaded by the closer shot.

The data analysis was therefore limited to the first arrival travel times at vertical geophones. The only horizontal geophones were six north-south/east-west pairs used with the MARS recorders.

### 5.3.2 The travel time data

The first arrivals were picked as described in chapter 2, and the maximum observational error associated with each travel time was estimated. The complete travel time data set is given in tables 5.3 (profile A) and 5.4 (profile B).

The arrivals from the Quenby 1 and Holwell shots into

profile B were digitized using an AR11 analogue to digital converter on the Leicester mainframe computer. The first arrivals for these events were picked from the digital records. The digitizing was done in order to test a newly established processing system, with a view to producing record sections of all the data. However the digitizing process was found to be very time consuming and of limited value if the interpretation was to be restricted to the first arrival data.

Because of the large number of quarry blasts recorded by the Geostore recorders it was necessary to compile a representative data set of arrivals from the three quarries into all the recording sites. This provided a way of checking the accuracy of the first arrival picks and removing dubious events.

The quarry blasts at Mountsorrel came from four separate faces (A,B,C,D table 6.2). Face A was at a lower level than the other three which lay on a line perpendicular to profile A. The signals from the different faces were checked by graphical correlation to ensure that they were compatible. As described in chapter 2 the position of a blast within a quarry will not significantly affect the received seismic signal.

The final data set for profile A consisted of 102 travel times from 10 shotpoints into 21 recording sites. For profile B there were no quarry blast data and therefore the data set consisted of 66 travel times from 6 shotpoints into 23 recording sites.

QUARRY BLASTS

MS 234 (B) 12-35-45.600

| STN | D km | T sec | E sec |
|---|---|---|---|
| A19 | 1.01 | 0.260 | 0.010 |

MS 241 (B) 12-33-29.945

| STN | D km | T sec | E sec |
|---|---|---|---|
| A21 | 2.23 | 0.485 | 0.020 |
| A22 | 4.60 | 0.895 | 0.010 |
| A24 | 10.11 | 1.870 | 0.010 |
| A25* | 10.34 | 1.910 | 0.010 |

MS 245 (C) 12-33-50.465

| STN | D km | T sec | E sec |
|---|---|---|---|
| A5 | 13.27 | 2.460 | 0.020 |
| A8 | 10.51 | 1.965 | 0.020 |
| A9 | 10.12 | 1.895 | 0.020 |

MS 247 (B) 12-33-19.305

| STN | D km | T sec | E sec |
|---|---|---|---|
| A10 | 8.98 | 1.675 | 0.015 |
| A21 | 2.23 | 0.505 | 0.010 |
| A22 | 4.60 | 0.900 | 0.010 |
| A24 | 10.11 | 1.880 | 0.020 |

MS 252 UNTIMED

| STN | D km | T sec | E sec |
|---|---|---|---|
| A3 | 15.25 | 2.825 | 0.020 |
| A4 | 14.49 | 2.690 | 0.020 |
| A5 | 13.26 | 2.485 | 0.020 |
| A7 | 12.34 | 2.335 | 0.020 |
| A8 | 10.50 | 1.980 | 0.020 |
| A9 | 10.11 | 1.900 | 0.015 |
| A12 | 6.56 | 1.260 | 0.015 |

MS 253 UNTIMED

| STN | D km | T sec | E sec |
|---|---|---|---|
| A3 | 15.25 | 2.825 | 0.020 |
| A4 | 14.49 | 2.690 | 0.020 |
| A5 | 13.26 | 2.485 | 0.020 |
| A7 | 12.34 | 2.330 | 0.020 |
| A9 | 10.11 | 1.900 | 0.015 |
| A10 | 8.98 | 1.690 | 0.020 |
| A11 | 7.30 | 1.395 | 0.020 |
| A12 | 6.56 | 1.260 | 0.015 |
| A13 | 5.40 | 1.050 | 0.010 |
| A21 | 2.23 | 0.500 | 0.010 |

MS 255 12-31-03.540

| STN | D km | T sec | E sec |
|---|---|---|---|
| A3 | 15.25 | 2.825 | 0.020 |
| A5 | 13.26 | 2.480 | 0.020 |
| A11 | 7.30 | 1.395 | 0.020 |
| A12 | 6.56 | 1.280 | 0.015 |
| A13 | 5.40 | 1.055 | 0.020 |
| A21 | 2.23 | 0.485 | 0.020 |
| A22 | 4.60 | 0.890 | 0.020 |
| A23 | 6.63 | 1.280 | 0.020 |

WHITWICK 245 14-08-42.220

| STN | D km | T sec | E sec |
|---|---|---|---|
| A3 | 26.25 | 4.715 | 0.025 |
| A4 | 25.50 | 4.585 | 0.025 |
| A5 | 24.27 | 4.370 | 0.025 |
| A7 | 23.36 | 4.215 | 0.025 |
| A8 | 21.53 | 3.880 | 0.025 |
| A9 | 21.16 | 3.805 | 0.025 |
| A12 | 17.60 | 3.190 | 0.020 |

WHITWICK 248 09-55-50.593

| STN | D km | T sec | E sec |
|---|---|---|---|
| A3 | 26.25 | 4.710 | 0.025 |
| A5 | 24.27 | 4.365 | 0.025 |
| A7 | 23.36 | 4.210 | 0.025 |
| A8 | 21.53 | 3.875 | 0.020 |
| A9 | 21.16 | 3.805 | 0.025 |
| A10 | 20.02 | 3.595 | 0.020 |
| A12 | 17.60 | 3.195 | 0.020 |
| A22 | 6.76 | 1.210 | 0.010 |
| A24 | 2.79 | 0.535 | 0.010 |

WHITWICK 261 13-57-18.490

| STN | D km | T sec | E sec |
|---|---|---|---|
| A3 | 26.25 | 4.710 | 0.025 |
| A4 | 25.50 | 4.600 | 0.025 |
| A7 | 23.36 | 4.215 | 0.025 |
| A8 | 21.53 | 3.885 | 0.025 |
| A9 | 21.16 | 3.800 | 0.025 |
| A10 | 20.02 | 3.605 | 0.025 |
| A21 | 9.11 | 1.630 | 0.015 |
| A22 | 6.76 | 1.205 | 0.010 |
| A23 | 4.97 | 0.915 | 0.010 |
| A24 | 2.79 | 0.535 | 0.010 |
| A25* | 2.72 | 0.522 | 0.010 |

BARDON 262 12-29-06.340

| STN | D km | T sec | E sec |
|---|---|---|---|
| A21 | 8.16 | 1.485 | 0.010 |
| A22 | 5.74 | 1.035 | 0.010 |
| A23 | 3.72 | 0.705 | 0.010 |
| A24 | 0.23 | 0.040 | 0.010 |

Timed but not used:

| | |
|---|---|
| MS 232 (B) | 12-33-10.255 |
| MS 234 (D) | 12-35-45.600 |
| MS 246 (A) | 12-33-20.480 |
| BARDON 225 | 12-30-42.410 |
| BARDON 234 | 12-31-11.990 |
| BARDON 248 | 12-28-36.980 |

CONTROLLED SHOTS

01 (252) 16-23-05.670

| STN | D km | T sec | E sec |
|---|---|---|---|
| A1 | 2.37 | 0.715 | 0.010 |
| A3 | 0.93 | 0.330 | 0.010 |
| A4 | 1.69 | 0.542 | 0.010 |
| A5 | 2.92 | 0.755 | 0.010 |
| A7 | 3.83 | 0.925 | 0.015 |
| A8 | 5.68 | 1.215 | 0.010 |
| A9 | 6.11 | 1.285 | 0.010 |
| A10 | 7.21 | 1.470 | 0.010 |
| A12 | 9.61 | 1.900 | 0.010 |
| A13 | 10.79 | 2.105 | 0.015 |
| A21 | 18.33 | 3.380 | 0.015 |
| A22 | 20.76 | 3.730 | 0.015 |

02 (252) 15-58-53.310

| STN | D km | T sec | E sec |
|---|---|---|---|
| A1 | 4.06 | 0.965 | 0.010 |
| A3 | 0.77 | 0.275 | 0.010 |
| A7 | 2.14 | 0.585 | 0.010 |
| A8 | 3.99 | 0.885 | 0.010 |
| A9 | 4.42 | 0.965 | 0.010 |
| A10 | 5.51 | 1.150 | 0.010 |
| A12 | 7.92 | 1.570 | 0.010 |
| A13 | 9.09 | 1.780 | 0.010 |
| A21 | 16.64 | 3.040 | 0.015 |
| A22 | 19.06 | 3.400 | 0.015 |

03 (252) 15-58-53.310

| STN | D km | T sec | E sec |
|---|---|---|---|
| A3 | 2.09 | 0.670 | 0.010 |
| A4 | 1.34 | 0.400 | 0.010 |
| A5 | 0.10 | 0.050 | 0.010 |
| A7 | 0.82 | 0.250 | 0.010 |
| A8 | 2.66 | 0.630 | 0.010 |
| A9 | 3.10 | 0.715 | 0.010 |
| A10 | 4.19 | 0.895 | 0.010 |
| A11 | 5.87 | 1.195 | 0.015 |
| A12 | 6.60 | 1.330 | 0.015 |
| A13 | 7.77 | 1.545 | 0.020 |
| A14 | 8.39 | 1.645 | 0.020 |
| A15 | 9.57 | 1.840 | 0.020 |
| A21 | 15.31 | 2.790 | 0.015 |
| A22 | 17.74 | 3.145 | 0.015 |
| A24 | 23.25 | 4.120 | 0.020 |

Table 5.3 : Travel time data for profile A.

DALBY (252) 19-06-02.050

| STN | D km | T sec | E sec |
|---|---|---|---|
| A3 | 3.29 | 0.845 | 0.010 |
| A4 | 4.06 | 0.965 | 0.010 |
| A5 | 5.28 | 1.170 | 0.010 |
| A7 | 6.20 | 1.340 | 0.010 |
| A8 | 8.04 | 1.610 | 0.010 |
| A9 | 8.46 | 1.690 | 0.010 |
| A10 | 9.57 | 1.875 | 0.010 |
| A11 | 11.25 | 2.170 | 0.010 |
| A12 | 11.98 | 2.310 | 0.010 |
| A13 | 13.15 | 2.510 | 0.010 |
| A14 | 13.77 | 2.625 | 0.025 |
| A15 | 14.95 | 2.810 | 0.020 |
| A16 | 16.78 | 3.100 | 0.020 |
| A21 | 20.69 | 3.750 | 0.015 |
| A22 | 23.12 | 4.110 | 0.015 |
| A24 | 28.63 | 5.070 | 0.010 |

BARDON 1 (263) 12-28-57.285

| STN | D km | T sec | E sec |
|---|---|---|---|
| A3 | 24.97 | 4.555 | 0.025 |
| A9 | 19.80 | 3.560 | 0.020 |
| A10 | 18.69 | 3.365 | 0.020 |
| A17 | 10.04 | 1.895 | 0.015 |
| A18* | 9.74 | 1.835 | 0.020 |
| A19 | 8.83 | 1.660 | 0.015 |
| A20 | 8.29 | 1.555 | 0.010 |
| A21 | 7.56 | 1.405 | 0.010 |
| A22 | 5.14 | 0.950 | 0.010 |
| A23 | 3.11 | 0.620 | 0.010 |
| A24 | 0.38 | 0.070 | 0.010 |

QUENBY 1 18-35-27.060

| STN | D km | T sec | E sec |
|---|---|---|---|
| A1 | 11.69 | 2.370 | 0.015 |
| A3 | 10.66 | 2.155 | 0.020 |
| A4 | 10.52 | 2.150 | 0.020 |
| A8 | 10.63 | 2.085 | 0.010 |
| A9 | 10.41 | 2.045 | 0.010 |
| A10 | 11.06 | 2.130 | 0.010 |
| A11 | 11.78 | 2.260 | 0.010 |

HOLWELL (262) 18-45-02.180

| STN | D km | T sec | E sec |
|---|---|---|---|
| A1 | 7.54 | 1.820 | 0.015 |
| A3 | 8.03 | 1.965 | 0.020 |
| A4 | 8.35 | 2.020 | 0.010 |
| A10 | 12.01 | 2.580 | 0.010 |
| A11 | 13.57 | 2.845 | 0.010 |

(262) : Julian day numbers 1980

Shot times : HH-MM-SS.sss (BST)

MS : Mountsorrel faces A/B/C/D

* : dummy travel time (see text)

D : shot to receiver distance

T : travel time

E : estimated maximum observational error

Table 5.3 continued.

---

QUENBY 1 (262) 18-35-27.060

| STN | D km | T sec | E sec |
|---|---|---|---|
| B32 | 0.93 | 0.365 | 0.020 |
| B33 | 1.63 | 0.560 | 0.015 |
| B34 | 2.49 | 0.698 | 0.010 |
| B35 | 3.28 | 0.867 | 0.015 |
| B36 | 3.96 | 0.995 | 0.020 |
| B38 | 5.92 | 1.319 | 0.015 |
| B39 | 6.91 | 1.520 | 0.015 |
| B40 | 7.55 | 1.649 | 0.015 |
| B47 | 12.01 | 2.390 | 0.015 |
| B48 | 13.40 | 2.625 | 0.015 |
| B50 | 15.38 | 3.035 | 0.020 |
| B51 | 17.30 | 3.459 | 0.015 |
| B53 | 18.61 | 3.730 | 0.015 |

QUENBY 2 (353) 11-05-05.320

| STN | D km | T sec | E sec |
|---|---|---|---|
| B33 | 1.67 | 0.575 | 0.015 |
| B37 | 5.17 | 1.190 | 0.015 |
| B40 | 7.61 | 1.640 | 0.015 |
| B41 | 8.51 | 1.785 | 0.015 |
| B42 | 9.30 | 1.920 | 0.015 |
| B44 | 10.36 | 2.130 | 0.015 |
| B45 | 11.02 | 2.230 | 0.025 |
| B47 | 12.06 | 2.400 | 0.020 |

HOLWELL (262) 18-45-02.180

| STN | D km | T sec | E sec |
|---|---|---|---|
| B30 | 18.61 | 3.732 | 0.020 |
| B32 | 17.83 | 3.650 | 0.015 |
| B33 | 16.99 | 3.460 | 0.020 |
| B34 | 16.14 | 3.341 | 0.015 |
| B35 | 15.34 | 3.190 | 0.015 |
| B36 | 14.66 | 3.060 | 0.015 |
| B38 | 12.71 | 2.675 | 0.020 |
| B39 | 11.71 | 2.552 | 0.015 |
| B40 | 11.07 | 2.429 | 0.020 |
| B47 | 6.61 | 1.665 | 0.015 |
| B48 | 5.24 | 1.425 | 0.015 |
| B50 | 3.23 | 0.991 | 0.015 |
| B55 | 2.33 | 0.773 | 0.015 |
| B51 | 1.34 | 0.513 | 0.015 |

01 (252) 16-23-05.670

| STN | D km | T sec | E sec |
|---|---|---|---|
| B32 | 10.19 | 2.130 | 0.015 |
| B41 | 2.51 | 0.685 | 0.015 |
| B43 | 1.54 | 0.515 | 0.010 |
| B46 | 0.26 | 0.125 | 0.010 |
| B48 | 2.47 | 0.715 | 0.015 |
| B49 | 3.86 | 0.990 | 0.020 |
| B51 | 6.33 | 1.570 | 0.015 |

02 (252) 15-58-53.310

| STN | D km | T sec | E sec |
|---|---|---|---|
| B32 | 9.67 | 1.975 | 0.020 |
| B41 | 2.51 | 0.650 | 0.010 |
| B48 | 3.19 | 0.805 | 0.010 |
| B49 | 4.64 | 1.090 | 0.010 |
| B50 | 5.19 | 1.230 | 0.010 |

03 (252) 19-26-01.850

| STN | D km | T sec | E sec |
|---|---|---|---|
| B30 | 10.37 | 2.055 | 0.010 |
| B32 | 9.49 | 1.880 | 0.010 |
| B41 | 3.23 | 0.750 | 0.010 |
| B43 | 2.78 | 0.660 | 0.010 |
| B46 | 2.76 | 0.690 | 0.010 |
| B48 | 4.14 | 0.935 | 0.015 |
| B50 | 6.03 | 1.430 | 0.015 |

DALBY (252) 19-06-02.050

| STN | D km | T sec | E sec |
|---|---|---|---|
| B30 | 11.69 | 2.380 | 0.015 |
| B32 | 11.04 | 2.240 | 0.015 |
| B41 | 3.79 | 0.910 | 0.010 |
| B43 | 3.18 | 0.800 | 0.010 |
| B46 | 2.63 | 0.730 | 0.010 |
| B48 | 3.42 | 0.840 | 0.020 |
| B50 | 4.65 | 1.135 | 0.020 |
| B51 | 6.39 | 1.570 | 0.020 |
| B53 | 7.54 | 1.820 | 0.015 |

Table 5.4 : Travel time data for profile B.

## 5.4 REDUCED TRAVEL TIMES

### 5.4.1 Profile A

Figure 5.4 shows the reduced travel times for profile A. The reducing velocity of 5.7 $km.s^{-1}$ was found to give a visual best fit for the reversed shots into stations A3-A13. The overburden structure varies along the profile, thus complicating the interpretation of the reduced travel time sections. From A16 to A24 the stations were located on exposed, or shallow buried, basement rocks. From A15 to A8 the Keuper Marl underlies the Boulder Clay and there is little variation in the overburden structure. To the east of A8 the thickness of the Lias shales and Coal Measures increases eastwards (chapter 4). The effect of this will be to lower the average velocity of the sediments, with respect to the Keuper, by an amount equivalent to a Ø.Ø15 second increase in delay time between A8 and A3. The increase in station elevation to the east of A8 (table 5.2) could account for a similar increase in delay time between A8 and A1 (Dalby).

The reduced travel time sections for the shots from the eastern end of the line (Ø1,Ø2,Ø3,Dalby) compare very closely. This indicates that there is no detectable increase in velocity with depth in the refractor. The shots from Whitwick and Mountsorrel, which were about 11 kilometres apart, compare less closely but are still within the limits of the observational errors.

The reduced travel time sections can be considered in three parts:

Stations A1 to A7: This interval was located over the Melton

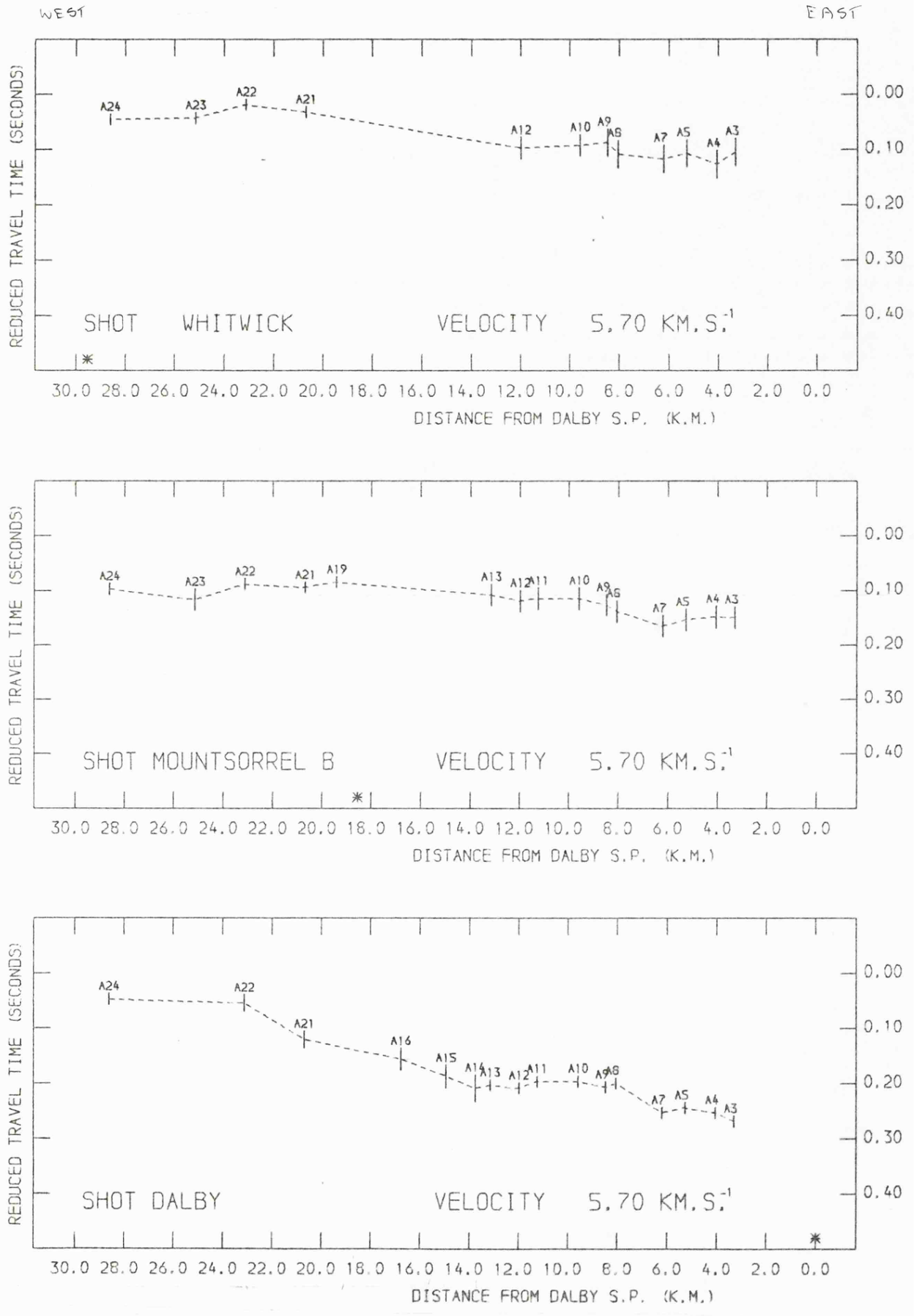


Figure 5.4 : Reduced travel time sections for profile A. The vertical bars indicate the maximum errors.

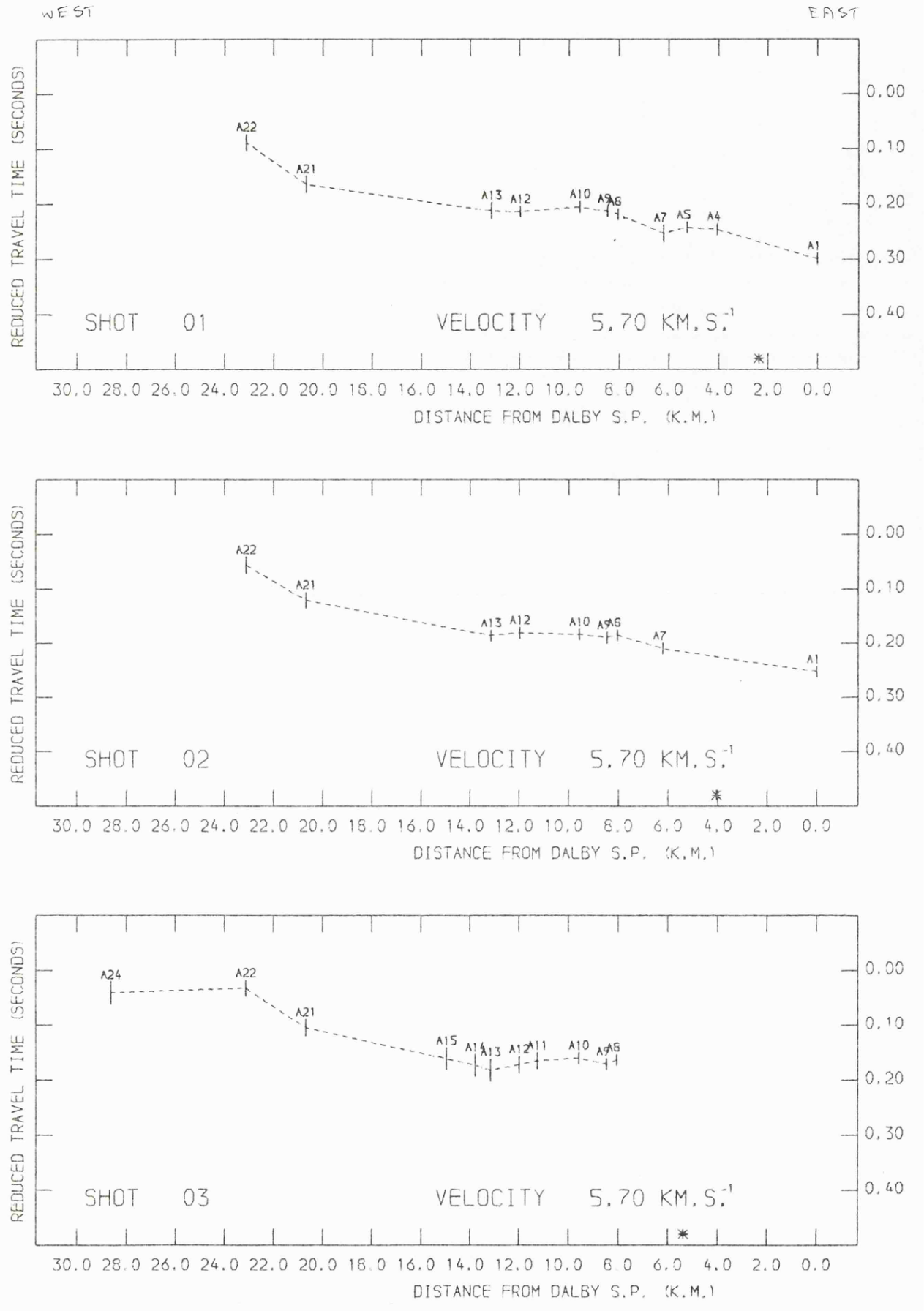


Figure 5.4 continued.

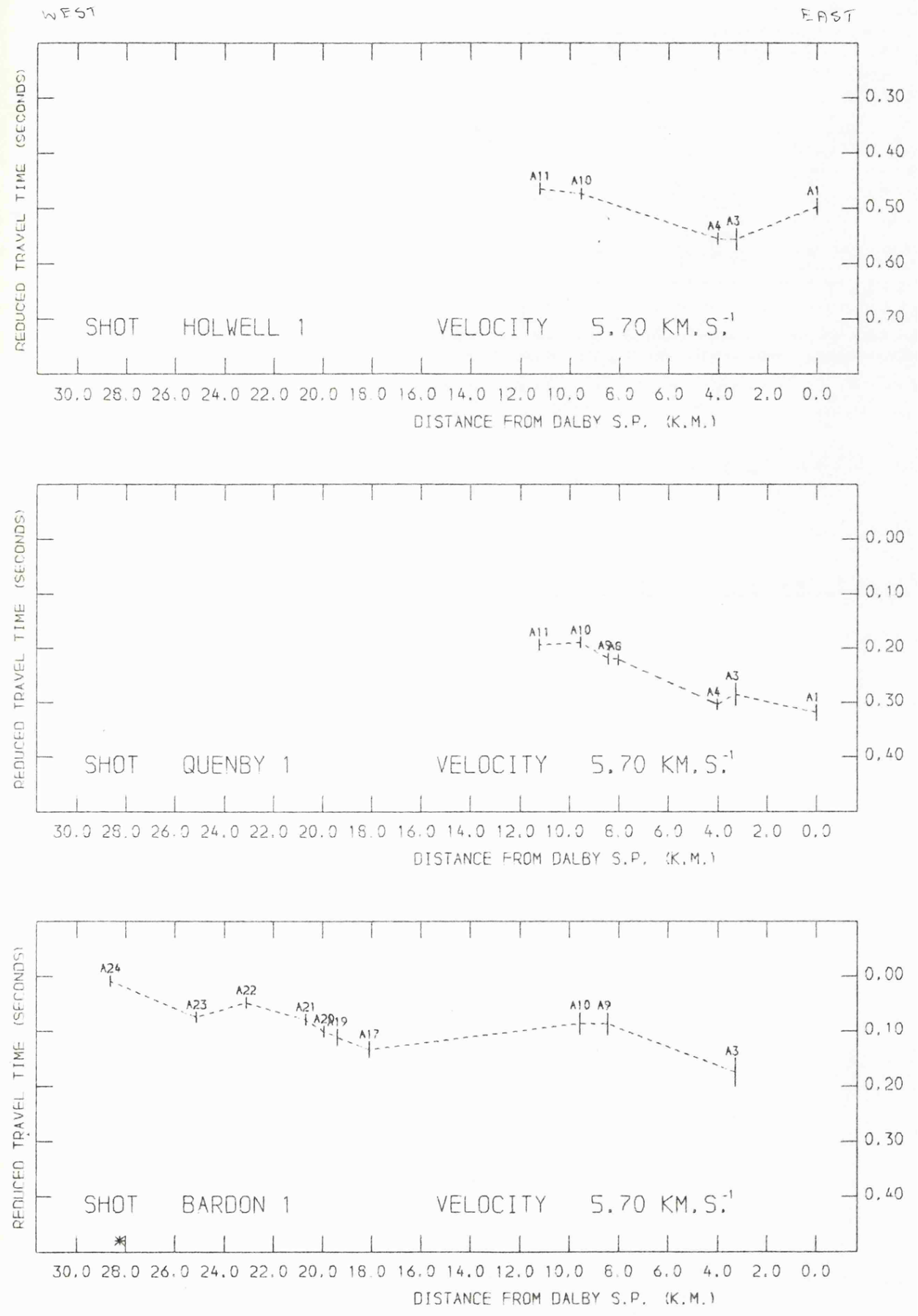


Figure 5.4 continued.

aeromagnetic anomaly. The resolution of the reduced travel times is limited by the lateral velocity changes within the sediments in this area. There is, however, no indication of a low velocity (i.e. 5.0 $km.s^{-1}$) refractor in this area.

The interval between stations A8 and A7 (a distance greater than the critical distance) lies on the the edge of the Melton magnetic anomaly and this is the point at which the overburden velocity starts to change. There is a discontinuity between stations A8 and A7 with a westward decrease in the reduced travel times. Since no lateral velocity change can be detected the discontinuity must be due to structure within the sediments or to topography on the refractor. The best quality data is from the Dalby shot which shows that the decrease in reduced travel times is greater than can be explained by a lateral thinning of the low velocity sediments (a maximum of about 0.020 seconds for the interval between A8 and A7).

Stations A8 to A16: The interval from A8 to A14 has the best reversed coverage on this profile and the most uniform overburden structure; the critical distance is about one kilometre. The reduced travel time sections give a good correlation for the reversed shots, indicating a refractor with negligible dip and a velocity of about 5.7 $km.s^{-1}$ . The changes in reduced travel times between adjacent stations are smaller than the estimated errors. The interval from A14 to the exposed Mountsorrel granodiorite at A16 was not reversed from the west due to the weak Bardon shot. The reduced travel times for the Dalby shot into stations A14-A16 indicate a westward shallowing of the refractor

which is consistent with the exposure of basement rocks at Mountsorrel.

Stations A18 to A24: These stations lie on or adjacent to the Charnian Inlier, although only A22 and A24 were on exposed Charnian rocks.

The Charnwood array of Whitcombe and Maguire (1980) indicated a velocity of 5.65 $km.s^{-1}$ for the Maplewell Series and 5.4 $km.s^{-1}$ for the older Blackbrook Series. Using the surface geology (figure 5.5) the relative proportions of the two lithologies that any arrival will pass through can be calculated. The proportion of Maplewell Series varies from 30 to 65%, which is equivalent to a variation in velocity of about 0.08 $km.s^{-1}$. The reduced travel time sections have been replotted for a reducing velocity of 5.6 $km.s^{-1}$ (figure 5.6). This velocity gives a better visual correlation for the reversed shots from the surrounding quarries than the reducing velocity of 5.7 $km.s^{-1}$. Since A22 and A24 were located on exposed Charnian rocks both stations should have near zero reduced travel times for the shots which were located in basement rocks. The Whitwick arrival at A22 shows this but the arrival at A24 has a positive reduced travel time indicating an apparent velocity of less than 5.6 $km.s^{-1}$. The near surface velocity of the Bardon Porphyroid and Slate Agglomerate is known, from shallow refraction surveys, to be about 5.0-5.2 $km.s^{-1}$. However, the reduced travel times for shots from Mountsorrel show a negative delay for A24 with respect to A22, indicating an apparent velocity of greater than 5.6 $km.s^{-1}$ between A22 and A24. It appears that the localised variations in apparent velocity are greater than

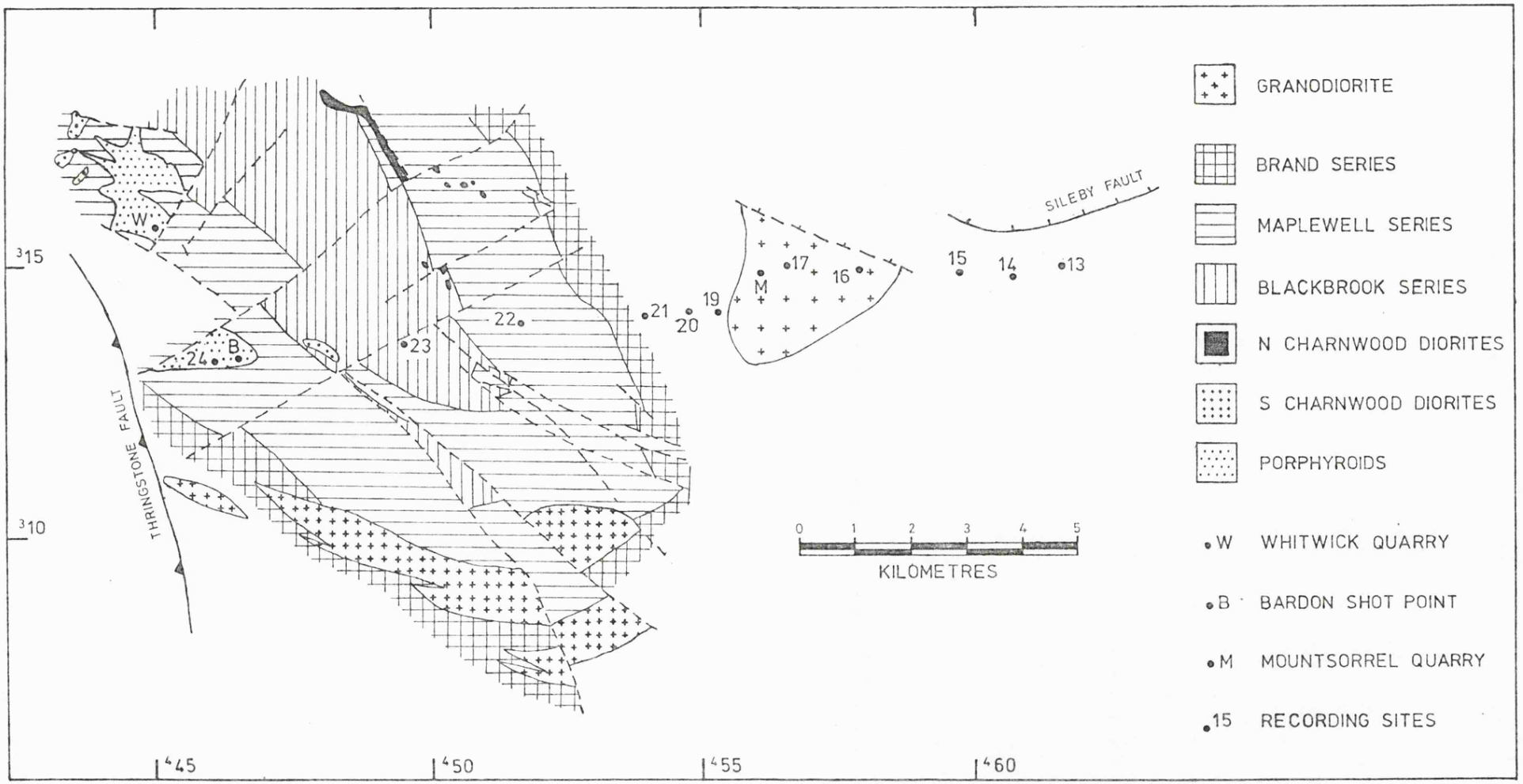


Figure 5.5 : The geology of Charnwood Forest (after Watts 1947) showing the locations of the recording sites.

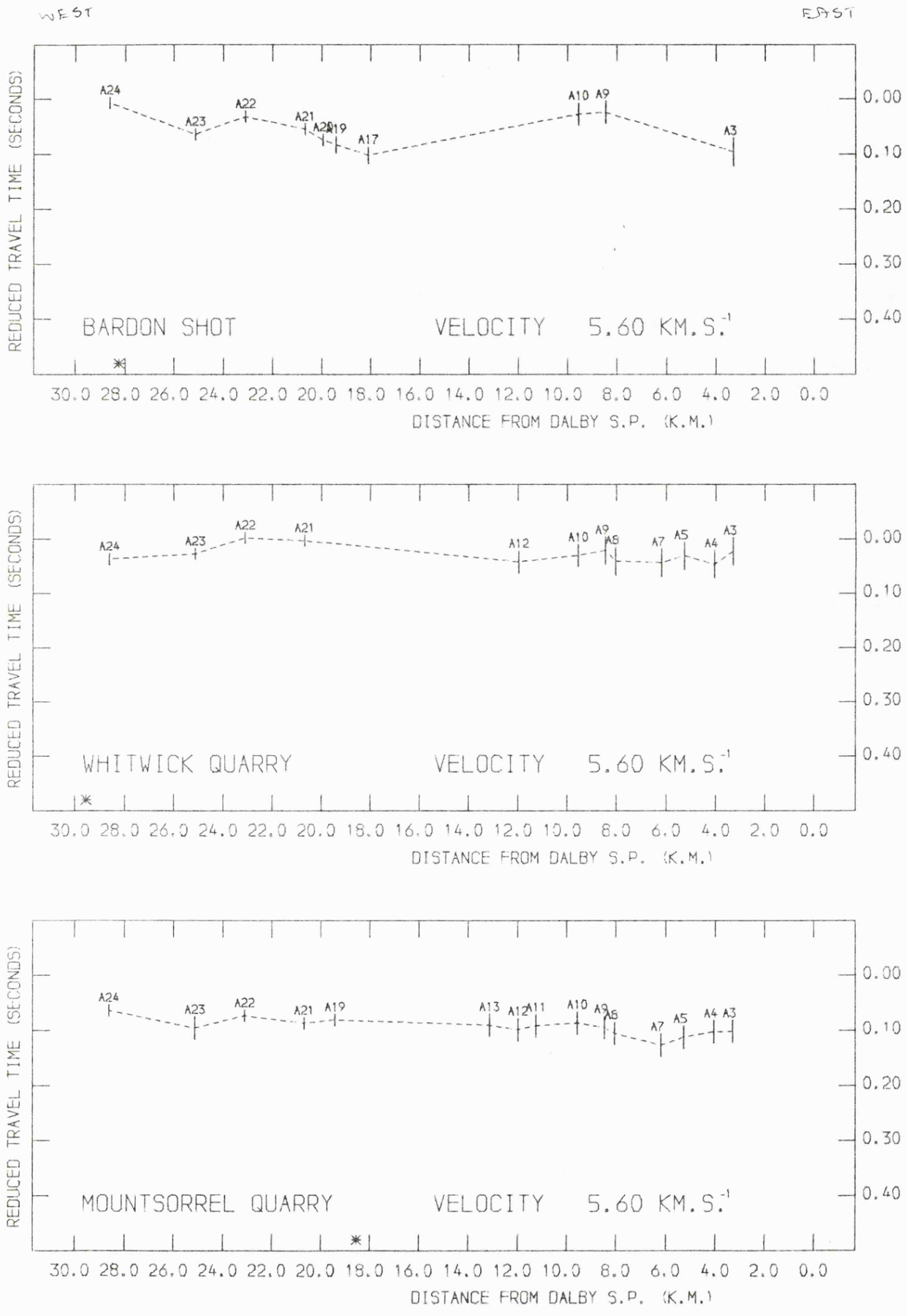


Figure 5.6 : Reduced travel time sections for profile A.

can be predicted by using the typical Maplewell and Blackbrook Series velocities described above.

The reduced travel times for the Mountsorrel shot also present a problem since they are about Ø.ØSØ seconds larger than the reduced travel times for the same stations from the other shotpoints. The Bardon shot into A17 (Mountsorrel) also shows a positive reduced travel time relative to A22. This suggests that there is a delay of up to Ø.ØSØ seconds associated with the Mountsorrel granodiorite. As discussed previously a low velocity refractor has been detected to the north of Mountsorrel and correlated with the northern extension of the intrusion. The problem of the Mountsorrel delay times is discussed below.

If there is a low velocity anomaly associated with the Mountsorrel intrusion then there is no indication, on the reduced travel time plots, that raypaths which pass through Mountsorrel are delayed. This suggests that the velocity anomaly is confined to shallow depths, this is consistent with the solution velocity for the Bardon to Holwell line which indicated a rapid increase in velocity with depth ($4.8+Ø.7z$ km.s$^{-1}$) within the low velocity refractor.

Of the stations not located on exposed basement rocks A21 and A23 show consistently small, positive, reduced travel times compared to A22. Arrivals from the Bardon shot were also recorded, to the east of the exposed Charnian, at stations A21 to A19 (figure 5.5). The reduced travel times here suggest an eastward deepening of the refractor or a lateral decrease in overburden velocity.

5.4.2 A possible basement to the Charnian

The shots from the eastern end of profile A, as plotted in figure 5.5, show a Ø.Ø7Ø second decrease in reduced travel times between A21 and A22. This is significantly larger than the difference in reduced travel times for the closer shots into these stations. Whitcombe and Maguire (198Ø) interpret a basement refractor with a velocity of 6.4 $km.s^{-1}$ at a depth of 2 to 4 kilometres beneath the Charnian. The apparent velocities observed between A21 and A22 were about 6.8 $km.s^{-1}$. However, the reduced travel time for A24 with respect to A22 fails to show an equivalent apparent velocity. If the high apparent velocity between A21 and A22 is due to a first arrival from a deeper refractor then it is possible that there is an increase in delay time, on this deeper refractor, at station A24. Such an increase might be due to the intrusion of the porphyroids, although these are not known to be deep rooted intrusions. Alternatively the refractor may be Ø.5 to 1.Ø kilometres deeper at the western edge of the Charnian Inlier.

Using velocities of 5.6 and 6.4 $km.s^{-1}$ for the two refractors suggests an offset of 3.6 to 7.2 kilometres for arrivals from a refractor at 2 to 4 kilometres depth. High velocity arrivals from all four shots (Ø1, Ø2, Ø3, Dalby) are observed between stations A21 and A22, indicating crossover distances of 16 to 22 kilometres. This suggests that the arrivals at A22 from the four shots must all originate from the same point on the refractor. The most likely place for this to happen is at the western edge of the Mountsorrel intrusion, which was 3.5 kilometres from A22. The variation in crossover distance suggests that the

higher velocity refractor is either deeper or not present to the east of Mountsorrel.

Similar high velocity arrivals are not detected at the eastern end of profile A, where the shot to receiver distances are up to 25 kilometres. This also suggests that, if present, the high velocity refractor is deeper here than it is under the Charnian Inlier. This is consistent with the results of the Melton Mowbray reflection profile (see below).

### 5.4.3 Profile B

With the exception of the northern part of profile B the reduced travel time sections (figure 5.7) show little structure on the refractor. The NCB seismic reflection data (chapter 4) showed an approximately north-south strike to the Jurassic sediments, and little variation in the thickness of the underlying sediments to the south of station B47.

The reduced travel time sections show that the first arrivals from the Holwell shot at stations to the north of B48 are not from the basement refractor. Similarly the Quenby 1 arrival at B32 is not from the basement refractor.

The rapid increase in reduced travel times to the north of B48 clearly shows the deepening of the basement associated with the margin of the Widmerpool Gulf. To the south of B48 there is only a small scale topography on the refractor and nothing to indicate a lateral change in refractor velocity over the Melton intrusion. The smaller reduced travel times in the vicinity of B37-38 and B33-34 could be due to basement highs or to localised velocity

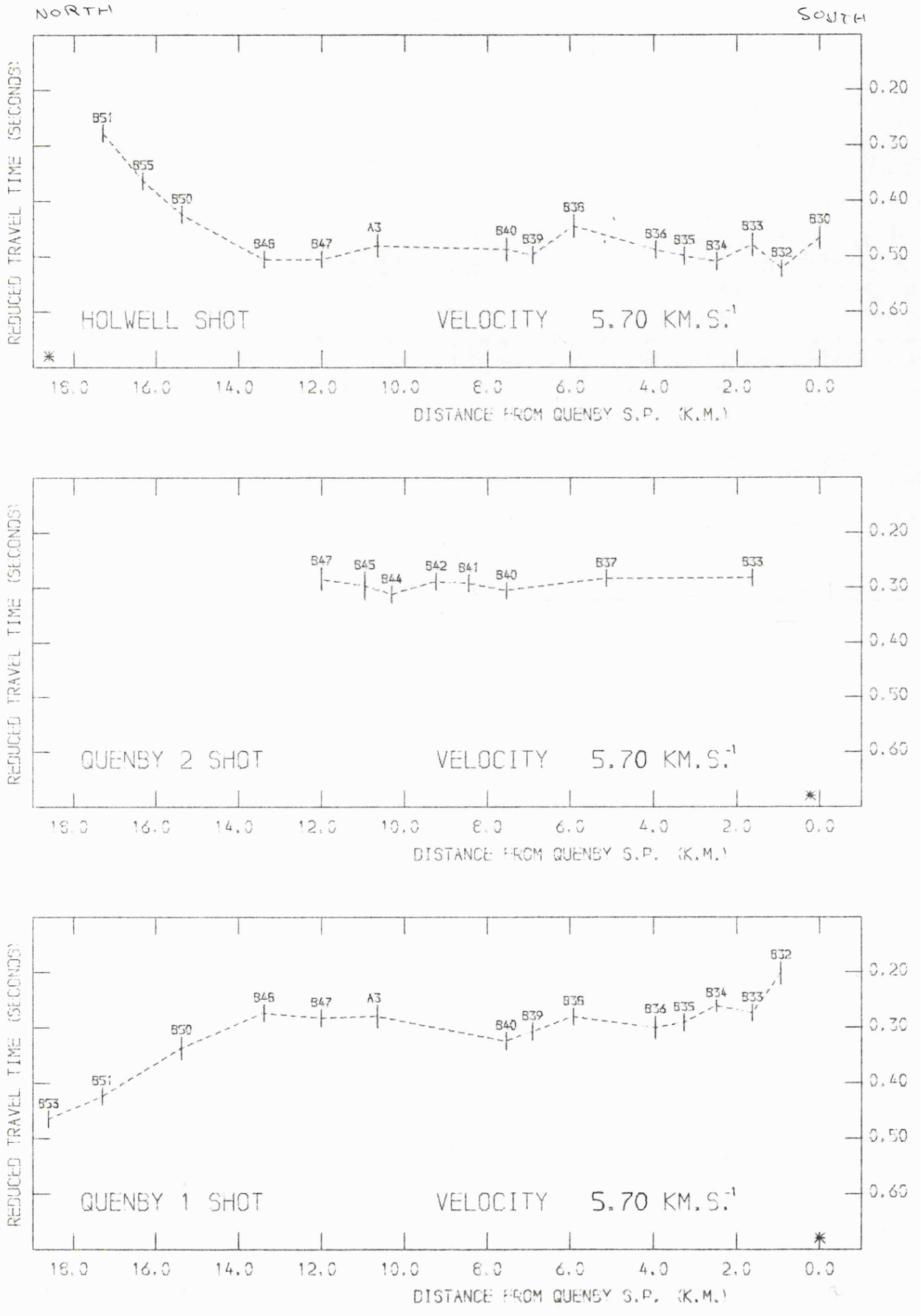


Figure 5.7 : Reduced travel time sections for profile B.

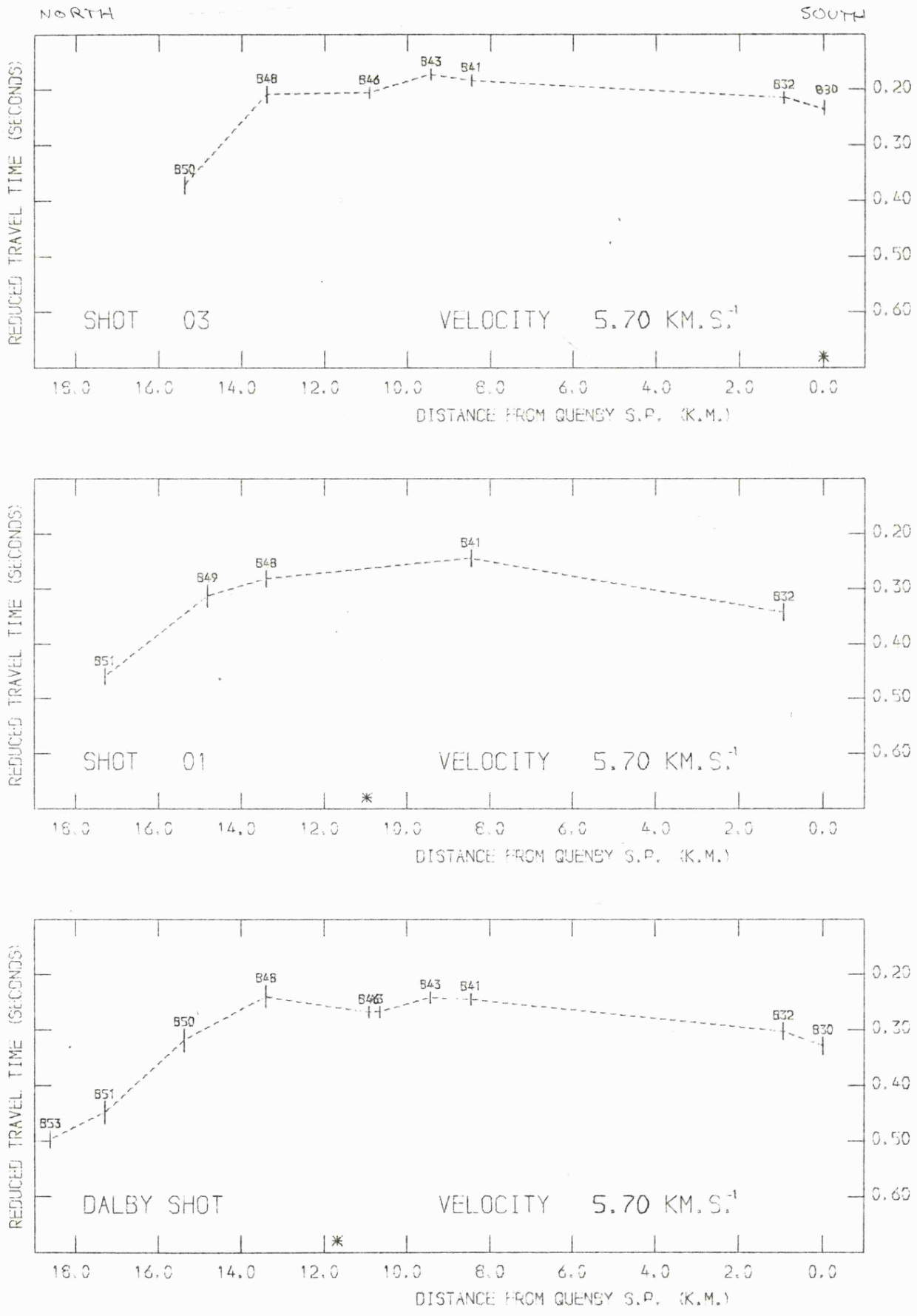


Figure 5.7 continued.

anomalies within the sediments.

The sections for the Holwell and Quenby 1 shots suggest a slight correlation between the reduced travel times and the shot to receiver distances between stations B32-33 and B40. Figure 5.8 shows the data for the Quenby and Holwell shots replotted at a reducing velocity of 5.55 $km.s^{-1}$ The visual correlation between the two sections for the interval from B33 to B40 is better than it was for the reducing velocity of 5.7 $km.s^{-1}$. Since B39 is located on the southern margin of the aeromagnetic anomaly it is possible that a southward decrease in the refractor velocity in this area could correspond to a southward transition from granitic to Charnian type basement. It is equally possible that there is a southward increase in the velocity of the overlying sediments, as would be the case if there was an increasing thickness of Lower Palaeozoic sediments overlying the basement to the south of the intrusion. Such sediments are found at depths of 100-200 metres below OD in boreholes around Leicester.

### 5.4.4 A deeper refractor under profile B

The reduced travel time sections for the Holwell shot (figure 5.7) show a 0.050 second decrease in reduced travel time between B32 and B30 (Quenby 1 shotpoint), at a distance of about 18 kilometres from the Holwell shotpoint. The closer Dalby and 03 shots show an increase in reduced travel times from B32 to B31. The Quenby arrivals at B51 and B53 (the Holwell shotpoint) also have smaller reduced travel times than the arrivals from the Dalby shot whereas for stations to the south of B51 the reduced travel times for

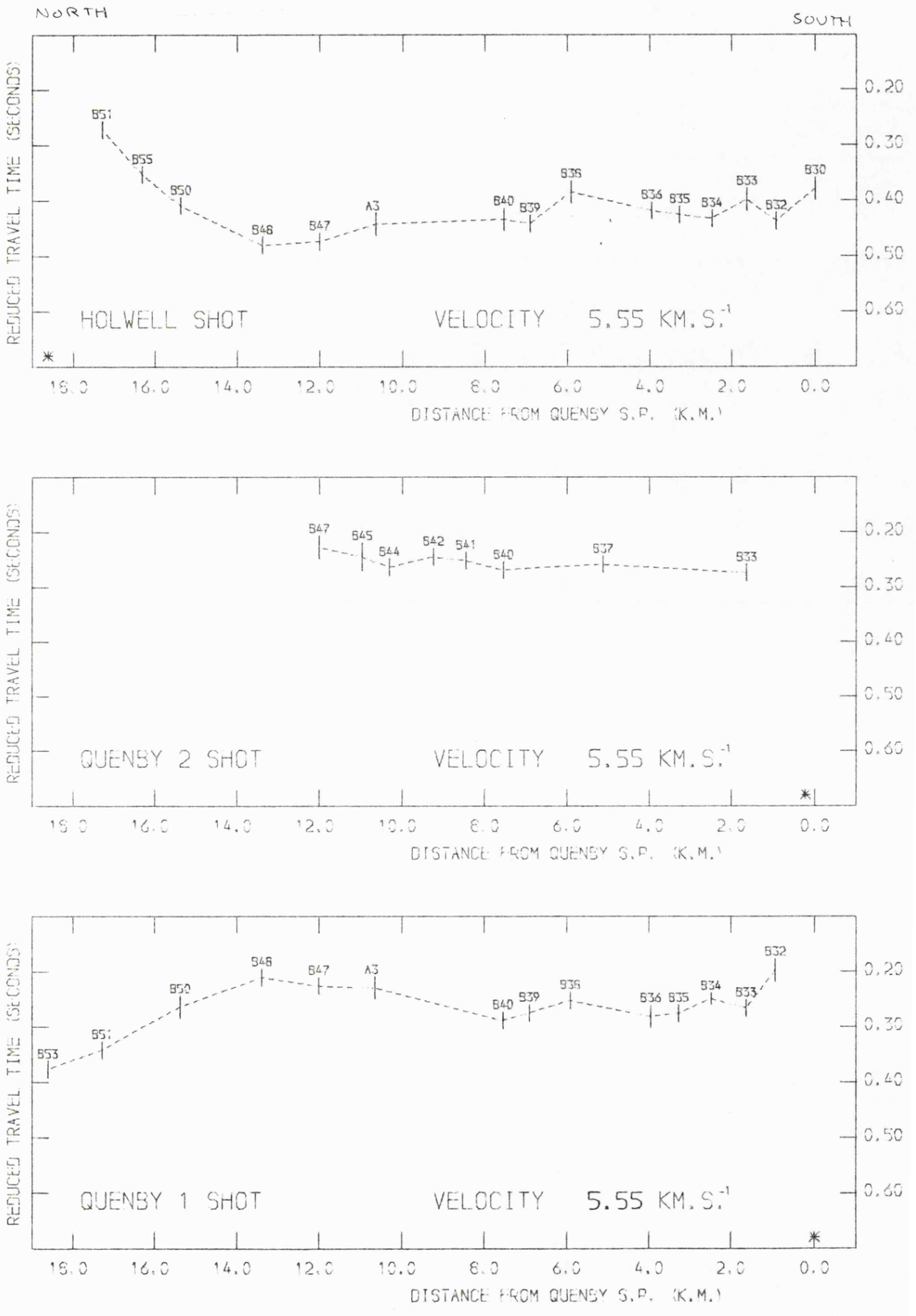


Figure 5.8 : Reduced travel time sections for profile B.

the Dalby and Holwell shots compare closely. The magnitude of the difference at the Holwell shotpoint is harder to determine because of the refractor dip but it is similar to the difference at B3Ø.

It is possible that profile B was just long enough to record first arrivals from a deeper refractor, such as may have been detected under the Charnian Inlier on profile A. If it is assumed that the high velocity refractor is not present beneath the Melton granite then the arrivals at Quenby and Holwell must have been refracted from the deeper layer within about 6 kilometres of the recording sites (using the magnetic anomaly to define the approximate margin of the granite). For velocities of 5.7 and 6.4 $km.s^{-1}$ the refractor would have to be less than 4 kilometres deep to give an offset of 6 kilometres.

## 5.5 TIME TERM SOLUTIONS FOR PROFILE A

As described in section 5.3.2 the quarry blast data were collated to give one set of travel times for each quarry into as many recording sites as possible. The time term solutions were all carried out using this data set, together with the data from each of the controlled shots.

The reduced travel time plots suggested that there were localised velocity variations over the Charnian Inlier. In order that the solution for stations to the east of Mountsorrel would not be affected by velocity variations across the Charnian Inlier profile A was divided at Mountsorrel, and the two parts treated separately in the time term solutions.

5.5.1 Bardon Hill to Mountsorrel (A24-A17)

Because the controlled shots from the eastern end of the profile appeared to indicate a deeper refractor the solution was confined to events from the surrounding quarries.

Station A17 was a telemetered outstation located at Mountsorrel Quarry for the purpose of recording arrivals from other shotpoints. Likewise A24, on Bardon Hill, was adjacent to the quarry. The time term method requires one or more shotpoint to shotpoint linking observations (equivalent to a reciprocal time) but in practice the permanent outstations had to be located up to 300 metres from the quarry faces. In order to make a time term solution possible dummy travel times linking Whitwick, Bardon Hill and Mountsorrel were calculated. These dummy times were determined using the events recorded at A17 and A24, and then calculating an adjusted travel time according to the distance between the two shotpoints compared with the distance to the recording site. The alternative way of dealing with the problem is to assume that the recording station and shotpoint will have the same time term and to treat them as one site. The disadvantage of this method is that it conceals any localised differences between the two time terms.

The first data set consisted of travel times for Mountsorrel, Whitwick and Bardon Hill quarry blasts, together with the Bardon shot, into stations A17 to A24. This gave a total of 7 recording sites, 4 shotpoints and 23 observations. The time term solution (number 1) is given in table 5.5, the solution velocity was 5.63 $km.s^{-1}$ and the F

ratio was 2.09. Given the limited number of recording sites this solution velocity is not significantly different to the previously determined velocities for the Charnian (see above).

A second solution (number 2) was carried out to exclude the arrivals from Whitwick Quarry, which was not used as a recording point and was off line. This gave a solution velocity of 5.57 $km.s^{-1}$ and an F ratio of 0.6 (figure 5.9, table 5.5).

The time terms for the two solutions were similar, the variations resulting largely from the slightly different solution velocities. The stations on exposed basement (A22,A24) and the Bardon Hill (A25) and Whitwick (A28) quarry blasts all had near zero time terms. The Bardon Hill controlled shot (A26) and Mountsorrel (A17,A18) had large positive time terms (0.030 to 0.070 seconds). As discussed above there appears to be a delay associated with the Mountsorrel granodiorite which affects both the shot and receiver time terms. The time term for the Bardon Shot cannot be explained in this way since neither the receiver (A24) nor the quarry blast (A25) have anomalous time terms.

The 0.030 second time term at A26 cannot be explained by site location or timing errors since this would affect the apparent velocity of 5.4 $km.s^{-1}$ determined from the arrival time at the nearby site A24. The Bardon shotpoint, which was not used as a recording station for any other shots, was located on the eastern edge of the Bardon Hill exposure, whereas the recording site and quarry blast were in the centre of the exposure. The basement to the east of the shotpoint (i.e. towards the recording profile) is thought to

dip away steeply. Jones (1927) studied the rocks of Bardon Hill in great detail and mapped a number of faults trending northwest to southeast across the quarry. It is therefore possible that the apparent Ø.Ø3Ø second delay is due to the structure of the basement immediately to the east of the shotpoint. This would not affect the travel times to station A24 which was to the west of the Bardon shotpoint.

The stations not located on exposed basement rocks have positive time terms of up to Ø.Ø57 seconds (table 5.5). In particular between stations A21 and A19 the time terms increase, suggesting that the basement refractor dips east away from the Charnian Inlier and towards the contact with the Mountsorrel granodiorite. A similar increase in time terms would be observed if there was a lateral decrease in either the refractor or overburden velocities.

### 5.5.2 Mountsorrel to Dalby (A18-A1)

The reduced travel times for this part of the profile suggested a refractor velocity of 5.7 $\pm$ Ø.1 km.s$^{-1}$ with a discontinuity between stations A7 and A8.

For an initial time term solution all the arrivals into stations A1 to A16 were used. This gave a data set of 57 observations from 7 shotpoints. No arrivals from the controlled shots were recorded at the Mountsorrel shotpoint.

The first solution (number 3, table 5.5) gave a velocity of 5.71 km.s$^{-1}$ and an F ratio of 1.2. Although no evidence for an increase in velocity with depth was detected from the reduced travel time sections a second solution, in which the arrivals from the more distant Whitwick quarry were excluded from the data set, was tried. The data set was

now restricted to arrivals which originated from shotpoints within the part of the profile being analysed.

The solution velocity for this data set (number 4) was unchanged at 5.71 $km.s^{-1}$ but the F ratio was reduced to Ø.6 (figure 5.9, table 5.5). The time terms for the two solutions compare to better than the observational errors. There is a general eastward increase in time terms and no evidence for deep basement in the area between the two intrusions. The discontinuity between A7 and A8 appears as an increase in time terms of about Ø.Ø3Ø seconds from A7 to A8.

From A14 there is a westward decrease in timeterms up to station A16, which was located on the Mountsorrel granodiorite. Despite being located on exposed basement neither A16 nor the Mountsorrel shotpoint (A18) have zero time terms.

The solution velocities obtained are consistent with previously defined velocities for presumed Precambrian basement in this area, and are significantly higher than any previously determined refractor velocity associated with inferred intrusive igneous basement (chapter 1). The F ratios of about unity indicate that the models are acceptable, but not necessarily unique.

Because of the discontinuity in the time terms between A7 and A8 (correlating with the edge of the magnetic anomaly) and the unexpectedly high velocity recorded over the Melton granite the data set was subdivided for two further solutions.

Stations A1 to A7: The arrivals into stations A1,A3,A4, A5,A7 from all the shotpoints were used. The shotpoint links were well controlled, but the loss of the data from the

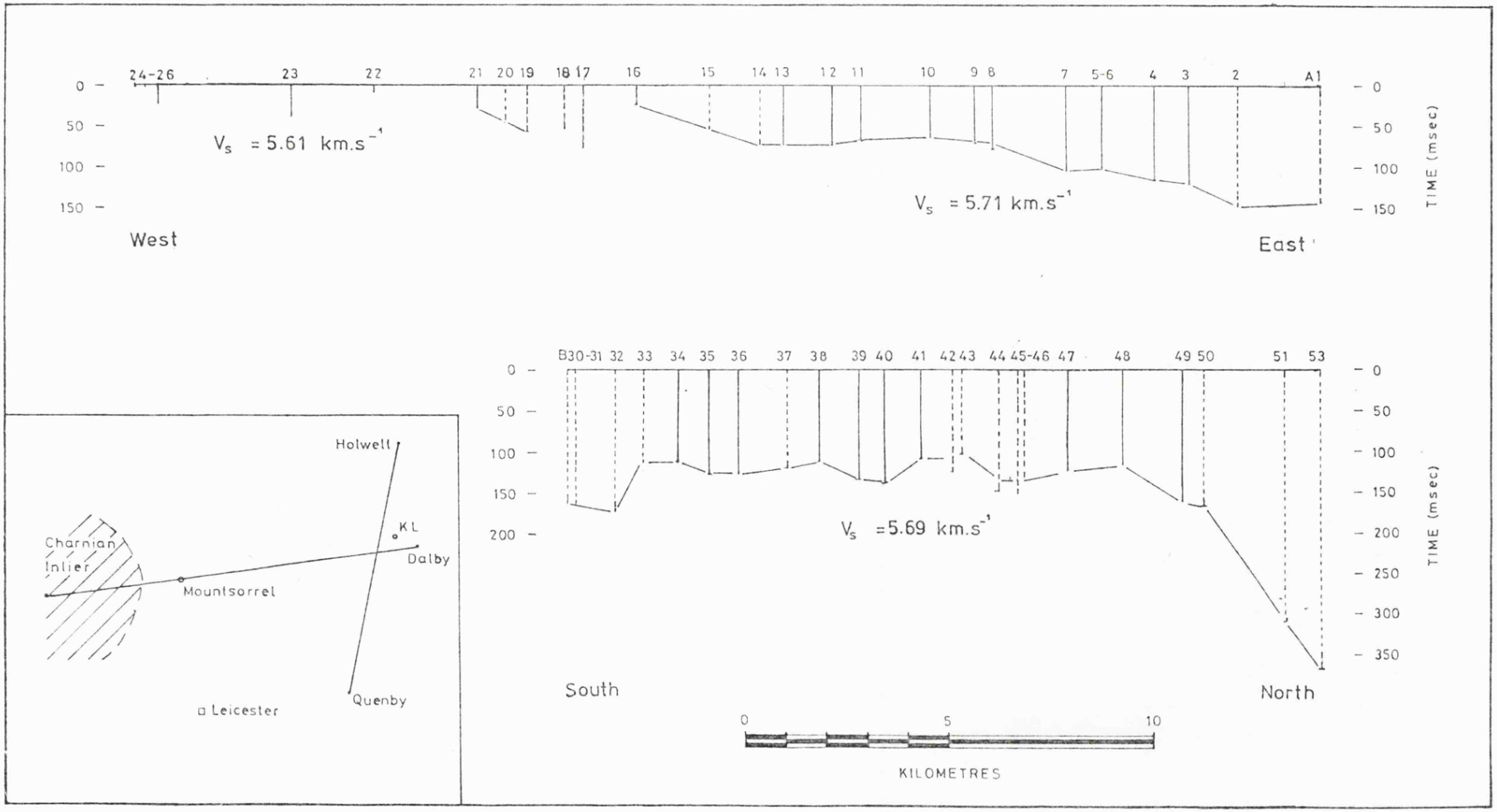


Figure 5.9 : Time term solutions. A dashed line indicates a single or unreversed observation.

Reading recorders limited the reversed cover on the refractor to about 3 kilometres.

The solution (number 5) gave a velocity of 5.79 $km.s^{-1}$ but with a standard error of Ø.Ø6 $km.s^{-1}$. The higher solution velocity, compared with solutions 3 and 4, meant that the excess travel times were taken up by the time terms for the shotpoints Ø1 and Ø2, which were increased by about Ø.Ø1Ø seconds.

Stations A8 to A18: The shotpoint links for this data set were restricted to arrivals from Mountsorrel into Ø2 and Ø3. All the other links involved raypaths outside the part of the profile being analysed. Had these links been used the solution time terms would have been affected by the velocity of the refractor between A1 and A7.

The solution velocity was 5.62 $km.s^{-1}$ and the F ratio about Ø.2. The time terms for this solution (number 6 table 5.5) agreed with those for solutions 3 and 4 within the limits of the observational errors. The values at stations A14 to A16 and the Mountsorrel shotpoint were reduced by up to Ø.ØZØ seconds, giving a near zero time term for A16 and Ø.Ø29 seconds for Mountsorrel. However the only arrival at A16 was from the Dalby shot which had passed through the region with a possible higher refractor velocity between A1 and A7.

### 5.5.3 Conclusions for profile A

The F ratios of solutions 4, 5 and 6 were all less than unity, therefore no one solution can be preferred. If the standard errors are reliable then the solution velocities for the subdivided data sets are significantly different. It

is tempting to say that the possible change in refractor velocity between A7 and A8 represents a transition from typical Charnian basement to a high velocity granitic basement.

For the stations on the Charnian Inlier solution 2 is preferred because of the lower F ratio. For the main part of profile A there is no reason not to use the general solution (4) when calculating depths. The possibility of a higher velocity over the intrusion can be investigated separately with the data from profile B.

## 5.6 TIME TERM ANALYSES FOR PROFILE B

### 5.6.1 An initial solution

The possibility of the Quenby to Holwell reciprocal times being arrivals from a deeper refractor was discussed in section 5.4.4. A first solution was tried using these arrivals, in order to avoid using arrivals from any of the shotpoints from profile A. This solution (number 7, table 5.5) gave a velocity of 5.74 $km.s^{-1}$ and an F ratio of 1.4. However the time terms in the centre of the profile were Ø.Ø3Ø to Ø.Ø6Ø seconds larger than the the solution time terms for the eastern part of profile A. In particular A3, which was used in both solutions, had a much larger time term in this solution, although the arrivals used in the two solutions were from azimuths 9Ø° apart. The increase in time terms cannot be explained by a difference in the solution velocities. If the Quenby to Holwell reciprocal times were arrivals from a deeper refractor then the shotpoint time terms would be underestimated and the receiving station time

| Soln. | 1 | 2 | 3 | 4 | 5 | 6 | | 7 | 8 | 9 | 10 |
|---|---|---|---|---|---|---|---|---|---|---|---|
| STN | | | | | | | STN | | | | |
| A1 | | | 0.143 | 0.142 | 0.159 | 0.107 | B30 | 0.135 | 0.168 | 0.156 | |
| A2 | | | 0.148 | 0.147 | 0.150 | | B31 | 0.140 | 0.162 | | 0.255 |
| A3 | | | 0.118 | 0.116 | 0.109 | | B32 | 0.190 | 0.168 | 0.138 | |
| A4 | | | 0.114 | 0.113 | 0.109 | | B33 | 0.146 | 0.110 | 0.110 | |
| A5 | | | 0.101 | 0.103 | 0.101 | | B34 | 0.152 | 0.117 | 0.114 | |
| A6 | | | 0.102 | 0.102 | | 0.087 | B35 | 0.162 | 0.127 | 0.123 | |
| A7 | | | 0.107 | 0.109 | 0.111 | | B36 | 0.161 | 0.126 | 0.122 | |
| A8 | | | 0.076 | 0.072 | | 0.074 | B37 | 0.150 | 0.120 | 0.106 | |
| A9 | | | 0.070 | 0.073 | | 0.070 | B38 | 0.153 | 0.112 | 0.092 | |
| A10 | | | 0.064 | 0.064 | | 0.063 | B39 | 0.170 | 0.134 | 0.131 | |
| A11 | | | 0.064 | 0.064 | | 0.063 | B40 | 0.173 | 0.138 | 0.129 | |
| A12 | | | 0.072 | 0.069 | | 0.072 | B41 | 0.163 | 0.109 | | 0.114 |
| A13 | | | 0.072 | 0.071 | | 0.066 | B42 | 0.160 | 0.124 | | 0.124 |
| A14 | | | 0.073 | 0.071 | | 0.062 | B43 | | 0.102 | | 0.104 |
| A15 | | | 0.054 | 0.052 | | 0.040 | B44 | 0.185 | 0.148 | | 0.159 |
| A16 | | | 0.024 | 0.021 | | 0.005 | B46 | | 0.128 | | 0.132 |
| A17 | 0.081 | 0.076 | | | | | B47 | 0.160 | 0.124 | | 0.147 |
| A18 | 0.072 | 0.062 | 0.053 | 0.052 | 0.088 | 0.029 | B48 | 0.160 | 0.115 | | 0.135 |
| A19 | 0.061 | 0.057 | | | | | B49 | 0.162 | | | |
| A20 | 0.052 | 0.047 | | | | | B50 | 0.221 | 0.166 | | |
| A21 | 0.018 | 0.027 | | | | | B51 | 0.311 | 0.308 | | |
| A22 | 0.002 | 0.008 | | | | | B53 | 0.355 | 0.366 | | |
| A23 | 0.030 | 0.037 | | | | | A1 | | 0.140 | 0.122 | 0.161 |
| A24 | -0.002 | 0.004 | | | | | A2 | 0.170 | 0.150 | 0.098 | 0.155 |
| A25 | 0.012 | 0.003 | | | | | A3 | 0.185 | 0.119 | | 0.139 |
| A26 | 0.031 | 0.027 | | | | | A4 | | | | 0.131 |
| A28 | 0.012 | | 0.029 | | 0.081 | 0.011 | A6 | | | | 0.103 |
| V | 5.63 | 5.61 | 5.72 | 5.71 | 5.80 | 5.62 | | 5.74 | 5.69 | 5.58 | 6.04 |
| se | 0.04 | 0.02 | 0.20 | 0.02 | 0.06 | 0.02 | | 0.05 | 0.04 | 0.05 | 0.24 |
| F | 0.5 | 0.1 | 0.9 | 0.6 | 0.3 | 0.2 | | 1.3 | 1.4 | 0.7 | 0.8 |

Table 5.5 : Time term solution values.

terms overestimated. The comparison with profile A suggests that this is the case. The Holwell to Quenby reciprocal times, together the Quenby arrival at B51, were therefore removed from the data set.

5.6.2 Solutions using the central shots

In order to provide some shotpoint linking observations the Dalby and Ø1 shots (stations A1,A2) were added to the data set. This gave pairs of reciprocal times between Dalby and Holwell/Quenby as well as Ø1 to Dalby and Quenby 2 (A31) to Ø1. In addition there were some arrivals into the central part of profile from the Dalby shot to fill in the gaps due to the non-recording of the Quenby 1 and Holwell shots.

The solution for this data set (number 8) gave a velocity of 5.69 $km.s^{-1}$ and an F ratio of 1.4. The time terms for the shotpoints and stations that were common to the solutions for profiles A and B agreed to better than the observational errors. The F ratio was small enough to indicate a good solution but, compared with the solutions for profile A, it is higher than might have been expected. If there is a lateral change in the refractor velocity, as was suspected from the reduced travel time data, this could be a source of variance in the solution.

The travel time data were therefore subdivided. The largely unreversed data to the north of B48 were not used and the profile was split between stations B4Ø and B41.

Stations B3Ø to B4Ø: Only one shotpoint (Quenby) was located within this part of the profile, therefore arrivals from the Holwell and Dalby shots also had to be used. The two Quenby shots were treated as one site. The solution velocity for

this data set (number 9) was 5.58 km.s$^{-1}$ and the F ratio was less than unity. The recording station time terms were comparable with those for solution 8, but the time terms for the Holwell and Dalby shotpoints were reduced because of the smaller solution velocity.

Stations B41 to B48: Since the solution for the southern section of the profile gave a lower velocity than the general solution it was to be expected that the solution for this part would give a higher velocity. Using the Quenby 2, Dalby, Ø1, Ø2 and Ø3 shots gave a solution velocity of 6.Ø4 km.s$^{-1}$ (number 1Ø table 5.5). Altering the combination of shotpoints used caused a variation of $\pm$ Ø.2 km.s$^{-1}$ in the solution velocity, although none of the solutions gave an F ratio of greater than unity.

The fact that high solution velocities were obtained from predominantly close range arrivals suggests that the refractor has a high velocity at its top surface. For this reason, together with the low F ratios obtained from the uniform velocity models, a solution in which the refractor velocity increased with depth was not considered.

### 5.6.3 Conclusions for profile B

As with profile A there is some evidence for an increase in refractor velocity correlated with the magnetic anomaly, and hence the Melton granite. The resolution and distribution of the data is such that no one model can be preferred with any statistical justification. The time terms from the general solution (number 8) will be used to calculate the depth models (see below).

The time terms for stations B41-B46 (figure 5.9) showed

a short wavelength variation between adjacent stations of up to Ø.ØØ4Ø seconds. Such a structure was not indicated on the NCB reflection sections (chapter 4). There is a correlation between shotpoint locations and time terms for these stations with the Dalby shot associated with small time terms, and the Quenby 2 shot with larger time terms. This suggests that arrivals from the Quenby 2 shotpoint have been slowed and/or arrivals from the Dalby shotpoint have been speeded up, relative to the 5.7 $km.s^{-1}$ solution velocity.

## 5.7 THE MELTON MOWBRAY SEISMIC REFLECTION LINE

During the course of the refraction experiment a seismic reflection profile was recorded in conjunction with the Institute of Geological Sciences. The reflection recording was in two parts:

1. A two kilometre long profile along a north-south line about one kilometre to the west of the Dalby shotpoint. The data were recorded to 12 seconds two way time (TWT) on a 24 channel Sercel recorder with geophone groups and shotpoints at 5Ø metre spacing, giving a nominal 12 fold cover.

2. A fixed spread, also using a 5Ø metre group interval, laid out westwards from the Dalby shotpoint to record the Dalby, Ø1, Ø2 and Ø3 shots.

The profile is described in Maguire et.al. (1982) and the final section is shown in figure 5.1Ø. From the top of the granite at Ø.25 seconds TWT to about 4.Ø seconds (about 12 kilometres) there are few coherent reflections. The reflectors between Ø.5 and 1.Ø seconds TWT are probably multiples. There are some impersistent reflectors at the

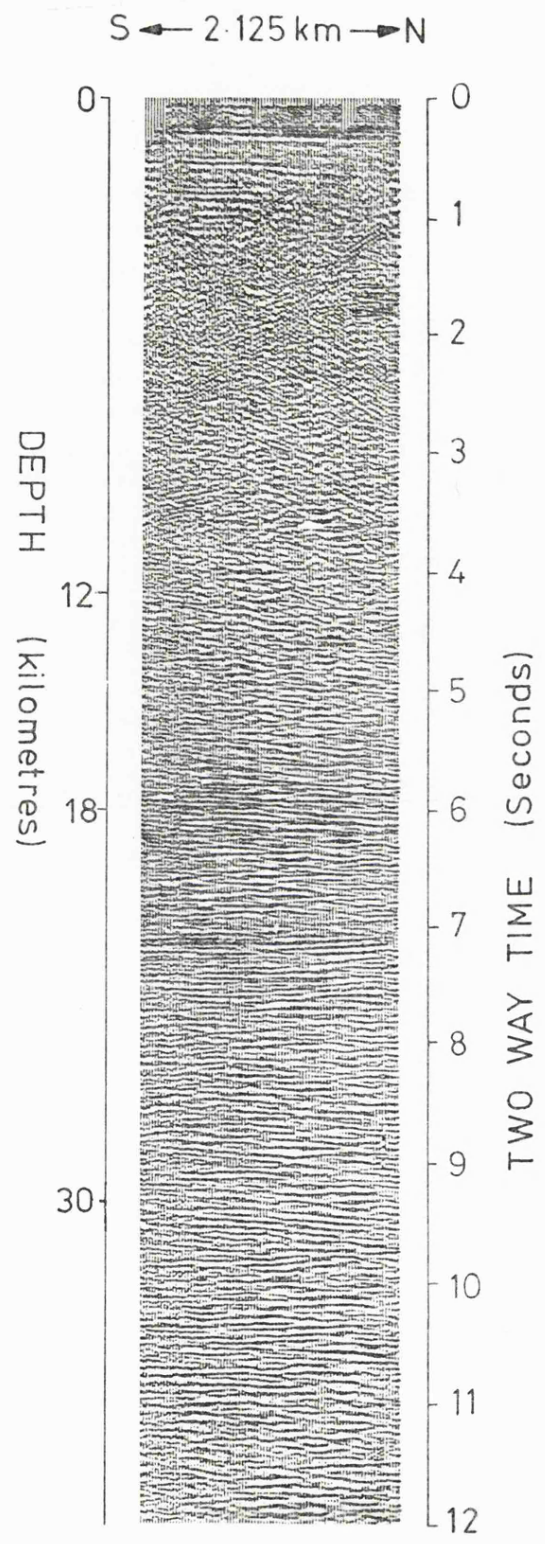


Figure 5.1Ø : The Melton seismic reflection profile.

north end of the profile at about 1.8 seconds TWT. It is difficult to assess the loss of information in this interval caused by to the groundroll, which was observed on the field records to persist to at least 3 seconds TWT. From 4.Ø to 6.Ø seconds there are a number of laterally impersistent reflectors which may indicate some structural or compositional change at the base of the granite. The band of strong reflections seen at 6.Ø seconds TWT (about 18 kilometres) may represent a lower crustal layer, such as was detected by the LISPB experiment.

The first breaks from some of the replotted digital records were picked to determine refractor velocities for the Keuper and, in one case, the basement. The picking accuracy was one sample (Ø.ØØ25 seconds). The velocities determined for the Keuper are as follows: (the peg number refers to the position of the shotpoint on the profile).

| SHOT | AZIMUTH | VELOCITY |
|---|---|---|
| Dalby | west | $3.4 \pm Ø.2$ km.s$^{-1}$ |
| Peg Ø8 | south | $3.2 \pm Ø.2$ km.s$^{-1}$ |
| Peg Ø9 | south | $3.2 \pm Ø.2$ km.s$^{-1}$ |
| Peg 19 | south | $3.5 \pm Ø.2$ km.s$^{-1}$ |

The Ø3 shot into the east-west spread was used to determine the basement refractor velocity. Recognisable first breaks were picked for 18 of the 24 channels at ranges of 4.28 to 5.43 kilometres (1.1 km west of Dalby to Ø.Ø5 km east). The amplitude of the first breaks was small due to the use of in-line arrays of geophones (12 at 4 metres). The refractor velocity, as determined by linear regression, was $6.ØØ \pm Ø.15$ km.s$^{-1}$. The error estimate is for the worst possible case of a systematic error along the recording line.

The line was unreversed and therefore susceptible to refractor dip and to lateral variations in the overburden velocity. The time term solutions in the previous sections, and the structure map for the basement reflector in chapter 4, indicate an eastward dip on the basement of about $1^{\circ}$. The structure map for the base Rhaetic reflector (chapter 4) showed that the Jurassic thickened eastwards by about 10-20 metres in the length of the reflection spread.

The available data suggest that $6.00 \pm 0.15$ km.s$^{-1}$ is a downdip velocity, both in terms of refractor dip and variation in overburden velocity, and is therefore a minimum estimate. This velocity supports the time term models in indicating a velocity for the granitic basement that is higher than typical p-wave velocities for the surrounding Charnian basement.

## 5.8 TIME TO DEPTH CONVERSION

### 5.8.1 Overburden structure

The interpretation of the NCB seismic reflection data (chapter 4) indicated that the Jurassic sediments thickened to the north and east. The Coal Measures and Millstone Grit thinned to the south against the basement high. By using the reflection interpretations, together with the Quenby refraction line (chapter 3B), it was possible to construct a model of the sediment structure along the two refraction profiles (figures 5.11, 5.12). The sedimentary dips in this area are low and the only rapid lateral changes in thickness occur at the two faults which cut the northern part of profile B (see chapter 4).

Only the Long Clawson borehole drilled through the Millstone Grit and into the Lower Carboniferous (gulf facies limestone shales). Extrapolation of the Ø3 "basement" reflector (see chapter 4), from the northern limit of the reflection lines to the Long Clawson borehole, suggested that this reflector represented the base of the Millstone Grit. The base of the Coal Measures could be extrapolated from the Great Framlands borehole to Long Clawson. Hence it was possible to predict the Carboniferous thickness at stations B51 and B53 (the Holwell shotpoint) which lay to the north of the reflection survey.

On the southern part of profile B the Trias was extrapolated southwards at a constant thickness of 225 metres. There is no evidence from south of the Widmerpool Gulf for a greater thickness of Triassic sediments. The sediments between the Trias and the basement refractor were assumed, by analogy with the boreholes around Leicester, to be Lower Palaeozoic shales with a velocity of 3.5 $km.s^{-1}$, as detremined by borehole logging (chapter 1). Carboniferous sediments are not found in boreholes in the area between the Widmerpool Gulf and Northampton (chapter 1).

### 5.8.2 Velocities of the sediments

The velocities used to calculate the depth sections were the same as those given in chapter 4. In addition velocities were required for the Lower Carboniferous and for the near surface weathered layer.

The NCB borehole logs showed velocities of 1.8-2.Ø $km.s^{-1}$ for the uppermost 2Ø-1ØØ metres of most boreholes. The Quenby refraction survey indicated a "weathered" layer 5Ø

metres thick with a velocity of 1.8 $km.s^{-1}$. Similar small scale refraction surveys at Bardon Hill Quarry have shown up to 50 metres of sediments with average velocities of 2.0 $km.s^{-1}$ overlying the Charnian basement. The refraction lines of Davies and Matthews (1966) described in chapter 1 indicated velocities of between 1.8 and 2.1 $km.s^{-1}$ down to a 4.0 $km.s^{-1}$ refractor at a depth of 50 to 65 metres.

The depths to basement were therefore calculated assuming a 50 metre thick weathered layer with a velocity of 2.0 $km.s^{-1}$. In areas where the Drift overlay Keuper a thinner layer (20-30 metres) was assumed to allow for the higher velocity of the weathered Keuper.

No measurements of Lower Carboniferous velocities are known from boreholes in this area. El-Nikhely (1981) derived velocities of 3.8 $km.s^{-1}$ for the Lower Carboniferous, and 4.1 km.s for the sub-Carboniferous, from stacking velocities in the NCB Loughborough prospect. In the absence of any better data a velocity of 4.0 $km.s^{-1}$ was used for the Lower Carboniferous.

The time terms were converted to depths by ray tracing through the sedimentary layercake models. Given that the individual layers were usually less than 250 metres thick, and that the NCB velocity logs did not show any marked velocity gradients within the formations, it was assumed that the layers were of constant velocity.

## 5.9 DISCUSSION

### 5.9.1 The depth sections

The depth sections in figures 5.11 and 5.12 agree with

the depth to the granitic basement in the Kirby Lane borehole and compare reasonably well with the interpretation of the NCB reflection lines (chapter 4). The refractor at the eastern end of profile A, and in the central part of profile B, is therefore interpreted as the top surface of the Melton granite.

The greatest differences between the two interpretations occur to the north of the Kirby Lane borehole where the depths to the refractor are up to 100 metres less than the depths to the 03 reflector. As the reflection lines were datumed to OD and the time terms were calculated relative to the station elevations these differences may be due to variations in the near surface velocities. The arrivals at B48-50 were mostly from updip shotpoints; these arrivals will be offset downdip by up to 0.5 kilometres and would therefore cause an underestimate of the refractor depth relative to the reflection interpretation. It is also possible that the first arrivals at B48-50 were head waves from a sill within the Carboniferous and not from the basement.

The refractor structure between B41 and B46 (figure 5.12) has been smoothed to remove the effects of the variation in time terms for shots at different ranges (see above).

The overburden structure on profile B may appear to be inconsistent in that there is a velocity decrease at the base of the Trias to the north of station B41 and an increase to the south. It was assumed, from the reflection interpretations, that the Carboniferous onlapped the basement high on the southern edge of the Widmerpool Gulf. As discussed above there is no evidence for a continuation

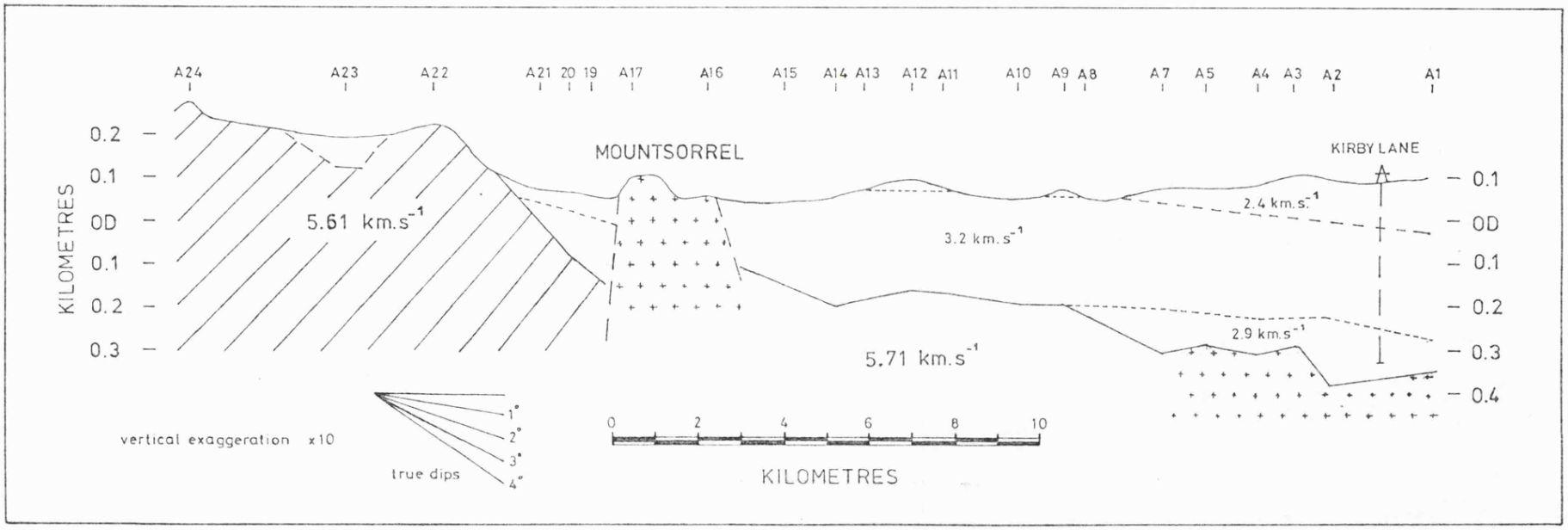


Figure 5.11 : Depth sections for profile A.

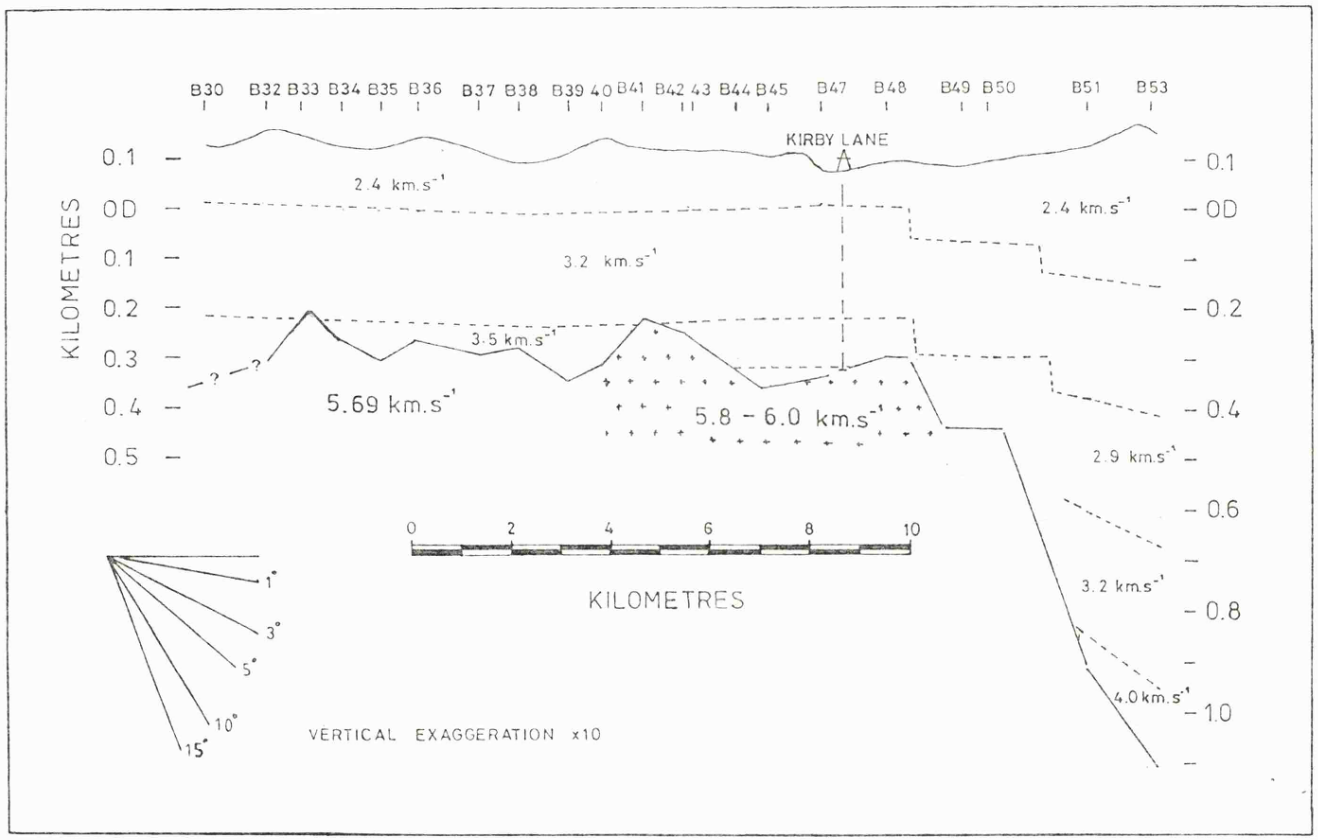


Figure 5.12 : Depth sections for profile B.

of the Carboniferous to the south of the basement high, but there is some evidence for the presence of Lower Palaeozoic shales. If the Melton granite is the same age as the Mountsorrel intrusion it would have been intruded into the Lower Palaeozoic shales, and subsequently eroded before deposition of the Carboniferous sediments.

The assumption that Lower Palaeozoic shales underlie the Trias on the southern part of profile B will cause an overestimate of the depth to basement of up to 50 metres if the sediments are Coal Measures or Millstone Grit.

The calculated depth at the Holwell shotpoint is about 800 metres less than that given by Whitcombe (1979) for the Bardon to Holwell line. The time terms for the shotpoint from the two profiles were similar and the difference in depths is due to the different velocity functions used for the overlying sediments.

The section for profile A shows a westward shallowing of the basement refractor, which agrees with the reflection interpretations. The discontinuity between A7 and A8 is not explained by the low velocity sediments to the east of A8 and is therefore interpreted as structure on the refractor.

### 5.9.2 Refractor velocities

The velocities recorded for the basement refractor over the Melton magnetic anomaly are significantly higher than have previously been observed for presumed igneous basement in this area (Whitcombe and Maguire 1981a). The velocities for the Melton granite lie in the range 5.7-6.0 (?6.2) $km.s^{-1}$ and were determined from the time term solutions of two separate profiles and from the first breaks on the reflect-

ion spread. This high velocity suggests a compositional difference between the Melton and Mountsorrel intrusions and also has important implications for the probable density of the Melton granite when interpreting the gravity anomalies in this area.

The refractor velocities determined for the non magnetic basement (5.55-5.7 $km.s^{-1}$) are consistent with previously determined velocities for the Charnian Inlier and for presumed Precambrian basement (chapter 1).

5.9.3 Mountsorrel

A feature of all the time term solutions for profile A was the large time term associated with the Mountsorrel shotpoint and recording stations. The best explanation for this anomaly is that the Mountsorrel granodiorite has a lower p-wave velocity than the time term solution velocities of 5.7 $km.s^{-1}$. The time term for A16 was about Ø.Ø3Ø seconds smaller than the value for the shotpoint (A18). The two stations were 1.8 kilometres apart, therefore the difference in time terms could be explained by an apparent velocity of 5.2 $km.s^{-1}$ across the granodiorite. The two recording stations at Mountsorrel (A16,A17) were never operational at the same time so that no apparent velocities were recorded. The time term at A16 (Ø.Ø22 seconds) could be accounted for if the arrivals from the Dalby shot had travelled about 1.3 kilometres at a velocity of 5.2 $km.s^{-1}$. A distance of 1.3 kilometres east from A16 is the Soar Valley and the western extension of the Sileby Fault. This could represent the eastern extent of the postulated low velocity granodiorite.

The p-wave velocities of six samples from one piece of

Mountsorrel pink granodiorite were measured under atmospheric conditions, and gave a velocity of 5.28 $\pm$ 0.16 km.s$^{-1}$ (G.Hickman 1980 pers.comm.).

## 5.10 SUMMARY AND CONCLUSIONS

The two profiles have demonstrated that Caledonian igneous intrusions in this area do not always have lower p-wave velocities than the Precambrian basement. There is some evidence to suggest that the Melton granite has a higher velocity than the surrounding basement. This could be taken as an explanation for the absence of a gravity anomaly associated with the intrusion (see chapter 7).

As a result of the absence of a velocity contrast it was not possible to delineate the margins of the Melton intrusion, as had been hoped.

The basement refractor to the east of Mountsorrel dips gently to the east towards the Kirby lane borehole. There is no evidence for a depression in the basement surface correlated with the magnetic low between the Mountsorrel and Melton intrusions.

The basement depths obtained from the refraction profiles will be used to constrain the modelling of the aeromagnetic anomalies (chapter 8A).

# CHAPTER SIX

# PETERBOROUGH SEISMIC REFRACTION PROFILES

## 6.1 INTRODUCTION

The Bouguer gravity map of the Peterborough area (figure 6.1) shows two negative anomalies to the north and northeast of Peterborough. There are a further two anomalies around The Wash. Some or all of these gravity anomalies have been interpreted as either fault bounded sedimentary basins (Allsop and Jones 1981) or granitic intrusions (Westbrook pers. comm.). Chroston and Sola (1982) interpreted a similar gravity anomaly in north Norfolk as a granitic intrusion.

Boreholes in the vicinity of Peterborough show Precambrian and Lower Palaeozoic rocks at depths of 200 to 500 metres below OD (chapters 1 and 9, appendix 1.1). In North Norfolk presumed late Precambrian basement, as seen in boreholes, correlates with refractor velocities of 5.7 to 6.0 $km.s^{-1}$ (Chroston and Sola 1982). Upper Palaeozoic rocks are only found in boreholes further south around Cambridge where they correlate with refractor velocities of 3.5 to 4.2 $km.s^{-1}$ (Bullard 1946, Chroston and Sola 1982).

The aeromagnetic map of the area (figure 6.2) shows that the gravity anomaly to the north of Peterborough correlates with a negative magnetic anomaly. There is, however, a belt of positive anomalies to the southwest of the Peterborough gravity anomaly (see chapter 7). This is a similar situation to the Norfolk anomaly interpreted as an

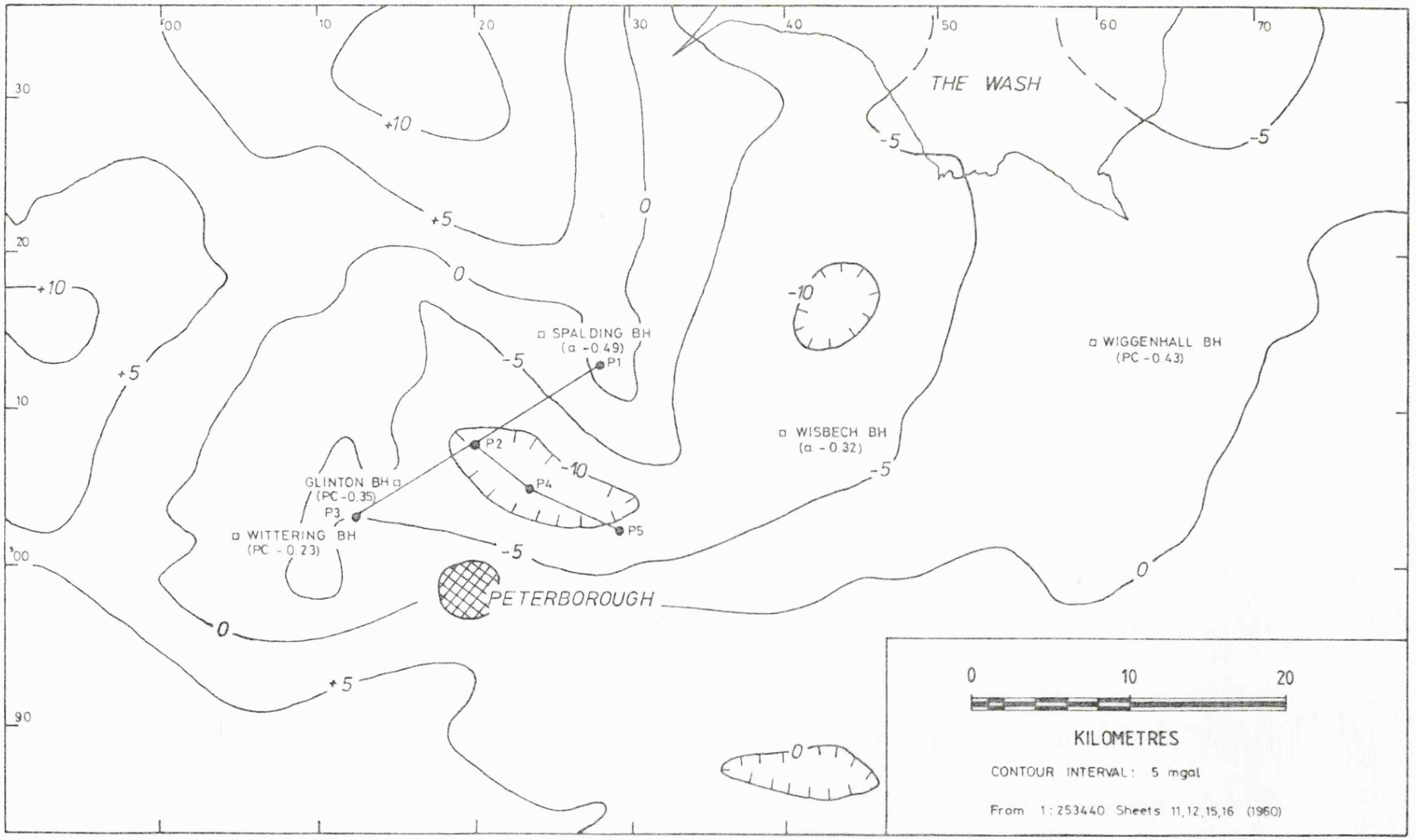


Figure 6. : Bouguer gravity map of the Peterborough area. P1-P5 are shotpoints.

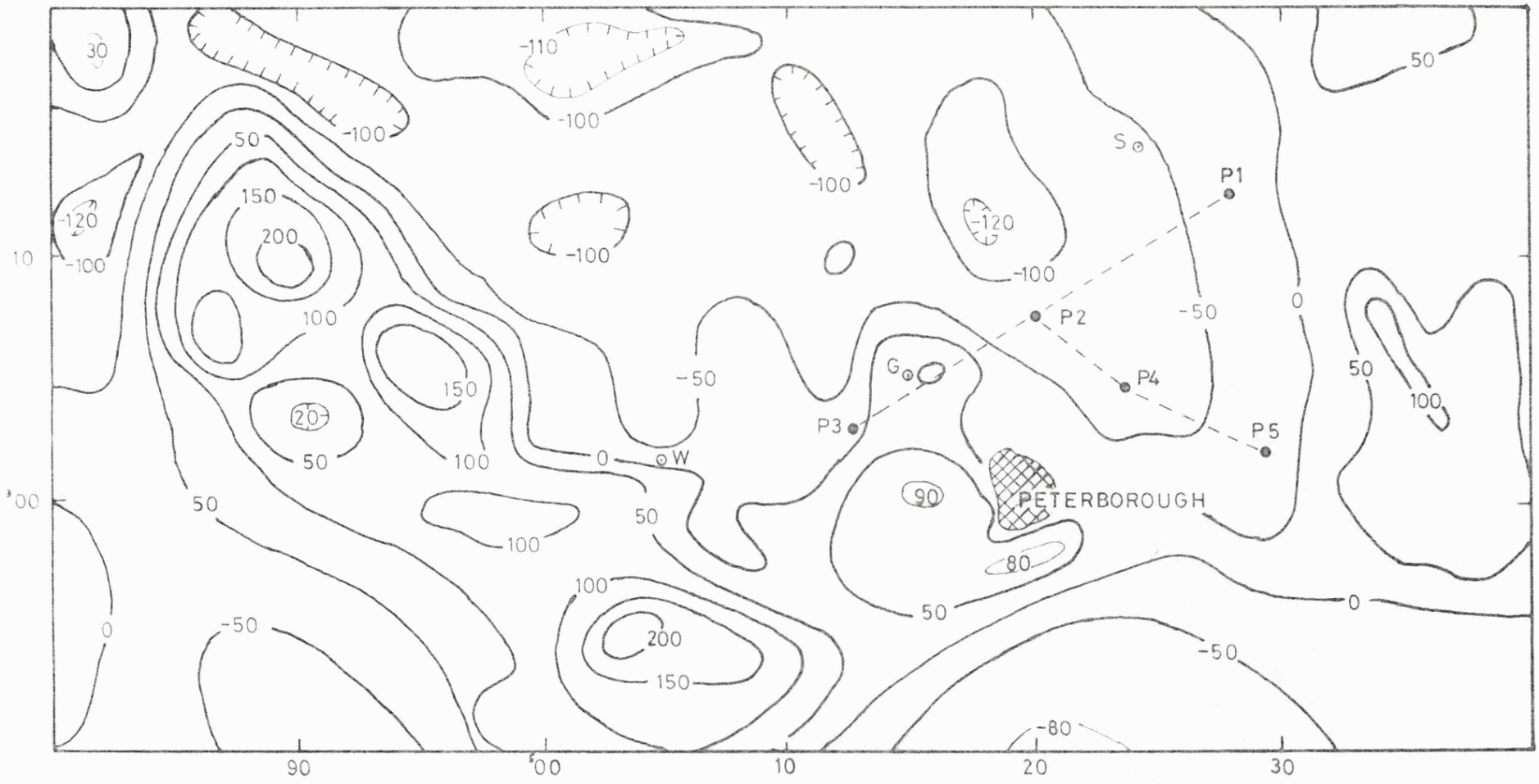


Figure 6.2 : Aeromagnetic anomaly map of the Peterborough area.

intrusion by Chroston and Sola (1982).

The Peterborough gravity anomaly was chosen for further investigation since it had the most pronounced closure and was in the most accessible location. In order to constrain the modelling of the gravity anomaly a seismic refraction experiment was undertaken to determine the depth to basement across the anomaly. The approximate location of the seismic lines is shown in figures 6.1 and 6.2, P1-P5 are the shotpoints used in the experiment.

## 6.2 THE EXPERIMENT

The experiment consisted of two recording profiles, each with three shotpoints (figure 6.3). Profile A was 18 kilometres long and ran southwest to northeast across the northern tip of the gravity anomaly. At its southwestern end (stations A23,24) the profile passed close to the Glinton borehole (Precambrian basement, density 2710 $kg.m^{-3}$ at 350 metres below OD). This profile was designed primarily to locate the margins of the postulated sedimentary basin.

Profile B was 11 kilometres long and ran southeast, from the central shotpoint on profile A, along the axis of the gravity anomaly. This profile was intended to examine the top surface of the granite intrusion, or the basement surface, if either were present at shallow (less than 1 kilometre) depth.

### 6.2.1 Shotpoints

The exact location of the profiles was determined by the availability of suitable shotpoints, as all the shots

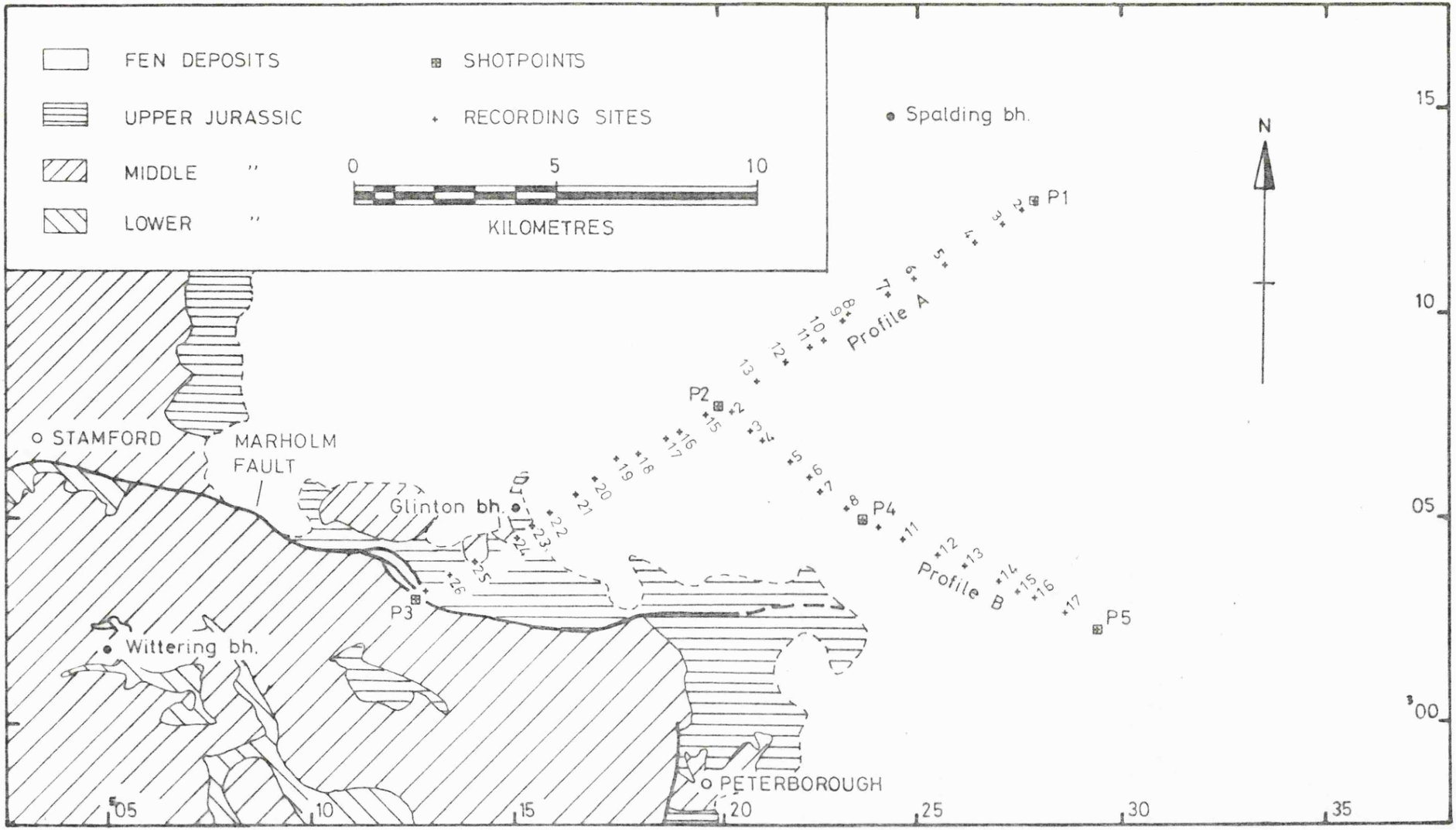


Figure 6.3 : Surface geology and recording station locations.

were to be borehole charges.

The Fenland deposits and the underlying Oxford Clay provided a good medium for auger drilling and gave good ground coupling. The only problems occurred at P1 where sandy deposits prevented deep holes from being drilled and a total of five holes had to be used. Shot P3 was drilled in the Lincolnshire Limestone in a small quarry at Helpston. Originally it was hoped to drill through the 10 metre thick limestone into the underlying clays but the lower sections of the holes cemented up. As a result the shot was fired in fractured sandy limestone and was considerably weaker than the shots fired in clay. This shot was not recorded by the more distant stations.

Where more than one shothole was required the holes were spaced about five metres apart in a line perpendicular to the recording profile. At P3 (Helpston quarry) this was not possible and four holes in a square array were used. The shotpoint data are given in table 6.1.

| SHOT | SITE | NGR E | NGR N | ELEV | CHARGE kg |
|---|---|---|---|---|---|
| P1 | (A1) | 527.90 | 312.59 | 1. | 50. |
| P2A | (A14) | 520.04 | 307.67 | 1. | 25. |
| P3 | (A28) | 512.54 | 302.99 | 25. | 50. |
| P2B | (B1) | 520.08 | 307.64 | 1. | 28. |
| P4 | (B9) | 523.63 | 304.86 | 1. | 15. |
| P5 | (B18) | 529.40 | 302.20 | 1. | 32. |

Table 6.1 : Shotpoint data

All the shots were fired in the early evening (17.ØØ to 19.ØØ BST). There was considerable background noise at the time of some of the earlier shots but it was not possible to shoot any later as the equipment had to be collected in each evening.

### 6.2.2 Recording Stations

The recording stations were sited between the shot-points at spacings of Ø.5 to 1.Ø kilometres (figure 6.3). The recording equipment comprised eight MARS sets, eight Reading single channel cassette recorders and ten Durham single channel recorders. The equipment is described in chapter 2. By using landlines from some of the MARS recorders, to give an extra vertical geophone station, it was possible to occupy 28 stations on profile A, plus shotpoints P4 and P5, for the recording of shots P1, P2, P3 on the first day of the experiment. For profile B, which was recorded on a separate day, 18 sites were occupied on the profile together with 1Ø sites on profile A. The sites on profile A (A4 to A13) were reoccupied to give a fan-shoot across the eastern margin of the gravity anomaly in order to delineate any lateral velocity change within the basement, although in the light of the Melton experiment such lateral changes were by no means certain.

The depth to basement at shotpoints P1 and P3 was thought, from nearby boreholes, to be less than 5ØØ metres, giving an expected crossover distance of less than two kilometres.

| SITE | NGR E | NGR N | ELEV | SEISMO. | | RECORDER | |
|---|---|---|---|---|---|---|---|
| | | | | day 1 | day 2 | 1 | 2 |
| A1 | 527.90 | 312.59 | 1 | HS10 | WII | M | D3 |
| A2 | 527.60 | 312.36 | 1 | HS10 | | c | |
| A3 | 527.11 | 312.06 | 1 | HS10 | | c | |
| A4 | 526.41 | 311.62 | 1 | WIII | WIII | D1 | D1 |
| A5 | 525.65 | 310.99 | 1 | WIII | WIII | D1 | D1 |
| A6 | 524.92 | 310.69 | 1 | WIII | WIII | D2 | D2 |
| A7 | 524.25 | 310.33 | 3 | WIII | WIII | D2 | D2 |
| A8 | 523.49 | 309.74 | 2 | WIII | WIII | D2 | D2 |
| A9 | 523.19 | 309.70 | 2 | WIII | WIII | D2 | D2 |
| A10 | 522.68 | 309.24 | 1 | WII | WII | D3 | D3 |
| A11 | 522.36 | 309.08 | 1 | WII | | D3 | |
| A12 | 521.76 | 308.72 | 1 | WII | HS10 | D3 | R |
| A13 | 521.02 | 308.24 | 2 | WII | WII | D3 | R |
| A14 | 520.06 | 307.65 | 1 | HS10 | | M | |
| A15 | 519.71 | 307.42 | 2 | HS10 | | c | |
| A16 | 519.05 | 306.99 | 3 | HS10 | | M | |
| A17 | 518.76 | 306.86 | 3 | HS10 | | c | |
| A18 | 518.06 | 306.47 | 3 | HS10 | | R | |
| A19 | 517.51 | 306.21 | 3 | HS10 | | M | |
| A20 | 516.94 | 305.90 | 4 | HS10 | | R | |
| A21 | 516.49 | 305.51 | 7 | HS10 | | M | |
| A22 | 515.86 | 305.04 | 10 | HS10 | | M | |
| A23 | 515.37 | 304.75 | 9 | HS10 | | M | |
| A24 | 515.03 | 304.44 | 8 | HS10 | | M | |
| A25 | 514.01 | 303.89 | 8 | WII | | R | |
| A26 | 513.37 | 303.53 | 10 | HS10 | | R | |
| A27 | 512.73 | 303.14 | 20 | WII | | R | |
| A28 | 512.54 | 302.99 | 25 | HS10 | | R | |

Table 6.2a : Recording site data for profile A

| SITE | NGR E | NGR N | ELEV | SEISMO. | | RECORDER | |
|---|---|---|---|---|---|---|---|
| | | | | day 1 | day 2 | 1 | 2 |
| B1 | 520.06 | 307.65 | 1 | | HS10 | | M (day 1=A14) |
| B2 | 520.36 | 307.46 | 1 | | HS10 | | M |
| B3 | 520.88 | 307.02 | 1 | | WII | | R |
| B4 | 521.17 | 306.79 | 1 | | WII | | D3 |
| B5 | 521.84 | 306.25 | 1 | | WII | | D3 |
| B6 | 522.30 | 305.87 | 1 | | HS10 | | M |
| B7 | 522.59 | 305.55 | 1 | | HS10 | | M |
| B8 | 523.25 | 305.16 | 1 | | HS10 | | M |
| B9 | 523.63 | 304.86 | 1 | WII | HS10 | R | M |
| B10 | 524.02 | 304.69 | 1 | | HS10 | | c |
| B11 | 524.64 | 304.38 | 1 | | HS10 | | M |
| B12 | 525.48 | 303.98 | 3 | | HS10 | | R |
| B13 | 526.09 | 303.71 | 2 | | HS10 | | R |
| B14 | 526.98 | 303.35 | 1 | | HS10 | | c |
| B15 | 527.39 | 303.11 | 1 | | HS10 | | M |
| B16 | 527.84 | 302.96 | 5 | | WII | | R |
| B17 | 528.58 | 302.59 | 1 | | WII | | R |
| B18 | 529.40 | 302.20 | 1 | WII | WII | R | R |

W = Willmore mk II/III  R = Reading cassette recorder

M = MARS recorder  c = cabled outstation (to MARS)

D1,D2,D3 = Durham type 1,2,3 recorders

Table 6.2b : Recording site data for profile B

The locations of the recording stations, and the details of the equipment used, are given in table 6.2. With the exception of the stations near Helpston quarry the station elevations were less than five metres above OD.

The MARS and Durham recorders were manned for all the shots and therefore the gain settings could be changed between shots. The Reading recorders were usually run in automatic mode and therefore the gain settings could not be changed when two shots were fired in the same shot window (P1,P2A and P4,P2B).

## 6.3 THE TRAVEL TIME DATA

Despite the variety of recording equipment used it was possible to establish, by graphical correlation, that the same phase was picked on all the records for each shot. Particular attention was paid to the polarity of the first arrival as a means of ensuring continuity.

The signal to noise ratios for the first arrivals were generally between three and ten to one. The only poor quality data were from the Durham type 2 recorders at A6 and A9, where the first arrivals from the more distant shots were very weak. This problem was due to an apparent 10 Hz. high cut in the recorded signals which was itself due to the very low carrier frequency used by these recorders (see chapter 2). The MSF time signal recorded by the Durham type 3 recorders at A10-13 and B4,5 was put onto the tape in unmodulated form; this produced a very noisy signal on replay. It was found that the most reliable location of the timing mark could be obtained from the high to low

transition at the end of the MSF pulse. This transition occurs at Ø.1ØØ or Ø.2ØØ seconds after the second epoch depending on the binary code which the pulse carries.

The first arrival onset times were picked as described in chapter 2. The shot times were corrected to a surface datum using the uphole times from the MSF-triggered automatic blaster or, if these were not available, the hole depths and an assumed near surface velocity of 1.8 $km.s^{-1}$ derived from the Nimbus recordings (see below). First arrivals for the weak shot from P3 could not be picked for stations to the east of A1Ø (except A2).

If recovered data are defined as the events that give a pickable first arrival time, the data recovery was as follows:

| | MARS | READING | DURHAM | TOTAL |
|---|---|---|---|---|
| No. of recorders/day | 8 | 8 | 1Ø | 26 |
| Max. possible events | 66 | 48 | 6Ø | 174 |
| No. events recovered | 58 | 4Ø | 33 | 131 |
| Recovery | 85% | 83% | 55% | 75% |

The final data set consisted of 131 events from five shotpoints recorded at a total of 41 sites (25 on profile A and 16 on profile B).

SHOT P1 15-09-81 19-06-00.869

| STN | D km | T sec | E sec |
|---|---|---|---|
| A28 | 18.11 | 3.468 | 0.010 |
| A27 | 17.87 | 3.435 | 0.010 |
| A26 | 17.12 | 3.270 | 0.015 |
| A24 | 15.23 | 2.915 | 0.015 |
| A23 | 14.78 | 2.865 | 0.020 |
| A22 | 14.21 | 2.761 | 0.015 |
| A21 | 13.43 | 2.626 | 0.020 |
| A20 | 12.84 | 2.534 | 0.010 |
| A19 | 12.19 | 2.431 | 0.020 |
| A18 | 11.59 | 2.332 | 0.010 |
| A17 | 10.79 | 2.185 | 0.020 |
| A16 | 10.47 | 2.135 | 0.010 |
| A15 | 9.69 | 2.002 | 0.010 |
| A14 | 9.27 | 1.935 | 0.010 |
| A12 | 7.26 | 1.588 | 0.015 |
| A11 | 6.56 | 1.488 | 0.020 |
| A10 | 6.20 | 1.414 | 0.010 |
| A9 | 5.53 | 1.282 | 0.015 |
| A8 | 5.25 | 1.223 | 0.020 |
| A7 | 4.29 | 1.055 | 0.020 |
| A4 | 1.78 | 0.593 | 0.010 |
| A3 | 0.95 | 0.358 | 0.010 |
| A2 | 0.38 | 0.176 | 0.010 |
| B9 | 8.83 | 1.783 | 0.010 |
| B18 | 10.50 | 2.176 | 0.010 |

SHOT P2A 15-09-81 18-49-59.994

| STN | D km | T sec | E sec |
|---|---|---|---|
| A28 | 8.84 | 1.877 | 0.010 |
| A27 | 8.60 | 1.849 | 0.010 |
| A26 | 7.85 | 1.685 | 0.015 |
| A24 | 5.96 | 1.325 | 0.010 |
| A23 | 5.51 | 1.259 | 0.010 |
| A22 | 4.94 | 1.157 | 0.010 |
| A21 | 4.16 | 1.022 | 0.010 |
| A20 | 3.57 | 0.926 | 0.010 |
| A19 | 2.92 | 0.824 | 0.010 |
| A18 | 2.32 | 0.717 | 0.010 |
| A17 | 1.51 | 0.575 | 0.010 |
| A16 | 1.20 | 0.521 | 0.010 |
| A12 | 2.02 | 0.698 | 0.015 |
| A11 | 2.71 | 0.816 | 0.015 |
| A10 | 3.07 | 0.878 | 0.015 |
| A9 | 3.75 | 0.985 | 0.020 |
| A7 | 4.98 | 1.193 | 0.020 |
| A6 | 5.74 | 1.342 | 0.020 |
| A3 | 8.32 | 1.780 | 0.010 |
| A2 | 8.90 | 1.895 | 0.010 |
| B9 | 4.56 | 1.117 | 0.015 |

SHOT P3 15-09-81 17-34-58.006

| STN | D km | T sec | E sec |
|---|---|---|---|
| A27 | 0.24 | 0.101 | 0.003 |
| A25 | 1.72 | 0.608 | 0.005 |
| A24 | 2.88 | 0.805 | 0.010 |
| A23 | 3.33 | 0.875 | 0.010 |
| A22 | 3.90 | 0.978 | 0.010 |
| A21 | 4.69 | 1.122 | 0.010 |
| A20 | 5.28 | 1.229 | 0.015 |
| A19 | 5.92 | 1.342 | 0.010 |
| A18 | 6.53 | 1.458 | 0.015 |
| A17 | 7.33 | 1.592 | 0.020 |
| A16 | 7.64 | 1.640 | 0.010 |
| A15 | 8.43 | 1.789 | 0.010 |
| A14 | 8.85 | 1.867 | 0.010 |
| A12 | 10.86 | 2.235 | 0.010 |
| A11 | 11.56 | 2.344 | 0.015 |
| A10 | 11.91 | 2.416 | 0.010 |
| A2 | 17.74 | 3.422 | 0.015 |

SHOT P2B 17-09-81 19-05-05.323

| STN | D km | T sec | E sec |
|---|---|---|---|
| B2 | 0.33 | 0.122 | 0.010 |
| B3 | 1.01 | 0.340 | 0.010 |
| B4 | 1.38 | 0.547 | 0.015 |
| B5 | 2.24 | 0.700 | 0.015 |
| B7 | 3.27 | 0.870 | 0.010 |
| B8 | 4.02 | 1.001 | 0.010 |
| B9 | 4.51 | 1.106 | 0.010 |
| B10 | 4.92 | 1.173 | 0.010 |
| B11 | 5.61 | 1.288 | 0.010 |
| B12 | 6.52 | 1.460 | 0.010 |
| B14 | 8.12 | 1.750 | 0.010 |
| B15 | 8.60 | 1.822 | 0.010 |
| B16 | 9.06 | 1.927 | 0.010 |
| B18 | 10.79 | 2.209 | 0.010 |
| A13 | 1.12 | 0.402 | 0.020 |
| A12 | 2.00 | 0.686 | 0.010 |
| A10 | 3.05 | 0.867 | 0.010 |
| A9 | 3.73 | 0.977 | 0.020 |
| A4 | 7.48 | 1.625 | 0.050 |

SHOT P4 17-09-81 18-49-41.967

| STN | D km | T sec | E sec |
|---|---|---|---|
| B1 | 4.53 | 1.114 | 0.015 |
| B2 | 4.18 | 1.054 | 0.010 |
| B3 | 3.50 | 0.935 | 0.010 |
| B4 | 3.13 | 0.842 | 0.010 |
| B5 | 2.27 | 0.710 | 0.010 |
| B7 | 1.25 | 0.514 | 0.010 |
| B8 | 0.48 | 0.201 | 0.010 |
| B11 | 1.12 | 0.402 | 0.010 |
| B12 | 2.05 | 0.674 | 0.010 |
| B14 | 3.67 | 0.972 | 0.010 |
| B15 | 4.15 | 1.047 | 0.010 |
| B16 | 4.62 | 1.150 | 0.010 |
| B17 | 5.45 | 1.296 | 0.015 |
| B18 | 6.35 | 1.431 | 0.010 |
| A13 | 4.27 | 1.083 | 0.010 |
| A12 | 4.29 | 1.097 | 0.010 |
| A10 | 4.48 | 1.149 | 0.010 |
| A9 | 4.86 | 1.193 | 0.015 |
| A8 | 4.88 | 1.192 | 0.015 |
| A7 | 5.51 | 1.275 | 0.020 |
| A6 | 5.97 | 1.377 | 0.015 |

SHOT P5 17-09-81 17-36-02.110

| STN | D km | T sec | E sec |
|---|---|---|---|
| B1 | 10.81 | 2.214 | 0.010 |
| B2 | 10.46 | 2.135 | 0.015 |
| B3 | 9.79 | 2.025 | 0.020 |
| B4 | 9.42 | 1.937 | 0.010 |
| B7 | 7.59 | 1.617 | 0.020 |
| B8 | 6.83 | 1.498 | 0.015 |
| B9 | 6.35 | 1.417 | 0.015 |
| B10 | 5.93 | 1.328 | 0.010 |
| B11 | 5.24 | 1.208 | 0.010 |
| B12 | 4.31 | 1.080 | 0.010 |
| B14 | 2.68 | 0.753 | 0.010 |
| B15 | 2.21 | 0.676 | 0.010 |
| A13 | 10.33 | 2.142 | 0.010 |
| A12 | 10.04 | 2.086 | 0.010 |
| A10 | 9.73 | 2.060 | 0.015 |
| A9 | 9.74 | 2.030 | 0.020 |
| A8 | 9.58 | 1.996 | 0.010 |
| A6 | 9.60 | 1.971 | 0.015 |

Table 6.3 : Travel time data for profiles A and B.

### 6.3.1 Errors

The maximum observational errors associated with the travel time data (table 6.3) reflect the confidence with which the various first arrivals could be picked. Most of the errors lie in the range $\pm$ Ø.ØlØ to Ø.Ø2Ø seconds. Given these errors any difference in delay time between two sites of less than Ø.Ø2Ø seconds cannot be regarded as significant. This gives a resolution limit on the refractor topography of about 7Ø metres for good quality data. In practice the technique of correlating graphically between arrivals at adjacent sites means that the relative delay time for a pair of recording sites is generally determined to better than Ø.Ø2Ø seconds. This feature is especially useful in the study of reduced travel time graphs for individual shots.

An estimate of the real travel time errors can be obtained from the reciprocal times between shotpoints (table 6.4). The differences in travel times were, in all the cases, less than the estimated maximum observational errors. The repeated shots from P2 into stations A9,AlØ,Al2 also show a close agreement in travel times, the differences being less than Ø.ØlØ seconds. The recorder at Al2 was a Durham type 3 for shot P2A and a Reading cassette for P2B. The agreement in travel times for this station indicates that the unmodulated MSF signal on the Durham recorder did not affect the accuracy of the travel time pick.

| SHOT | RECEIVER | TIME | DIFFERENCE |
|---|---|---|---|
| P3 | A14 | 1.865 | Ø.Ø12 |
| P2A | A28 | 1.877 | |
| P2A | A1 | 1.95Ø* | Ø.Ø15 |
| P1 | A14 | 1.935 | |
| P2A | B9 | 1.111 | |
| P2B | B9 | 1.11Ø | Ø.ØØ4 |
| P4 | B1 | 1.114 | |
| P2B | B18 | 2.211 | Ø.ØØ1 |
| P5 | B1 | 2.212 | |
| P4 | B18 | 1.431 | Ø.Ø14 |
| P5 | B9 | 1.417 | |

* : no arrival, time determined by linear regression

| RECEIVER | P2A TIME | P2B TIME | DIFFERENCE |
|---|---|---|---|
| A12 | Ø.694 | Ø.686 | Ø.ØØ6 |
| A1Ø | Ø.874 | Ø.867 | Ø.ØØ7 |
| A9 | Ø.981 | Ø.977 | Ø.ØØ4 |

Table 6.4 : Comparison of travel times

## 6.4 TIME:DISTANCE GRAPHS

Figures 6.4 and 6.5 are time distance graphs for profiles A and B respectively. The straight lines were fitted to the first arrival times by linear regression and indicate apparent velocities of 5.63 to 5.82 $km.s^{-1}$ for profile A and 5.43 to 5.64 $km.s^{-1}$ for profile B. Given the observational errors, which are shown by the vertical bars, most of the travel times lie on the regressed line indicating that there is no major structure on the refractor. The intercept times are in the range Ø.28 to Ø.33 seconds which suggests a shallow depth to the refractor along both profiles.

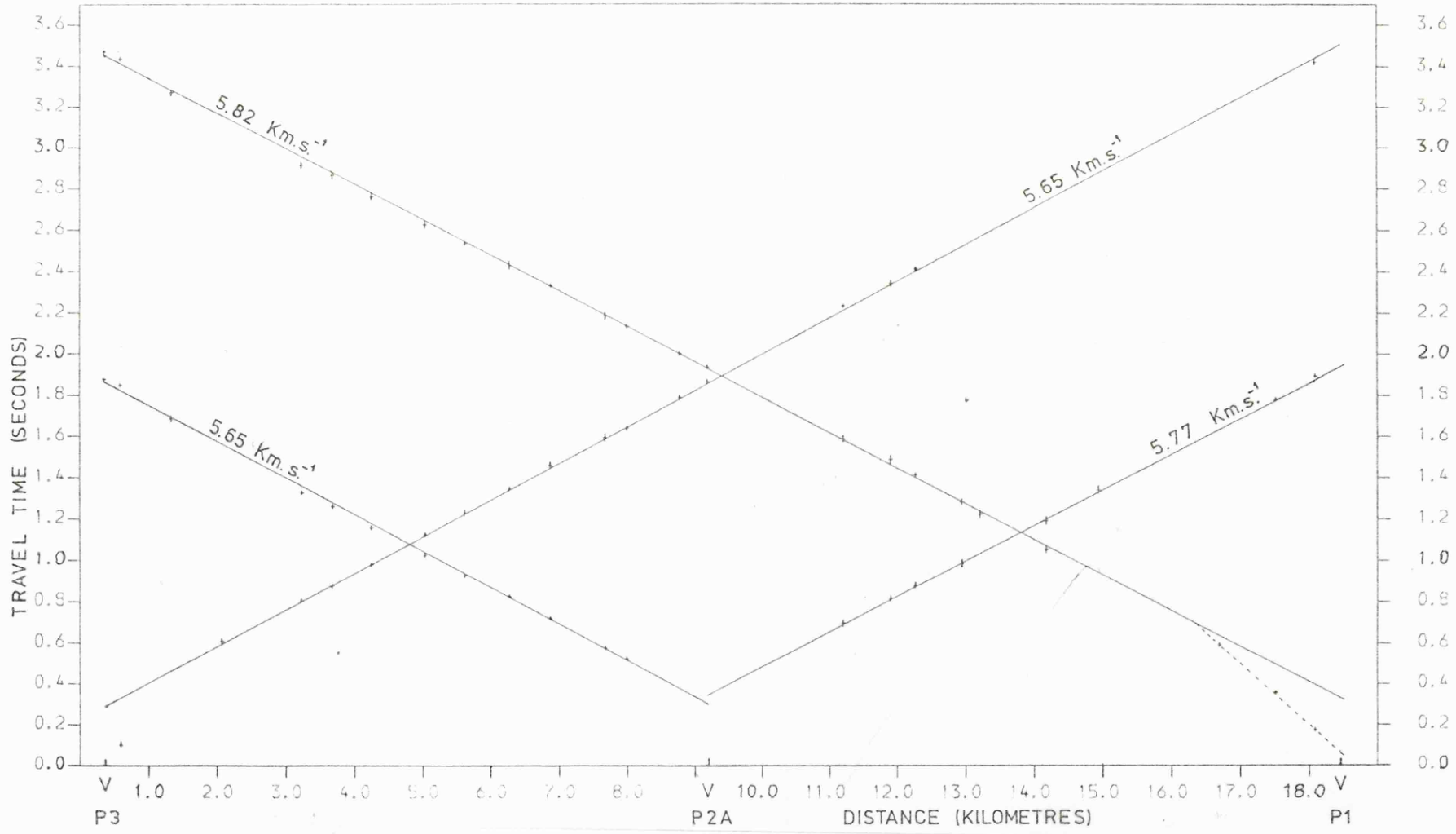


Figure 6.4 : Time-distance graphs for profile A.

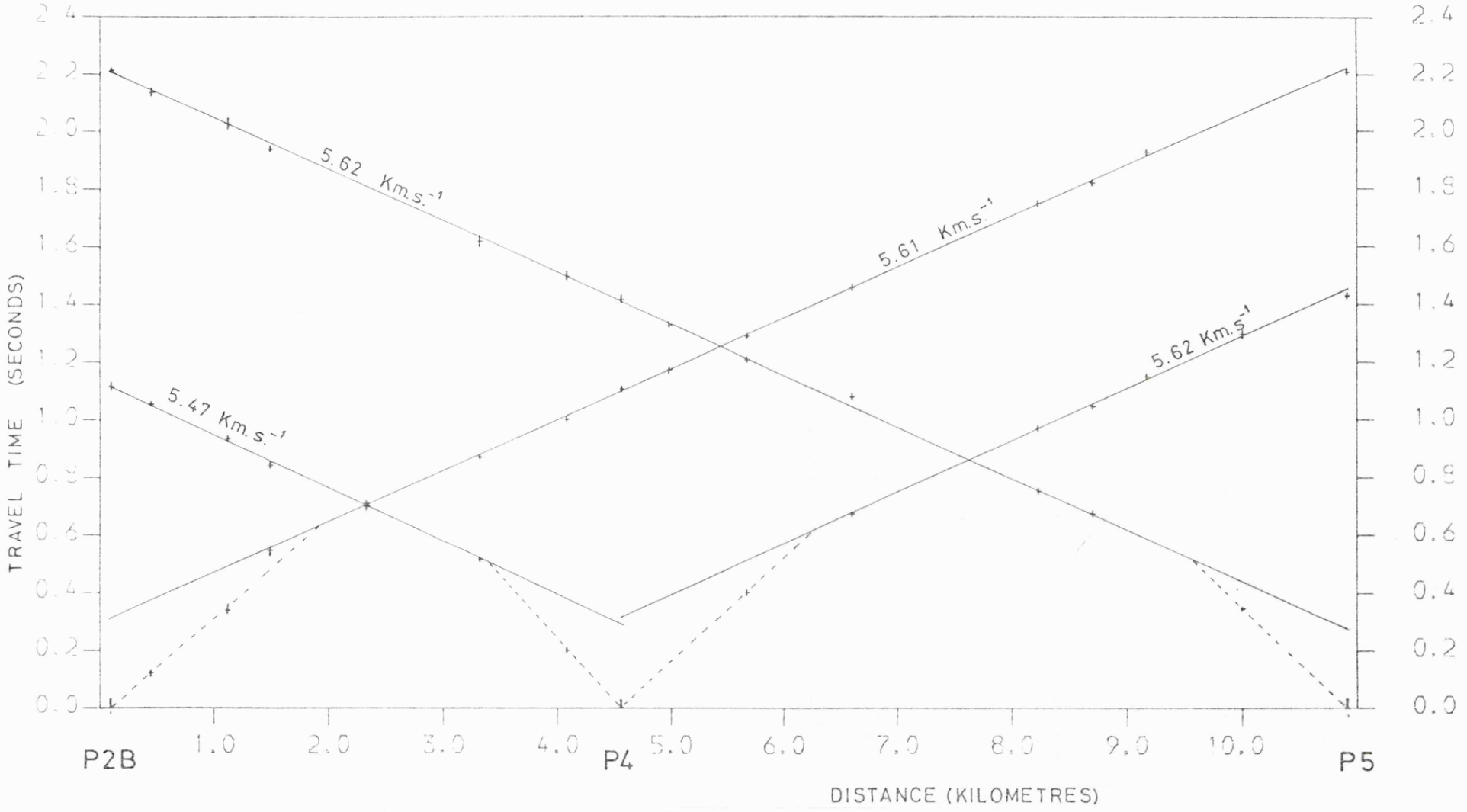


Figure 6.5 : Time-distance graphs for profile B.

## 6.5 REDUCED TRAVEL TIME SECTIONS FOR PROFILE A

As described in chapter 2, reduced travel time sections are useful in examining the topography on a refractor before the structure becomes smeared by the addition of two or more delay time surfaces.

### 6.5.1 Stations A14 to A24

Reduced travel time profiles were plotted for profile A (figure 6.6) using a reducing velocity of 5.75 $km.s^{-1}$, as indicated by the linear regression of the time:distance data. There is a good visual correlation between the reduced travel time sections for the three shots into the section from A14 to A24, which suggests that the reducing velocity is a good approximation of the refractor velocity. The reduced travel times increase eastwards from A24 to A14 indicating that there is either an easterly dip on the refractor or a systematic lateral change in the velocity of the overlying sediments. The sections for shots P1 and P2A into stations A16-23 compare closely and therefore show that there is not a detectable increase in velocity with depth within the refractor.

### 6.5.2 Stations A24 to A28

The interval between stations A24 and A28 is anomalous, but unfortunately this section is not reversed by shot P3. The reduced travel time sections for shots P1 and P2 have a very similar pattern. Both shots show that there is a marked lateral reduction in either the refractor or overburden velocity, or a rapid deepening of the refractor. If the

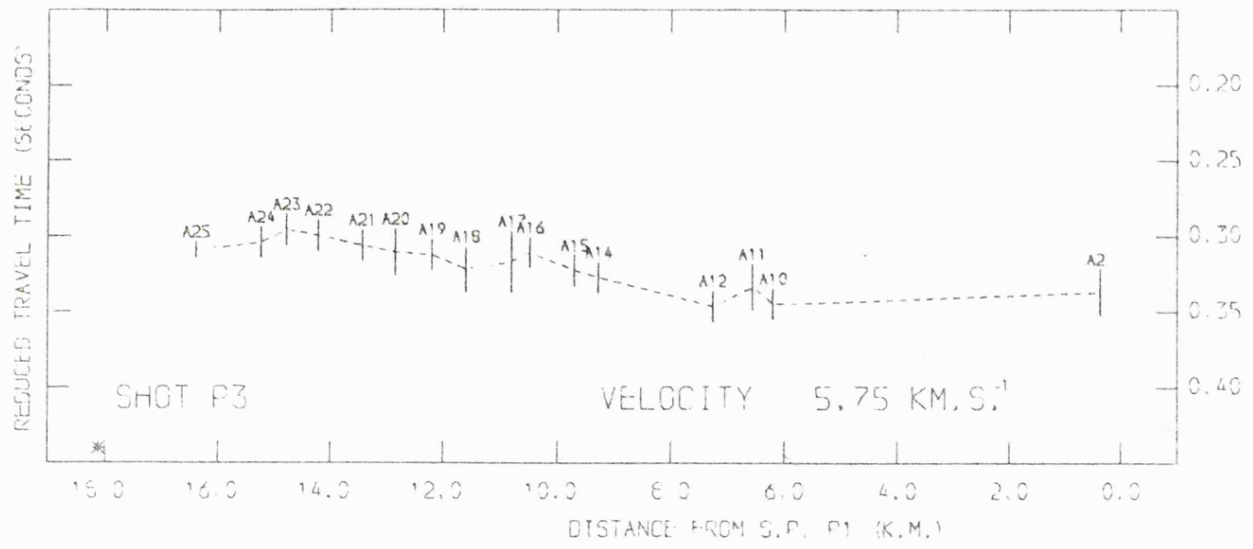


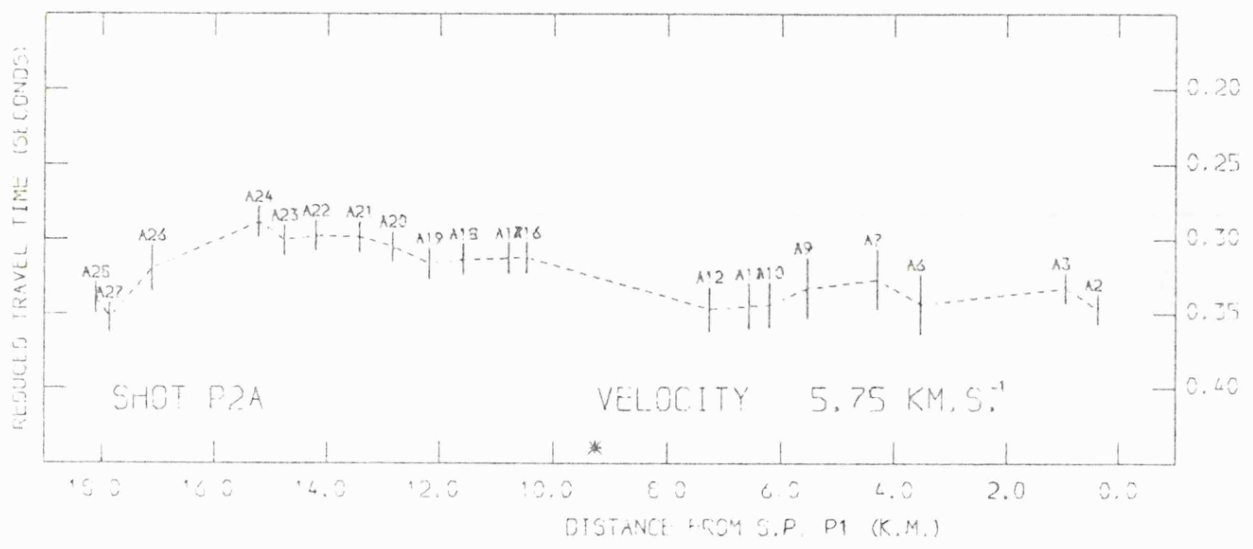


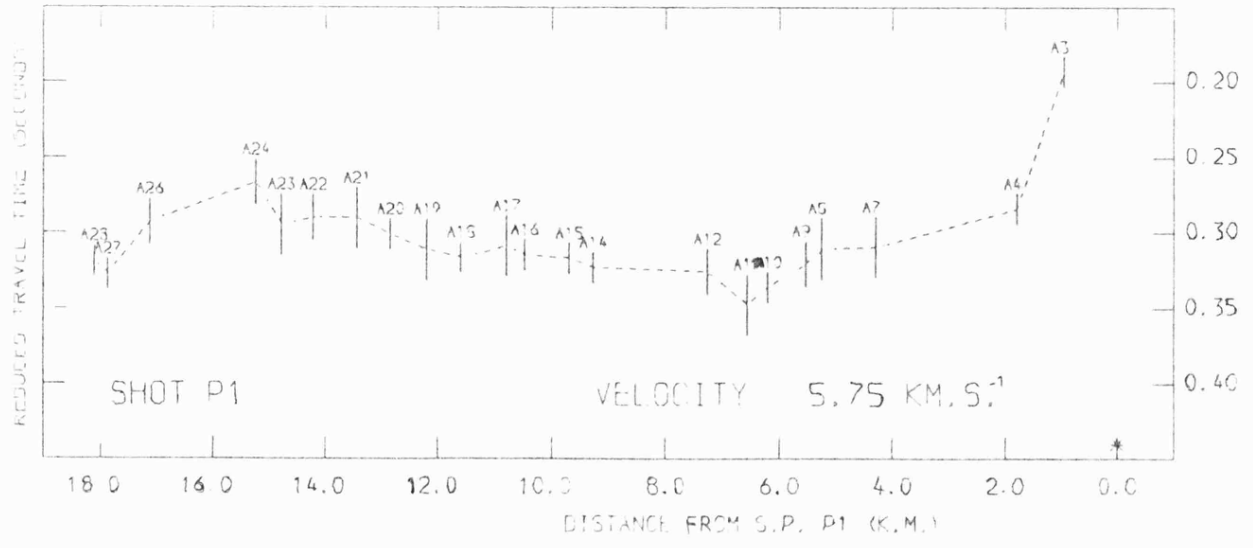


Figure 6.6 : Reduced travel time sections for profile A.
The vertical bars indicate the maximum error.
The * marks the position of the shot.

latter interpretation were to be correct the increase in depth would be about 200 metres in three kilometres. This is in direct contradiction to the borehole evidence which indicates a westward shallowing of the Precambrian basement from Glinton (350 metres below OD) to Wittering (230 metres below OD). There are some variations in the near surface structure at the Marholm fault (throw about 25 metres) but these are too small to cause the 0.5 $km.s^{-1}$ reduction in the average sedimentary velocities that is necessary to produce the observed 0.050 second increase in the reduced travel times. The interpretation of the increase in reduced travel times as being due to a lateral change in refractor velocity is preferred. This gives a velocity of about 5.2 $km.s^{-1}$, if this part of the refractor is assumed to be horizontal.

### 6.5.3 Stations A1 to A14

Because of the weak shot at P3, and problems with the recording equipment at some of the sites, the data in this section of poorer quality and ha several gaps. The reduced travel time sections for shots P1 and P2A have a similar pattern, with smaller reduced travel times at stations A7 to A9 than at A10 to A12. This suggests a reduction in the depth to the refractor under stations A7 to A9. The repeated shots from P2 (table 6.4) show that the repe errors for A10 and A12 were smaller than the estimated maximum observational errors which are plotted as error bars.

For an average overburden velocity of 3.0 $km.s^{-1}$ the angle of incidence of critically refracted energy would be about 30° to the vertical, giving an offset, away from the

shotpoint, of about 300 metres for a refractor 500 metres deep. Station A11 shows an increased reduced travel time for shot P1 compared with P2A and P3. The maximum errors at this site are the same size as the reduced travel time anomaly. A depression in the basement under A10 could cause this anomaly. Given an offset of 300 metres, the depression would not be seen by shots P2A and P3 into A10 provided that it did not extend as far east as A11. The distance between A10 and A9 is about equal to the critical distance, therefore the depression would have to end midway between A10 and A9 in order not to be detected by shot P1 into A10 or P2A into A9.

### 6.5.4 Refractor topography

The general trend for profile A, as shown by the reduced travel time sections, is for an apparent dip from southwest to northeast. The dip is very small, being about 0.050 seconds (of the order of 150 metres) in 15 kilometres. It is possible that this apparent structure is due to a lateral variation in overburden velocity along the profile.

The difference in reduced travel times between adjacent stations, and therefore refractor topography, is usually less than the estimated maximum observational errors, as shown by the error bars on the reduced travel time sections.

### 6.5.5 Shots P2B, P4, P5

Figure 6.7 shows the reduced travel time sections for shot P2B and the fan shoot from P4 and P5 into stations A4 to A13. There is a good visual correlation between the sections for shots P2A (figure 6.6) and P2B, indicating that the two shots, which were 50 metres apart, could be treated

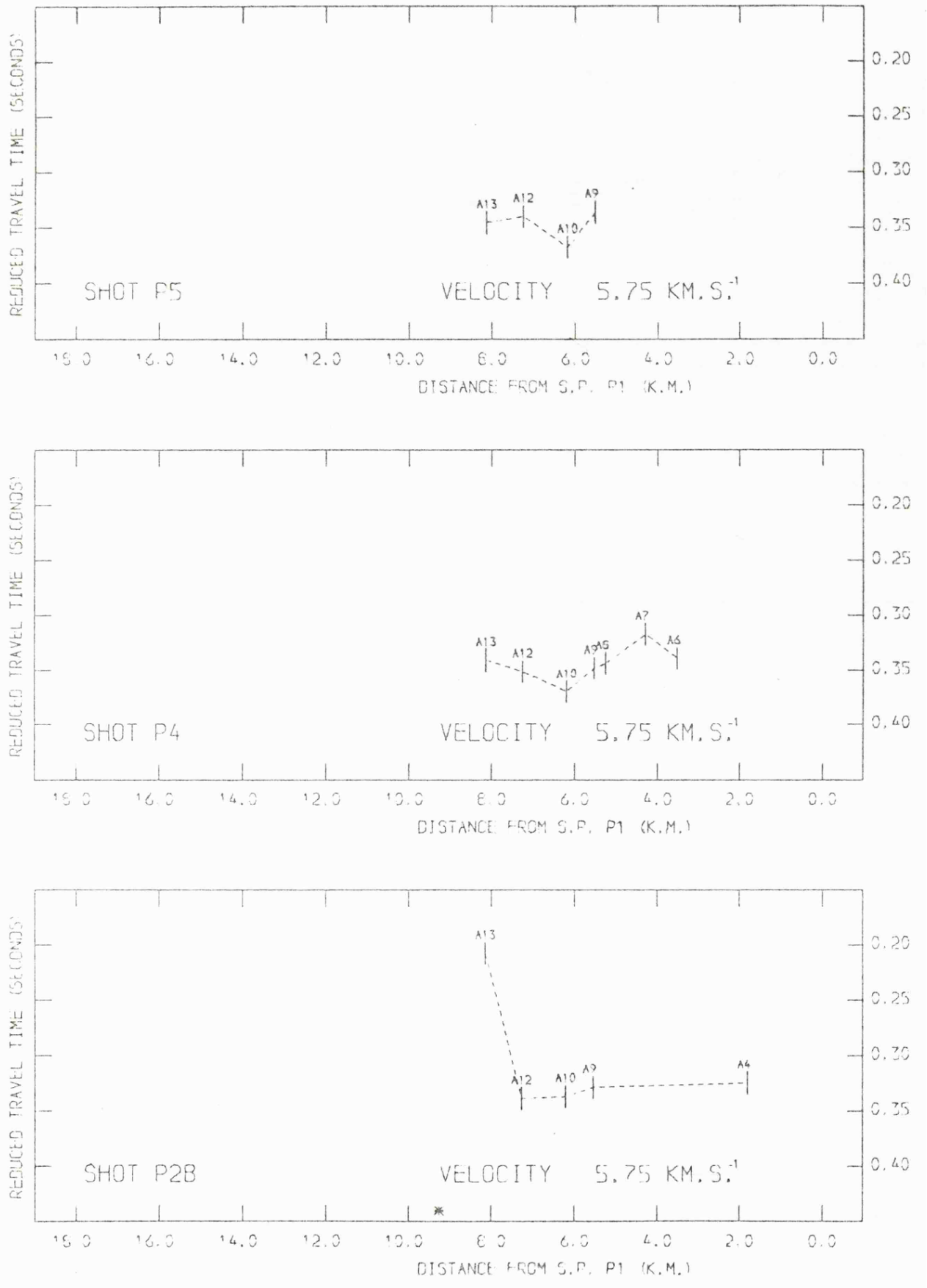


Figure 6.7 : Reduced travel time sections for profile A.

as one shotpoint in any time term solution for profile A.

Because of the orientation of the two profiles, the variation in shot to receiver distances for P4 and P5 into stations A6 to A13 is much smaller than is apparent when the stations are plotted against their positions along profile A.

If T1 and T2 are travel times to stations at distances of X1 and X2 respectively, the reduced travel times TR1, TR2 are given by:

$$TR1 = T1 - X1/Vr \qquad TR2 = T2 - X2/Vr$$

The difference in reduced travel times $\Delta t$ is therefore:

$$\Delta t = TR1-TR2 = (T1 - X1/Vr) - (T2 - X2/Vr)$$

$$= T1 - T2 + (X1-X2)/Vr$$

If X1 and X2 are approximately equal, as they are in a fan shoot, the reduced travel time sections will be largely independent of the reducing velocity used (Vr) and should show up any lateral change in refractor velocity across the fan.

In the case of profile A the reduced travel time sections have a similar shape to the sections for the on-line shots; this suggests that these sections are also showing the refractor topography under the recording stations and that there are no lateral velocity changes in the area covered by the fan shoot.

One exception to this is at station A1Ø. Here the reduced travel times for P4 and P5 are anomalously large. The arrivals from P4 and P5 will be travelling almost perpendicular to profile A, the reduced travel time anomaly is therefore consistent with a basement depression, or a velocity anomaly immediately above the basement, under A1Ø

trending perpendicular to the recording profile (see 6.5.3).

## 6.6 REDUCED TRAVEL TIME SECTIONS FOR PROFILE B

The reversed cover on the refractor along this profile is less than eight kilometres and there are a maximum of nine recording stations at which the reduced travel time sections can be compared.

The linear regression indicated that the refractor velocities on profile B were slightly lower than for profile A. Accordingly the reduced travel time sections in figure 6.8 have been calculated for a reducing velocity of 5.6 $km.s^{-1}$. The reduced travel time sections for the three shots show little structure on the refractor and only two small scale features can be correlated between the shots.

Stations B1 to B3 have larger reduced travel times than B4, this suggests a deepening of the refractor by up to 100 metres at the northern end of profile B. The section for shot P5 shows an increase in reduced travel times at stations B8 and B9, shot P2B shows a similar increase at B9 and B10. Given an offset of about 300 metres (see above), the reduced travel times are consistent with a narrow (500 metre) depression in the refractor centred under station B9. A time term type solution would tend to smooth out such small scale variations since it adds delay time surfaces without making allowances for critical angle offset.

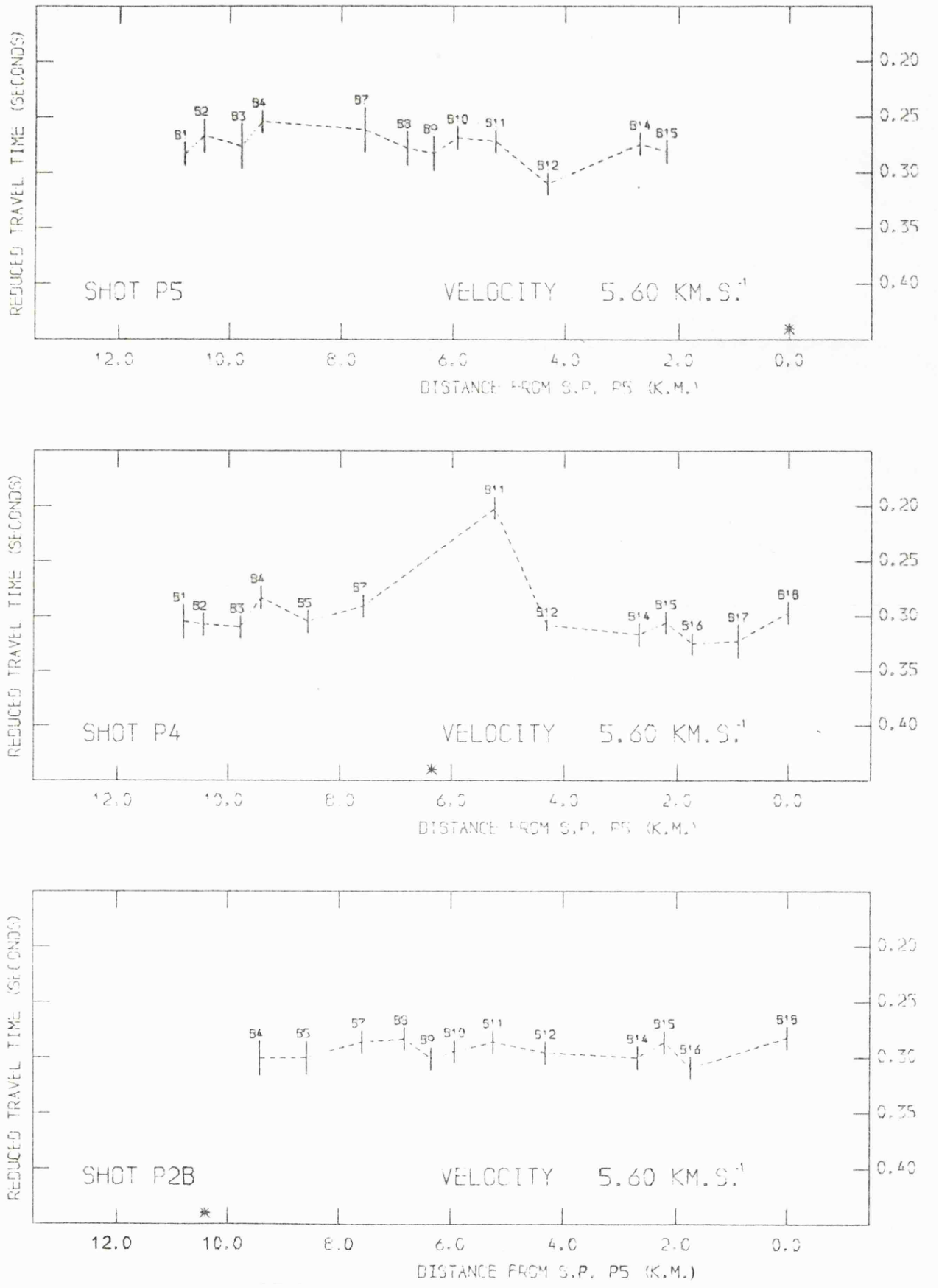


Figure 6.8 : Reduced travel time sections for profile B.

## 6.7 TIME TERM SOLUTIONS

### 6.7.1 Profile A

Figure 6.9 shows a time term solution for profile A. The calculated delay times are plotted at the station locations to give a time section. This solution was obtained using a data set containing all the first arrival data for the on-line shots P1,P2A,P2B,P3. This represents a total of 60 observations for 25 receiving stations. As described above, the reduced travel time sections for shots P2A and P2B were very similar. These shots were treated as two separate shotpoints in the initial solution as a way of checking the solution.

Even with this large data set the F ratio of the solution (the ratio of the solution variance to the observational error variance) was 0.5, indicating that the solution was as good as the observational errors would allow, but not necessarily unique. The solution velocity was 5.77 $km.s^{-1}$ and the time term for shot P2A was 0.006 seconds larger than that for P2B, this difference is smaller than the observational errors. The solution time terms are given in table 6.5.

The time terms show a steady increase from 0.130 seconds at A24 to 0.180 seconds at A10. The interval from A25 to A28 had anomalously large time terms as a result of the probable change in refractor velocity discussed above.

Although the F ratio was less than unity an attempt was made to refine the model by removing the unreversed arrivals from either end of the profile (and hence the data from A25 to A28). The resulting solution gave a velocity of 5.76 $km.s^{-1}$.

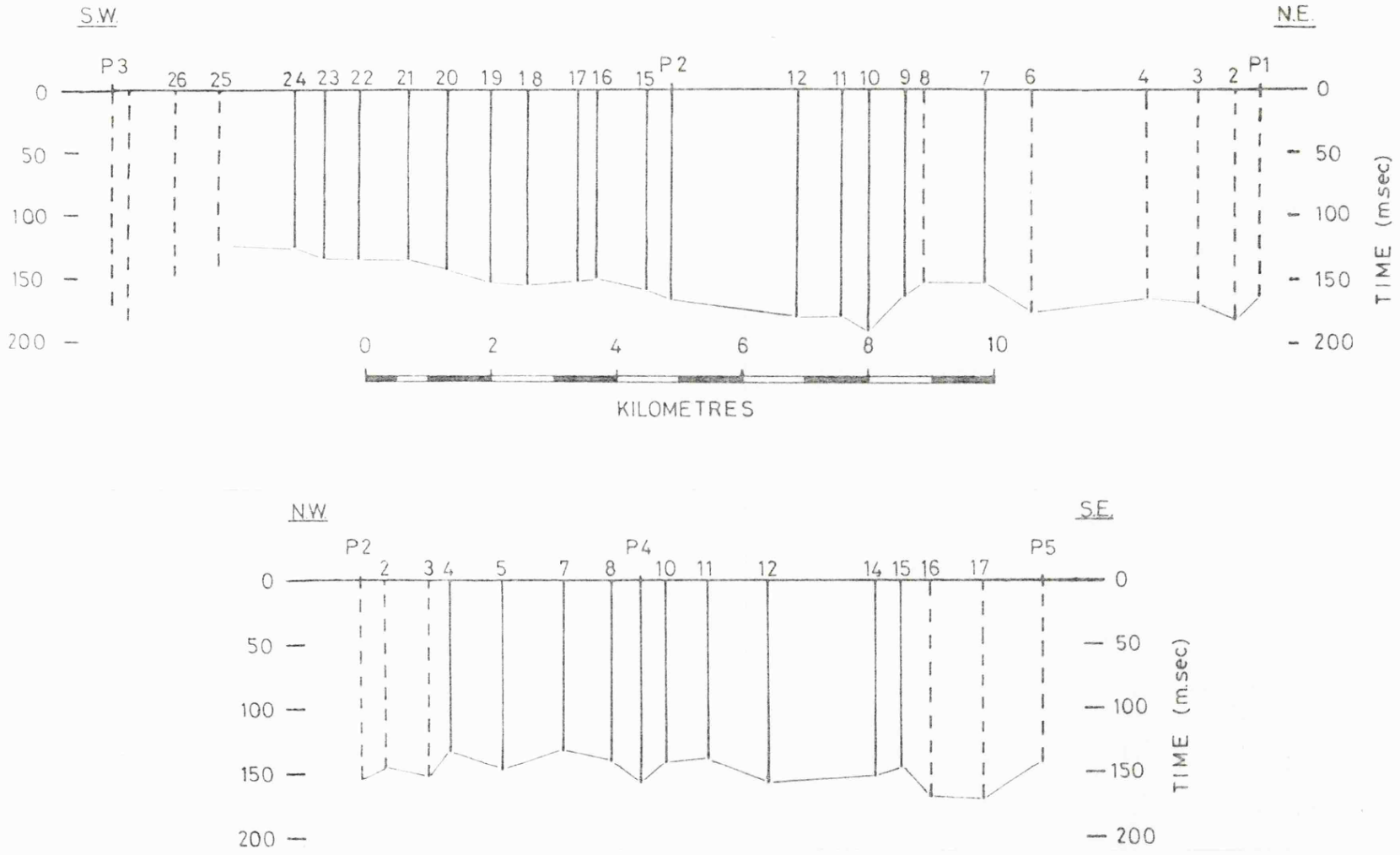


Figure 6.9 : Time term solutions, a dashed line indicates a single or unreversed observation.

None of the station time terms changed by more than Ø.ØØ5 seconds. The solution for the full data set is therefore considered as good as can be obtained from a simple non-iterative time term solution.

The data from shots P4 and P5 into profile A was not used since there was very little variation in shot to receiver separation and therefore the data were not suited to a time term type of analysis.

### 6.7.2 Profile B

A similar procedure was adopted for the data from profile B, a data set comprising 35 travel times for 16 receiving stations was assembled.

The time term solution for this data set is also shown in figure 6.9. The solution velocity was 5.65 $km.s^{-1}$ and the F ratio Ø.98. The variation in time terms along the profile is of the same magnitude as the observational errors. Once again nothing could be gained from a subdivision of the data set.

The time terms reflect the slight variations in refractor topography deduced from the reduced travel time data. The time term obtained for shot P2B was Ø.ØØ6 seconds smaller than the value obtained for the same shotpoint in the solution to profile A, a difference which is, again, less than the observational error. The solution time terms are given in table 6.5.

| | | | | | |
|---|---|---|---|---|---|
| A1 | Ø.161 | A19 | Ø.153 | B1 | Ø.156 |
| A2 | Ø.18Ø | A2Ø | Ø.143 | B2 | Ø.148 |
| A3 | Ø.169 | A21 | Ø.136 | B3 | Ø.153 |
| A4 | Ø.166 | A22 | Ø.134 | B4 | Ø.134 |
| A6 | Ø.178 | A23 | Ø.135 | B5 | Ø.148 |
| A7 | Ø.156 | A24 | Ø.125 | B7 | Ø.134 |
| A8 | Ø.152 | A25 | Ø.142 | B8 | Ø.141 |
| A9 | Ø.166 | A26 | Ø.148 | B9 | Ø.16Ø |
| A1Ø | Ø.178 | A27 | Ø.182 | B1Ø | Ø.142 |
| A11 | Ø.179 | A28 | Ø.168 | B11 | Ø.139 |
| A12 | Ø.177 | | | B12 | Ø.159 |
| A14 | Ø.168 | | | B14 | Ø.152 |
| A15 | Ø.16Ø | | | B15 | Ø.147 |
| A16 | Ø.15Ø | | | B16 | Ø.17Ø |
| A17 | Ø.15Ø | | | B17 | Ø.172 |
| A18 | Ø.155 | | | B18 | Ø.141 |

Solution velocities A: 5.77 $km.s^{-1}$ B: 5.64 $km.s^{-1}$

Table 6.5 : Time term solutions for profiles A and B

## 6.8 VELOCITIES OF THE OVERLYING SEDIMENTS

In order to convert the delay time data into depth sections it is necessary to estimate the velocities of the overlying sediments. The following sections outline the available data.

### 6.8.1 Nimbus recordings

A 12 channel Nimbus seismograph was deployed at shotpoint P2A during the recording of profile A and at P4 during the recording of profile B. Near surface apparent velocities were recorded with a 35 metre geophone spacing. The first arrival data is shown in the time-distance graphs in figure 6.10.

A simple horizontal layer interpretation of this data gives the following structures:

Shot P2A layer 1: velocity 1.8 $km.s^{-1}$ thickness 21 m.
layer 2: velocity 3.2 $km.s^{-1}$

Shot P4 layer 1: velocity 1.8 $km.s^{-1}$ thickness 34 m.
layer 2: velocity 3.2 $km.s^{-1}$

Both shotpoints were drilled in Oxford Clay and this would appear to be the low velocity layer 1. The high velocity for layer 2 is unlikely to be due to dip on the refractor since the two lines had different orientations and yet the sediments in this area have uniform shallow dips (0.5 to 1.0°) to the east.

Shotpoint P4 was located less than two kilometres from the Thorney borehole which proved 2 metres of Drift and 45 metres of Oxford Clay underlain by 17 metres of Middle

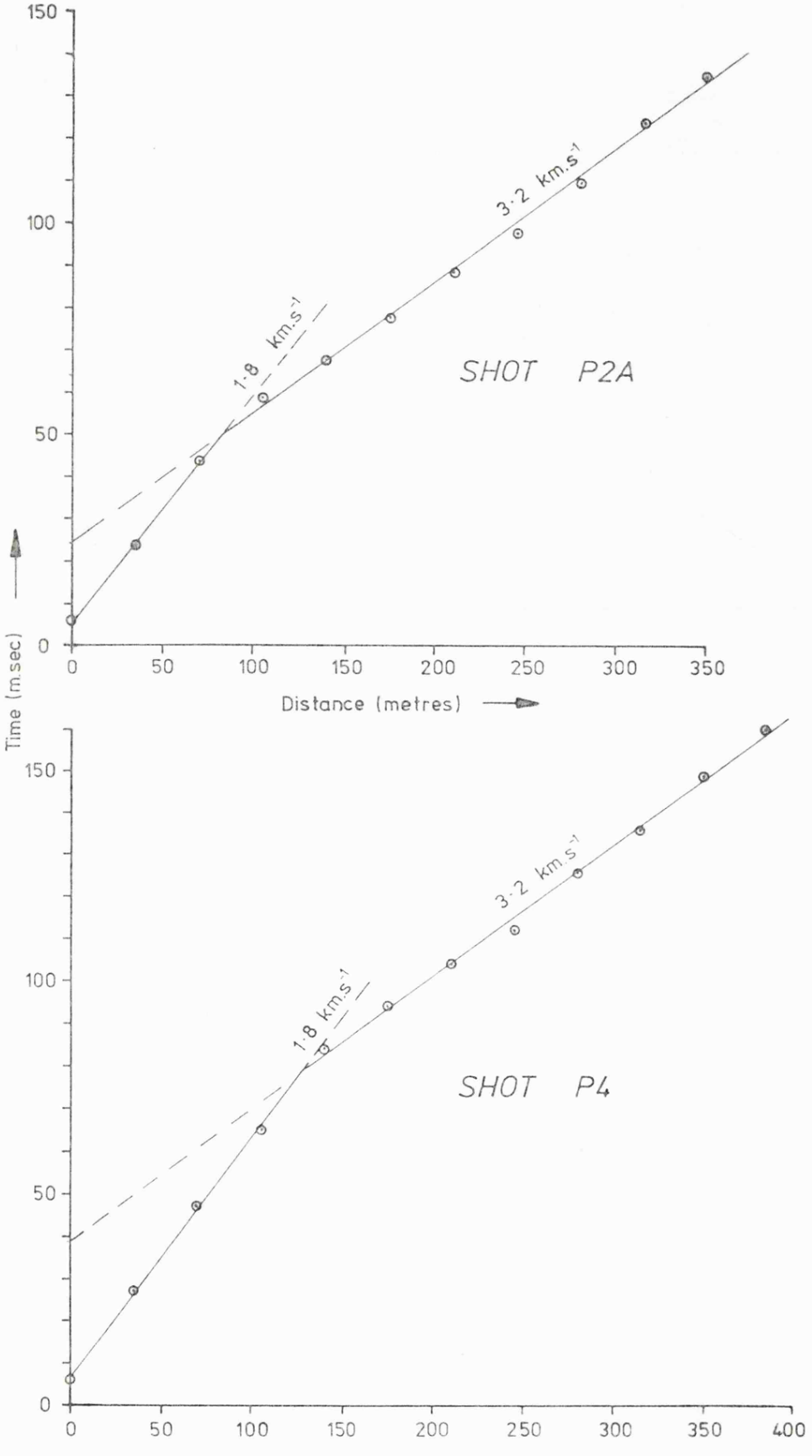


Figure 6.1Ø : Time-distance graphs for the Nimbus data.

Jurassic (Cornbrash, Great Oolite, Upper Estuarines).

The 3.2 $km.s^{-1}$ refractor is most likely to be a thin unit, such as a well lithified limestone, within the Middle Jurassic. Such a layer would effectively hide any underlying units of lower velocity.

### 6.8.2 Direct arrival data

The time distance graphs for profiles A and B show crossover distances of less than two kilometres. With a station spacing of Ø.5 to 1.Ø kilometres only one or two direct arrivals will have been recorded at each shotpoint. It was not possible to move the recording sites between the shots in order to record extra direct arrival data. However, the time terms for the shotpoints all lie in the range Ø.14Ø to Ø.17Ø seconds, it is therefore possible to combine all the Nimbus and direct arrival data, together with the short range refractions, on one time-distance graph (figure 6.11)

This graph reveals that all the "direct" arrivals are coming from a layer with a velocity of about 3.1 $km.s^{-1}$. A second set of arrivals, those from the basement refractor, are seen at distances of as little as 1.2 kilometres, with at least four such arrivals between 1.2 and 2.Ø kilometres. Extrapolation of the 3.1 $km.s^{-1}$ line suggests a crossover distance of about 2.Ø kilometres. Clearly 3.1 $km.s^{-1}$ is not the true average velocity of the sediments above the basement refractor and units of a lower velocity are being hidden by the high velocity arrivals.

### 6.8.3 Borehole velocity measurements

The Thorney borehole indicated that the high velocity

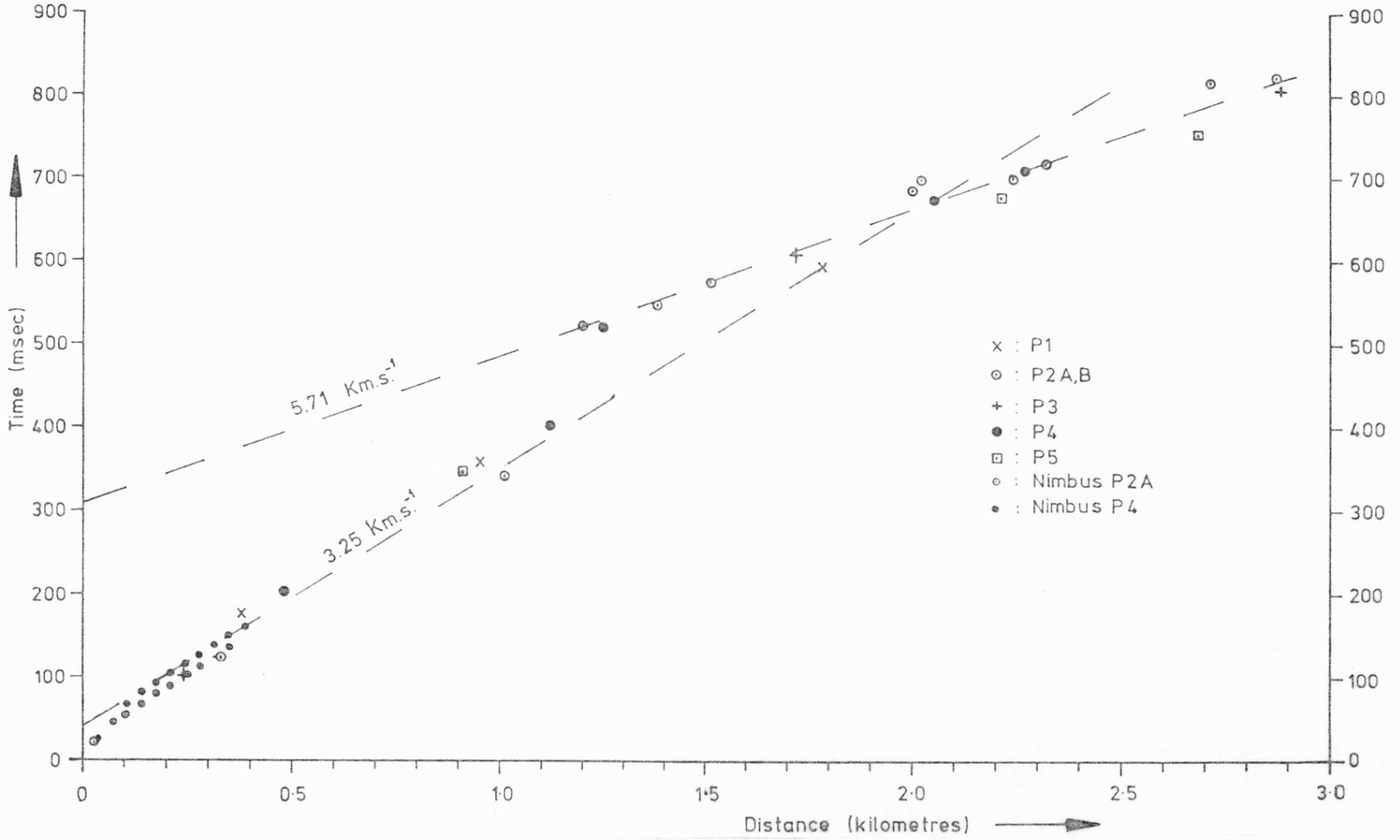


Figure 6.11 : Combined time-distance data for all arrivals up to 3 km.

was probably due to a refractor within the Middle Jurassic sediments. Sonic logs are available for some of the more recent boreholes in the area and these have been analysed to obtain velocities for the sedimentary succession. The velocities were obtained by blocking the logs into representative intervals and then converting the interval transit times into velocities.

Table 6.6 is a compilation of the velocities obtained. The borehole locations and other details can be found in appendix 1.1.

| | WISBECH | WIGGENHALL | SPALDING | HUNTINGDON |
|---|---|---|---|---|
| OXFORD CLAY | | 2.Ø3 | | |
| M JURASSIC | | 3.6 | | 1.6-3.8 |
| LIAS SHALE | 2.Ø-2.Ø5 | 2.Ø4 | 2.Ø-2.2 | 1.9-2.1 |
| LIAS LIMESTONE | 2.5-3.4 | 3.4-4.Ø | 2.5-3.8 | 3.Ø-3.8 |
| AVERAGE JURASSIC | 2.Ø7 | 2.21 | 2.16 | |
| KEUPER | 3.3-3.6 | 2.9 | 3.2 | |
| BUNTER | | 3.4 | | |
| ORDOVICIAN | | | | 3.8-4.2 |
| PRECAMBRIAN | | 5.85-6.1 | | |

Table 6.6 : Interval velocities measured from sonic logs

The log for the Wiggenhall borehole shows a ten metre thick interval, with a velocity of 3.6 $km.s^{-1}$, between the Kellaways and the Upper Lias. There are about 2Ø metres of Middle Jurassic in the Huntingdon (Mill Lane) borehole, the velocities vary considerably but the highest values, about

3.8 km.s$^{-1}$, occur in the Cornbrash and Great Oolite.

In addition to the Middle Jurassic there are thin, high velocity, limestones in the Lias shales in all the boreholes. The highest of these limestones, stratigraphically, is at the base of the Upper Lias. The interval velocities measured for the Lias are about Ø.4 km.s$^{-1}$ lower than velocities measured at similar depths in the Melton area.

### 6.8.4 Refraction from thin layers

The borehole logs confirm that velocities in excess of 3.Ø km.s$^{-1}$ can occur in limestone beds in the Middle Jurassic. O'Brien (1967) suggests that the attenuation of energy refracted along a thin bed will be "several db per wavelength", where thin means less than half a wavelength. This contrasts with "several tenths of a db per wavelength" for typical thick porous formations.

The Nimbus data were recorded with 14Hz. HSJ geophones at ranges of up to 385 metres. The other direct arrival data was recorded with 2Hz. HS1Ø geophones at ranges of Ø.25 to 1.Ø kilometres. Because of the close proximity to the shot most of the records were overloaded and only first break times could be obtained. From the few complete seismograms the frequency of the first arrivals was measured at about 25 Hz. for the Nimbus data and 1Ø to 2Ø Hz. for the other arrivals. For a velocity of 3.2 km.s$^{-1}$, frequencies of 1Ø, 2Ø and 25 Hz. are equivalent to wavelengths of 32Ø, 16Ø and 128 metres respectively.

The Nimbus records for the four most distant geophones at shot P2A were not overloaded and the same gain setting

was used on all four channels. The amplitude of the first cycle decreased rapidly across the four traces, a distance of 1Ø5 metres. The dynamic range of the recorder was not known exactly but can be assumed to be 4Ø±1Ø db. The peak to peak amplitudes of the four traces were measured from the replayed digital records, and the amplitudes corrected for geometrical spreading ($A = A_0 / r$, where A is the amplitude and r the distance from the source). The amplitudes of the four traces then showed an attenuation of 2.7±Ø.5 db/1ØØ metres or 2.85-4.15 db per wavelength of a 25 Hz. pulse.

The attenuation evidence indicates that the 3.2 $km.s^{-1}$ refractor was a thin layer within the Middle Jurassic sediments.

6.8.5 Previous surveys

Bullard et.al. (1946) tabulate the results of 28 seismic refraction surveys in eastern England. The velocities of the refractors above the basement were calculated and assigned to various formations by comparison with outcrop and borehole data. The mean velocities and standard deviations for the Jurassic, with the number of observations in brackets, are as follows:

| | | | |
|---|---|---|---|
| Oxford Clay | (8) | 1.75 $km.s^{-1}$ | sd Ø.22 |
| Great Oolite | (12) | 3.42 $km.s^{-1}$ | sd Ø.36 |
| Upper Lias | (4) | 2.16 $km.s^{-1}$ | sd Ø.27 |
| Lower Lias | (9) | 2.45 $km.s^{-1}$ | sd Ø.18 |

## 6.9 TIME TO DEPTH CONVERSION

### 6.9.1 Structure of the supra-basement sediments

A structure contour map on the base Jurassic was prepared in connection with the interpretation of the gravity data (chapter 8B). This map was used to predict the thickness of the Jurassic sediments along the two seismic profiles. An average velocity of 2.3 $\pm$ Ø.2 km.s$^{-1}$ was used for the Jurassic sediments, this is slightly higher than was indicated by the borehole logs, but lower than typical Lias velocities from the Melton area where the borehole velocity data were better than it is in this area. The velocity of the underlying sediments was taken as 3.2 $\pm$ Ø.2 km.s$^{-1}$, this represents an average of the available data for the Permo-Triassic. The refractor velocity was taken to be the time term solution velocity for the profile (5.77 km.s$^{-1}$ for A and 5.65 km.s$^{-1}$ for B).

The assumptions made about the thickness of layer 1 mean that all the variations in station time terms are translated into variations in the thickness of the lower, higher velocity, layer. This is reasonable since the Permo-Trias was deposited on an erosion surface and is known from the boreholes to vary in thickness. The borehole logs did not indicate any vertical velocity gradients within the sediments.

### 6.9.2 Discussion of the depth sections

The depth sections are shown in figure 6.12. The calculated depths to the basement refractor at stations A23 and A24 are less than the depth to basement in the nearby

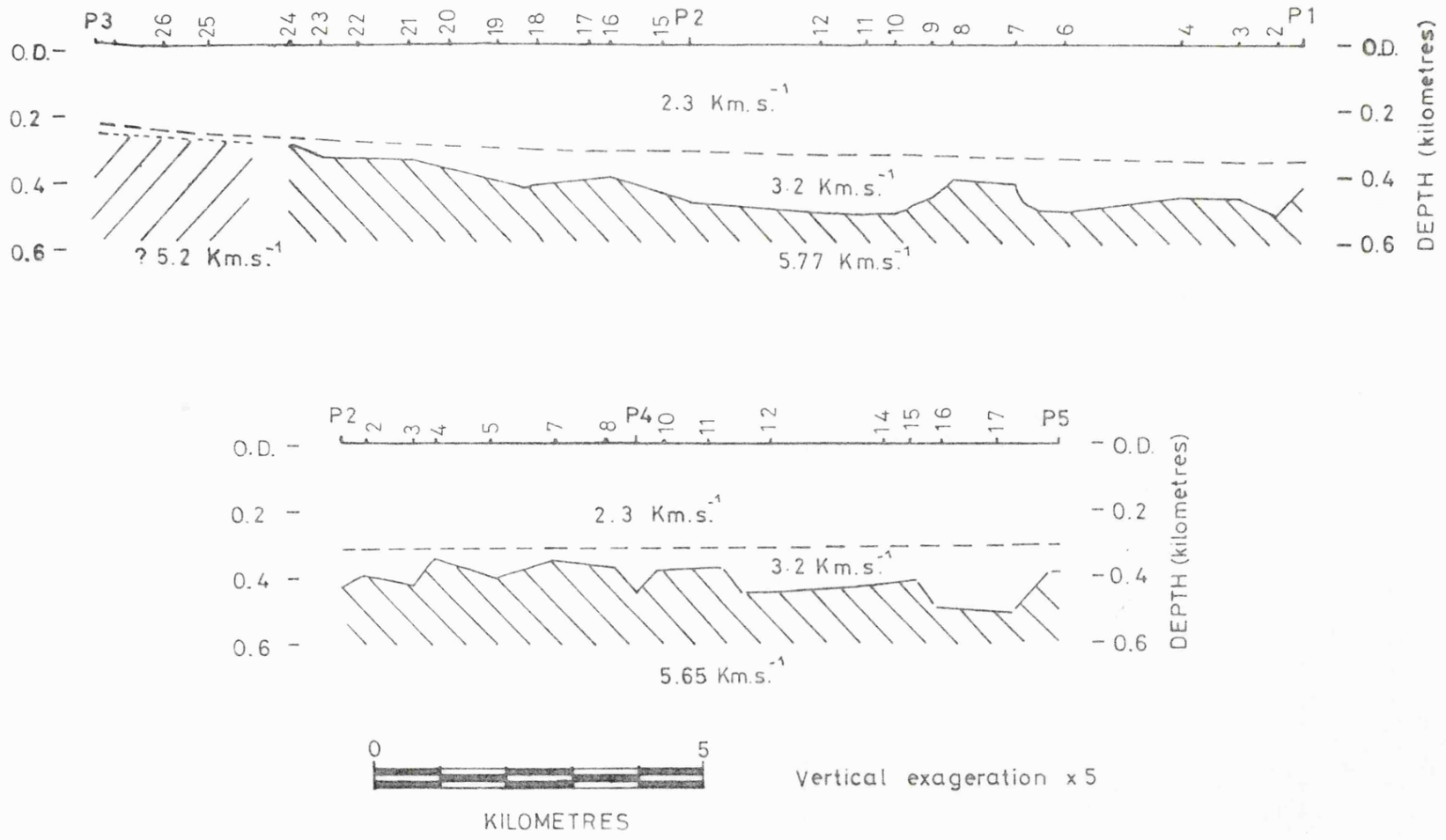


Figure 6.12 : Depth sections for profiles A and B.

Glinton borehole by 5 and 40 metres respectively.

There is no recognisable lateral change in refractor velocity and therefore the simplest conclusion is that the Precambrian basement seen in the Glinton borehole forms the refractor along both seismic lines. The velocity of the basement refractor (5.65-5.77 $km.s^{-1}$) is equivalent to velocities reported by Chroston and Sola (1982) for presumed Precambrian basement in North Norfolk.

The time term solution velocities for profiles A and B give velocities that are different by 0.12 $km.s^{-1}$, the standard error estimates on the solution velocities for profiles A and B are 0.014 and 0.029 $km.s^{-1}$ respectively. Profile A has a general dip of 1 to 2° towards shotpoint P1. The solution velocity (v') is related to the true velocity (v) by:

$$v' = v/\cos a \qquad \text{where a is the dip.}$$

Therefore a dip of 2° would alter "v'" by less than 0.004 $km.s^{-1}$. The average shot to receiver distances on profile A are larger than those on profile B. If there were a slight increase in velocity with depth in the refractor then the solution to profile A would give a higher velocity. Such an increase in velocity was not indicated by the reduced travel times for shots P1 and P2A into stations A16 to 24 (see section 6.5).

If the standard error estimates are accepted as meaningful, and the variation in velocities is not the result of a systematic variation in the sedimentary velocities, then there is an azimuthal variation in the refractor velocity. Such an anisotropy could be caused by fracture orientation or structural grain.

The low refractor velocity (about 5.2 $km.s^{-1}$) detected to the west of station A24 occurs to the southwest of the 100 nT magnetic high that is situated over the Glinton borehole (figure 6.2). It seems unlikely that low velocity intrusive basement would occur on the edge of the magnetic anomaly that runs south from Glinton to southeast of Peterborough. The low velocity could be due to fracturing of the basement, the surface expression of which is the Tinwell-Marholm fault. This structure can be traced for 20 kilometres from Peterborough to Stamford, but since the low velocity zone is 1 to 2 kilometres wide a fracture zone does not seem likely.

The simplest explanation for the low apparent velocity is for a compositional change within the Precambrian basement. Bullard et.al. (1946) report a refractor velocity of $5.17 \pm 0.15$ $km.s^{-1}$ for the Precambrian basement close to the Great Oxendon borehole. The Precambrian volcanic agglomerate in the Upwood borehole had a velocity of 4.57 $km.s^{-1}$ (Bullerwell 1967). The available evidence suggests that a velocity of over 5.0 $km.s^{-1}$ is too high to be associated with Lower Palaeozoic sediments.

The depths to the refractor along the two profiles are, in general, deeper than was predicted by correlating between the various boreholes. It must, however, be remembered that not all the boreholes penetrate Precambrian basement. Spalding, and possibly Wisbech, bottom in Cambrian quartzites, whilst boreholes to the south of Peterborough prove Devonian or Ordovician rocks with only Upwood reaching the Precambrian. The Wyboston borehole, located 50 kilometres south of Peterborough, proved 110 metres of Old Red

Sandstone and Devonian overlying Cambrian. Although the pre-Permian basement surface in this area is gently undulating and lies at shallow depth there is a considerable variation in lithology and age of the basement rocks.

The refractor detected by the seismic lines is not the pre-Permian unconformity surface but the Precambrian basement. At Glinton the two surfaces are the same and the depth calculated from the seismic data agrees with the borehole depth. In other areas, such as south of the Spalding borehole, the calculated depth to the refractor would be expected to be greater than the borehole depth, thus giving an estimate of the thickness of the Palaeozoic.

The evidence from the boreholes is that the Permo-Trias is between 30 and 100 metres thick in this area whilst the calculated thickness for the sub-Jurassic sediments along the seismic lines is 20 to 200 metres. The refractor may therefore be overlain, in places, by up to 100 metres of Palaeozoic sediments. The assumption of a velocity of 3.2 $km.s^{-1}$ for the interval from the base Jurassic to the basement refractor will be a reasonable approximation if the Palaeozoic sediments are Old Red Sanstone conglomerates (the most likely interpretation). The depths to basement will be underestimated by up to 40 metres if the rocks are Lower Palaeozoic mudstones and quartzites, which have velocities of 3.4 to 4.0 $km.s^{-1}$. Errors of $\pm$ 0.2 $km.s^{-1}$ in the assumed velocities for the Jurassic and Permo-Trias would cause a maximum error of $\pm$ 40 metres in the calculated depth to basement. The errors due to uncertainty in the first arrival travel times will be about 30 to 60 metres for errors of $\pm$ 0.010 to 0.020 seconds.

## 6.10 SUMMARY AND CONCLUSIONS

The two seismic profiles proved a refractor of velocity 5.65 to 5.75 $km.s^{-1}$ at depths of 350 to 500 metres both across and along the axis of the Peterborough gravity anomaly. By comparison with the Glinton borehole, and with basement refractor velocities in north Norfolk (Chroston and Sola 1982) and in Leicestershire (chapter 1), the refractor is interpreted as Precambrian basement.

No lateral changes in the refractor velocity were detected over the gravity anomaly. An apparent refractor velocity of 5.2 $km.s^{-1}$ was detected to the southwest of the Glinton borehole. This may represent a compositional change within the Precambrian basement.

A short wavelength structure with an amplitude of about 100 metres was detected along both profiles. This probably represents a combination of refractor topography and localised variation in the velocities of the overlying sediments.

The results of the seismic experiments clearly preclude the Palaeozoic sedimentary basin model for the gravity anomaly (unless the basin was filled with a high velocity sediment that was less dense than the surrounding Precambrian rocks but had a similar velocity).

The granite model is clearly favoured and will be analysed further in chapter 8B.

# CHAPTER SEVEN

# POTENTIAL FIELD INTERPRETATION

## 7.1 INTRODUCTION

This chapter is in three parts:

1. A review, together with some new measurements, of the densities and magnetic properties of the basement rocks found in the East Midlands.

2. A description of the theory of the modelling techniques used to interpret the East Midlands gravity and magnetic data.

3. A discussion of the gravity and magnetic anomaly maps for the East Midlands, including some simple modelling.

In the context of this and the following two chapters, "basement" is taken to mean the pre-Carboniferous surface proved in boreholes. Therefore it comprises Lower Palaeozoic and Precambrian rocks together with igneous intrusions and some Devonian sediments. This basement does not always correspond with the Precambrian metasediments and the igneous intrusions which formed the seismic basement detected by the Melton and Peterborough refraction lines.

A second term, "Proterozoic basement" is used in the same context as pre-Charnian basement or sub-Charnian refractor, was used when discussing the seismic refraction experiments.

As will be shown below, only the Precambrian and Caled-

onian igneous intrusions, and possibly the Proterozoic basement, have significant magnetic susceptibilities. These can be considered as representing magnetic basement.

## 7.2 ROCK DENSITIES

Maroof (1973) made a large number of density measurements on samples from the Charnian Inlier and Mountsorrel, as well as some measurements on cuttings from deep boreholes. The mean values obtained from these measurements are given in table 7.1. Also included in the table are some measurements made on borehole samples by Bullerwell (1967) and some measurements made on samples from the Malvern Hills (Brooks 1968).

### 7.2.1 New measurements

Saturated densities have been measured on a selection of "basement" rocks from boreholes and outcrop in the East Midlands. In order to show the range of densities obtained for each suite of rocks all the measurements made are given in table 7.1 The restricted sampling for each group of samples does not permit a meaningful statistical analysis to be made.

The samples, which weighed Ø.Ø5 to Ø.4 kg, were dried in an oven and then put in a vacuum flask for several days. The samples were then immersed in water and left to saturate under atmospheric pressure for several days. The saturated samples were weighed in air and in water using a beam balence (reading accuracy > Ø.1 gram). The sample densities are given by:

$$\text{saturated density} = \rho_S = W_1 \,/\, (W_1 - W_2)$$

$$\text{dry density} = \rho_D = W_3 \,/\, (W_1 - W_2)$$

$$\text{porosity} = \phi = (\rho_S - \rho_D) \,.\, 100\%$$

where: $W_1$ = saturated weight in air

$W_2$ = saturated weight in water

$W_3$ = dry weight in air

The dry densities measured are not included in table 7.1. Of the samples measured only the Hartshill Quartzite (3.7%) and the weathered Kirby Lane granite (5.5%) had porosities of over 2%. Porosities of less than 2% are reasonable for unweathered, fine grained, metasediments, and for igneous rocks. Had it been possible to saturate the rocks under realistic confining pressures the measured porosities might have been higher, due to the saturation of microfractures. In the case of the Kirby Lane granite the porosity was due to the presence of chlorite and kaolinite. If the samples were not fully saturated the density measurements will be under-estimated.

### 7.2.2 Density : rock type

The density measurements from table 7.1 are grouped by age and/or rock type in figure 7.1. Clearly there is a considerable range of densities associated with each grouping. It is therefore difficult to assign typical densities to any of the rock units found in the area.

The South Leicestershire and Mountsorrel intrusions are less dense than the Precambrian pyroclastics and metasediments, but the Warboys diorite is significantly more dense. The sample of Melton granite is excluded since it was weathered. The samples from the South Charnwood Diorites

PRECAMBRIAN METASEDIMENTS AND VOLCANICS

| | | | | |
|---|---|---|---|---|
| Charnian Blackbrook Series | | (13) | 2630 ± 30 | 1 |
| " Beacon Hill Beds | | (10) | 2700 ± 20 | 1 |
| " Slate Agglomerate | | ( 8) | 2790 ± 20 | 1 |
| " Swithland Slate | | ( 7) | 2780 ± 20 | 1 |
| Sproxton bh. phyllitic shale | | ( 8) | 2840 ± 90 | 1 |
| Upwood bh. tuffaceous agglomerate | | | 2680 | 2 |
| Glinton bh. tuff | BDB 4342 | (359.3) | 2704 ± 10 | 3 |
| " " " | BDB 4343 | (360.2) | 2703 ± 10 | 3 |
| " " " | BDB 4344 | (363.3) | 2775 ± 10 | 3 |
| " " " | BDB 4345 | (375.8) | 2688 ± 10 | 3 |
| " " " | BDB 4346 | (376.4) | 2670 ± 10 | 3 |
| Wittering bh. tuff | BZ 461 | (232.1) | 2795 ± 10 | 3 |
| Hollowell bh. agglomerate | | (175.0) | 2714 ± 10 | 3 |
| " " " | | " | 2696 ± 10 | 3 |
| " " " | | " | 2697 ± 10 | 3 |

PRECAMBRIAN IGNEOUS INTRUSIONS

| | | | | |
|---|---|---|---|---|
| Malverian granitic rocks | | | 2630 ± 20 | 4 |
| Malverian basic-ultrabasic rocks | | | 2680-3070 * | 4 |
| Markfield diorite | | (39) | 2800 ± 10 | 1 |
| Groby diorite | | (34) | 2720 ± 10 | 1 |
| Whitwick porphyroid | | ( 4) | 2700 ± 80 | 1 |
| Bardon Hill porphyroid | | (29) | 2840 ± 10 | 1 |

CAMBRIAN - ORDOVICIAN SEDIMENTS

| | | | | |
|---|---|---|---|---|
| Nuneaton Hartshill Quartzite | | | 2610 ± 10 | 3 |
| Merry Lees Stockingford Shale | | ( 7) | 2750 ± 20 | 1 |
| Deanshanger bh. Tremadocian shale | | | 2520 | 2 |
| Great Paxton bh. Ordovician mudstone | | | 2550 | 2 |
| Eyham bh. silty mudstone | | (11) | 2750 ± 10 | 1 |
| GH 3 bh. siltstone | BDA 3917 | (152.4) | 2684 ± 10 | 3 |
| " " | BDA 3918 | (153.3) | 2693 ± 10 | 3 |
| " " | BDA 3919 | (153.9) | 2682 ± 10 | 3 |
| Thorpe-by-Water bh. | BDF 2812 | (331.3) | 2788 ± 10 | 3 |
| " " " " | BDF 2813 | (332.3) | 2774 ± 10 | 3 |

| | | | | |
|---|---|---|---|---|
| Thorpe-by-Water bh. | BDF 2819 | (335.4) | 2790 ± 10 | 3 |
| " " " " | BDF 2823a | (338.5) | 2770 ± 10 | 3 |
| CALEDONIAN IGNEOUS INTRUSIONS | | | | |
| Mountsorrel granodiorite | | (60) | 2660 ± 10 | 1 |
| " " | | | 2687 ± 10 | 3 |
| " " | | | 2638 ± 10 | 3 |
| " " | | | 2669 ± 10 | 3 |
| " " | | | 2652 ± 10 | 3 |
| Enderby microtonalite | | | 2679 ± 10 | 3 |
| " " | | | 2674 ± 10 | 3 |
| Kirby Lane bh. biotite granite | | | 2559 ± 10 | 3 |
| " " " " " | | | 2564 ± 10 | 3 |
| Warboys bh. diorite | BX 7294 | (156.8) | 2839 ± 10 | 3 |
| " " " | BX 7313a | (167.2) | 2813 ± 20 | 3 |
| " " " | BX 7313b | (167.2) | 2781 ± 20 | 3 |
| " " " | BX 7364 | (187.3) | 2866 ± 10 | 3 |
| " " " | BX 7375 | (192.8) | 2725 ± 10 | 3 |
| " " " | BX 7377 | (193.1) | 2813 ± 10 | 3 |
| " " " | | | 2820 | 2 |
| DEVONIAN SEDIMENTS | | | | |
| Ellingham bh. mudstone-slate | | | 2630 ± 30 | 5 |
| Lakenheath bh. siltstone | | | 2620 ± 40 | 5 |
| Four Ashes bh. shale | | | 2670 ± 33 | 5 |
| Little Chiswell bh. mudstone | | | 2610 ± 20 | 5 |

Sources : 1. Maroof 1973. Number of samples used in brackets.
2. Bullerwell 1967.
3. New measurement. For borehole samples the figure in brackets is the depth in metres below OD and the ID's are the IGS sample numbers.
4. Brooks 1968. * = densities > 3000 kg.$m^{-3}$ very rare.
5. Chroston and Sola 1982.

Table 7.1 : Densities of basement rocks in the East Midlands and adjacent areas.

D : Deanshanger borehole
GP : Great Paxton borehole
GH : G H 3 borehole
E : Eyham borehole
ML : Merry Lees drift
T : Thorpe-by-Water borehole
B : Blackbrook Series
SA : Charnian Slate Agglomerate
SS : Swithland Slate
BH : Beacon Hill Beds
G : Glinton borehole
S : Sproxton borehole
U : Upwood borehole
H : Hollowell borehole
W : Wittering borehole
MS : Mountsorrel Granodiorite
SL : South Leicestershire Diorites
W : Warboys borehole
BP : Bardon Hill Porphyroids
WP : Whitwick Porphyroids
MD : Markfield Diorite
GD : Groby Diorite
M : Malvernian granitic intrusions

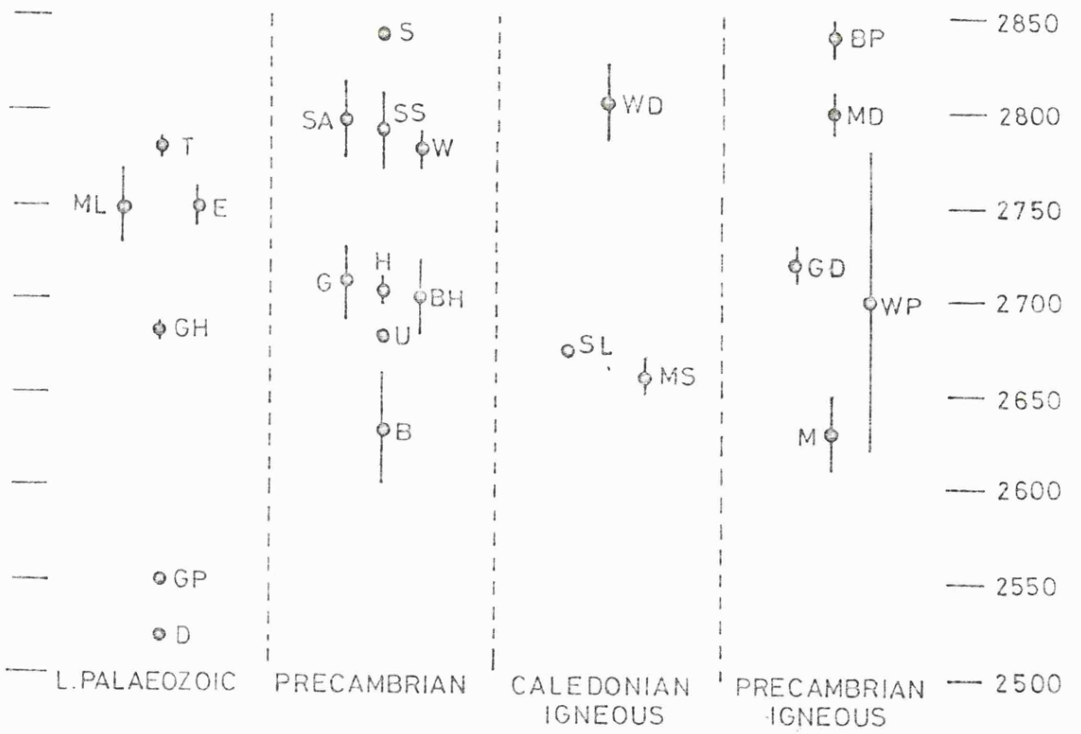


Figure 7.1: Density variations for different lithologies, based on the data in table 7.1. The points represent the means of the measured samples, the error bars show the standard error estimates.

show that a considerable variation in density is possible within a single intrusion, with values of 2720 $kg.m^{-3}$ from Groby and 2800 $kg.m^{-3}$ from Markfield.

The Lower Palaeozoic mudstones and shales from the Great Paxton and Deanshanger boreholes have lower densities than any other basement rocks in the area. The pyritised siltstones from the Thorpe-by-Water borehole and the Stockingford Shales from the Merry Lees drift are more dense than several of the Precambrian samples. In the context of the gravity interpretations carried out here, it is reasonable to class the Lower Palaeozoic sediments as basement.

### 7.2.3 Density : p-wave velocity

Some of the samples on which densities have been measured come from localities where the basement velocity has been measured by seismic refraction or borehole logging. These data are shown in figure 7.2, part of the curve of Nafe and Drake (1963) is included for reference.

These data should be treated with some caution, especially when comparing the different measurements. The Deanshanger and Great Paxton mudstone velocities were determined from borehole logs. The other velocity data come from seismic refraction surveys and represents a bulk velocity for the formation. The Nafe and Drake measurements were on laboratory specimens. The points plotted in figure 7.2 are from several different lithologies; the igneous rocks (Mountsorrel, South Leicestershire and Warboys) and the fine grained Precambrian metamorphic rocks (Maplewell and Blackbrook Series and Glinton borehole) do show a positive correlation between velocity and density. The scatter of

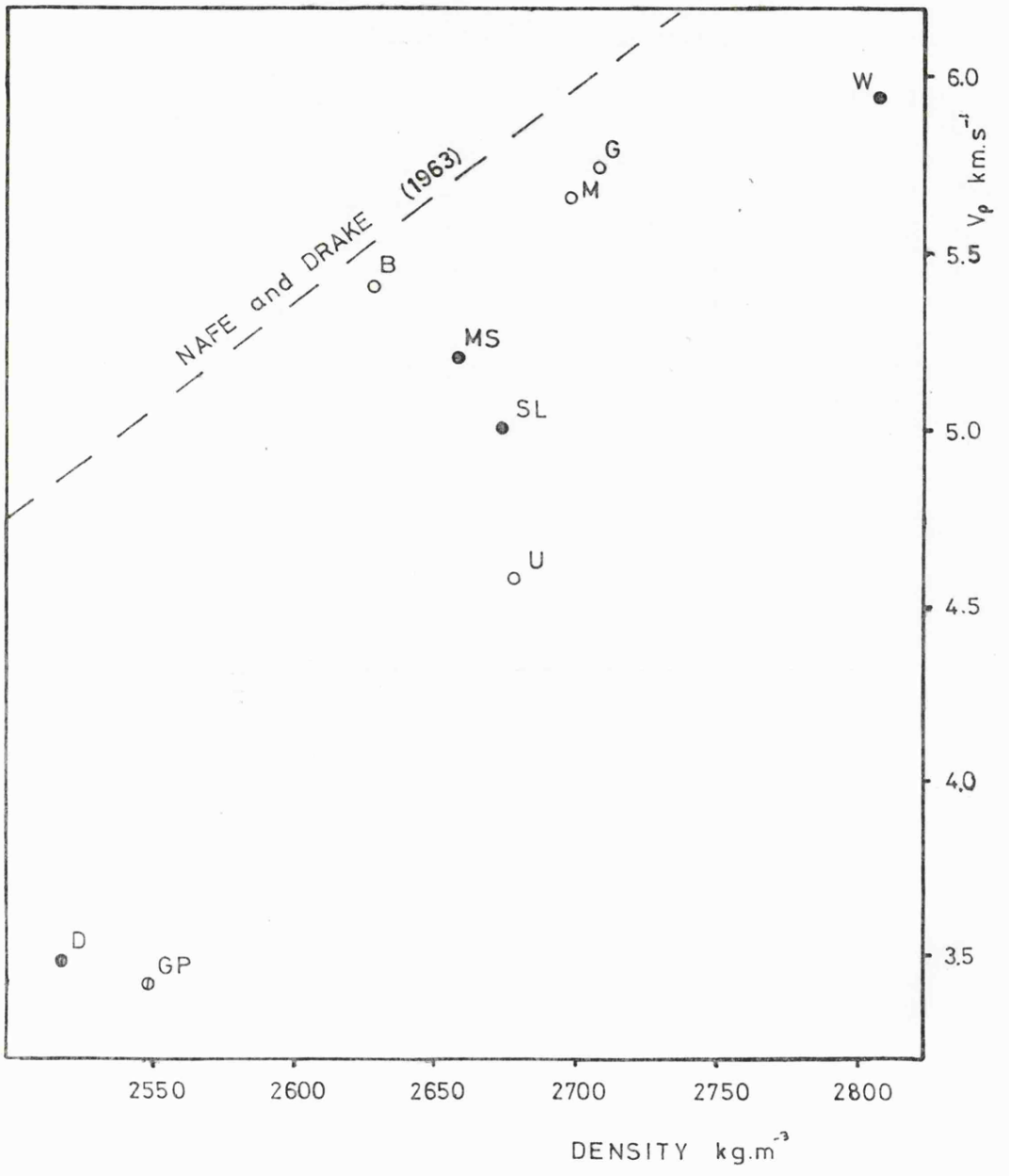


B : Blackbrook Series
D : Deanshanger borehole
G : Glinton borehole
GP : Great Paxton borehole
M : Maplewell Series
MS : Mountsorrel granodiorite
SL : South Leicestershire Diorites
W : Warboys borehole
U : Upwood borehole

Figure 7.2 : The relation between density and p-wave velocity.

points shows that the igneous rocks cannot be distinguished from the Precambrian basement rocks even if both p-wave velocity and density are known.

The interpretation of the Melton refraction profiles (chapter 5) indicated a velocity of 5.8 to 6.Ø km.$s^{-1}$ for the Melton granite. This suggests a density at least as high as those of the Precambrian tuffs in the Glinton borehole and the Maplewell Series (Beacon Hill Beds) of the Charnian.

The high density for the Thorpe-by-Water siltstone, which may have been due to disseminated pyrite, suggests a high p-wave velocity. However the seismic refraction surveys of Bullard et.al. (1946), located 5 to 1Ø kilometres from the borehole, indicated a 5.43 to 5.69 km.$s^{-1}$ refractor about 1ØØ metres deeper than the top of the siltstone. This suggests that either the siltstone has a high velocity but thins laterally and was not detected, or that the high density does not correlate with a high p-wave velocity. The refractor could have been the siltstone, a change in depth of 1ØØ metres over a few kilometres seems reasonable, but would be atypical for this area (see chapter 9).

### 7.2.4 Densities of the supra-basement sediments

No new direct density measurements have been made on these rocks in the course of the present study. Maroof (1973) measured chip samples from the Sproxton borehole and quotes densities of 249Ø $\pm$ 15 kg.$m^{-3}$ for the Lias and 24ØØ $\pm$ 9 kg.$m^{-3}$ for the Trias.

Brooks (1966) analysed 56 samples of Keuper Marl from The Midlands; these gave a mean density of 245Ø $\pm$ 2Ø kg.$m^{-3}$.

Compensated formation density logs are available for

the Huntingdon and Wisbech boreholes. These logs were blocked to obtain average densities for the various formations:

| | | | |
|---|---|---|---|
| WISBECH | Middle Lias shale | 2100-2200 | $kg.m^{-3}$ |
| | Basal Lias | 2310 | " |
| | Trias sandstone | 2420 | " (ø 16-20%) |
| HUNTINGDON | Middle Jurassic | 2050 | $kg.m^{-3}$ |
| | Lias | 2050-2200 | " |
| | Keuper | 2200 | " |

## 7.3 MAGNETIC PROPERTIES

The magnetic properties referred to here are all given in SI units, the following relationships are used:

Susceptibility: k (SI) = k' (cgs) . $4\pi$ (dimensionless)

Magnetisation: M (SI) $A.m^{-1}$ = M (cgs) . $10^{-3}$

Magnetic dipole moment: md (SI) $A.m^2$ = md (cgs) x $10^3$

Permeability of free space: $\mu_o = 4\pi . 10^{-7}$

Magnetic intensity (remanence) = M (cgs) . $4\pi . 10^5$ nT

The details of the conversion of electromagnetic units to SI are given by Reilly (1972).

### 7.3.1 Magnetic susceptibility and remanence

Maroof (1973) measured the magnetic susceptibilities of samples from the igneous intrusions of Mountsorrel and Charnwood Forest. These measurements indicated a considerable variation in susceptibility within each rock type:

| Sample | mean k (SI) | 95% confidence limit |
|---|---|---|
| Mountsorrel granodiorite | 0.0264 | 0.0117 |
| Markfield diorite | 0.0787 | 0.0321 |
| Groby diorite | 0.0045 | 0.0045 |
| Bardon Hill porphyroid | 0.0009 | 0.0004 |

One new measurement has been made on a sample (IGS BX 7313) from the Warboys diorite, which gave a value of 0.028 $\pm$ 0.01 (SI). A single measurement such as this can only serve as an indication that the susceptibilities of the diorite are the same magnitude as those of the Mountsorrel granodiorite.

Brooks (1968) made susceptibility and remanence measurements for the Precambrian rocks of the Malvern Hills. The remanence intensities below have been converted from emu to SI as described above:

| | k (SI) | Remanence nT |
|---|---|---|
| Warren House lavas | 0.003-0.010 | 300-1000 |
| Malvernian | 0.002-0.004 | 200-380 |

For field strengths of about 50000 nT these measurements indicate a Koenigsberger ratio (Q) of about one.

Recent measurements by Duff (1980) on the South Leicestershire, South Charnwood and Mountsorrel intrusions yielded NRM intensities of $10^{-3}$ to 1 $A.m^{-1}$ (1.25-1250. nT). Piper (1979) gives values of 0.4 to 150 nT for the late Proterozoic rocks of the Midland craton (NB the values were quoted in $A.m^{2}.kg^{-1}$ and have been converted assuming a density of 3000. $kg.m^{-3}$).

Six samples from three intrusions have been measured in

a spinner magnetometer to determine the intensity of the remanence. As the samples came from borehole cores it is possible to calculate the inclination if the core is assumed to have been vertical. The remanence in all the samples was weak, and the values of Q very low (see below) as was to be expected for such coarse grained acidic rocks. The initial measurements were sufficient to show the weakness of the remanent magnetization and therefore the samples were not demagnetized.

| | Magnetization nT | I | Q |
|---|---|---|---|
| Mountsorrel | 302 | 86 ± 20° | 0.3 |
| " | 82 | 67 ± 20° | 0.1 |
| Warboys BX 7377 A | 94 | 65 ± 20° | 0.1 |
| " " " B | 120 | 69 ± 20° | 0.1 |
| Kirby Lane 71380 | 1.9 | - | 0.002 |
| " " 71383 | 4.6 | - | 0.005 |

Declination and inclination measurements for basement rocks from the Midlands craton are given by Brooks (1963) and Piper (1979):

| | | D° | I° |
|---|---|---|---|
| Late Proterozoic basement: | Rushton schist | 274* | 51* |
| | Church Stretton | 282 | 51 |
| | Malvernian | 127 | 77 |
| Late Precambrian: | West Uriconian | 136 | 25 |
| | East Uriconian | 078 | 17 |
| | Warren House | 233 | 77 |

* corrected for the dip of the overlying Cambrian sediments.

Duff (1980) measured samples from 11 sites in the Leicestershire intrusions. The mean NRM direction before demagnetization was D=24°, I=62° which is not significantly different from the present position at the 95% confidence limit. Of the 11 sites sampled only three (Enderby, Markfield and Bradgate quarries) gave stable, scatter free, NRM directions after demagnetization. The calculated pole for these sites was 141E 63N (D=18°, I=48°) which is typical of late Precambrian and early Cambrian pole positions. If the U-Pb date of 452 m.yr. for the South Leicestershire diorites (chapter 1) is accurate, then the determination of an early Cambrian pole position for the Enderby diorite is anomalous. The older, Late Proterozoic, rocks from the Midlands craton give pole positions of 235-285E 13-37N (Briden and Duff 1981).

The available data do not indicate any significant remanence intensities for the Midlands granitic rocks. However the late Precambrian pole positions are such that the the magnetic anomalies would be affected by any bodies with a significant component of remanent magnetization.

## 7.4 POTENTIAL FIELD MODELLING

The two and three dimensional gravity and magnetic models in this and the following chapter have been prepared using pre-existing computer programs. The theory of the techniques is well documented and is summarized below.

### 7.4.1 Two-dimensional gravity modelling

This method is described by Talwani et.al. (1959). It is based on the approximation of a 2-dimensional body by an n-sided polygon. The gravity effect of this polygonal body at any point outside the body is then given by a line integral around the perimeter of the body.

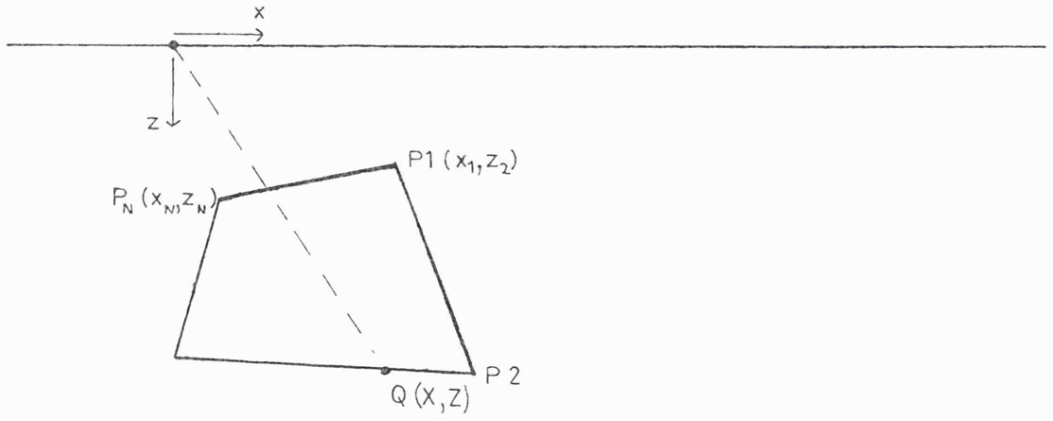


$$\Delta g(0) = 2.G.\rho. \oint \tan^{-1} \frac{X}{Z} \, .dz \qquad (7.1)$$

The i th side of the polygon is given by:

$$X = a_i . Z + b_i$$

where : $a_i = (x_{i+1} - x_i)/(z_{i+1} - z_i)$, $b_i = (x_i . z_{i+1} - x_{i+1} z_i)/(z_{i+1} - z_i)$

Integrating (7.1) gives a numerical solution for i = 1,n. For the n th. side $(x_{i+1}, z_{i+1}) = (x_n, z_n)$. A complete profile can be calculated by moving the position of O horizontally

by some suitable value $\Delta x$. The values of $z_i$ in the summation will be unchanged whilst the $x_i$ values will be incremented by $\Delta x$.

## 7.4.2 Two-dimensional magnetic modelling

Talwani and Heirtzler (1964) published a Fortran IV computer program for the calculation of the horizontal, vertical and total intensity anomalies caused by a 2-dimensional, polygonal body.

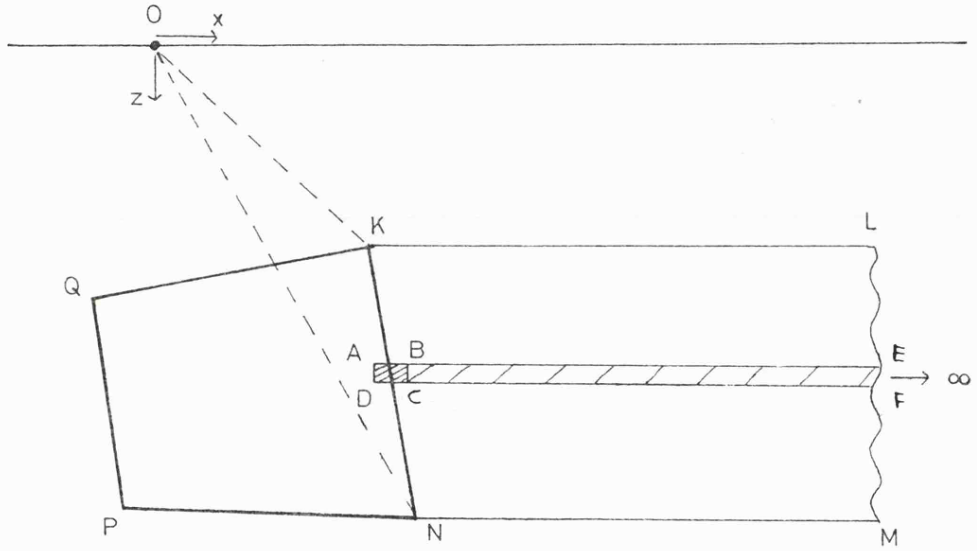


The horizontal (H) and vertical (V) field strengths at the origin (O) due to the semi-infinite two-dimensional prism KLMN can be determined by first calculating the effect of the prism element ABCD which extends to $\pm \infty$ in the y direction. Integrating with respect to x gives expressions for H and V for the semi-infinite horizontal lamina ABEF. These expressions can then be integrated with respect to z, taking into account the orientation of the side KN, to give the values of H and V due to KLMN. This is repeated for each side of the polygon and the successive values of H and V

summed. The position of O is then moved and the process repeated.

### 7.4.3 Three-dimensional iterative gravity inversion

A program based on the method of Cordell and Henderson (1968) was used to interpret the Peterborough gravity anomaly (chapter 8B).

This method simulates the geological model by means of a rectangular array of vertical square prisms, each prism being centred on a known data point. This requires the observed data to be on a square grid. The vertical dimensions of the prism are calculated with respect to a predefined reference plane at the top, bottom or centre of the model. A first estimate of the prism lengths is obtained from a Bouguer slab approximation. Successive iterations are performed by comparing the observed and calculated gravity at each grid node and adjusting that prism accordingly. One of the limitations of this method is that the density contrast has to be constant for the entire body.

The gravitational attraction of each prism at each grid node is calculated in two stages.

1. For the prism at the grid node:

$$\Delta g = 2.\pi.G.\rho \left[ t - \left((d+t)^2 + w^2/\pi\right)^{1/2} + \left(d^2 + w^2/\pi\right)^{1/2} \right]$$

where d = depth to the top of the prism, t = prism thickness and w = grid spacing (length of prism sides).

2. For all other prisms:

$$\Delta g = G.\rho.w^2 \left[ \left( R^2 + d^2 \right)^{-1/2} - \left( R^2 + (d+t)^2 \right)^{-1/2} \right]$$

this is the formula for a vertical line element, where R = the distance from the prism centre to the grid node.

The attraction due to all the prisms can then be summed at each grid node and the thicknesses adjusted:

$$t_{n+1} = t_n . (g_{obs} / g_{calc})$$

In practice it was found that rapid oscillations occurred in the values of "t". Therefore the adjustment of "t" was progressively damped with the amount of change being limited to 50% of the value of "t" for the first 5 iterations, 10% for the next 3 and 5% thereafter.

The calculated anomaly will be due only to mass beneath the grid nodes, i.e. within the area of the model. If the observed data does not completely cover the causal body this can create an edge effect in which the prisms around the model become too large in an attempt to compensate for the material outside the model. If the regional field is not removed the model will also include a horizontal slab to accommodate this component.

An attempt was made to reduce the edge effects by calculating the gravitational attraction, at each grid node, of 12 right rectangular prisms arrayed around the edge of the model. The calculation used the formula of Nagy (1966). The external prisms were of preset thickness and had sides equal to half the length of the equivalent side of the input data array. The computation of the gravity anomaly of these prisms was found to take about the same time as one iteration of a 30 x 30 grid of data points. The computationally

faster line element approximation could not be used because of the size of the external prisms. Better definition would be obtained if more prisms were used but this would increase the computation time still further. Using these prisms helped to isolate the anomaly being modelled at the expense of a slight distortion in the observed data (see chapter 8B).

7.4.4 Three-dimensional gravity modelling

This method, after Talwani and Ewing (1960) is a forward modelling technique as opposed to the inversion of observed data in the iterative method. The method is a development of the two-dimensional method described above and is based on an expression for the gravitational attraction, at an external point, of a horizontal lamina defined by an irregular polygon. Horizontal laminae are preferred since any three-dimensional body can be defined by a number of surface contours which can then be replaced by laminae represented by n-sided polygons.

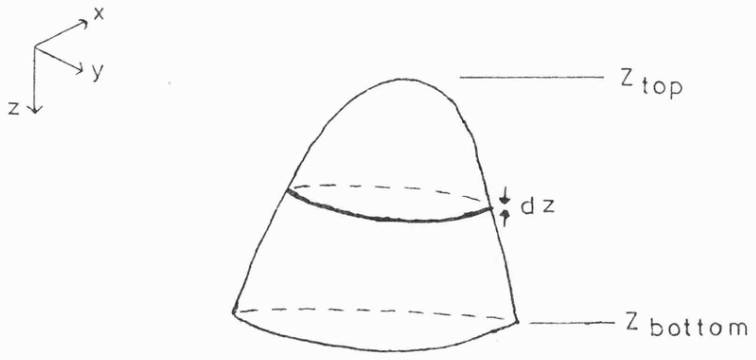


The gravitational attraction at a surface point P due to a polygonal lamina of infinitesimal thickness dz will be:

$$\Delta g = V.dz$$

where V is the anomaly per unit thickness of the polygon,

this can be determined from the evaluation of two line integrals around the polygon. The total anomaly at P due to the body will be:

$$\Delta g = \int_{z_{bottom}}^{z_{top}} V.dz$$

This can be solved graphically by plotting V:z and drawing a smooth curve. The area between this curve and the z axis will give $\Delta g$. In practice the problem is solved by numerical integration with parobolas fitted to successive groups of three points. The accuracy is therefore dependent on the accuracy with which the body is defined by the contours.

### 7.4.5 Three-dimensional magnetic modelling

A program to calculate the magnetic anomalies of three-dimensional polygonal bodies, after Barnett (1976) was used in the interpretation of the aeromagnetic data. This program was developed by Dr. W.H. Owens of Birmingham University. A number of bodies of differing but constant magnetic susceptibility could be modelled and the anomaly due to each body summed. Each body is defined by a number of polygonal sections (templates) which, in the simplest case, would be vertical and coplanar. The polygonal body is then reconstructed by joining the vertices of the templates to form triangular facets. To preserve the triangular faceting it would be necessary to specify apices at either end of the body. This is circumvented by using the expressions of Okabe (1979) for the magnetic attraction of a polygonal facet. The program therefore used the first and last templates to define the ends of the body.

## 7.5 GRAVITY AND MAGNETIC ANOMALIES IN THE EAST MIDLANDS

### 7.5.1 Magnetic anomalies

Figure 7.3 is a reduction of the IGS 1:250000 aeromagnetic map of the East Midlands; the area described here lies to the east of the Thringston Fault (TF).

Several of the magnetic anomalies can be correlated with the surface or borehole geology; the late Precambrian South Charnwood Diorites (E) and the Caledonian intrusions of Mountsorrel (B), Melton Mowbray (C), and South Leicestershire (D) are all recognisable. The Mountsorrel and Melton intrusions lie in a belt of 100 to 250 nT positive anomalies which is truncated, to the west of anomaly A, along the line of the Thringston Fault. To the east of anomaly C the belt swings southeastwards to form a 35 kilometre ridge of positive anomalies (G-H-I-J). A longer wavelength, lower amplitude, anomaly (K) lies to the south of the Melton intrusion. If all these anomalies are grouped together they form an area of about 2500 $km^2$ of positive, mostly short wavelength, anomalies. The Warboys diorite (F) is located to the southeast of this area. Simple depth estimates using the techniques of Steenland (1951) suggest that the top surfaces of the sources of these anomalies are at depths of one to three kilometres.

The belt of anomalies A-C, G-I lies along the northern margin of the region of shallow Precambrian-Lower Palaeozoic basement, as proved by boreholes (see chapter 9), and can be thought of as representing a hinge line between the Midlands Platform to the south and the Carboniferous basins to the north.

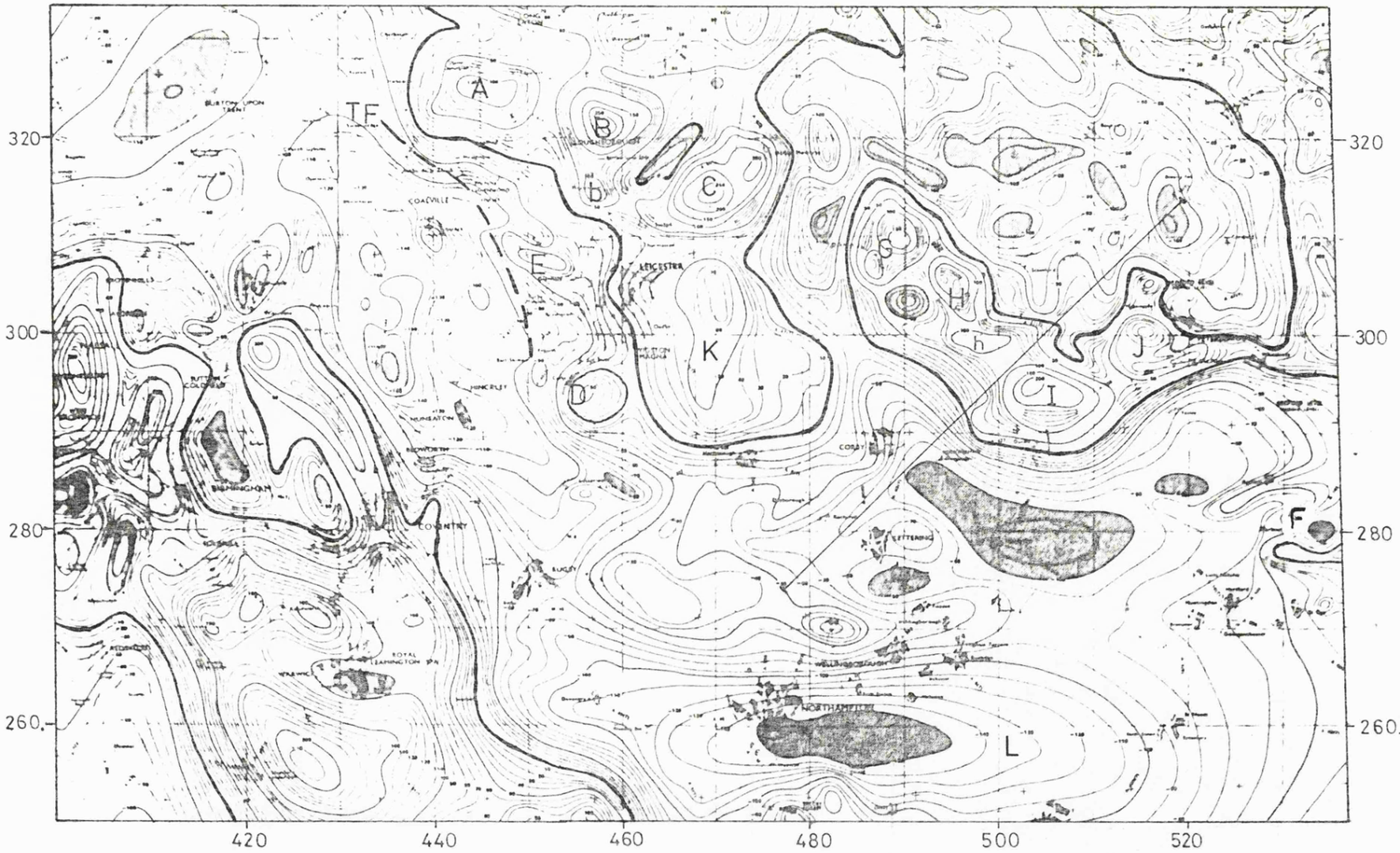


Figure 7.3 : Aeromagnetic map of the East Midlands. Bold contour is Ø nT, negative closures shaded.

To the south of the positive anomalies there is a long wavelength, east-west trending, negative anomaly (L). The depth to magnetic basement here is probably greater than six kilometres.

### 7.5.2 Gravity anomalies

The gravity map (figure 7.4) also shows the locations of, and depths to the pre-Carboniferous basement in, the boreholes in the area. The magnetic anomalies A-J are marked on the gravity map for reference. There is little visible correlation between the gravity anomalies and sediment thicknesses, the negative anomaly P is due to the Carboniferous sediments of the Widmerpool Gulf. Low Q is the Peterborough gravity anomaly (chapters 6 and 8B); low R is located over the shallowest Precambrian basement in the area (excluding Charnwood Forest).

The positive anomaly S is due to the southern end of a basement ridge that connects the Derbyshire Dome to the Charnian Inlier (the Derby-Melbourne causeway). This positive anomaly extends eastwards to the south of the Mountsorrel and Melton intrusions, and then swings southeast (anomaly T), parallel to, but some 10 kilometres south of, the magnetic ridge (anomalies G-H-I-J). These ridges therefore follow a northwest to southeast "Charnoid" trend.

At the eastern end of the gravity ridge is a small positive anomaly (F) located over the Warboys diorite intrusion. The density data in table 7.1 shows that this intrusion has a higher density than the Precambrian agglomerates in the nearby Upwood borehole.

A second positive ridge (V) with a similar trend to T

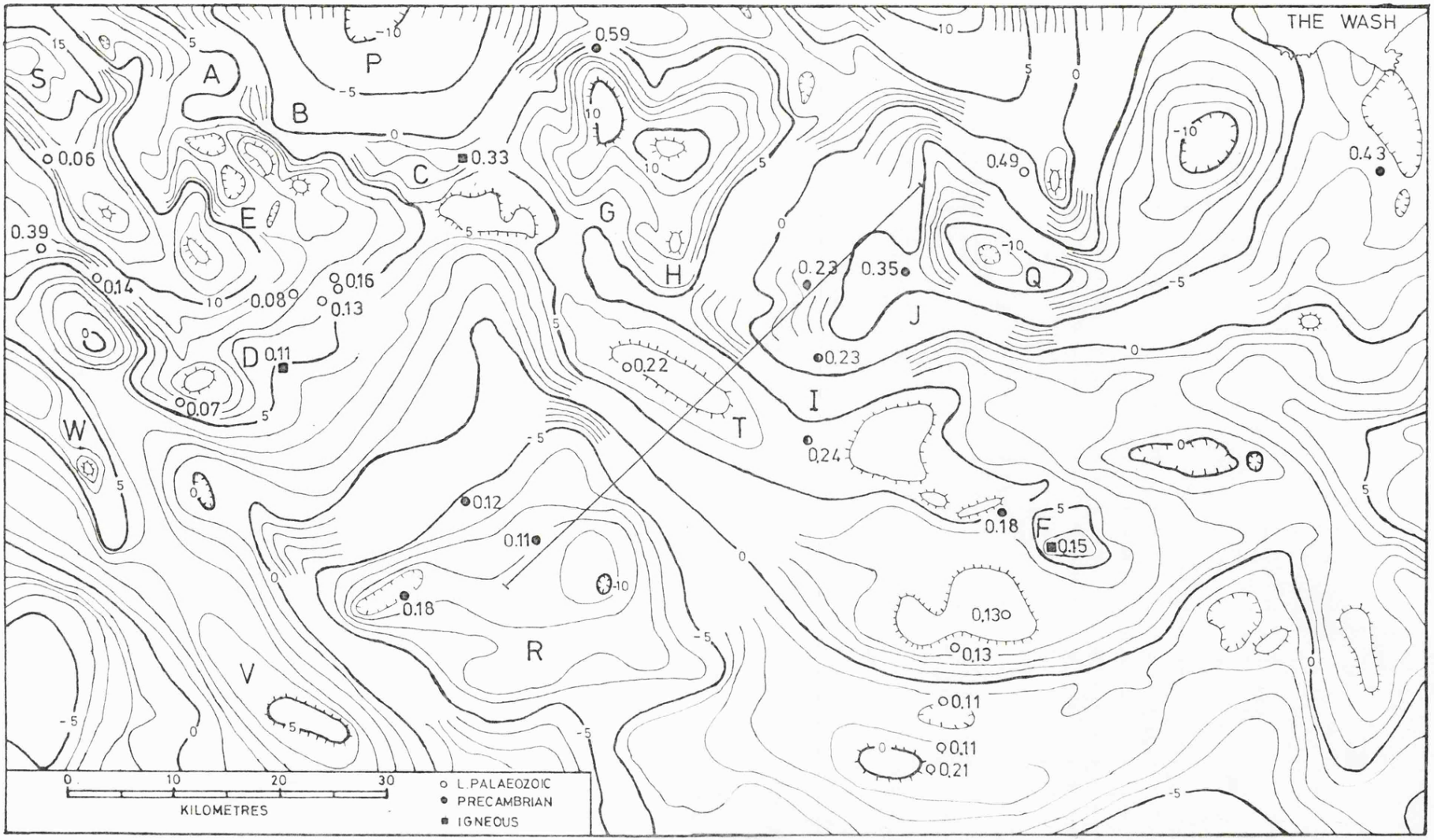


Figure 7.4 : Bouguer gravity map of the East Midlands with depths to basement.

lies to the southwest of the low R. At the northwest end of this ridge is the Nuneaton Inlier (W). Low R broadens out to the south to form a large negative anomaly which covers much of the London Platform.

Although the Mountsorrel intrusion has a lower density than the surrounding Precambrian basement there is no discernable associated negative gravity anomaly. This suggests that the density contrast decreases with depth. The Holwell seismic line (Whitcombe and Maguire 1981a) indicated a large vertical velocity gradient within the intrusion, this would be consistent with the density of the granite increasing more rapidly with depth than the density of the surrounding basement. The density of the Melton granite was dicussed above in relation to the high p-wave velocity observed over the intrusion. The velocity data suggest that the granite does not have a negative density contrast with the Precambrian basement. In the case of both the Mountsorrel and Melton intrusions the negative anomaly of the Widmerpool Gulf may be masking any small anomalies due to the intrusions. The seismic reflection line and detailed gravity profile in progress at Leicester should provide enough control to accurately remove the effects of the sediments and detect any residual anomaly due to the northern extension of the Mountsorrel intrusion.

In general it appears that the observed gravity anomalies cannot be explained by variations in the depth to basement. A wide range of densities have been measured for the Precambrian-Lower Palaeozoic rocks and it is possible that these variations might account for some of the observed anomalies. Imformation on the thickness of the Lower

Palaeozoic is scarce but what there is suggests a thin veneer of mudstones overlying the Precambrian. Therefore the larger gravity anomalies are likely to be due to structures within the Precambrian basement. One such anomaly is investigated below.

### 7.5.3 Simple two-dimensional modelling

The Charnoid trend of the positive gravity ridge T and the thin post-Carboniferous sediment cover (figure 7.4) suggest that the anomaly may be due to an intra-basement structure. The two possible sources of such a structure are a horst of Proterozoic basement rocks, possibly analogous to the rocks exposed in the west of the Midlands craton; or a linear igneous intrusion. Either model might also explain the ridge of magnetic anomalies.

A density contrast of 130 $kg.m^{-3}$ was used for the two-dimensional model. This implies a density of about 2880 $kg.m^{-3}$ for the anomalous body, given a Charnian type basement density of about 2750 $kg.m^{-3}$. The Markfield Diorites, which intrude the Charnian , have a density of 2800 $kg.m^{-3}$ and a magnetic susceptibility of 0.08 (SI), although other late Precambrian intrusions in the area are neither as dense nor as magnetic. The only clue to the density of the Proterozoic basement is the 6.4 $km.s^{-1}$ refractor velocity determined for the deep refractor beneath Charnwood Forest, and for the LISPB "$a_1$" refractor (see chapter 1).

The line of the profile chosen for gravity modelling is shown in figures 7.3 and 7.4. The model for the observed data is shown in figure 7.5, a reasonable fit has been obtained with a simple (8 sided) body, the calculated points

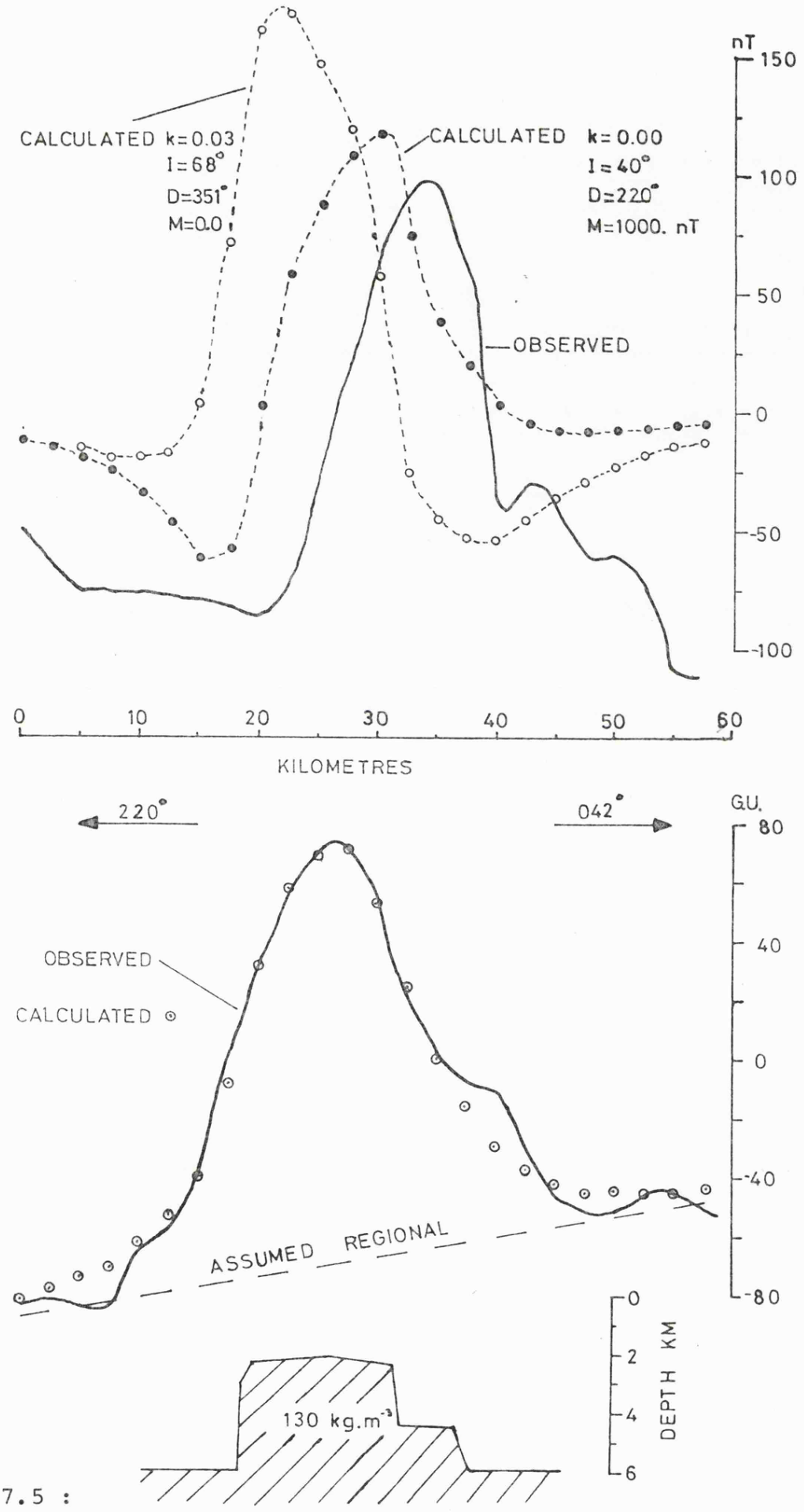


Figure 7.5 :

2-D gravity and magnetic models for the basement ridge.

are at intervals of 2.5 kilometres.

In order to model the edges of the profile it was necessary to assume a regional gradient, of about Ø.7 gu/km, rising to the northeast. The boreholes in the area indicate that the thickness of the supra-basement sediments increases to the northeast. The gravity effect of these sediments has not been removed separately, if it were the regional gradient would be increased by up to Ø.5 gu/km. The required regional cannot therefore be explained by sediment thicknesses and is most likely to be due to the non two-dimensional nature of the anomalies to the northeast of the gravity ridge. In particular the profile passes close to the Peterborough gravity anomaly (Q). The misfit of the calculated points is worst at the ends of the profile, especially on the northeast side. The densities in table 7.1 show a variation in density within the Precambrian-Lower Palaeozoic basement, this could also account for a regional gradient, although there are insufficient data to map the variations in basement density.

For the chosen density contrast it was necessary to use a model with near verical sides in order to fit the steep slopes of the observed profile. This indicates that the depth to the top of the model (two kilometres) can be considered a maximum value.

This simple model suggests that it is possible to explain the gravity ridge by a 4 kilometre horst structure within the basement. The size of this structure could be reduced to a thickness of about two kilometres if a density of 3ØØØ $kg.m^{-3}$ were used, such a density can be considered as an upper limit for shallow Proterozoic basement.

The observed total field magnetic anomaly along the profile is also shown in figure 7.5. Two possible anomalies have been calculated for the body modelled from the gravity data. In the first model (open circles) the magnetization was assumed to be induced with a susceptibility of Ø.Ø3 (SI). This is a higher value than those given above, but was necessary to satisfy the amplitude of the observed anomaly; this suggests that the magnetic body might have a greater thickness than the 4 kilometres of the gravity model. The main problem with the calculated magnetic profile is that the peak is shifted slightly to the southwest of the centre of the body whereas the peak of the observed anomaly is 1Ø kilometres to the northeast of the gravity anomaly. Clearly if the gravity and magnetic anomalies are due to the same source body the magnetization must be dominantly induced with a declination to the southwest.

In practice any calculated anomaly would be the resultant of the remanent and induced magnetizations. In order to investigate the maximum possible shift of the anomaly, in the plane of the profile, the magnetic anomaly was recalculated for an apparent remanent magnetization of 1ØØØ.Ø nT with D = 22Ø° and I = 4Ø° and no induced component, this is not necessarily the orientation of the actual remanence.

The calculated anomaly (solid circles) is displaced towards the observed anomaly but still lies to the southwest of it. At inclinations of less than 4Ø° the displacement is slightly greater but the negative lobe on the southwest side of the peak becomes unreasonably large. It therefore seems unlikely that the gravity and magnetic anomalies are due to the same source body. This does not mean that the two

anomalies are unrelated, their similar trend suggests that they may well be related. It is possible that a non-magnetic, high density, intra-basement horst structure is flanked, on one side, by a ridge of strongly magnetic intrusions which have little or no density contrast with the Precambrian basement. The magnetic ridge is composed of of number of separate peaks (eg. G,H,I,J), these might be explained in terms of a number of cupolas extending upwards from a plutonic body. The magnetic anomalies are investigated further in the following section.

### 7.5.4 Magnetic anomalies G H I J

These four anomalies are the most prominent highs in the belt of magnetic anomalies that runs from east of Melton Mowbray to Peterborough. The individual anomalies have a similar areal extent to the anomaly due to the South Leicestershire Diorites (D) but are of a larger amplitude. As described above the individual anomalies lie within a larger, ridge like, positive anomaly (figure 7.6).

The three-dimensional modelling program (see 7.4.5) was used to calculate the anomalies due to a group of simple prismatic bodies. The object was to obtain a reasonable representation of each of the observed peaks and then to see if these anomalies would coalesce to form the background ridge.

The prisms were defined by horizontal polygonal contours with four or five sides, an extra contour was sometimes added to the top of the body to create a sharper apex. The sides of the prisms were sub-vertical and outward sloping. A base level of 8 kilometres was used, with the

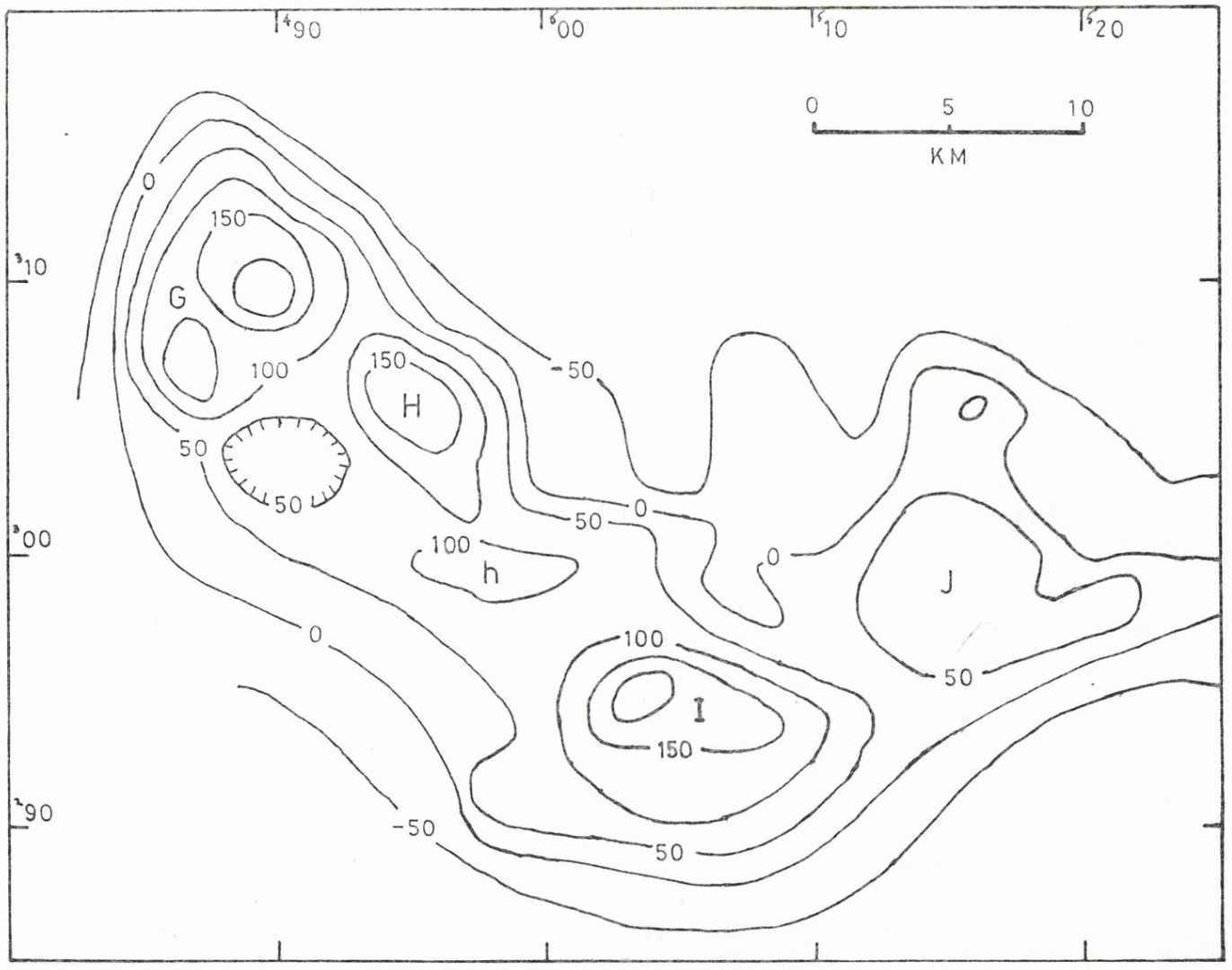


Figure 7.6 : Magnetic anomalies G H h I J, contour interval 5Ø nT.

depths to the tops of the prisms and the susceptibility contrast being adjusted to control the shape and amplitude of the anomalies. Deeper base levels were found to give too broad an anomaly, even when lower susceptibility contrasts were used.

By using five such prisms to model the most prominent peaks a reasonable representation of the observed anomalies was obtained (figure 7.7). The contour map is for the total field anomaly in nT at a datum of Ø.5 kilometres above OD (the flight line elevation); in this and the following figures the mapped area is the same as in figure 7.6 and the upper map shows the horizontal templates used to define the model and their depths in kilometres below OD. The anomaly was calculated, and the data contoured, on a 1 kilometre square grid which measured 46 by 31 kilometres.

The calculated anomalies in figure 7.7 have merged to some extent, and the contours on the north side of the anomaly fit the observed data well. On the south side the anomaly falls off too sharply. This model suggests that the prism model is a good first approximation of the observed anomaly but that extra magnetic material is required to explain the ridge that surrounds the prism anomalies. The tops of the prisms are at depths of one to two kilometres, which is similar to the depths to the intrusions to the west.

The next stage of the modelling was to join the prisms together with an underlying slab. In the example shown in figure 7.8 the base of the slab was at 7.Ø kilometres and the top at 4.Ø kilometres. The shapes of the prisms were not altered and therefore they protruded from the slab by two to

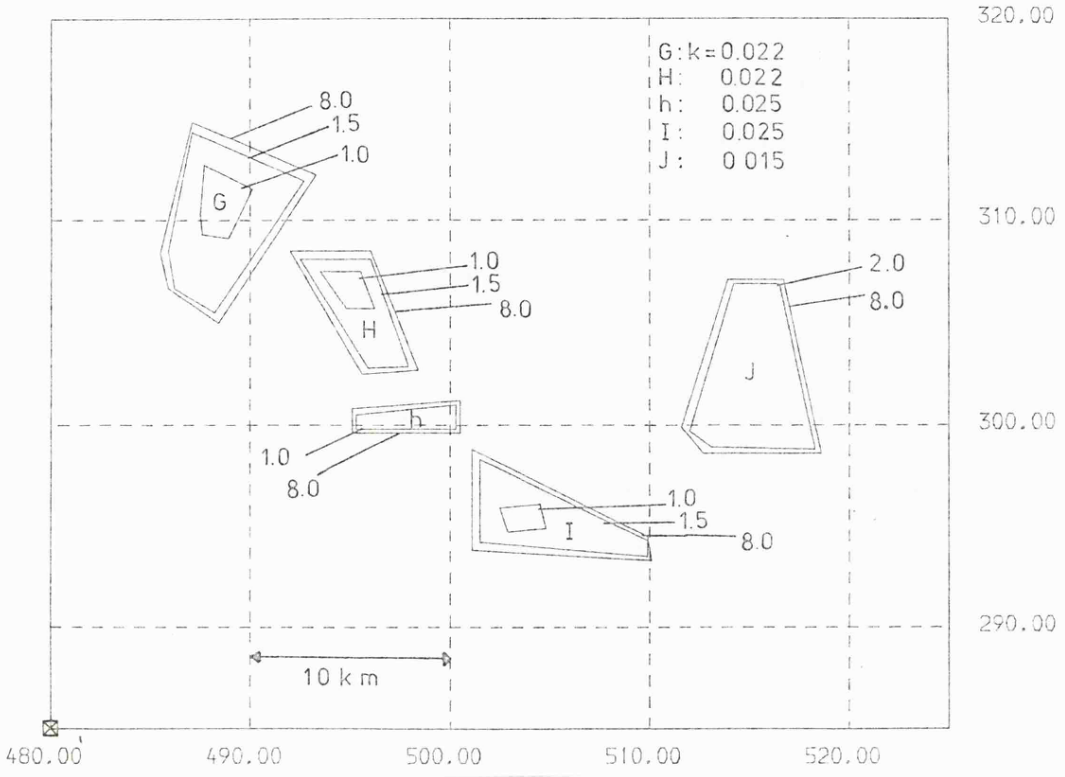


Figure 7.7 : 3-D magnetic model for five prisms. The body templates (above) are horizontal with depths in km, k is the susceptibility contrast. The calculated anomaly (below) is in nT.

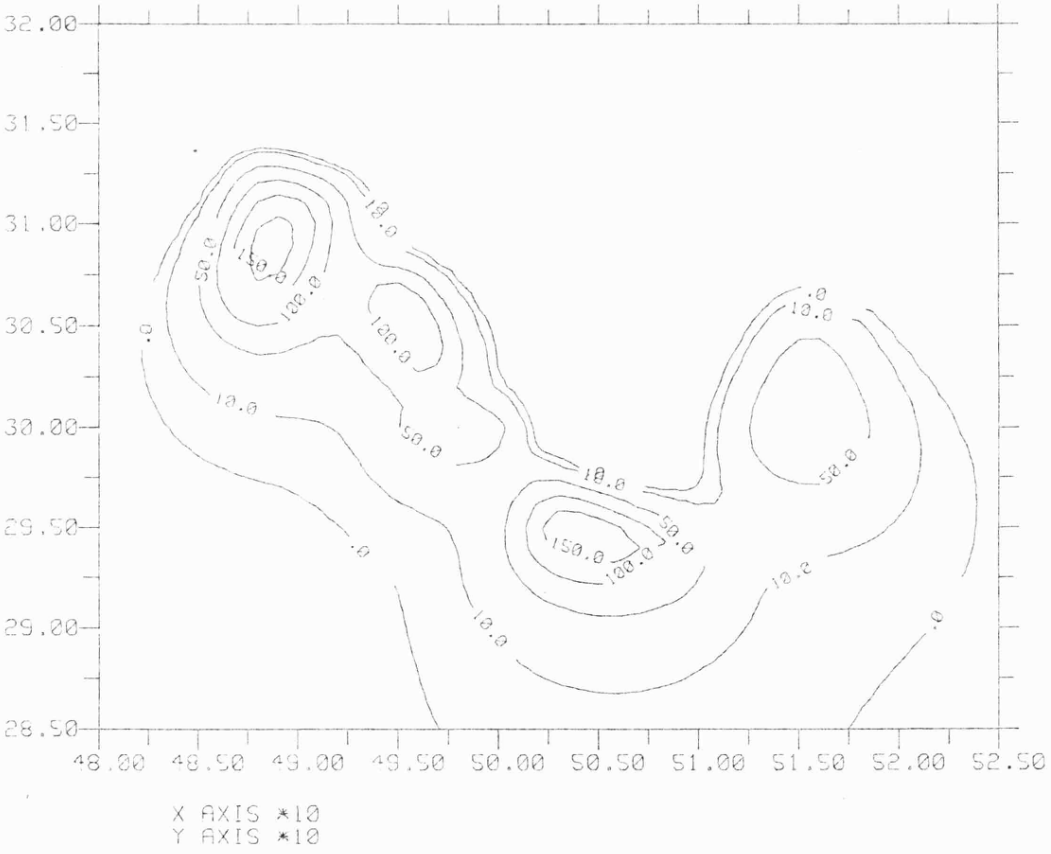

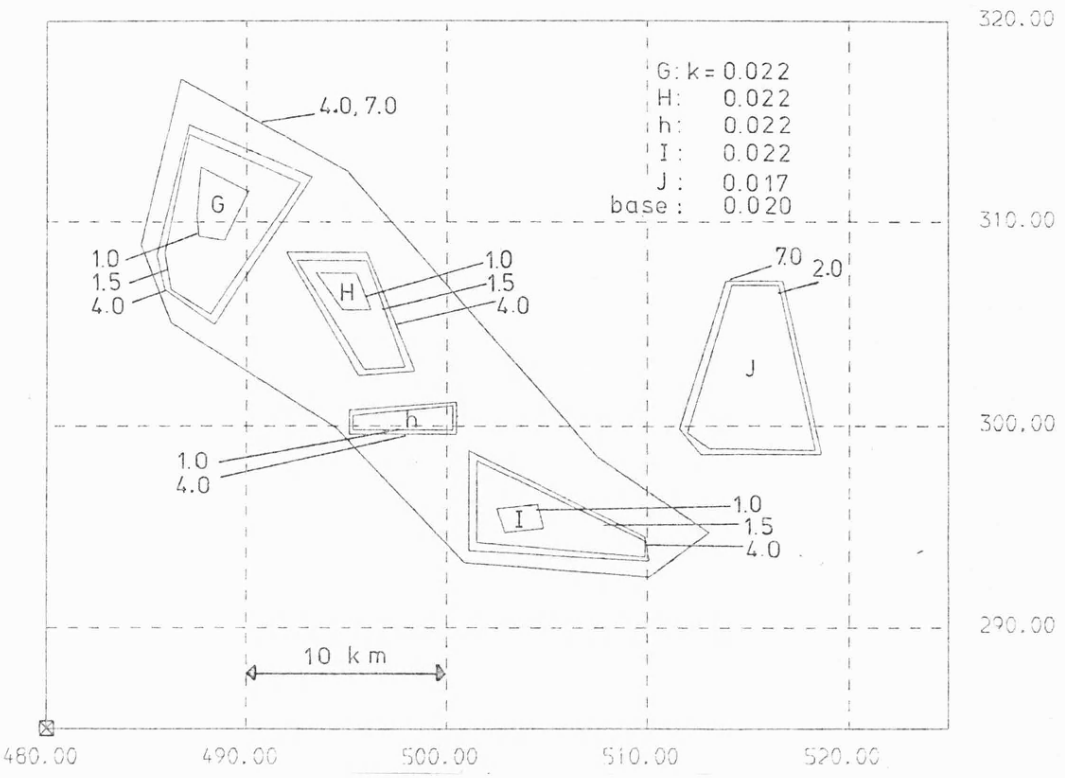


Figure 7.8 : 3-D magnetic model including a basal slab.

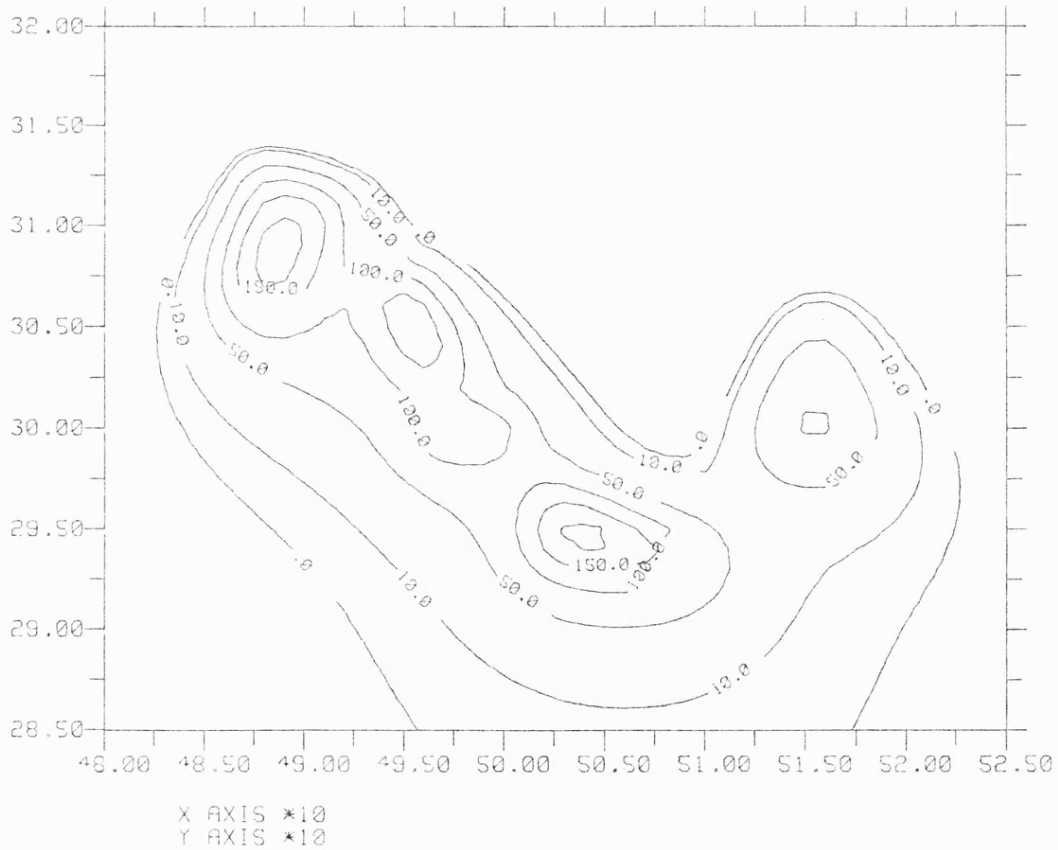

three kilometres. The correlation with the observed data is much improved, the 50 nT contour fits the data well. The position of the 0 nT contour on the calculated anomaly is largely a function of the contouring, the 10 nT contour is included as this gives a more reliable estimate of the edge of the anomaly.

With the base of the slab at greater depths the anomaly became too broad to fit the observed data. The depth to the top of the slab was not well constrained since it was affected by the susceptibility contrasts used for the prisms and the slab.

The body on the east of the model (J) was not attached to the rest of the model. The amplitude of the anomaly for this body is 100 to 150 nT lower than the others and it is not connected to the other anomalies by the 50 nT contour. For consistency the base of this body was kept at the same depth as the rest of the model, therefore a lower susceptibility contrast had to be used. It is possible that this body had a smaller depth extent than the others and a similar susceptibility contrast.

The two-dimensional models suggested that the gravity and magnetic anomalies were not due to the same source body. The gradients on the margins of the observed anomaly are also consistent with the magnetism being induced.

It is possible to test the effect of remanent magnetism on the model to see if the calculated anomalies can be moved sufficiently far to the north or northeast (about 10 kilometres) for the source bodies to lie on the gravity ridge. For this purpose the magnetization was assumed to be totally remanent with an intensity of 1000.0 nT and a

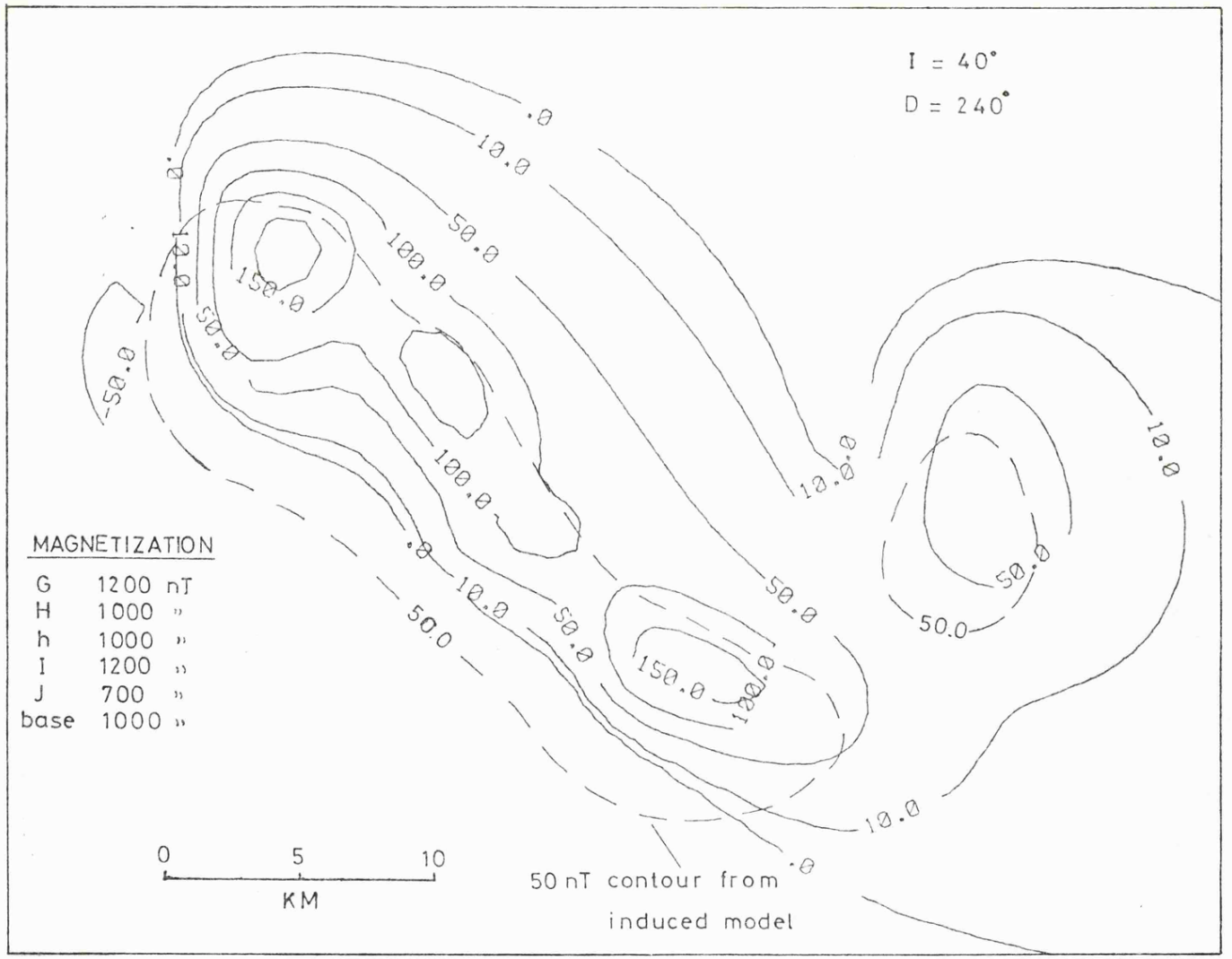


Figure 7.9 : 3-D magnetic model for the body in 7.8, but assuming remanent magnetization. The dashed line is the 50 nT contour from 7.8.

declination of 240°.

The example shown in figure 7.9 is for the same model as in figure 7.8. An inclination of 40° was used. The anomalies are shifted by considerably less than 10 kilometres and are distorted when compared with the observed anomalies. A common source body for the gravity and magnetic anomalies therefore seems improbable.

The model bodies used in these examples suggest a degree of refinement that is probably not justified. The exact depths to the upper surfaces and the fine detail of the template outlines will not have a significant effect on the calculated anomaly since the anomaly was calculated on a one kilometre grid at a height of 1.5 to 2.5 kilometres above the bodies.

## 7.6 SUMMARY AND CONCLUSIONS

The 3-dimensional modelling suggests that magnetic anomalies G,H,I,J can be interpretated as a ridge of magnetic material with prismatic cupolas protruding from its upper surface. The steep gradients on the flanks of the ridge require a shallow body to be used, although the base depths will not necessarily define the base of the body but the lower limit of the susceptibility contrast. The depth extent of the model is similar to that of the two-dimensional gravity model for anomaly T.

On the basis of this modelling it is unlikely that the linear gravity and magnetic anomalies (ridge T and G,H,I,J) have a common source. Furthermore the positions of the individual prisms used to construct the magnetic model do

not correlate with any minor anomalies on the flanks of the gravity ridge.

Inspection of the gravity and magnetic maps for the East Midlands suggests that the anomalies are dominantly intra-basement in origin. The tabulated density measurements show a considerable variation in density for the basement rocks. This variation is not, however, systematic with lithology or geologic age. The most striking potential field anomalies are the positive magnetic anomalies associated with Caledonian igneous intrusions. These anomalies include the proven intrusions of Mountsorrel, the South Leicestershire Diorites and Warboys, and the probable ridge of intrusions investigated in the previous section. All these anomalies suggest a high level of emplacement within the upper crust.

With the exception of the Warboys diorite, which has a small positive gravity anomaly, the intrusions inferred from magnetic anomalies do not have associated gravity anomalies. This may be due to the large variation in densities for these rocks and for the surrounding basement. In the case of the intrusions which appear to have a lower density than the surrounding basement, such as Mountsorrel, the density contrast may be nullified by a more rapid increase in density with depth in the intrusion than in the basement.

# CHAPTER EIGHT

## A. MELTON-MOUNTSORREL MAGNETIC MODELLING

### 8A.1 INTRODUCTION

Due to the absence of a lateral velocity contrast with the surrounding basement, the Melton seismic refraction profiles (chapter 5) failed to resolve the margins of the Melton granite. The depths to the top of the intrusion were well defined by the refraction profiles and the NCB reflection survey (chapter 4). Profile A of the refraction experiment also proved continuous shallow (<Ø.3 km.) basement between Mountsorrel and the Kirby Lane borehole.

The Melton deep reflection line (chapter 5) indicated a possible base to the granitic intrusion at about 12 kilometres. El-Nikhely (198Ø) showed, from NCB seismic reflection data, that the basement depths over the northern Mountsorrel magnetic anomaly were about 1.5 kilometres.

The magnetic properties of the Mountsorrel rocks have been described in chapter 7. There is no evidence for any significant remanent magnetization in these rocks.

The ammount of control data available warranted more detailed modelling than was attempted for the ridge of anomalies to the east of Melton (chapter 7). The aim was to develop some three-dimensional models which gave an acceptable fit to the observed anomalies and then to test the compatibility of these models with the seismic interpretation. In particular it was hoped to determine if the

margins of the Melton intrusion correlated with the slight increase in time term solution velocities obtained for stations to the north of B40 and east of A8 (see chapter 5). The original flight line data were used, in preference to the IGS 1:250000 map, in order to check the short wavelength components of the anomalies.

8A.1.1 Flight line data

The survey was carried out in 1955 with east-west lines two kilometres apart and north-south tie lines at 10 kilometres, the mean terrain clearance was about 500 metres.

The magnetometer profiles covering the Melton and Mountsorrel areas were digitized on a table digitizer and then converted into x,y,z coordinates by tying the fiducial marks on the profiles to the equivalent points on a digitized flight line basemap (original scale 1:253440). The digitized basemap is shown in figure 8.1, the small dots show the locations of the position fixes. The resulting data set was gridded onto a 1 kilometre square grid (see appendix 2) and contoured. The only regional removed from the data was a linear trend drawn on the profiles at the time of the survey. When the data were plotted the contour values were about 75 nT larger than the equivalent contours on the IGS 1:250000 map. Therefore 75 nT was removed from all the data before plotting the contour map in figure 8.2. Comparison with figure 5.2, which was based on the IGS map, shows that the two maps are very similar, except for the peak of the north Mountsorrel anomaly which is 200 nT on the flight line data and 250 nT on the IGS map. This similarity indicates that the IGS map would have been an acceptable source of the

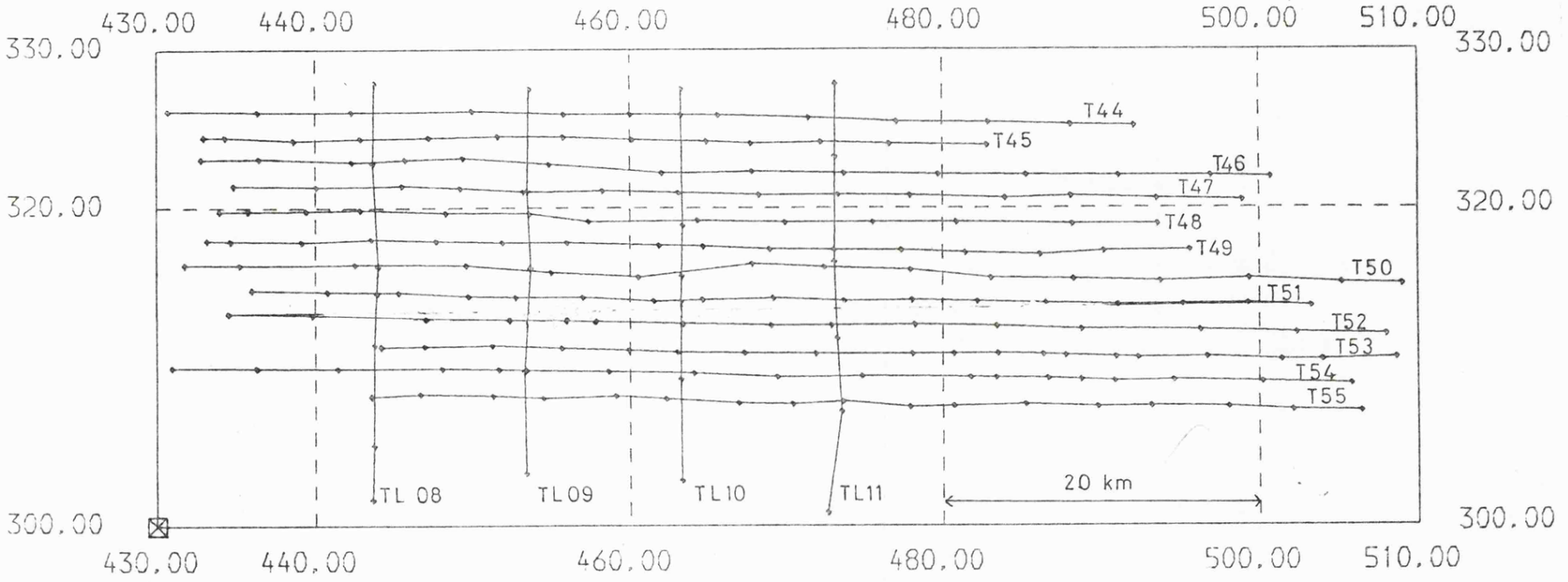


Figure 8.1 : Aeromagnetic flight line basemap for the Melton area.

observed data for simple comparison with the calculated anomalies.

The accuracy of the digitized magnetometer values, as shown by the line ties, was a few nT. The positioning was probably accurate to better than Ø.5 kilometres. Since the data was gridded onto a one kilometre grid this is not a serious inaccuracy.

## 8A.2 THREE-DIMENSIONAL MODELLING

In order to avoid the problems of defining planar sections in 3-dimensional space only horizontal templates were used, consequently all the models are flat topped. The seismic interpretations indicated a flat top surface for the Melton intrusion, and the deep reflection profile indicated horizontal layering within and/or beneath the intrusion. The modelling program required that all the templates have the same number of vertices, as a result some of the templates have more vertices than are actually needed to define their shapes and may appear overcomplicated. The flanks of all the bodies were outward sloping and near vertical. Three bodies were defined: 1) the Melton granite, 2) the exposed area of the Mountsorrel granodiorite, 3) the presumed northern extension to the Mountsorrel intrusion. The number of vertices on the templates was gradually increased, and templates added at different levels, as the model was refined. The anomalies for the model bodies were calculated on a one kilometre square grid at a reference datum of Ø.5 kilometres above OD. At each stage a contour map of the calculated anomaly was produced and compared visually with the observed

anomalies. The gridded data from the flight lines was used to plot contour maps for comparison with the models, and to produce maps of the residuals for some of the better models.

The Mountsorrel anomaly merges to the west with another anomaly (A in figure 7.3), the sources of these two anomalies may be connected at depth. The separation of the Melton and Mountsorrel anomalies is more clearly defined, and does not suggest a connection between the two source bodies. The exception to this is the southern margin, just south of the refraction profile, where the two anomalies are joined at the 40 nT contour.

8A.2.1 An initial model

Initially the base of the model was fixed at 12 kilometres, as suggested by the Melton deep reflection profile, and the susceptibility of each of the three bodies was adjusted according to the amplitude of the calculated anomalies. Using this method the susceptibility contrasts required were 0.02 or less, which was compatible with the properties given in chapter 7. The shape of the Melton anomaly was largely controlled by the shallow templates and was not very susceptible to changes in the base depth.

The Mountsorrel anomaly proved difficult to model using such a large base depth. This was because the top surface was constrained to a minimum depth of 1.5 kilometres but the peak of the anomaly was 200 nT (250 nT on the IGS map) which was similar to the anomaly for the shallower Melton intrusion. Therefore it was necessary to use a higher susceptibility contrast for the north Mountsorrel intrusion than for Melton. When a 12 kilometre base was used, the

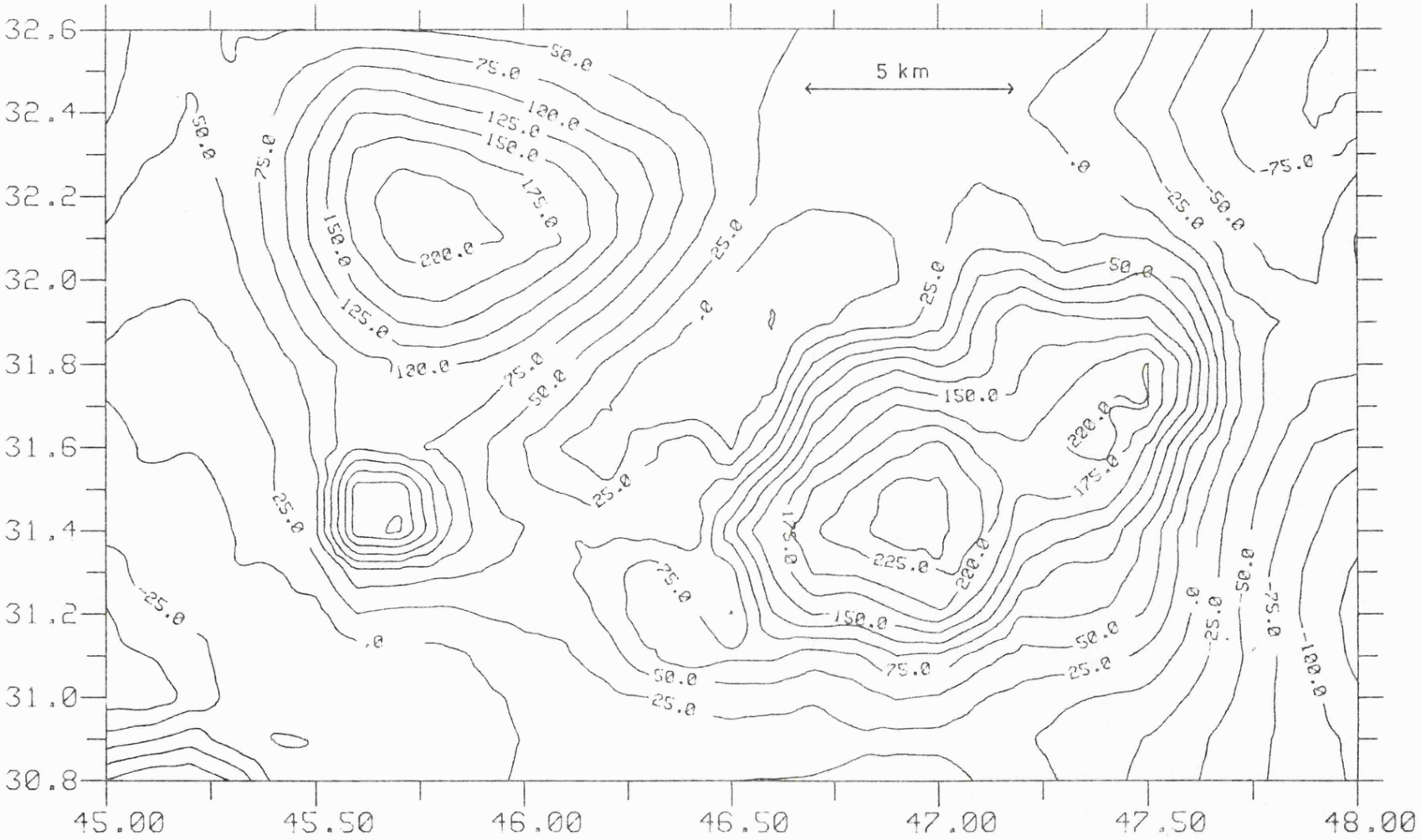


Figure 8.2 : Melton-Mountsorrel magnetic anomaly contoured from the digitized flight line profiles. Contour interval 25 nT.

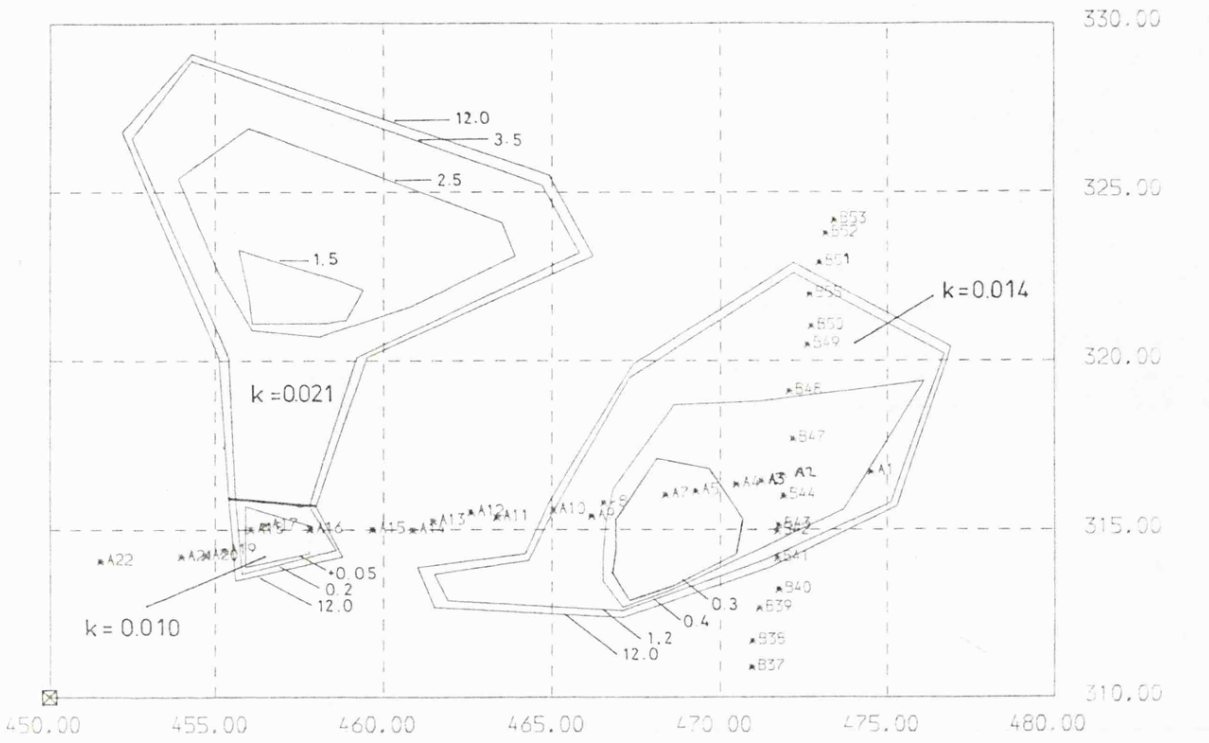


Figure 8.3 : Magnetic model for a 12 km base depth. The upper figure shows the template outlines, the lower figure shows the calculated anomaly in nT at a datum of 0.5 km. above OD. the dashed line is the 50 nT contour from the observed data. Refraction recording sites marked: * A3.

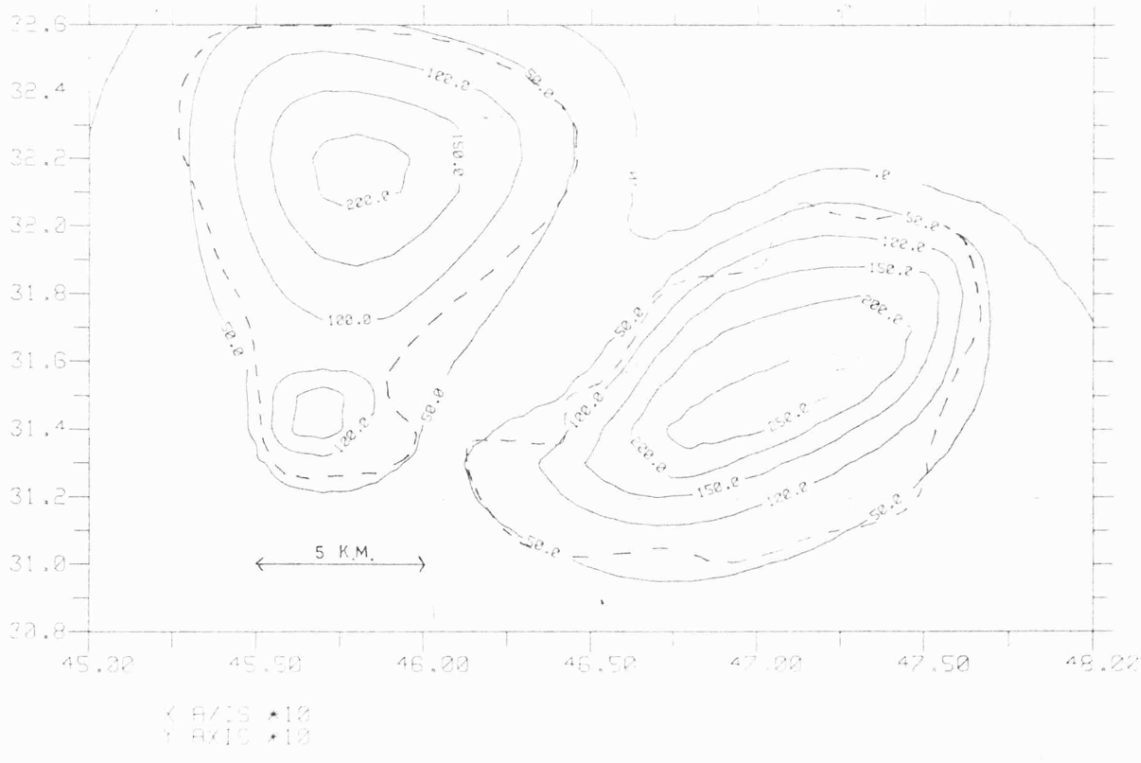

Mountsorrel anomaly, as defined by the 50 nT contour, was too broad (figure 8.3). In subsequent models the base depth was reduced to 7 kilometres. This can be considered as the limiting depth of the susceptibility contrast.

Apart from the indication that the base depth was too large, this model provided a reasonable agreement with the observed data, suggesting that the basic shape of the models was correct. Having reduced the base depth to 7 kilometres this model was refined, initially using the same three bodies (Melton, Mountsorrel and the northern extension of Mountsorrel), as described below.

8A.2.2 A model with a 7 kilometre base

The final version of the three body model is shown in figure 8.4 and the calculated anomaly in figure 8.5. This model was used to test the relation between the magnetic and seismic interpretations, and to develop more complex models in an attempt to refine certain aspects of the modelling. The choice of depths for the upper templates was controlled initially by the seismic data. The intermediate templates were added in an attempt to vary the slope of the top and sides of the model body, in response to variations in the observed anomaly. The choice of depths for these templates was somewhat arbitary and it is likely that a number of equally valid models exist. However, for a given base depth or susceptibility contrast, the areal extent of the model will not vary by very much in the different models. The greatest assumption that has to be made is that the magnetization is homogenous, this is most unlikely to be the case. Even within the small Mountsorrel intrusion there is

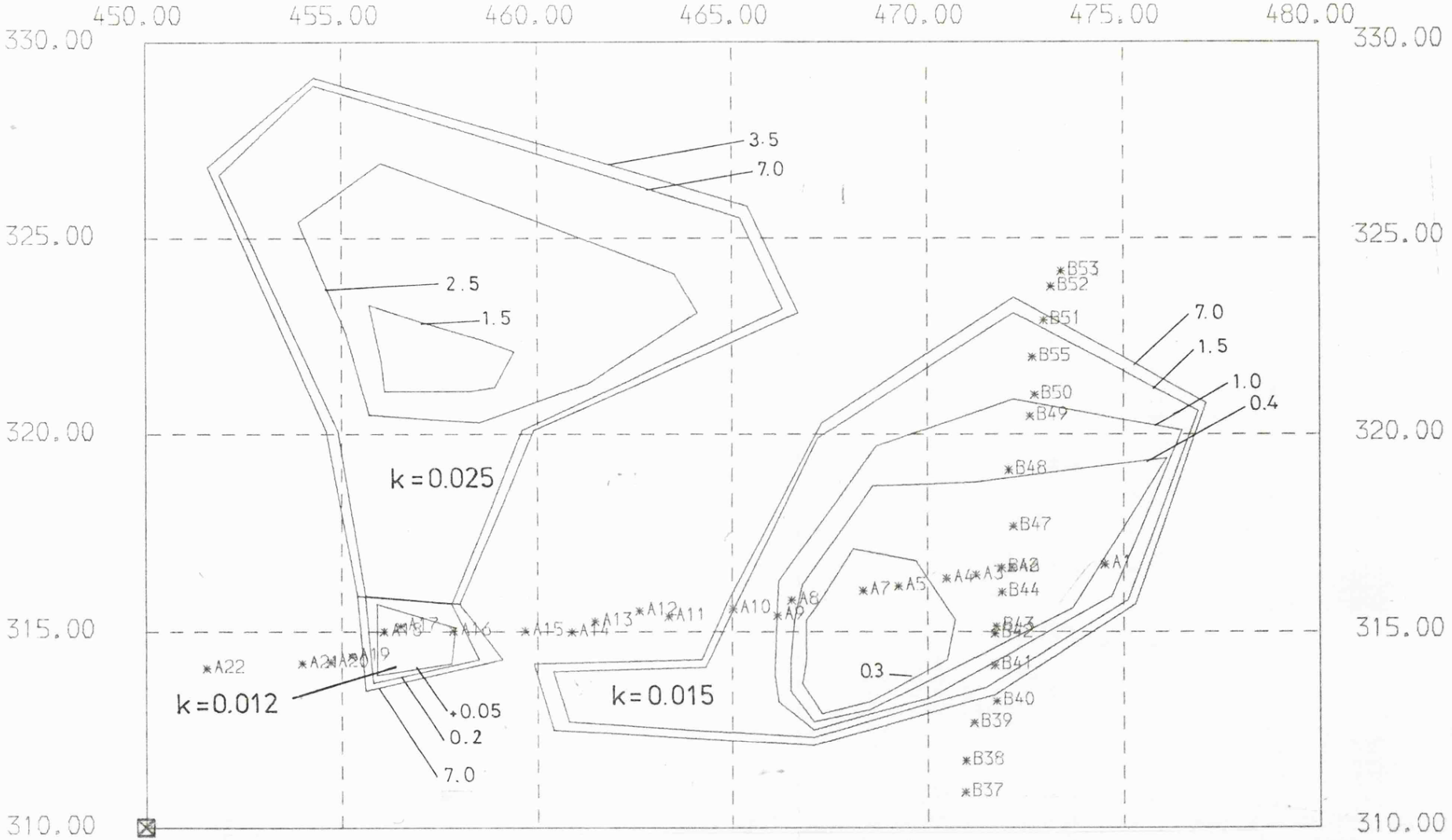


Figure 8.4 : Template plans for a model with a 7 km. base depth.

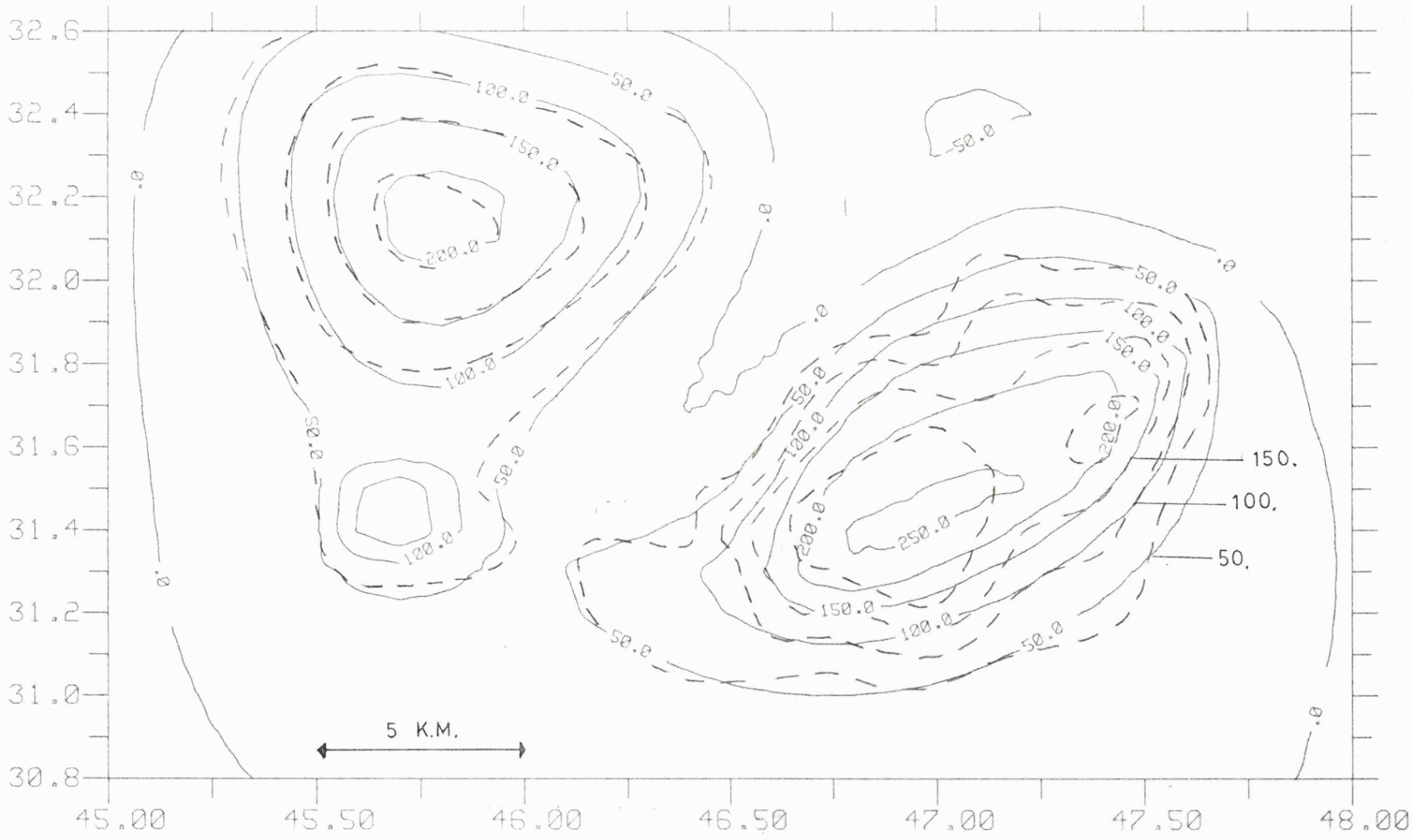


X AXIS *10
Y AXIS *10

Figure 8.5 : Calculated anomaly for the model in figure 8.4.

an outcrop of gabbro on the margin of the granodiorite.

The model for the Mountsorrel granodiorite includes a template at Ø.Ø5 kilometres above OD to represent the exposed rock. The susceptibility contrast used for this body (Ø.Ø12 SI) was lower than the measured values tabulated in chapter 7.

A high susceptibility contrast of Ø.Ø25 was required for the northern Mountsorrel anomaly. This was because the peak of the anomaly had to be 2ØØ+ nT but the top surface of the intrusion was constrained to a minimum depth of 1.5 kilometres. However, once this high susceptibility was used, the anomaly was relatively simple to model because of the smooth, evenly spaced, contours on the observed data.

The two Mountsorrel models were joined together to the north of the exposed granodiorite. The doubling of the susceptibility contrast, and the 3 kilometre increase in depth, at this junction are clearly an over-simplification. The depth to the model along the Bardon to Holwell seismic line is about 3 kilometres, this is at least double the depth to the low velocity refractor in the seismic interpretation (Whitcombe and Maguire 1981a and chapter 1). This difference indicates that the high susceptibility need not be extended as far south as the position of the seismic line and that it could be replaced by a body, at shallow depth, with a lower susceptibility contrast. As a refinement the Mountsorrel model was subsequently divided into three parts (see below).

Despite the wealth of control on the depth to the upper surface of the intrusion, the Melton anomaly proved more difficult to model. This was due to the short wavelength variations in the anomaly which could not be adequately

modelled using a single body. In particular the two peaks of the anomaly had to be merged together. As with the Mountsorrel models, this body was subsequently split into two bodies.

With the base at 7 kilometres and the uppermost templates at Ø.3 to Ø.4 kilometres a susceptibility contrast of Ø.Ø15 was needed. The model shows that the Melton anomaly can be modelled by a body with a shallow top surface, as defined by the seismic interpretations.

8A.2.3 Further refinements to the model

Having developed a basic model, which fitted the observed data acceptably well, two aspects of the model were chosen for further refinement. These alterations also indicate the type of changes that have to be made in order to produce a significant variation in the calculated anomaly, and the changes that can be made without significantly affecting the calculated anomaly.

Mountsorrel anomaly: the northern extension of the Mountsorrel model was split into two parts. The depth to the top surface of the southern part was adjusted to agree more closely with the Holwell to Bardon seismic line (Whitcombe and Maguire 1981a). The susceptibility contrast for this body was reduced to compensate for the reduced depth to the top surface. There is still a large change in susceptibility contrast at the junction of the northern and central bodies. A more realistic model would probably have a core of high susceptibility contrast at depth within the northern body.

The calculated anomaly (figure 8.7) is very similar to that in figure 8.5 and demonstrates the ambiguity in this

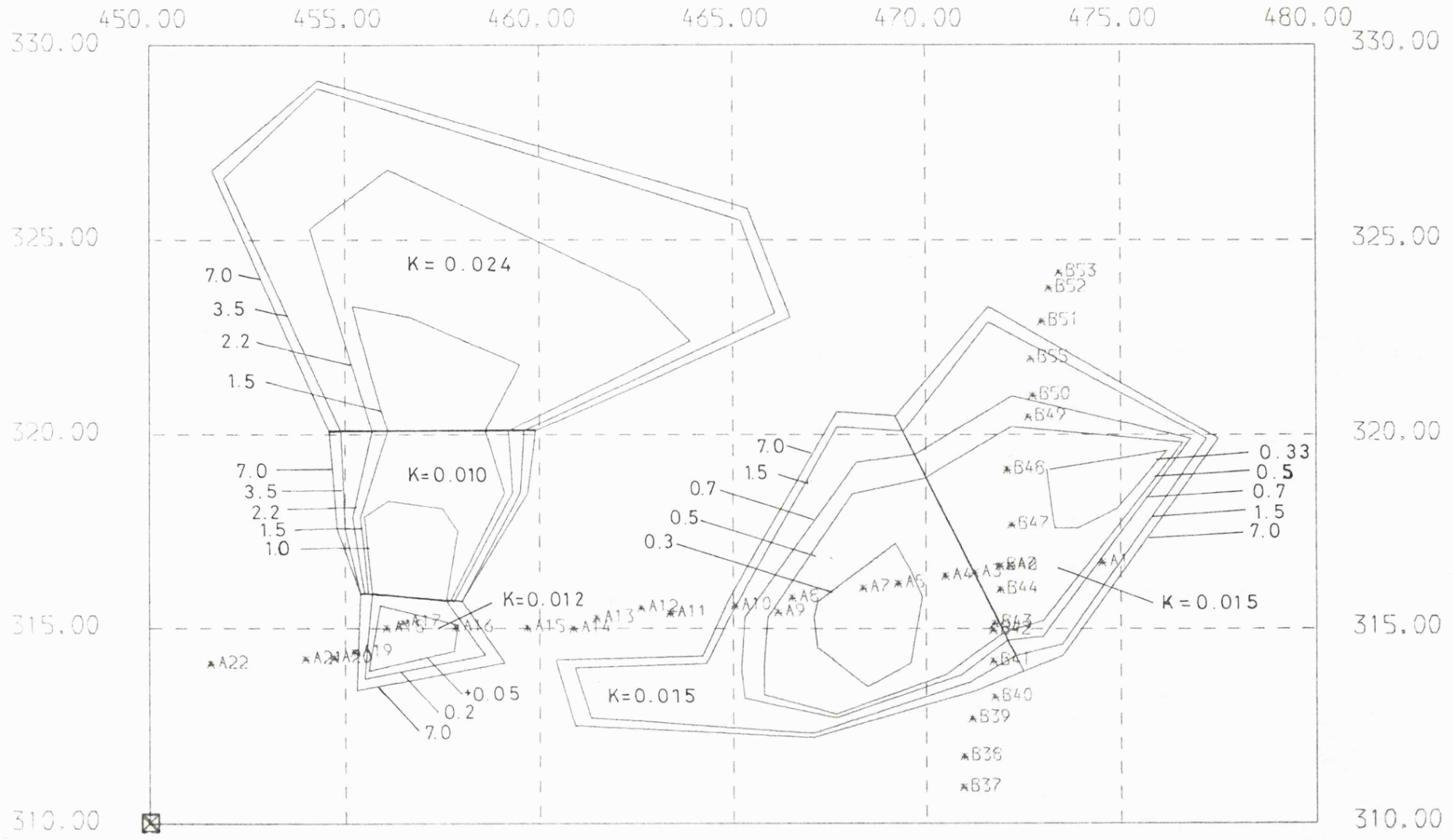


Figure 8.6 : Template plans for a 5 body model with a 7 km. base depth.

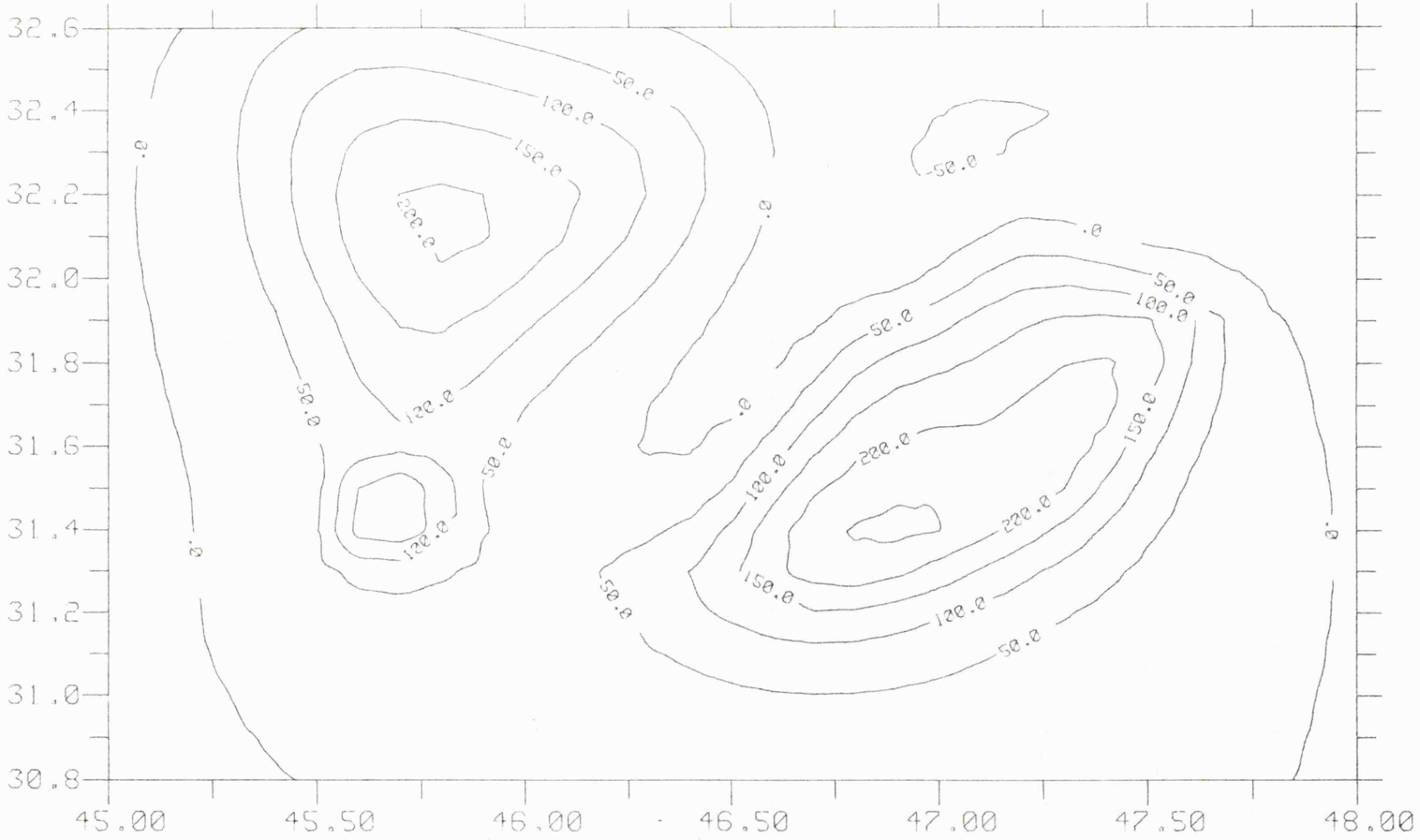


X AXIS *10
Y AXIS *10

Figure 8.7 : Calcualted anomaly for the model in figure 8.6.

type of modelling.

Melton anomaly: the alterations made to this model were less successful. The model was split into two parts so that the two separate peaks on the observed anomaly could be represented by two high points on the model bodies, a feature that could not be created with a single model. Because the top surface of the body was already at its minimum depth it was necessary to create a depression on the top of the model in order to define the two highs. Such a depression was not indicated in the seismic interpretations and must be thought of as a variation in the depth to the magnetic material, and not to the surface of the intrusion. The two parts of the body were given the same susceptibility contrast. The calculated anomaly in figure 8.7 shows the development of two separate peaks, although they are less pronounced than on the observed anomaly. The larger peak of the Melton anomaly could also be explained by a localised variation in susceptibility contrast. The observed anomaly in figure 8.2 shows that this peak extends further to the south than can be modelled without distorting the contours on the southern margin of the body.

As noted in chapter 4, it is common to find 10 to 20 metres of dolerite sills within the Coal Measures of the North East Leicestershire Coalfield. These sills would be unlikely to affect the aeromagnetic anomaly. However, if a greater thickness, such as is observed in the Asfordby borehole, is present with a significant lateral extent this could be the source of short wavelength anomalies.

The Melton and Mountsorrel intrusions have not been joined at depth in these models. It would be possible to

connect the two bodies at depth without affecting the calculated anomaly, but such a connection would not be significant.

Figure 8.8 shows the observed profile along flight line T51, projected onto an east-west line at NGR 314.3 N. The dashed line shows the anomaly along this line for the body in figure 8.6, calculated at intervals of Ø.2 kilometres. It is not possible to model all the short wavelength features of the observed anomaly using the 3-dimensional method. However, the calculated anomaly fits the main features of the observed profile acceptably well. Some of the differences arise from the fact that the calculated anomalies were compared with contour maps of the digitized data and not with the original profiles. The agreement is best on the western margin of the Melton intrusion, and supports the correlation of the magnetic and seismic interpretations (see below).

8A.2.4 Comparing the seismic and magnetic interpretations

In the 3-body model in figure 8.4 the northern margin of the body dipped away more steeply than was indicated by the seismic interpretations. In the 5-body model in figure 8.6 the depth to the third template has been changed so that the two interpretations agree more closely. It was subsequently found that altering the depth to this template from 1.Ø to Ø.7 kilometres had no significant effect on the calcualted anomaly for the 3-body model.

The maps of the models in figures 8.4 and 8.6 also show the positions of the seismic refraction stations. Figure 8.9 shows cross sections along both seismic profiles to compare

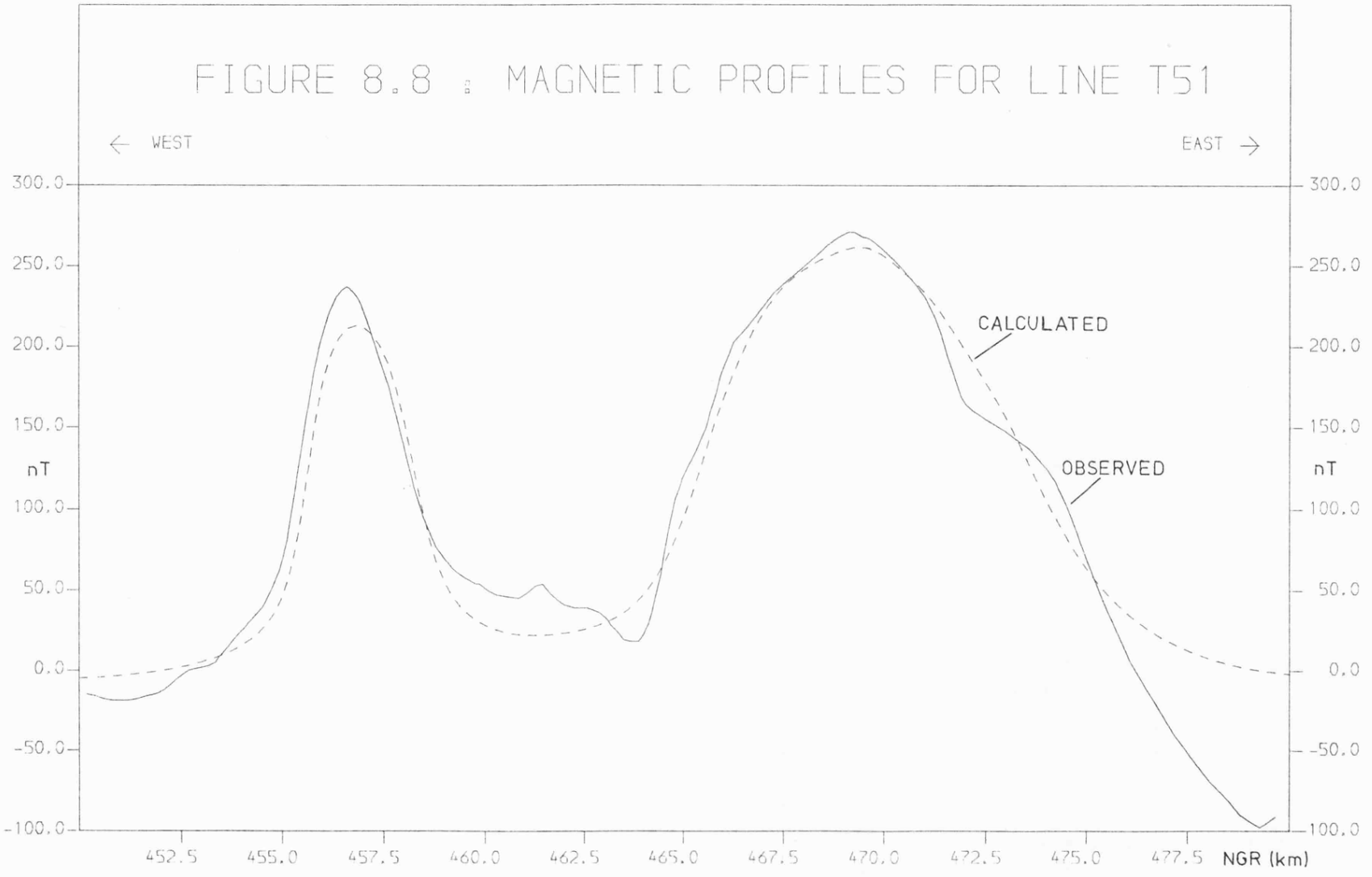
FIGURE 8.8 : MAGNETIC PROFILES FOR LINE T51
← WEST
EAST →
300.0
250.0
200.0
150.0
nT
100.0
50.0
0.0
-50.0
-100.0
CALCULATED
OBSERVED
452.5
455.0
457.5
460.0
462.5
465.0
467.5
470.0
472.5
475.0
477.5
NGR (km)

the seismic and magnetic interpretations. The western edge of the Melton intrusion occurs at station A1Ø whereas, in the seismic interpretation, a possible change in refractor velocity was detected between A7 and A8. However the cross section shows the top surface of the magnetic models dipping away, beneath the refractor, from A8 westwards. Similarly the interval between B4Ø and B41 (the position of the other possible velocity change) agrees less closely with the break in slope on the top surface of the model, which was to the north of B41.

The anomaly was calculated for a model in which the Ø.3 kilometre template (eqivalent to the basement refractor) extended west to station A1Ø. This model did not give as good a fit to the observed data and was rejected. The uncertainty in the magnetic models is such that the apparent correlation with the seismic interpretation cannot be taken as conclusive proof that the margins of the Melton intrusion were located between stations A7 and A8 but the available evidence supports this possibility.

The possibility of a deeper refractor beneath profile B, as deduced from the reduced travel time sections, was discussed in chapter 5 (5.4.4). The magnetic models indicate a northern margin to the Melton intrusion about 2 kilometres south of the Holwell shotpoint (B53). This would appear to preclude the possibility of a first arrival, at B53, from a sub-Charnian refractor.

The western margin of the Mountsorrel extension crosses the Bardon to Holwell seismic line (Whitcombe 1979, Whitcombe and Maguire 1981a) between stations 15 and 16, as opposed to between 17 and 18 as deduced from the seismic

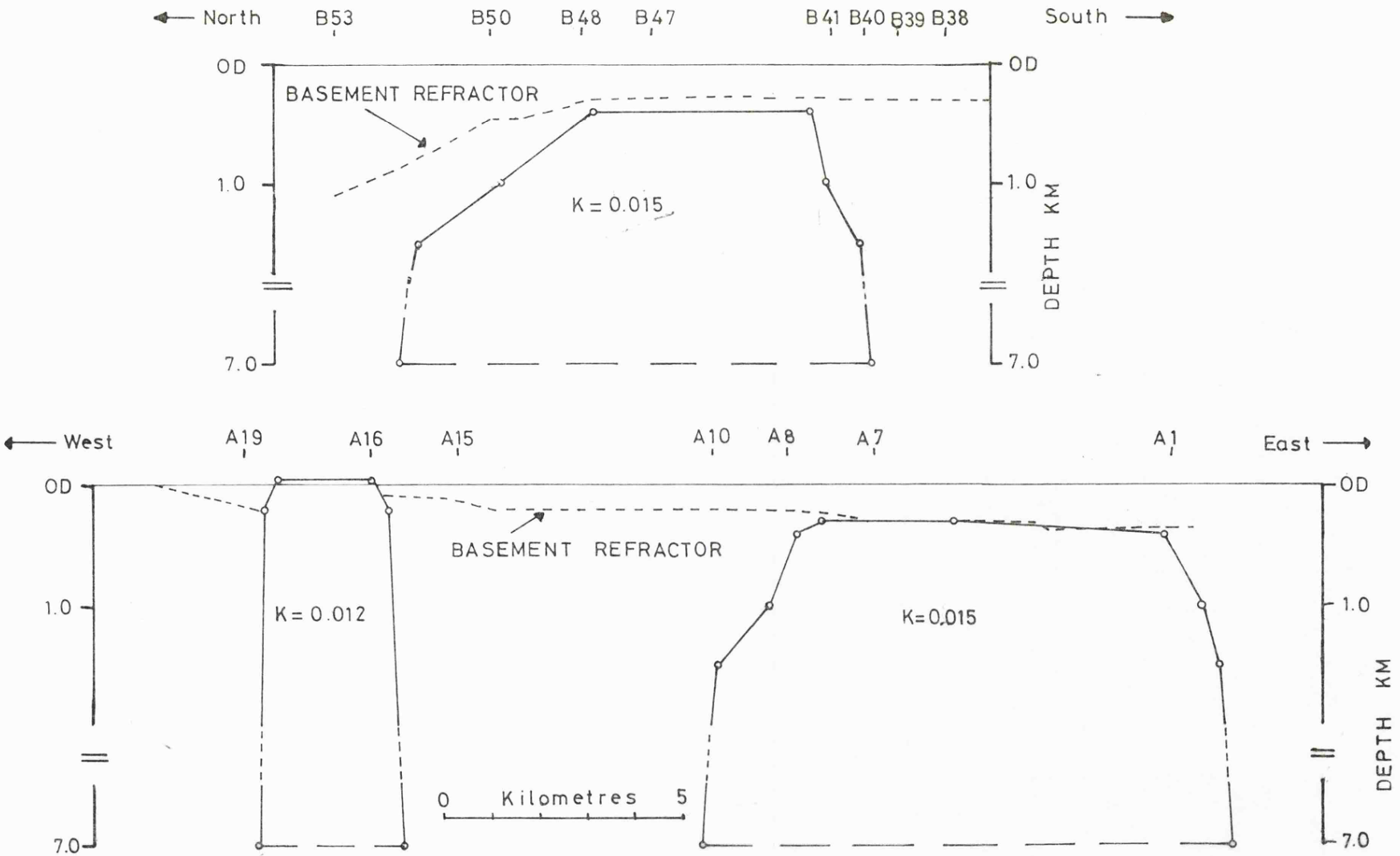


Figure 8.9 : Cross sections to compare the seismic and magnetic interpretations.

data (see figure 1.5). If the low refractor velocity on the Bardon to Holwell line is taken to indicate that the granite is exposed at the basement surface, at a depth of 1.Ø to 1.5 kilometres, and the Loughborough prospect seismic data indicates a basement depth of at least 1.5 kilometres, it follows that there is a major downfaulting of the basement to the north of Mountsorrel and the northeast of Charnwood Forest. The "CHARM" reflection profile should define this faulting more accurately.

## 8A.3 SUMMARY

The three-dimensional modelling shows that the Melton and Mountsorrel intrusions can be fitted by models with a susceptibility contrast of Ø.Ø1 to Ø.Ø25 (SI), extending to depths of about seven kilometres. This agrees with the models in chapter 7 for the ridge of intrusions to the east of Melton. The modelled position of the western margin of the Melton intrusion agrees with the location of the change in time term solution velocities. The modelled position of the southern margin of the intrusion is to the north of station B41, whereas the change in solution velocity was to the south of B41.

# B. PETERBOROUGH GRAVITY MODEL

## 8B.1 INTRODUCTION

The Peterborough seismic profiles (chapter 6) were designed to determine the depth to basement over the Peterborough gravity anomaly. The experiment proved probable Precambrian basement at shallow depth along the axis of the anomaly, and therefore indicated that the anomaly was intra-basement in origin. Using the seismic and borehole control on the depth to the basement surface, the gravity data were modelled to investigate the shape of the anomalous body, which was presumed to be a low density intrusion.

### 8B.1.1 Gravity data

A total of 692 gravity stations for the 30 x 30 kilometre area east and north of NGR 510.0 290.0 were used in the interpretation. The data, in the form of Bouguer gravity values and 10 metre National Grid coordinates were supplied by Durham University. This data set represented all the IGS gravity stations in the area, together with some additional Durham stations. The station distribution was fairly even across the area and the data were gridded (appendix 2) onto a one kilometre square grid and contoured (figure 8.10).

### 8B.1.2 Constraints on the model

The seismic lines did not indicate a lateral velocity decrease over the gravity anomaly. This can be interpreted in two ways: 1) the intrusion was not exposed at the

basement surface; or 2) the intrusion was exposed at the basement surface but had a similar p-wave velocity to the surrounding basement, the Warboys and Melton intrusions would fit this model. The latter assumption would imply that there was a negligible density contrast between the basement and the intrusion which conflicts with the observed gravity data. Therefore it can be assumed that the intrusion is not exposed at the basement surface.

The density of the Glinton borehole samples was about 2710 $\pm$ 20 $kg.m^{-3}$ , samples of Precambrian basement from other locations (see chapter 7.2) indicated a considerable variation in densities. A density of 2720 $kg.m^{-3}$ was taken as a reasonable approximation for the near surface basement rocks for the purpose of stripping off the overlying sediments.

The density of the intrusion can only be guessed at; by analogy with the Leicestershire intrusions 2650 $kg.m^{-3}$ is a reasonable value. It should be noted, however, that the Leicestershire intrusions have strong positive magnetic anomalies and the Peterborough gravity anomaly correlates with a magnetic low, this indicates that there may be petrological differences between the two types of intrusion and hence possible differences in density. Since the intrusion has a considerable depth extent a density of 2750 $kg.m^{-3}$ was assumed for the surrounding basement rocks, giving a density contrast of 100 $kg.m^{-3}$ . A density of 2720 $kg.m^{-3}$ was assumed for the rocks at the basement surface, when stripping the sediments, therefore using a density of 2750 $kg.m^{-3}$ implies a density gradient with depth in the top kilometre of the basement. The density contrast may decrease

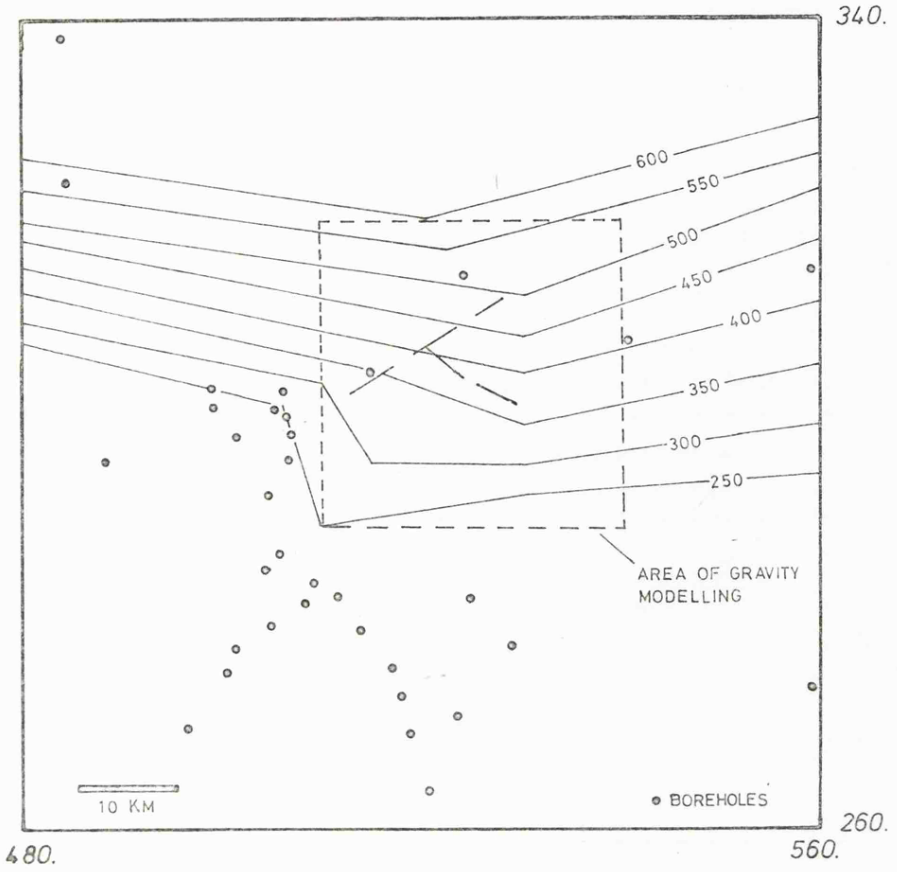


Figure 8.11 : Stratum contours used to remove the sedimentary cover.

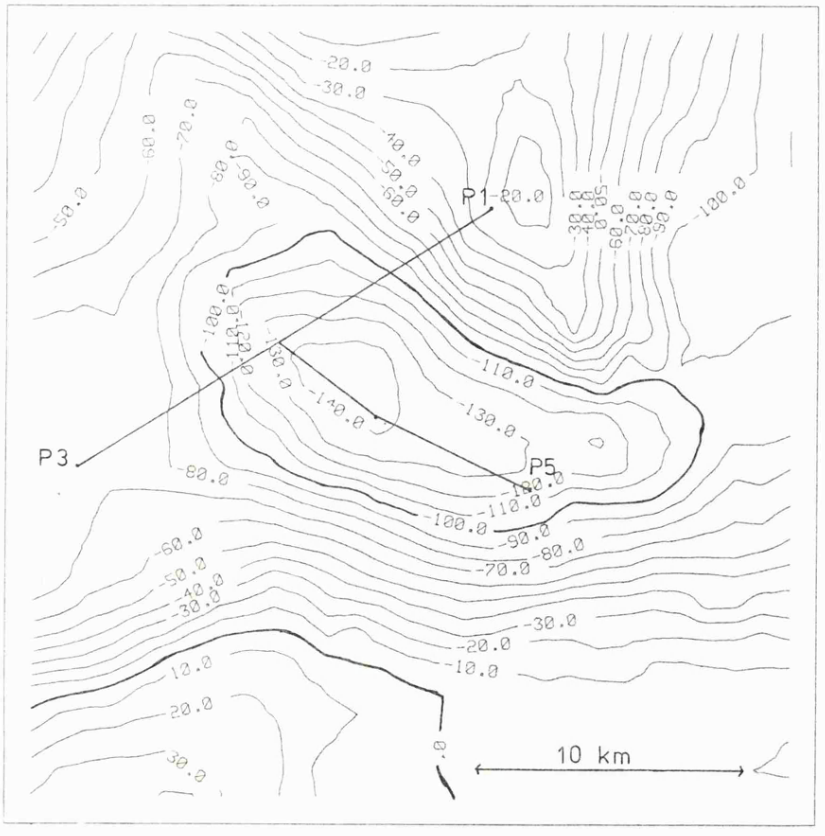


Figure 8.10 : Bouguer gravity map for the Peterborough area.

with depth, due to greater compaction within the intrusion, but this cannot be allowed for in a simple iterative model.

## 8B.2 MODELLING

### 8B.2.1 The sedimentary cover

The extensive borehole information in this area shows that the pre-Carboniferous unconformity is a smooth surface which dips northwards (chapters 1 and 9). Typical depths are 150 to 200 metres below OD in the Huntingdon area and 400 to 600 metres below OD to the north of the gravity anomaly.

There is a considerable variation in the lithology and geologic age, and hence density, in the rocks beneath the unconformity but little is known about the detailed structure or thickness of the Palaeozoic and Precambrian rocks. In the area surrounding the Peterborough anomaly the boreholes prove mainly Precambrian tuffs with some Cambrian quartzites.

The gravity effect of the sediments was calculated for a three-dimensional model, defined by a set of structure contours on the basement surface, using the method of Talwani and Ewing (1960). The contoured surface (figure 8.11) represents the estimated depths below datum of the Precambrian basement. The structure along the seismic lines has been smoothed out to remove localised variations in the depth to the refractor.

Initially an extra model was used to calculate the effect of the Middle Jurassic sediments. These have a lower density than the underlying Lias and Keuper and thicken in the same direction as the other sediments. Calculating the

gravity effect of this layer separately from the underlying Lias and Trias caused a difference of less than 5 gu. in the residual gravity. Therefore all the sediments were treated as one body.

A density of 2450 $kg.m^{-3}$ would be acceptable for the Lias and Keuper Marl (chapter 7), this was reduced to 2400 $kg.m^{-3}$ when calculating the effect of all the sediments in order to allow for the lower density Middle Jurassic and any Triassic (and possibly ORS) sandstones. This gave a density contrast of 320 $kg.m^{-3}$ between the sediments and the near-surface basement rocks.

Figures 8.12 and 8.13 show, respectively, the computed gravity for the sediments and the residual gravity anomaly after the removal of the sedimentary effect.

8B.2.2 Anomaly separation

The dominant trend of the Peterborough gravity anomaly is east-west, there is an extension to the northwest and a connection with a second negative anomaly to the northeast. In order to produce a simple iterative gravity model for the Peterborough anomaly it was assumed that, other than the effect of the supra-basement sediments which had been corrected for (figure 8.12), there was no regional gravity gradient over the mapped area. This assumption is consistent with the work of Maroof (1973) who filtered, and fitted polynomial surfaces to, the gravity anomalies of Southern Britain. This analysis showed that the regional gravity in the Peterborough area has a gentle gradient to the north or northeast.

If a larger area of gravity data were to be used for

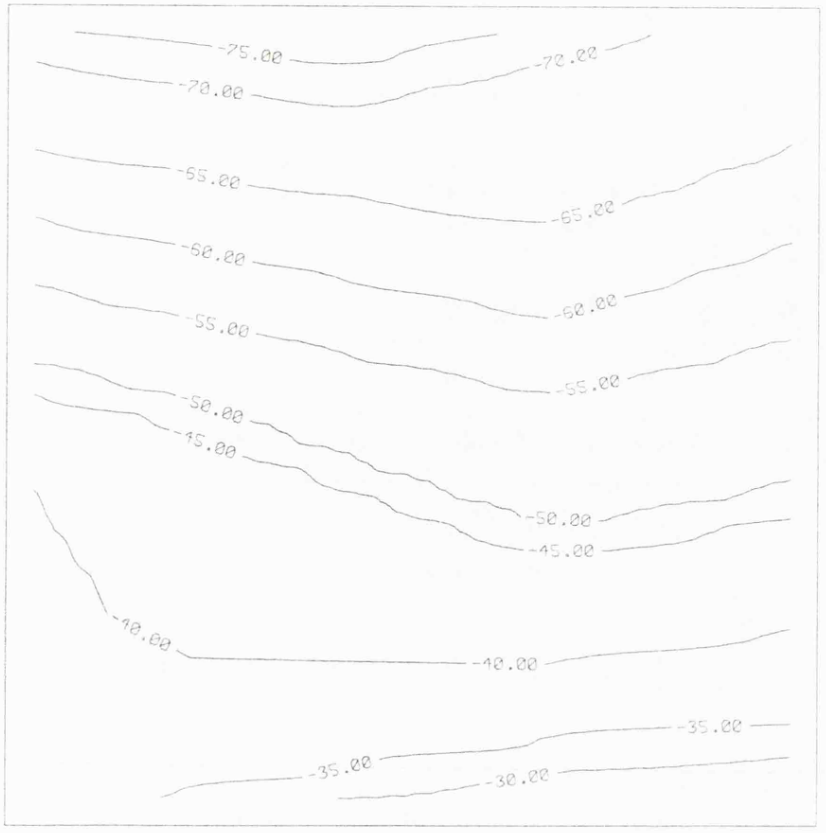


Figure 8.12 : The calculated effect of the sediments.

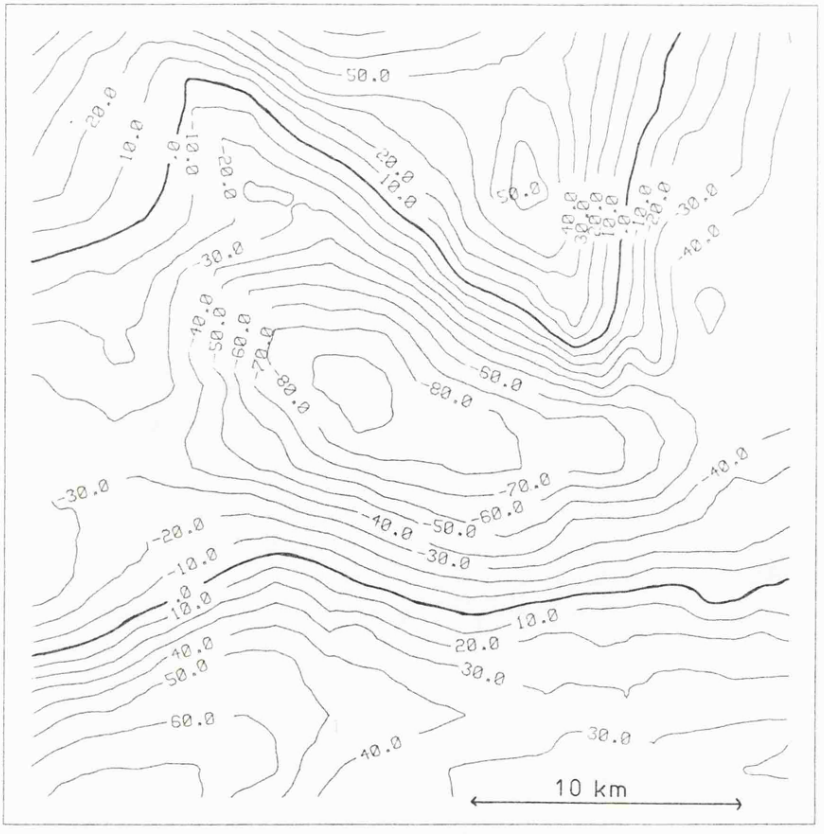


Figure 8.13 : The anomaly corrected for the effect of the sediments.

the modelling it would be possible to separate out the Peterborough anomaly by some form of empirical gridding.

For an iterative model confined to a small area of data the criterion for an acceptable model is that the residual gravity for the model is not correlated with the shape of the causal body. From figure 8.13 it can be seen that the 30 g.u. contour on the south side of the anomaly follows the east-west trend of the anomaly, whereas the 40 gu. contour does not. The situation is more complex on the north side of the anomaly due to a large (100 gu.) positive anomaly to the north of the mapped area and a smaller positive anomaly within the area. However, the 30 to 40 gu. contours are the highest that are closely associated with the outline of the negative anomaly. The complexity of the other anomalies surrounding the Peterborough anomaly is shown on the Bouguer anomaly map (in milligals) in figure 7.4. This complexity makes it difficult to separate the Peterborough negative anomaly from the surrounding anomalies.

8B.2.3 Iterative modelling

The gravity data shown in figure 8.13 were used as the starting point for the modelling. The 1.0 kilometre grid was resampled to give a data array of 15 by 15 stations at 2.0 kilometre intervals. Reducing the ammount of data in this way reduced the computation time for the models by an order of magnitude.

As can be seen in figure 8.13 the anomaly to be modelled is not closed, but opens out to the east and west. It was found that edge effects in the modelling resulted in a ridge of excess material on the eastern and western margins of the model body. To suppress this feature the gravity effect of 12 external vertical square prisms, each with the same density contrast as the model, was subtracted from the gravity data before input to the modelling program. The thickness of the prisms was increased, where necessary, to minimize the ridges on the edge of the calculated model. The model was not, however, restricted to within the area of the gravity data; the aim was to let the body extend smoothly to the edges of the mapped area.

The depths to the tops of the prisms are shown in

figure 8.14. The bases were fixed at the same depth as the base depth of the model, which was 7.0 kilometres in the final version.

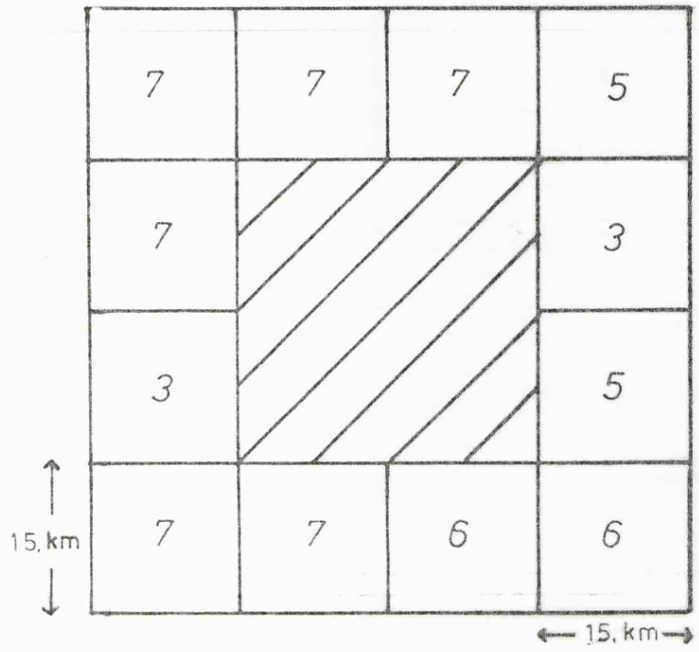


Figure 8.14 : The depths (in km.) to the tops of the external prisms. The shaded area contains the modelled data.

The calculated gravity anomaly for the external prisms is shown in figure 8.15 and the anomaly after removal of the effect of the prisms in figure 8.16.

The lateral extent of the model was allowed to increase until the the calculated anomaly was sufficiently large to account for the 30 gu. contour in figure 8.13 (equivalent to the 40 gu. contour in figure 8.16), and therefore leave no residuals correlated with the edge of the model.

Initially a 10.0 kilometre base depth was used for the model. The calculated anomaly fitted the central part of the negative anomaly but was too large, in a negative sense, on the flanks. this caused a residual on the edge of the body. A base depth of 7.0 kilometres was subsequently chosen; this was the minimum depth possible, for a density contrast of 100 $kg.m^{-3}$, if the top of the model was not to protrude through the basement surface defined by the seismic experiment.

The calculated anomaly is shown in figure 8.17 and the

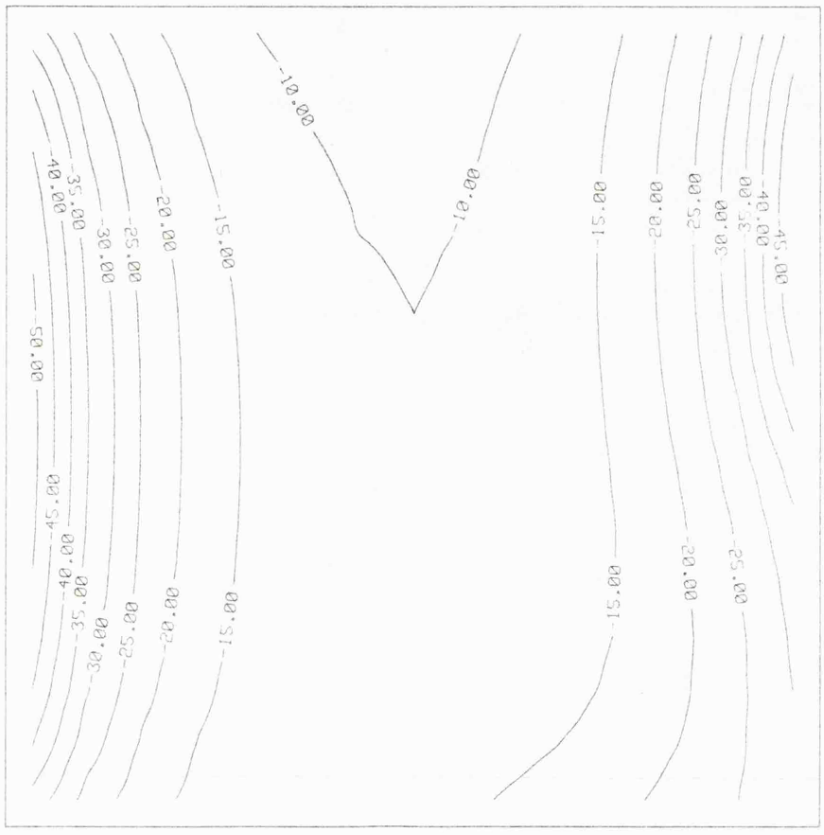


Figure 8.15 : Calculated gravity effect for the 12 external prisms, contour interval 5 g.u.

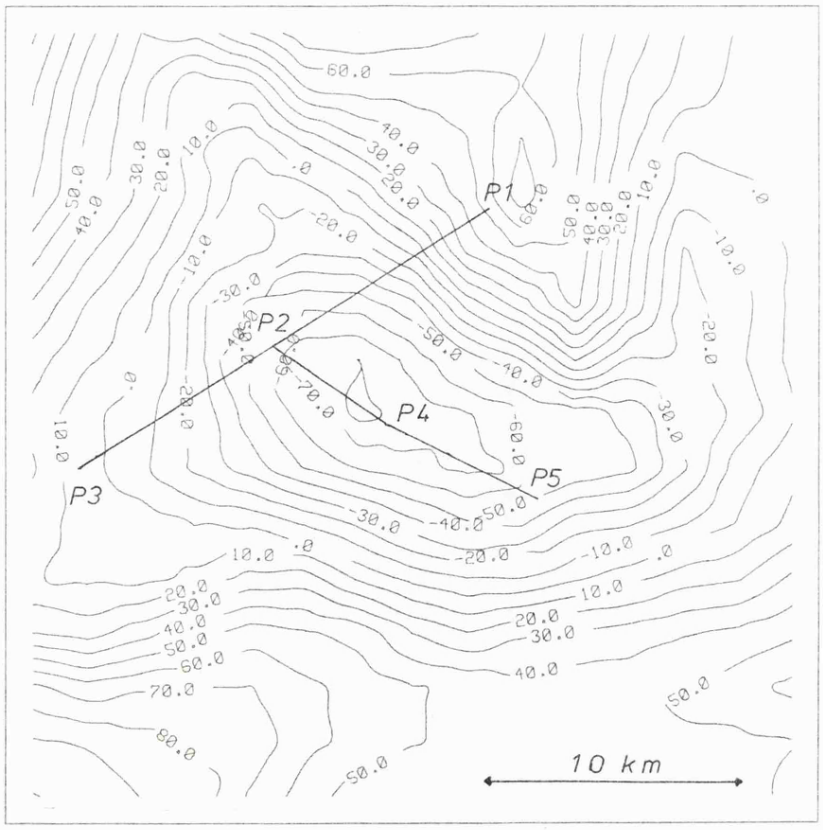


Figure 8.16 : The anomaly in figure 8.13 after removal of the effect of the external prisms, contour interval 10 g.u.

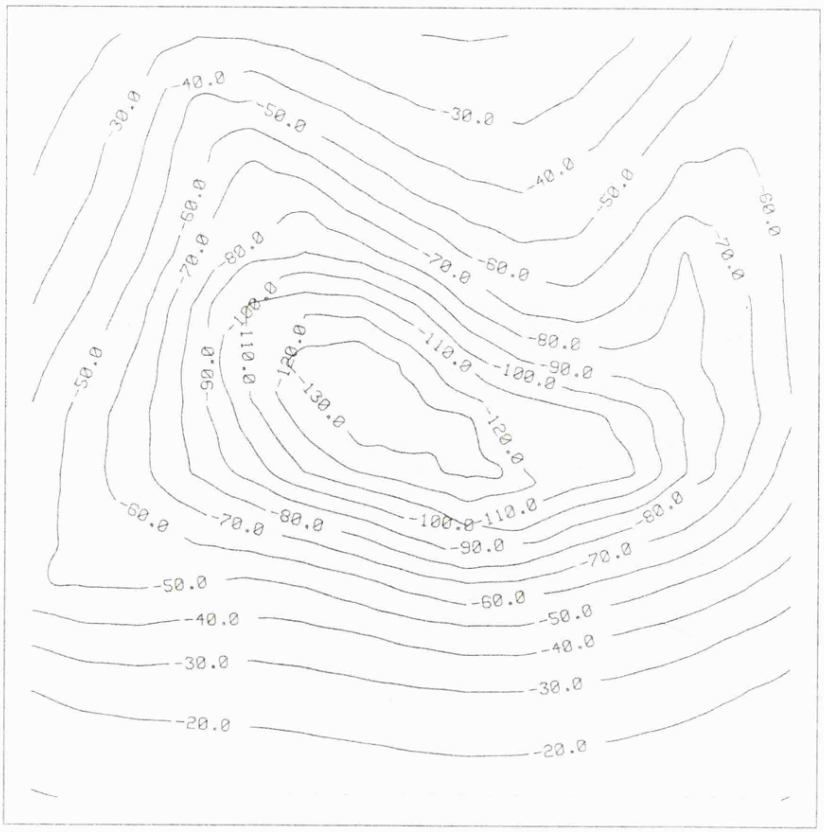


Figure 8.17 : Calculated gravity anomaly for a model with a 7 km. base depth and 100 kg.m density contrast, contour interval 10 g.u.

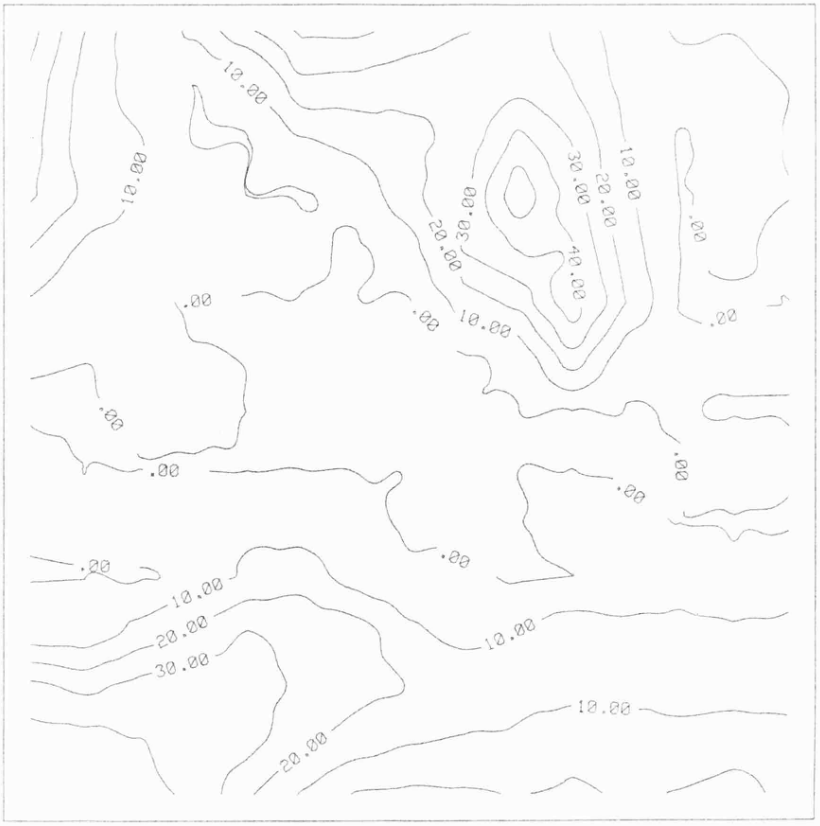


Figure 8.18 : Residual gravity for the model, contour interval 10 g.u.

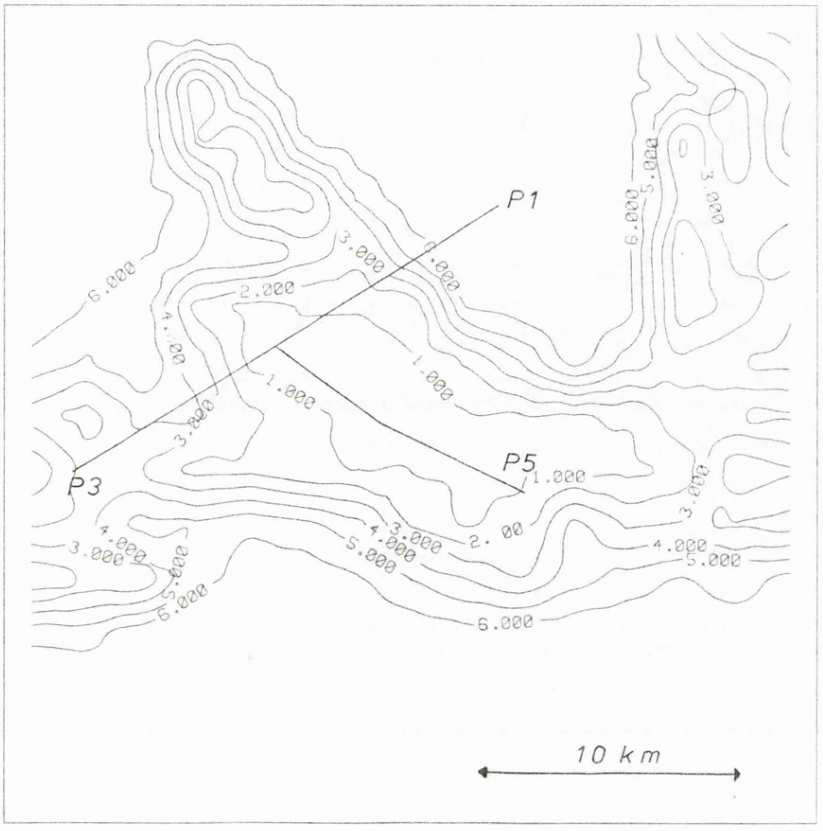


Figure 8.19 : The anomalous body as determined by the iterative modelling, shown as a contour map, in km., of the depth to the top surface of the body (above), and as an isometric projection (below).

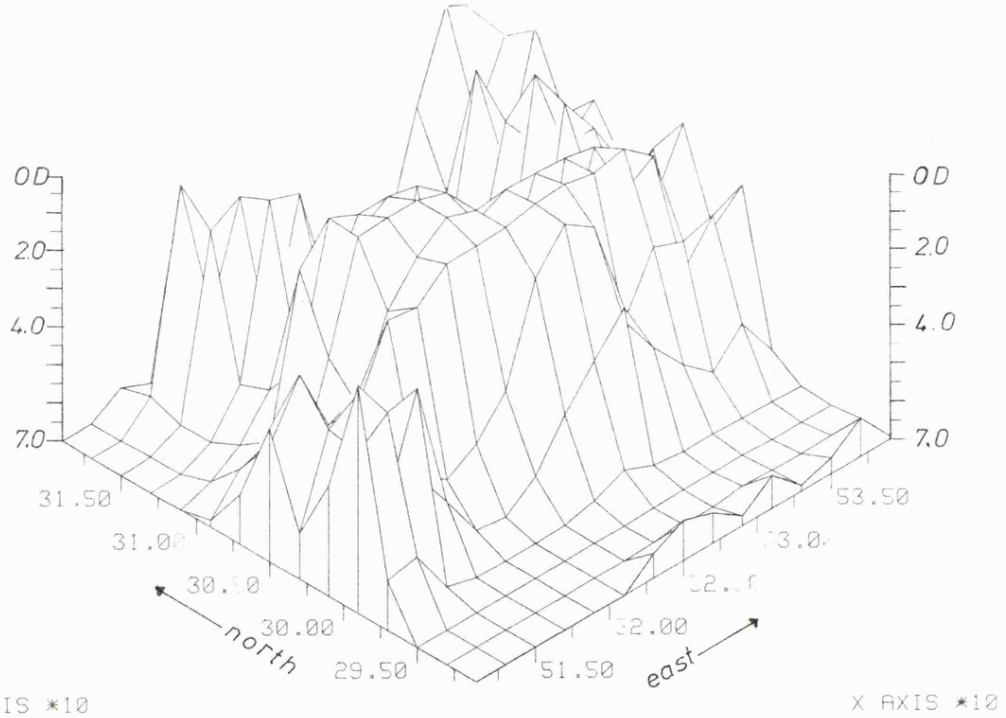

residuals for the model in figure 8.18. Similar residual maps were obtained for density contrasts of up to 130 $kg.m^{-3}$ and base depths as shallow as 5.0 kilometres. There is still a misfit, as shown by the 10 gu. contour in figure 8.18. This misfit cannot be removed using simple iterative models with a single density contrast. If the anomaly is due to a granitic intrusion a decrease in density contrast with depth might be expected. Such a variation would help to reduce the wavelength of the calculated anomaly and hence the residuals.

Figure 8.19 shows the modelled body as a contour map of the depth to its top surface, and as an isometric projection. The use of the external prisms has suppressed, but not removed, the edge effects. The causal body clearly extends to the east and the low gravity values on the western edge of the mapped area have caused an extension of the model to the west. It is possible, however, that the low Bouguer gravity in the east is due to a decrease in the density of the Precambrian basement rocks and not to a westward extension of the body. The seismic refraction experiment indicated a low refractor velocity in the vicinity of shotpoint P3 (see figure 8.16).

## 8B.3 SUMMARY

The iterative model of a low density, intra-basement, intrusion is acceptable but by no means perfect. The steep gradients on the flanks of the observed anomaly require that the top of the model is at shallow depth (<1.0 km.) for the best fit. The fit of the model to the observed anomaly is worst on the flanks of the anomaly. Allsop and Jones (1981) noted that a sedimentary basin model, with inward sloping sides, gave a better fit on the flanks of the anomaly than an intrusion with outward sloping sides. However the seismic data appear to preclude the sedimentary basin model. The intrusion model could be improved if a larger area of data were to be used and, possibly, if the density contrast was allowed to decrease with depth.

# CHAPTER NINE

# THE DEEP GEOLOGY OF THE EAST MIDLANDS

## 9.1 SUMMARY

### 9.1.1 Seismic experiments

The small refraction survey over the South Leicestershire Diorite intrusion (chapter 3) indicated a velocity of about 5.0 $km.s^{-1}$ for a refractor considered to be the top of the intrusion. This was comparable with previous experiments in Leicestershire which had also indicated a significantly lower velocity for the Caledonian igneous intrusions than for Charnian type basement (velocity 5.5-5.7 $km.s^{-1}$).

The Melton experiment, however, indicated a refractor velocity of greater than 5.7 $km.s^{-1}$, at depths equivalent to the depth to granitic basement in the Kirby Lane borehole, over the Melton granitic intrusion. Time term solutions for subdivided data sets indicated a possible increase in velocity over the Melton granite, compared with velocities for the surrounding Charnian type basement. These velocity determinations were supported by an apparent velocity of over 6.0 $km.s^{-1}$ measured from the first arrivals on a 1.1 kilometre seismic reflection spread.

Anomalously large delay times were found to be associated with the stations on the Mountsorrel granodiorite. This was taken to indicate that the Mountsorrel intrusion has a lower velocity than the time term solution velocities of about 5.7 $km.s^{-1}$. The delay time anomaly suggested a

velocity of 5.2 $km.s^{-1}$, which would be compatible with the results of a previous refraction profile to the north of Mountsorrel.

The velocities determined for the basement refractor to the south of the Melton intrusion, and on the Peterborough experiment, were in the range 5.55 to 5.75 $km.s^{-1}$. Such velocities are consistent with previously determined velocities for exposed Charnian basement. An apparent velocity of about 5.2 $km.s^{-1}$ was detected to the southwest of the Glinton borehole on profile A of the Peterborough experiment. This was interpreted as a localised velocity change within the Precambrian basement.

With the exception of the margin of the Widmerpool Gulf, neither the Melton or Peterborough experiments detected any significant structure on the basement refractor, which was typically less than Ø.5 kilometres deep.

A short wavelength structure, with an amplitude of 5Ø to 1ØØ metres, was detected along the seismic lines. This could have been due to topography on the basement refractor, or to variation in the velocity structure of the refractor or the overlying sediments.

### 9.1.2 Potential field data

The main potential field anomalies in this area are interpreted as being intra-basement in origin. Models of some of the magnetic anomalies, and of the Peterborough gravity anomaly, show intrusions emplaced within the top 1Ø kilometres of the crust, with their top surfaces less than two kilometres below the suface.

Models of the Melton magnetic anomaly are compatible with the seismic reflection and refraction interpretations and show that the intrusion can be modelled by a body with a flat top surface at Ø.3 to Ø.4 kilometres depth.

The belt of magnetic anomalies to the east of Melton can be interpreted as a ridge of igneous intrusions four kilometres deep, with prismatic cupolas protruding from its upper surface to depths of one or two kilometres. These intrusions lie on the northern flank of a positive gravity anomaly, which is interpreted as a horst structure of pre-Charnian material, possibly equivalent to the LISPB "$a_1$" refractor. Both anomalies have a Charnoid trend.

## 9.2 PRE-CARBONIFEROUS PALAEOGEOLOGICAL MAPS

Figures 9.1, 9.2 and 9.3 show, repectively; the locations of boreholes and seismic refraction lines; a contour map of the depth to the pre-Carboniferous basement; a palaeogeological map of the pre-Carboniferous basement surface. Figure 9.3 is an attempt to update the maps of Wills (1973, 1978) for the East Midlands area, incorporating the currently available borehole and geophysical data.

The pre-Carboniferous surface has been chosen, in preference to the more usual pre-Permian unconformity, in order to exclude the thick Carboniferous deposits which occur in the coalfield areas around Leicester. Since Carboniferous deposits are scarce to the south and east of Leicester the mapped surface is generally equivalent to the pre-Permian unconformity in this area. In fact the Permian

is also absent and it is usually the Keuper or Bunter which lies on the Palaeozoic basement.

The post-Caledonian Old Red Sandstone has been included on the map since it occupies a large portion in the south-east of the mapped area, where little is known about the deeper basement. The evidence from the Wyboston borehole is that the ORS is thin and overlies Lower Palaeozoic mud-stones. Red conglomerates occuring beneath the Lower Carboniferous in the Dukes Wood borehole have been excluded along with the Carboniferous.

The boundaries to the different units in figure 9.3 are highly speculative, there being no apparent connection between basement lithology and potential field anomalies. The exception to this are the outlines of the igneous intrusions which are based on the magnetic anomalies (chapters 7 and 8A) and on the Peterborough gravity anomaly (chapter 8B).

In figure 9.3 the annotations have been superimposed where there is some geophysical evidence for the presence of Precambrian basement, or igneous intrusions, beneath the Palaeozoic basement.

The Precambrian has been mapped as one unit. All the different lithologies found in boreholes can be described as "Charnian" in the loosest sense of the word, in that they are tuffs and volcanic agglomerates of probable late Precambrian age. For example Le Bas (pers. comm.) has described the material from the recent Hollowell borehole as a rhyolitic-dacitic agglomerate indicative of a nearby volcanic source. There is no direct equivalent to this rock in the Charnian Inlier, but dacites similar to the fragments

in the Hollowell agglomerate are found in some of the Charnian porphyroids. The coarse grained agglomerate in the Upwood borehole suggests another volcanic centre.

The Lower Palaeozoic: there is a distinct division in the lithology of the Lower Palaeozoic rocks found in the mapped area. To the west and south of Leicester the Lower Palaeozoic comprises shales and siltstones, of probable Cambrian age, analogous to the Stockingford Shales. Ordovician shales are found in the southeast of the area. In the north of the mapped area, from Eakring to The Wash, the Lower Palaeozoic comprises fine grained, pale grey or white, quartzites. This unit is only found in five boreholes (including Wisbech) but can be tentatively correlated with the Lower Cambrian Hartshill Quartzite of Nuneaton. The occurrence of the quartzite in the Wisbech borehole must be regarded as dubious since only two metres were drilled and no core was recovered. The depth to the quartzite is also shallower than in surrounding boreholes.

Igneous intrusions: the proven and possible intrusions are shown in figure 9.3. The proven intrusions are all associated with positive aeromagnetic anomalies, as is the ridge of possible intrusions to the east of Melton Mowbray. The possible Peterborough intrusion represents a second group of intrusions with negative gravity anomalies and no positive magnetic anomaly. The negative gravity anomaly to the northeast of the Peterborough anomaly is tentatively included in this group, although it has not been investigated here. The two gravity anomalies around the Wash

are not included since it is believed that the IGS have some seismic reflection data which indicates a sedimentary basin in this area.

There are two other occurences of granitic rocks in the area which may be relevant. The Trias pebble beds in the Wiggenhall borehole contained fragments of "pink granite". Pebbles of "granite" were found in the Middle Lias at the bottom of the Bletchley borehole, to the south of Northampton. This borehole was located over a positive aeromagnetic anomaly.

Key to figures 9.1, 9.2, 9.3.

Figure 9.1 : Location map.

- ● : borehole to pre-Carboniferous basement
- o : other boreholes
- ◌ : outcrop of pre-Carboniferous rocks
- ——— or ⧄ : seismic refraction profiles

Figure 9.2 : Structure contour map on the pre-Carboniferous.

- 40° ● : boreholes to pre-Carboniferous basement with dip of beds if known
- ⊥ ⊥ ⊥ : normal faults
- ⏃ — ⏃ : reversed faults
- ⟡ ⟡ : anticlinal axes
- (1.5) : depth to "Charnian" basement refractor (km.)
- — 0.5 — : structure contours in km. below OD

Figure 9.3 : Pre-Carboniferous palaeogeological map

- ● : borehole to pre-Carboniferous basement
- ⬭ : outcrop
- — : conjectured boundary
- ≡ : Precambrian
- |||| : Cambrian argillaceous rocks and quartzites
- /// : Ordovician argillaceous rocks
- \\\ : Devonian-ORS, predominantly conglomerates
- (+++) : exposed or drilled igneous intrusions
- (···) : unproven igneous intrusions (magnetic)
- (ooo) : unproven igneous intrusions (gravity)

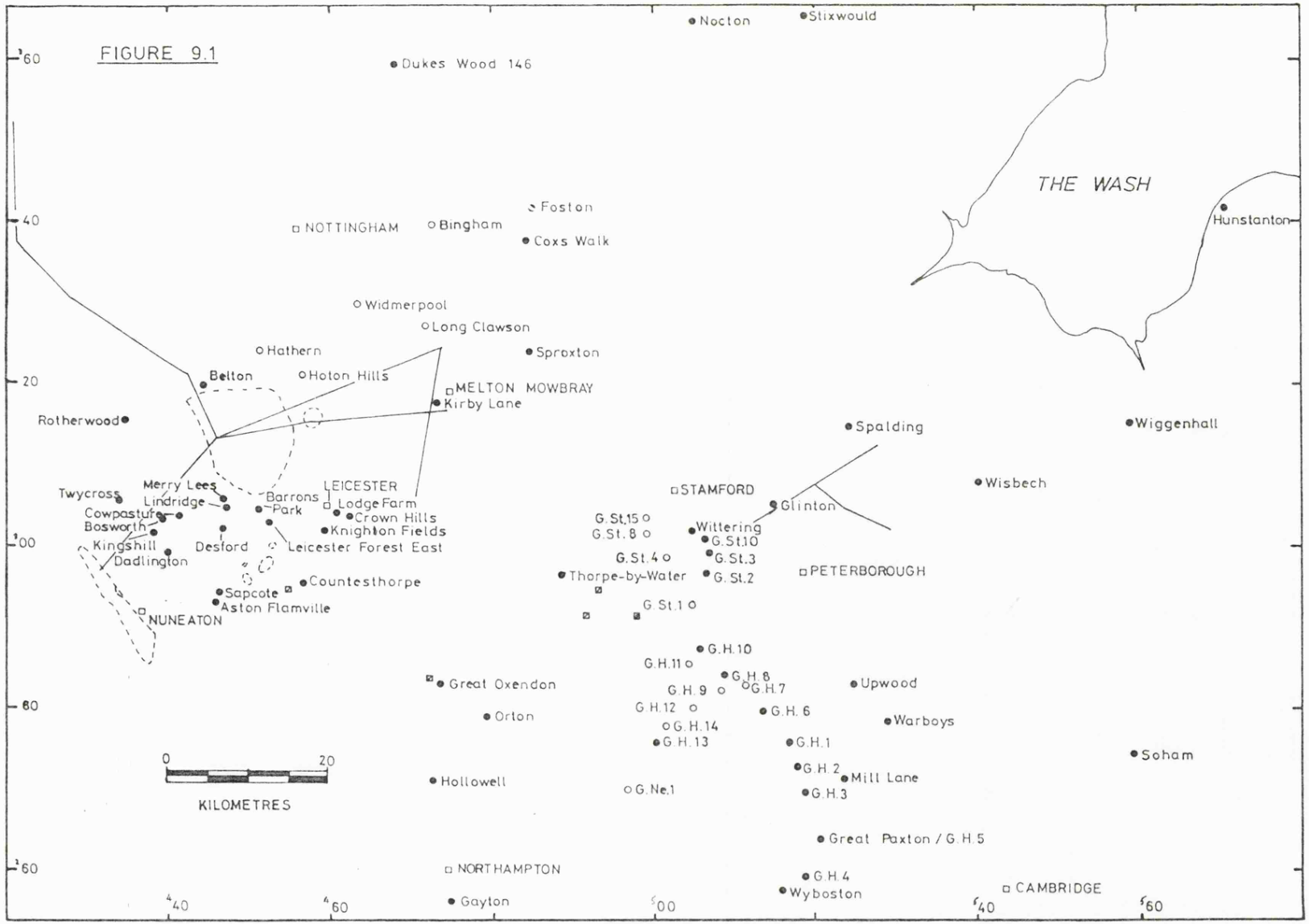
FIGURE 9.1
Nocton
Stixwould
Dukes Wood 146
THE WASH
Hunstanton
Foston
NOTTINGHAM
Bingham
Coxs Walk
Widmerpool
Long Clawson
Hathern
Sproxton
Belton
Holton Hills
MELTON MOWBRAY
Kirby Lane
Rotherwood
Spalding
Wiggenhall
Wisbech
STAMFORD
Glinton
Twycross
Merry Lees
Lindridge
Barrons Park
LEICESTER
Lodge Farm
Crown Hills
Knighton Fields
Leicester Forest East
Cowpastures
Bosworth
Kingshill
Dadlington
Desford
G.St.15
G.St.8
Wittering
G.St.10
G.St.4
G.St.3
G.St.2
Thorpe-by-Water
PETERBOROUGH
G.St.1
Countesthorpe
Sapcote
Aston Flamville
NUNEATON
G.H.10
G.H.11
G.H.8
G.H.9
G.H.7
Upwood
G.H.12
G.H.6
Warboys
G.H.14
G.H.13
G.H.1
Great Oxendon
Orton
Soham
G.H.2
Mill Lane
G.Ne.1
G.H.3
Hollowell
Great Paxton / G.H.5
NORTHAMPTON
G.H.4
Wyboston
CAMBRIDGE
Gayton
0
20
KILOMETRES

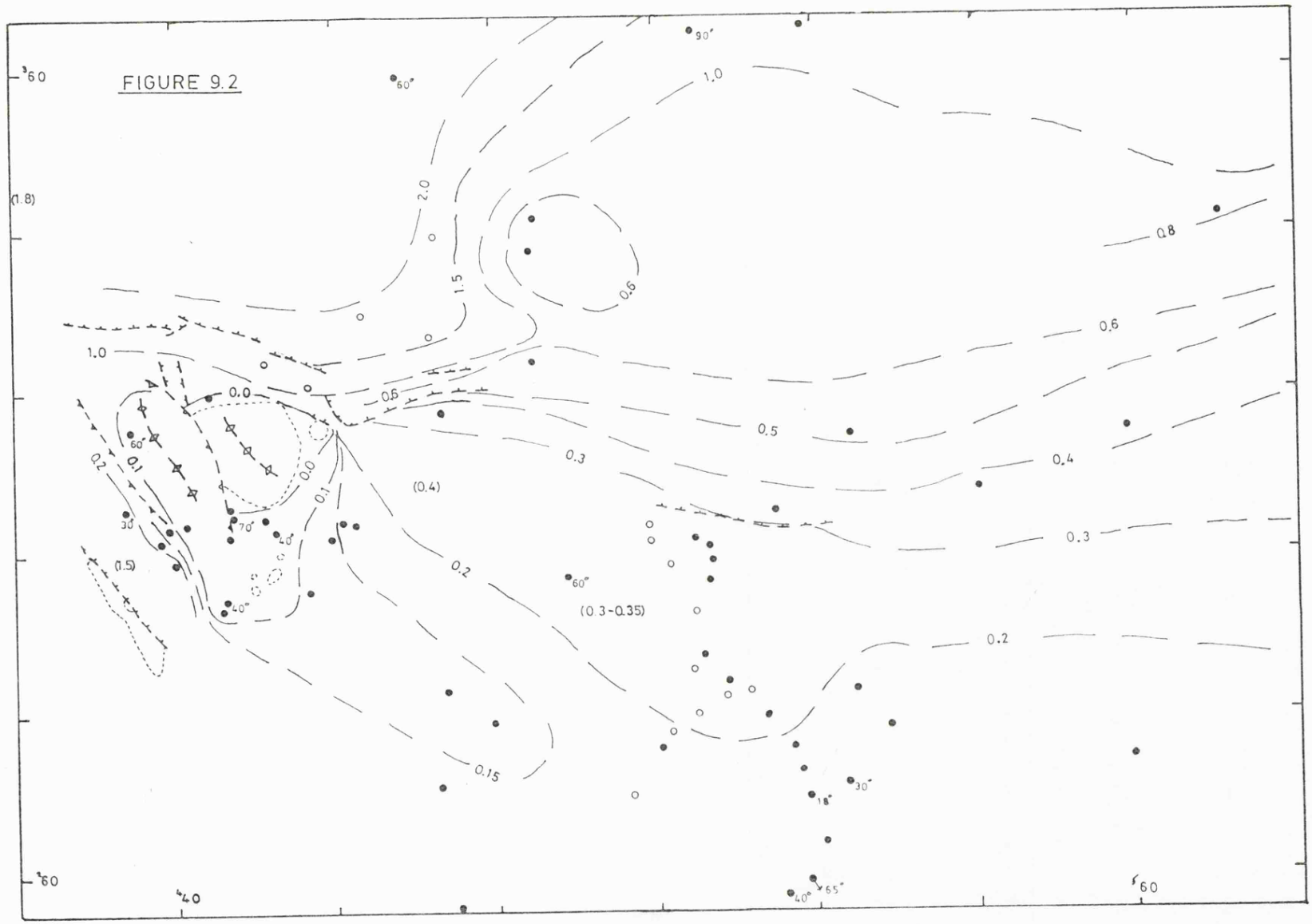
FIGURE 9.2
360
(1.8)
60°
90°
1.0
2.0
1.5
0.5
0.8
0.6
0.5
0.3
0.4
0.3
0.2
0.15
1.0
0.0
0.5
0.2
0.1
0.0
0.1
(0.4)
(1.5)
30°
70°
40°
60°
40°
(0.3-0.35)
18°
30°
40°
65°
360
340
360

FIGURE 9.3

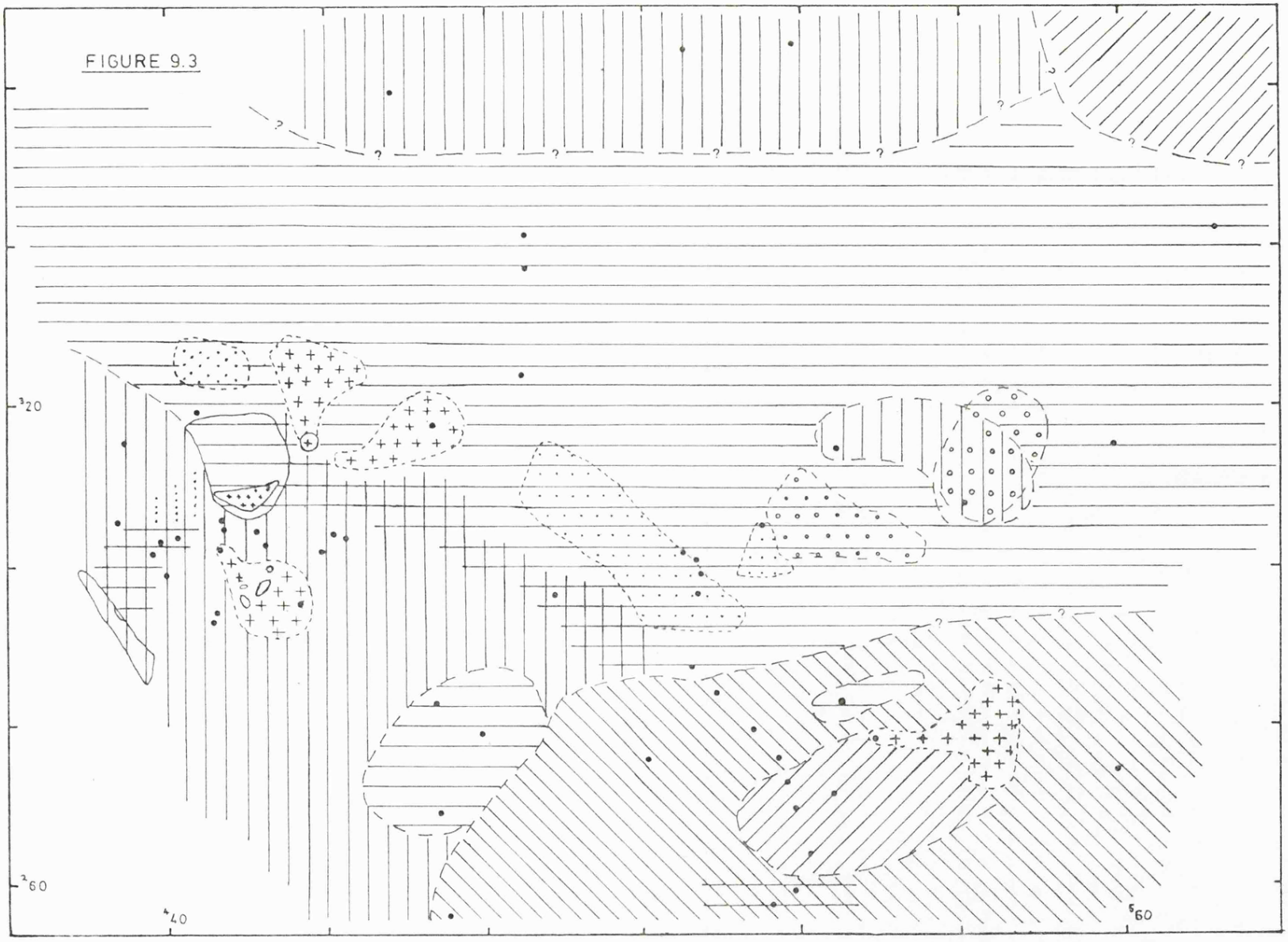

## 9.3 DISCUSSION

The maps discussed in the previous section show the distribution and type of the interpreted intrusions in the East Midlands. The ridge of shallow Precambrian basement can be traced from Charnwood Forest to Norfolk. The intrusions lie on or to the south of this ridge. No evidence has been found for a cross-cutting Caledonian aulacogen, as proposed by Evans (1979). The Ordovician mudstones located in the southeast of the mapped area may represent the northern extension of the thick accumulation of folded Lower Palaeozoic sediments found to the north and south of The Thames, and generally interpreted as a westward extension of the Brabant Massif.

### 9.3.1 Late Precambrian basement

The variations in density of the late Precambrian basement rocks, as tabulated in table 7.1, reflect the observable variations in lithology. However the p-wave velocities from the Melton and Peterborough experiments, as well as those from previous experiments, show that on a broader scale the late Precambrian basement across the whole of the East Midlands in characterized by p-wave velocities of 5.55 to 5.75 $km.s^{-1}$. Surveys in Norfolk (Chroston and Sola 1982) indicate slightly higher velocities (up to 6.Ø $km.s^{-1}$). Insufficient work has been done on the petrology of the basement rocks to say if this increase correlates with either an increase in metamorphic grade or a compositional change. Lower velocities have been noted for the Upwood borehole agglomerate, close to the Great Oxendon borehole,

and possibly on profile A of the Peterborough experiment.

Measured densities for the late Precambrian basement rocks range from 2700 to 2800 $kg.m^{-3}$, no samples of the late Precambrian basement in this area are known to have significant magnetic suscetibilities or remanence.

9.3.2 Igneous intrusions

Two groups of igneous intrusions can be identified:

1) intrusions with a high magnetic susceptibility contrast but no density contrast relative to the surrounding basement;

2) intrusions with negligible magnetic susceptibilities and negative density contrasts. Modelling suggests that both types are emplaced within one to two kilometres of the surface and extend to depths of seven to ten kilometres. Since the surrounding Precambrian basement shows little variation in physical properties across the area the two groups must represent two different types of intrusions.

The magnetic susceptibilities of the first group are in the range 0.01 to 0.025 (SI), assuming a non-magnetic surrounding basement, this together with the lack of positive density contrasts suggests an acid to intermediate composition. These intrusions can be referred to as "Mountsorrel type". P-wave velocities appear to range from 5.0 to 6.0 $km.s^{-1}$. Since high velocity gradients have been noted for the lower velocity refractors no division in composition is suggested by the range in velocities. The lower velocities have only been observed at ranges of a few kilometres.

No examples of the second group of intrusions are found at outcrop, or in boreholes, in the East Midlands. The low

density and susceptibility suggest that these intrusions can be expected to have a more acid composition than the Mountsorrel type; this group can be termed "Peterborough type". Two of these intrusions are shown in figure 9.3. If the Norfolk intrusion of Chroston and Sola (1982) is added to these there is a geographical division between the Mountsorrel type to the southwest, and the Peterborough type to the northeast.

The belt of Mountsorrel type intrusions to the east of Melton Mowbray has a northwest to southeast "Charnoid" trend and is associated with a positive gravity anomaly. This gravity anomaly is interpreted as an intra-basement horst structure which suggests that the intrusions may be following a Charnoid line of weakness. The possibility cannot be ruled out that some of the Mountsorrel type intrusions are Precambrian. The late Precambrian diorites of Charnwood Forest have similar physical properties to this group. However, there is no geological reason why both groups of intrusions cannot be Caledonian.

### 9.3.3 Older basement

The positive gravity anomaly that runs southeast, from east of Melton Mowbray to south of Peterborough, is interpreted as an intra-basement feature. No equivalent structure is detectable at the basement surface (figure 9.2) although the Lower Palaeozoic has a Caledonian deformation. This indicates a pre-Caledonian origin for the intra-basement structure, as does the Charnoid trend. The high density that must be assumed for this feature can be correlated with the 6.4 $km.s^{-1}$ refractor velocity detected at between two and

four kilometres beneath the Charnian Inlier and, by inference, the LISPB "$a_1$" refractor. The gravity ridge broadens out to the west and connects with the Charnian Inlier. It also passes to the south of the Melton intrusion, where a high velocity refractor may have been detected at the southern end of profile B of the Melton experiment. The absence of a magnetic anomaly associated with this feature indicates that the deeper Precambrian basement also has a negligible magnetic susceptibility.

It is therefore possible to deduce four types of igneous or Precambrian basement in this area, of these only two are found at outcrop or in boreholes.

1) Mountsorrel type intrusions, similar density to non-igneous basement, high magnetic susceptibility, p-wave velocities range from 5.Ø to 6.Ø $km.s^{-1}$.

2) Peterborough type intrusions, low density, negligible magnetic susceptibilities relative to non-igneous basement.

3) Charnian type basement, non magnetic, density 27ØØ to 28ØØ $kg.m^{-3}$, velocity 5.55 to ?6.Ø $km.s^{-1}$.

4) Pre-Charnian basement, high density, non magnetic, velocity ? 6.4 $km.s^{-1}$, minimum depth about two kilometres, possibly equivalent to the LISPB "$a_1$" layer.

## 9.4 RECOMMENDATIONS FOR FUTURE WORK

Seismic refraction surveys, of the type described in previous chapters, have been carried out by Leicester University in this area for the past 10 years, and by other workers for considerably longer. These surveys have continued to support the scattered borehole and outcrop evidence in indicating a ridge of late Precambrian and granitic basement extending eastwards, at shallow depth, from Charnwood Forest to Norfolk. "Charnian" type basement has also been detected, at depths of one to two kilometres, beneath the Upper Palaeozoic basins to the north and southwest of Charnwood Forest.

The fact that this basement is present at shallow depths makes it a good target for relatively short (10 to 30 kilometre) refraction profiles. Such profiles continue to prove useful in the interpretation of the potential field data from this area, which in turn continues to supply increasing evidence for a major (? Caledonian) igneous province. The resolution of such surveys is limited by the picking accuracy of first arrival travel times, say 0.010 seconds for good quality data. Resolution is also poor in areas of structural complexity with lateral velocity variations within the refractor or the overlying sediments.

Away from the Charnian Inlier, where refraction and teleseismic studies have yielded some information, very little is known about the sub-Charnian basement. A deeper refractor has been detected by some of the seismic profiles around the Charnian Inlier, but this refractor has never been resolved in terms of velocity or depth. The simple

gravity interpretation described in chapter 7 also suggests sub-Charnian basement at a depth of a few kilometres.

A study of the deeper structure of the Precambrian basement would be most useful in the geological interpretation of the Midlands craton, and would provide greater constraints on any potential field modelling. At the start of this project it was intended to record a 60 kilometre refraction profile running southeast from Charnwood Forest towards Peterborough. The Precambrian basement along this profile is at shallow depth (figures 9.2, 9.3) and no short wavelength structures are indicated on the potential field maps. This profile could therefore provide a simple velocity structure for the Charnian and sub-Charnian basement.

A second possibility, would be to rotate the profile through 90° to run southwest to northeast, across the strike of the gravity and magnetic ridges discussed in chapter 7. Because of the expected lateral variation in basement structure, this profile would be harder to interpret but potentially much more informative. A deep reflection profile would be the best option for this profile, but in order to have good velocity control it would be necessary to have some shots at long offsets, or else to record a refraction profile along the same line.

If any further short refraction profiles are to be recorded the best target would be the other negative gravity anomalies between Peterborough and The Wash. This could be backed up by further potential field modelling. In particular the relative distributions of the two types of intrusion could be investigated over a wider area.

A few new physical property measurements have been made

as part of this work. There is, however, a need for a thorough study of the physical properties of representative suites from the basement rocks. The Melton refraction survey indicated that the granitic intrusions in this area cannot be assumed to have low p-wave velocities relative to the Precambrian basement. If further refraction lines are to be carried out in this area, with a view to delineating other intrusions, greater attention should be paid to recording s-wave arrivals in order to use p/s velocity ratios as a means of detecting lateral variations in the basement refractor. This would require laboratory measurements of p and s-wave velocities, including the effects of pressure, for samples of both the granitic and Precambrian basement. The samples of the Melton granite from the Kirby Lane borehole are too weathered to yield meaningful velocities in the laboratory. Velocity measurements on samples of Mountsorrel granodiorite would be useful in the light of the conflicting results of the Melton and Bardon to Holwell refraction profiles, and the apparent delay associated with the Mountsorrel granodiorite in the solutions to profile A of the Melton experiment.

Work on the detailed petrology of borehole samples of the Precambrian basement is now in progress at Leicester. Recently the shallow water facies of the Lower Palaeozoic sediments has been questioned by Evans (1979), who suggested an "East Midlands Aulacogen"; and Le Bas (1982), who suggested a series of Lower Palaeozoic island arcs. Therefore it would seem sensible to study both the Lower Palaeozoic sediments, and the Caledonian intrusions, in detail, to see if this problem can be resolved.

## REFERENCES CITED

ALLEN,J.R.L. 1968. The Cambrian and Ordovician systems. In Sylvester-Bradley,P.C. & Ford,T.D. (eds). The Geology of the East Midlands. Leicester University Press. 20-40.

ALLSOP,J.M. & JONES,C.M. 1981. A pre-Permian palaeogeological map of the East Midlands & East Anglia. Trans. Leics. Lit. & Phil. Soc. 75, 28-33.

ANDERTON,R., BRIDGES,P.H., LEEDER,M.R. & SELLWOOD,B.W. 1979. A Dynamic Stratigraphy of the British Isles. George Allen & Unwin, London, 301pp.

ARAB,N. 1972. Seismic reflection and gravity investigation of the Widmerpool gulf in the East Midlands with a study of linear seismic sources and data processing techniques involving computer graphics. Unpublished Ph.D. thesis. University of Leicester.

BAMFORD,D., NUNN,K., PRODEHL,C. & JACOB,B. 1977. LISPB-III. Upper crustal stucture of Northern Britain. J. Geol. Soc. London 133, 481-8.

BAMFORD,D., NUNN,K., PRODEHL,C. & JACOB,B. 1978. LISPB-IV. Crustal structure of Northern Britain. Geophys. J. R. Astr. Soc. 54, 43-60.

BAMFORD,S.A.D. 1973. An example of the iterative approach to time term analysis. Geophys. J. R. Astr. Soc. 31, 365-372.

BARNETT,C.T. 1976. Theoretical modelling of the magnetic and gravitational fields of an arbitrarily shaped three-dimensional body. Geophysics 41 (6) 1353-1364.

BERCKHEMER,H. 1976. Standard equipment for deep seismic sounding. In Giese,P., Prodehl,C. & Stein,A. (eds). Explosion Seismology in Central Europe. 115-119.

BIRCH,A.F. 1958. Interpretation of the seismic structure of the crust in the light of experimental studies of wave velocities in rocks. In Beniott,H. et al (eds). Contributions in Geophysics, Int. Series. Mon. Earth Sciences. 1. Pergamon Press, New York, 158-170.

BRIDEN,J.C. & DUFF.B.A. 1981. Pre-Carboniferous paleomagnetism of Europe north of the Alpine orogenic belt. In McElhinny,M.W. & Valencio,D.A. (eds). Paleoreconstruction of the continents. A.G.U. geodynamics series 2. 137-150.

BROOKS,M. 1963. Rock groups of the Malvern Hills. Nature, London 198, 567-568.

BROOKS,M. 1966. A study of density variations in the New Red Sandstones of the English Midlands. Geol. Mag. 103, 61-69.

BROOKS,M. 1968. The geological results of gravity and magnetic surveys in the Malvern Hills and adjacent districts. Geol. J. 6(1) 13-30.

BONNEY,T.G. 1895. Supplementary note on the Narborough District (Leicestershire). Quart. J. Geol. Soc. Lond. 51, 24-34.

BULLARD,E.C., GASKELL,T.F., HARLAND,W.B. & KERR-GRANT,C. 1946. Seismic investigations of the Palaeozoic floor of East England. Phil. Trans. Roy. Soc. Lond. A 239, 29-94.

BULLERWELL,W. 1967. In discussion pp38-39 following: STUBBLEFIELD,C.J. & BULLERWELL,W. Some results of a recent Geology Survey boring in Huntingdonshire. Proc. Geol. Soc. Lond. 1637, 35-38.

BURKHARDT,H & VEES,R. 1976. Seismic signals from quarry blasts. In Giese,P., Prodehl,C. & Stein,A. (eds). Explosion seismology in Central Europe. 62-72.

BUTTERLY,A.D. & MITCHELL,G.H. 1946. Driving of two drifts by the Desford Coal Co. Ltd. at Merry Lees, Leics. Trans. Inst. of Mining Engineers. 104, 703-13.

CHROSTON,P.N. & SOLA,M.A. 1982. Deep boreholes, seismic refraction lines and the interpretation of gravity anomalies in Norfolk. J. Geol. Soc. Lond. 139 (3), 255-264.

CORDELL,L. & HENDERSON,R.G. 1968. Iterative three-dimensional solution of gravity anomaly using a digital computer. Geophysics 33 (4) 596-601.

CRIBB,S.J. 1975. Rubidium Strontium ages and Strontium isotope ratios from the igneous rocks of Leicestershire. J. Geol. Soc. Lond. 131, 203-212.

DAVIES,D. & MATTHEWS,D.H. 1966. Geophysical investigations on the boundaries of the Mountsorrel granite. Geol. Mag. 103 (6) 534-547.

DEWEY,J.F. 1969. Evolution of the Appalacian/Caledonian orogen. Nature, London, 222, 124-129.

DUFF,B.A. 1980. Palaeomagnetism of late Precambrian or Cambrian diorites from Leicestershire UK. Geol. Mag. 117, 479-483.

EVANS,A.M. 1964. Note on the Orton boring,Northamptonshire. Jnl. N'hants. Nat. Hist. Soc. 34, 247.

EVANS,A.M. 1968. Precambrian rocks. In Sylvester-Bradley,P.C. & Ford,T.D. (eds) The Geology of the East Midlands. Leicester University Press. 1-12.

EVANS,A.M. 1979. The East Midlands aulacogen of Caledonian age. Mercian Geol. 7 (1), 31-42.

FALCON,N.L. & KENT,P.E. 1960. Geophysical results of petroleum exploration in Britain 1945-1957. Geol. Soc. Lond. Memoir 2.

FOX-STRANGWAYS,C. 1903. The geology of the country near Leicester, (sheet 156). Mem. Geol. Surv. England & Wales.

HAGEDOORN,J.G. 1959. The Plus-Minus method of interpreting seismic refraction sections. Geophysical Prospecting 7, 158-182.

HAINS,B.A. & HORTON,A. 1969. British regional geology, Central England. 3rd ed. Institute of Geological Sciences London. H.M.S.O.

HARRIS,A.L., HOLLAND,C.H. & LEAKE,B.E. (eds) 1979 The Caledonides of the British Isles reviewed. Spec. Publ. Geol. Soc. Lond. 8. 768pp.

HARRISON,W.J. 1884. The syenites of South Leicestershire. Midlands Naturalist 7, 7-11 & 41-2.

HARRISON,W.J. 1885. On the pre-Carboniferous floor of the Midlands. Midlands Naturalist 8, 133.

HILL,E. & BONNEY,T.G. 1878. The pre-Carboniferous rocks of Charnwood Forest - part 2. Quart. J. Geol. Soc. Lond. 34, 199-239.

INSTITUTE OF GEOLOGICAL SCIENCES. Annual reports 1965-
(continues from Summary of Progress of the Geological Survey of Great Britain.)

INSTITUTE OF GEOLOGICAL SCIENCES Special Reports:
73/12 The geology of Peterborough.
74/7 IGS boreholes 1973
78/21 IGS boreholes 1977
79/12 IGS boreholes 1978

JONES,F. 1927. A structural study of the Charnian rocks and of the igneous intrusions associated with them. Trans. Leics. Lit. & Phil. Soc. 28, 24-41.

JONES,P.A. 1981. National Coal Board exploration in Leicestershire. Trans. Leics. Lit. & Phil. Soc. 75, 34-40.

JUKES-BROWN,A.J. 1889. The occurence of granite in a boring at Bletchley. Geol. Mag. 16, 356-361.

KENT,P.E. 1947. A deep boring at North Creake, Norfolk. Geol. Mag. 84, 2-18.

KENT,P.E. 1968. The buried floor of Eastern England. In Sylvester-Bradley,P.C. & Ford,T.D. (eds). The Geology of the East Midlands. Leicester University Press. 138-148.

LE BAS,M.J. 1968. Caledonian igneous rocks. In Sylvester-Bradley,P.C. & Ford,T.D. (eds). The Geology of the East Midlands. Leicester University Press. 41-58.

LE BAS,M.J. 1972. Caledonian igneous rocks beneath Central and Eastern England. Proc. Yorks. Geol. Soc. 39 (1) 71-86.

LE BAS,M.J. 1981. The igneous basement of southern Britain with particular reference to the geochemistry of the pre-Devonian rocks of Leicestershire. Trans. Leics. Lit. & Phil. Soc. 75, 41-57.

LE BAS,M.J. 1982. Geological evidence from Leicestershire on the crust of Southern Britain. Trans. Leics. Lit. & Phil. Soc. 76, 54-67.

LEES,G.M. & TAITT,A.H. 1946. The geological results of the search for oilfields in Great Britain. Quart. J. Geol. Soc. of London 101, (for 1945) 255-317.

LONG,R.E. 1974. A compact portable seismic recorder. Geophys. J. R. Astr. Soc. 37, 91-98.

LOWE,E.E. 1926. The igneous rocks of the Mountsorrel district. Leics. Lit. & Phil. Soc. 49pp.

LOWE,E.E. 1928. In Bennet,F.W. et al. The geology of Charnwood Forest. Proc. Geol. Assoc. 39, 241-98.

MAGUIRE,P.K.H., ANDREWS,E.M., ARTER,.G., CHADWICK,.R.A., HILL,I.A., KENOLTY,.N. & KHAN,M.A. 1982. A deep seismic reflection profile over a Caledonian granite in Central England. Nature, London 297, 671-673.

MARO F,S.I. 1973. Geophysical investigations of the Carboniferous and pre-Carboniferous formations of the East Midlands of England. Unpublished Ph.D. thesis. University of Leicester.

McKERROW,W.S. & ZIEGLER,A.M. 1972. Silurian palaeo-geographic developments of the proto Atlantic Ocean. 24th Intl. Geol. Congress 6, 4-10.

MENEISY,M.Y. & MILLER,J.A. 1963. A geochronological study of the crystalline rocks of Charnwood Forest, England. Geol. Mag. 100, 507-523.

MILLER,J.A. & PODMORE,J.S. 1961. Age of the Mountsorrel granite. Geol. Mag. 98, 86-88.

NAFE,J.E. & DRAKE,C.L. 1963. Physical properties of marine sediments. In Hill.M.N. (ed). The Sea 3. Interscience. 794-815.

NAGY,D. 1966. The gravitational attraction of a right rectangular prism. Geophysics 31 (2) 362-71.

O'BRIEN,P.N.S. 1967. The use of amplitudes in seismic refraction survey. In Musgrave,A.W. (ed) Seismic Refraction Prospecting. SEG.

OKABE,M. 1979. Analytical expressions for gravity anomalies due to homogenous polyhedral bodies and translations into magnetic anomalies. Geophysics 44, 730-41.

PHILLIPS,W.E.A., STILLMAN,C.J. & MURPHY,T. 1976. A Caledonian plate tectonic model. J. Geol. Soc. Lond. 132, 579-609.

PIDGEON,R.T. & AFTALION,M. 1978. Cogenetic and inherited Zircon U-Pb systems in granites: Paleozoic granites of Scotland and England. In Bowes,D.R. & Leake,B.E. (eds) Crustal evolution in Northwest Britain and adjacent regions. Seel House Press, Liverpool. 183-220.

PIPER,J.D.A. 1979. Palaeomagnetic study of late Precambrian rocks of the Midland Craton of England and Wales. Phys. Earth. Plan. Sci. 19, 59-72.

REILLY,W.I. 1972. Use of the international system of units (SI) in geophysical publications. N.Z. J. Geology & Geophysics. 15 (1) 148-156.

RICHARDSON,L. 1931. Wells and springs of Leicestershire. Memoirs of the Geological Survey. England. H.M.S.O.

RICHARDSON,S.W. & OXBURGH E.R. 1978. Heat flow, radiogenic heat production and crustal temperatures in England and Wales. Jnl. Geol. Soc. Lond. 135 (3) 323-337.

SPINK,K. & FORD,T.D. 1979. The Coal Measures. In Sylvester-Bradley,P.C. & Ford,T.D. (eds). The Geology of the East Midlands. Leicester University Press. 95-111.

STEENLAND,N.C. 1951. Depth estimates from slopes. In Vacquier,V., Steenland,N.C., Henderson,R.G. & Zeitz,I. Interpretation of Aeromagnetic Maps. Geol. Soc. Am. Mem. 47, 9-41.

STUBBLEFIELD,J. 1967. Some results of a recent geological survey boring in Huntingdonshire. Proc. Geol. Soc. 1637, 35-38.

TALWANI,M. & EWING,M. 1960. Rapid computation of gravitational attraction of three-dimensional bodies of arbitrary shape. Geophysics 25, 203-25.

TALWANI,M. & HEIRTZLER,J.R. 1964. Computation of magnetic anomalies caused by two-dimensional structures of arbitary shape. Computers in the geosciences. Stamford University Publication. 464-497.

TALWANI,M., WORZEL.J.L. & LANDISMAN,M. 1959. Rapid gravity computations for two-dimensional bodies with application to the Mendocino submarine fracture zones. Jour. Geophys. Res. 64, 49-59.

THORPE,R.S. 1972. The geochemistry and correlation of the Warren House, the Uriconian and the Charnian volcanic rocks from the English Precambrian. Proc. Geol. Assoc. 83, 269-284.

WATTS,W.W. 1947. Geology of the ancient rocks of Charnwood Forest, Leicestershire. Leics. Lit. & Phil. Soc. 160pp.

WHITAKER,W. 1922. Water supply of Cambridgeshire, Huntingdonshire and Rutland. H.M.S.O.

WHITCOMBE,D.N. 1979. Seismic studies of the Upper Crust in Central England. Unpublished Ph.D. thesis. University of Leicester.

WHITCOMBE,D.N. & MAGUIRE,P.K.H. 1979. The response of the time term method to simulated crustal structures. Bull. Seismological Soc. Am. 69 (5) 1455-73.

WHITCOMBE,D.N. & MAGUIRE,P.K.H. 1980. An analysis of the velocity structure of the Precambrian rocks of Charnwood Forest. Geophys. J. R. Astr. Soc. 63.

WHITCOMBE,D.N. & MAGUIRE,P.K.H. 1981a. A seismic refraction investigation of the Charnian basement and granitic intrusions flanking Charnwood Forest. J. Geol. Soc. Lond. 138 (6) 643-52.

WHITCOMBE,D.N. & MAGUIRE,P.K.H. 1981b. Seismic refraction evidence for a basement ridge between The Derbyshire Dome and the west of Charnwood Forest. J.Geol. Soc. Lond. 138 (6) 653-60.

WILLMORE,P.L. & BANCROFT,A.M. 1960. The time term approach to refraction seismology. Geophys. J. Roy. Astr. Soc. 3, 419-32.

WILLS,L.J. 1973. A palaeogeographic map of the Palaeozoic floor below the Permian and Mesozoic formations in England and Wales. Memoir 7 Geol. Soc. London.

WILLS,L.J. 1978. A palaeogeographical map of the lower Palaeozoic floor below the cover of the upper-Devonian, Carboniferous and later formations. Memoir 8 Geol. Soc. London.

WOODWARD,H.B. & THOMPSON,B. 1909. Water supply of Bedfordshire and Northamptonshire. Memoirs Geol. Survey England and Wales.

WYROBEK,S.M. 1959. Well velocity determinations in the English, Trias, Permian and Carboniferous. Geophysical Prospecting 7, 218-30.

EL-NIKHELY,A.H.D. 1980. Seismic reflection, gravity and magnetic studies of the geology of the East Midlands. Unpublished Ph.D. thesis. University of Leicester.

# APPENDIX ONE

## BOREHOLE DATA

This appendix is in two parts:

1.1 Boreholes that reach pre-Carboniferous basement.

1.2 Boreholes that bottom in Carboniferous or younger formations.

The details are as complete as possible, more detailed descriptions of the formations and of the supra-basement stratigraphy will be found in the quoted references. Where no reference is given the details were obtained from borehole logs or by personal communication from the IGS Deep Geology Unit.

The depths and locations are given to as many significant figures as possible. The formation names are as given in the source and have not been changed to conform to any standard of stratigraphical nomenclature.

The format of the data is as follows:

BOREHOLE NAME (DATE)  NGR E  NGR N  ELEVATION (m AOD)

REFERENCES (if available)

FORMATION NAME  DEPTH TO BASE (from surface datum)

## APPENDIX 1.1

ASTON FLAMVILLE (NCB 1977) 445.813 293.121 90

| | | |
|---|---|---|
| TRIAS | 167 | |
| CAMBRIAN | to TD | Stockingford Shales. |

---

BARRON'S PARK (1830) 451.2 304.5 80.16

Harrison 1884 Richardson 1931 Le Bas 1968

| | | |
|---|---|---|
| KEUPER | 36 | |
| ? IGNEOUS | 60.12 TD | "Syenite of Charnwood Forest type". |

---

BELTON (NW Leics. Water 1971) 444.37 319.57 71.63

| | | |
|---|---|---|
| ALLUVIUM | 3. | |
| KEUPER MARL | 53.0 | |
| KEUPER SANDSTONE | 74.37 | |
| PRECAMBRIAN | 81.38 TD | Greyish-red-purple tuff. Dip 15, cleaved throughout |

---

BOSWORTH WHARF (1880-2) 439.2 303.3 91.44

Richardson 1931

| | | |
|---|---|---|
| BOULDER CLAY | 8.2 | |
| KEUPER MARL | 116.4 | |
| L KEUPER SANDSTONE | 171.0 | |
| BUNTER PEBBLE BEDS | 226.8 | |
| ? TRIAS BRECCIA | 229.8 | |
| CAMBRIAN | 405.4 | Middle or Upper Stockingford Shales. |
| ? CAMBRIAN | 415.7 TD | Quartz breccia, ? Hartshill Quartzite. |

---

BURMAH 47/29 1-A 53.1508 N 01.6108 E 28.7

| | | |
|---|---|---|
| TOP PERMIAN | 1328.9 | |
| TOP NAMURIAN | 1503.9 | |
| TOP ORDOVICIAN | 1675.5 | |
| TD | 1790.7 | Llanvirn/Arenig. |

---

COUNTESTHORPE (1892) 456.7 295.5 86

Fox-Strangways 1903 Richardson 1931 Le Bas 1968,1972

| | | |
|---|---|---|
| DRIFT | 26.5 | |
| TRIAS MARL | 192.9 | |
| MICROTONALITE | 194.4 TD | |

---

COWPASTURE (1878) 441.3 303.8 116

Richardson 1931

| | | |
|---|---|---|
| BOULDER CLAY | 12. | |
| TRIAS | 103.3 | |
| ? TRIAS BRECCIA | 115.3 | |
| CAMBRIAN | 166.5 TD | Fine grey slate, ? Stockingford Shales. |

---

COX'S WALK (NCB) 404.115 338.077 56.00 (KB)

| | | |
|---|---|---|
| NAMURIAN | 499.70 | |
| DINANTIAN | 566.20 | Limestone. |
| PRE CAMBRIAN | 800.60 TD | Similar to Charnian Maplewell Series. |

CROWN HILLS (LEICESTER) (1879-80) 462.4 303.7 92

Fox-Strangways 1903 Richardson 1931 Le Bas 1968

| | | |
|---|---|---|
| L LIAS | 60. | |
| RHAETIC | 95. | |
| KEUPER MARL | 223. | |
| KEUPER SANDSTONE | 255 | |
| TREMADOCIAN | 305 TD | Fossiliferous Stockingford Shales. |

---

DADLINGTON (NCB 1977) 439.840 299.100 90

| | | |
|---|---|---|
| TRIAS | 314 | |
| STOCKINGFORD SHALES | to TD | |

---

DUKE'S WOOD 146 468.075 359.450 104.24

Lees and Taitt 1946

| | | |
|---|---|---|
| CARBONIFEROUS | 1917.82 | |
| ? ORS | 2194.54 | Pink-red congl. |
| ? CAMBRIAN | 2267.14 | Brecciated phyilitic mudstone, dip 60. |
| ? CAMBRIAN | 2278.7 TD | Grey fine grained quartzite, dip 60. |

---

FOSTON 1 484.894 341.470 28.35

Lees and Taitt 1946 Kent 1968

| | | |
|---|---|---|
| PERMIAN | 466.34 | |
| DINANTIAN | 614.17 | S2 D2 Limestone. |
| ? PRE CAMBRIAN | 782.28 TD | Similar to Charnian Brand Series, highly contorted purplish and green phyilitic shales. |

---

GAYTON N'HANTS (1884) 475. 256. 85.9

Woodward and Thompson 1909

| | | |
|---|---|---|
| RECENT | 2.54 | |
| M LIAS | 33.02 | |
| L LIAS | 177.09 | |
| RHAETIC | 188.06 | |
| TRIAS | 213.06 | |
| L CARBONIFEROUS | 270.97 | |
| ORS | 302.97 TD | |

---

GLINTON (BP 1961) 515.00 305.28 9.5

IGS 73/12

| | | |
|---|---|---|
| RECENT | 1.5 | |
| U JURASSIC | 10.6 | |
| M JURASSIC | 51.8 | |
| U LIAS | 103.6 | |
| M+L LIAS | 303.9 | |
| RHAETIC | 324.9 | |
| KEUPER | 358.1 | |
| PRE CAMBRIAN | 387.4 TD | Massive rhyolitic crystal tuff. |

---

HOLLOWELL (NCB 1982) 468.3 271.8 165.

| | | |
|---|---|---|
| TRIAS | 340. | |
| PRECAMBRIAN | to TD | Volcaniclastic breccia, dacite fragments. |

HUNSTANTON 1 (1970) 569.23 342.70 10.7

| | | |
|---|---|---|
| CHALK | 21.9 | |
| JURASSIC | 530.7 | |
| TRIAS | 835.5 | |
| ? PRE CAMBRIAN | 861.3 TD | |

---

GREAT OXENDON (1934) 473.6 283.0 114.05

Summ. Prog. Geol Surv. 1934

| | | |
|---|---|---|
| U+M LIAS | 31.7 | |
| L LIAS | 206.66 | |
| RHAETIC | 212.14 | |
| KEUPER | 231.65 | |
| PRE CAMBRIAN | 246.89 TD | Quartz felsite. |

---

GREAT PAXTON (1966) 520.88 263.89 23.01

ICS Ann. Rpt 1966 Stubblefield 1967

| | | |
|---|---|---|
| PLEISTOCENE | 7.0 | |
| OXFORD CLAY | 42.4 | |
| KELLAWAYS | 47.3 | |
| M JURASSIC | 65.1 | |
| U LIAS | 75.4 | |
| (M)+L LIAS | 135.8 | |
| ORDOVICIAN | 201.1 TD | Llanvirn mudstone, dip 60-75 to south east. |

---

KINGSHILL SPINNEY (1880-82) 438.2 301.7 91.4

Richardson 1931

| | | |
|---|---|---|
| BOULDER CLAY & SANDS | 38.4 | |
| KEUPER MARL | 113.4 | |
| KEUPER SANDSTONE | 211.5 | |
| BUNTER CONGL. & SANDS | 249.3 | |
| CAMBRIAN | 321.3 TD | Stockingford Shales. |

---

KIRBY LANE (NCB 1975) 473.239 317.589 71.45

Jones 1981

| | | |
|---|---|---|
| LIAS | 67. | |
| RHAETIC | 87. | |
| KEUPER | 267. | |
| BUNTER | 288. | |
| L COAL MEASURES | 381.5 | |
| MILLSTONE GRIT | 402. | |
| "GRANITE" | 413.94 TD | |

---

KNIGHTON FIELDS (LEICESTER) (1892) 459.3 302.0 65.53

Fox-Strangways 1903 Le Bas 1968

| | | |
|---|---|---|
| KEUPER | 189.58 | |
| SILURIAN/CAMBRIAN | 251.46 TD | Blue and black shales, highly inclined. |

---

LEICESTER FOREST EAST (IGS 1978) 452.46 302.83 104.3

IGS 79/12

| | | |
|---|---|---|
| PLEISTOCENE | 2.81 | |
| TRIASSIC | 119.51 | Mudstone/siltstone. |
| TRIASSIC | 156.84 | Sandstone/mudstone. |
| CAMBRIAN/ORDOVICIAN | 179.00 TD | Probably Tremadocian, dark grey mudstone, dip c. 40, cleavage c. 50 in opposite direction to bedding. |

LEXHAM (1972) 585.0 318.0 70.7

| | | |
|---|---|---|
| CHALK | 196.6 | |
| M JURASSIC | 316.1 | |
| LIAS | 409.4 | |
| PRE CAMBRIAN | 437.4 TD | |

---

LINDRIDGE 1 (1875) 447.2 304.8 C.99

Le Bas 1968

| | | |
|---|---|---|
| U KEUPER SANDSTONE | 6.7 | |
| RED MARL & GYPSUM | 20.1 | |
| L KEUPER SANDSTONE | 82.3 | |
| ? PRE CAMBRIAN | 117.0 TD | "Slatey rocks" ? Charnian, dip 70. |

---

LODGE FARM (LEICESTER) (1878) 460.8 304.2 64.0

Richardson 1931 Le Bas 1968

| | | |
|---|---|---|
| KEUPER MARL | 190.65 | |
| L KEUPER SANDSTONE | 225.19 | |
| SILURIAN/CAMBRIAN | 249.62 TD | Shales, slatey lower down, highly inclined. |

---

MERRY LEES DRIFTS 1,2 446.8 305.9 109.7 (entrance)

Butterly and Mitchell 1946

| | | |
|---|---|---|
| NEW RED SANDSTONE | 36.14 | B.O.D. c.377 m. slope distance S.W. of entrance. |
| TREMADOCIAN | | Highly inclined weathered slates at top then dark grey hard shales, Tremadoc fauna. |

---

MILL LANE (HUNTINGDON) (1966) 523.691 271.430 13.53

IGS Ann. Rpt 1966

| | | |
|---|---|---|
| NO SAMPLES | 50.29 | |
| CORNBRASH | 51.9 | |
| BLISWORTH CLAY | 52.2 | |
| GT OOLITE | 58.25 | |
| U & L ESTUARINE | 67.89 | |
| U LIAS | 80.5 | |
| (M) & L LIAS | 151.5 | |
| KEUPER MARL | 172.6 | |
| ORDOVICIAN | 235.9 TD | Mudstone dip 30, pendant graptolites with rarer trilobites. |

---

NOCTON 1 505.106 304.661 28.04

Lees and Tait 1946

| | | |
|---|---|---|
| M JURASSIC | 34.44 | |
| LIAS | 278.89 | |
| RHAETIC | 288.95 | |
| NAMURIAN | 914.40 | |
| DINANTIAN | 1173.79 | Limestone C1, ?S2. |
| CAMBRIAN | 1181.7 TD | Banded light grey fine grained quartzites, lithologically similar to Nuneaton quartzites. |

---

NORTH CREAKE (1945) 585.7 337.9 21.64

Kent 1947

| | | |
|---|---|---|
| CRETACEOUS | 212.24 | |
| JURASSIC | 545.59 | |
| TRIAS | 742.19 | |
| PRE CAMBRIAN | 802.24 TD | Dark greenish grey tuff of Charnian type. |

ORTON (1884) 479.3 279.0 196.7

Harrison 1885 Summ. Prog. Geol Surv. 1934 Evans 1964

| | | |
|---|---|---|
| U LIAS | 14.63 | |
| M LIAS | 41.15 | |
| L LIAS | 203.00 | |
| RHAETIC | 209.7 | |
| KEUPER | 218.1 | |
| PRE CAMBRIAN | 240.5 TD | Quartz porphyrite or quartz felsite, cleavage 70. |

---

ROTHERWOOD (1977) 434.580 315.587 109.5

ICS 78/21

| | | |
|---|---|---|
| NAMURIAN | 61.49 | |
| DINANTIAN | 173.90 | 4 m. of grey sst. & congl. with Cambrian pebbles at base. |
| U CAMBRIAN | 199.00 TD | Pre Tremadocian mudstone (low grade slate) bedding dips 60-70, cleavage perpendicular to bedding. |

---

SAPCOTE FREEHOLT (1871) 446.3 294.3 98.

Harrison 1884 Le bas 1968

| | | |
|---|---|---|
| TRIAS | 164.6 | |
| PALAEOZOIC | 504.5 TD | (Depths may be wrong) Probably Stockingford Shales. |

---

SOHAM (1958) 559.28 274.48 5.2

Summ. Prog. Geol Surv. 1955 Stubblefield 1967

| | | |
|---|---|---|
| OXFORD CLAY | 76.8 | |
| U ESTUARINE | 90.5 | |
| L LIAS | 132.9 | |
| NEW RED SANDSTONE | 162.8 | |
| DEVONIAN | 242.2 TD | Dips 40-80 to 045. |

---

SOUTH CREAKE (1969) 585.75 334.00 41.8

| | | |
|---|---|---|
| CHALK | 160.5 | |
| KIMMERIDGE CLAY | 272.8 | |
| LIAS | 545.6 | |
| PERMO-TRIAS | 739.1 | |
| ?PRE CAMBRIAN | 772.4 TD | Phyllitic shales, quartzites & arkoses. |

---

SPALDING (Texaco 1971) 524.344 314.781 1.97

| | | |
|---|---|---|
| PLEISTOCENE | 13.11 | |
| OXFORD CLAY & KELLAWAYS | 94.18 | |
| U ESTUARINES | 116.13 | |
| LINCS. LIMESTONE | 131.67 | |
| U LIAS | 178.61 | |
| M (L) LIAS | 282.22 | |
| RHAETIC | 385.88 | |
| KEUPER | 452.93 | |
| PERMO-TRIAS | 492.39 | Basal conglomerate. |
| ? CAMBRIAN | 500.18 TD | White to light grey very hard quartzite. |

SPROXTON (1945) 484.51 323.91 130.54

Falcon and Kent 1960

| | | |
|---|---|---|
| TRIAS | 528.22 | |
| COAL MEASURES | 700.43 | |
| MILLSTONE GRIT | 714.15 | |
| ? PRE CAMBRIAN | 918.05 TD | Metamorphosed tuffs, mudstones and phyllitic shales. |

---

STIXWOULD 518.846 365.308 8.23

| | | |
|---|---|---|
| BOULDER CLAY | 8.84 | |
| U JURASSIC | 142.95 | |
| M JURASSIC | 194.77 | |
| LIAS | 437.39 | |
| RHAETIC | 445.62 | |
| ? | | |
| NAMURIAN | 1386.84 | |
| DINANTIAN | 1441.70 | |
| ? CAMBRIAN | 1454.2 TD | Grey/white feldspathic sandstone. |

---

STOCKS HOUSE (DESFORD) (1904) 446.7 302.2 C.122

Richardson 1931 Le Bas 1968

| | | |
|---|---|---|
| DRIFT | 12.19 | |
| KEUPER | ? | |
| COAL MEASURES | 140.2 | |
| MILLSTONE GRIT | 143.9 | |
| CARBONIFEROUS LIMESTONE | 152.4 | |
| QUARTZ DIORITE | 163.7 TD | Same petrology as Barrow Hill Earl Shilton. |

---

TATTENHOE (1970) 482.89 234.37,102.4

IGS Ann. Rpt. 1970

| | | |
|---|---|---|
| PLEISTOCENE & RECENT | 39.0 | |
| JURASSIC | 142.8 | Minimum depth. |
| TREMADOCIAN | 213.4 TD | |

---

THORPE BY WATER (1972-3) 488.57 296.48 63.0

IGS Ann. Rpt. 1972 IGS 74/7

| | | |
|---|---|---|
| U LIAS | 3.66 | |
| M LIAS | 30.10 | |
| L LIAS | 221.46 | |
| RHAETIC | 233.9 | |
| KEUPER MARL | 278.49 | |
| ? L PALAEOZOIC | 359.75 TD | Strongly cleaved siltstone. |

---

TOWCESTER 2 (1964) 471.79 241.97 125.88

Summ. Prog. Geol Surv. 1964 IGS Ann. Rpt. 1965

| | | |
|---|---|---|
| KEUPER | 270.2 | |
| TREMADOCIAN | 299.4 TD | Mudstone, dip 50 max. |

---

TOWCESTER 10 (DEANSHANGER) (1964) 476.52 238.80 69.69

Summ. Prog. Geol Surv. 1964 IGS Ann. Rpt. 1965

| | | |
|---|---|---|
| L LIAS | 115.75 | |
| KEUPER | 191.64 | |
| TREMADOCIAN | 259.08 TD | Shales and siltstones. |

TWYCROSS (IGS 1978) 433.87 305.64 122.0

IGS 79/12

| | | |
|---|---|---|
| PLEISTOCENE | 17.40 | |
| TRIASSIC | 484.20 | |
| PERMIAN | 503.30 | |
| IGNEOUS ? SILL | 506.95 | |
| ? CAMBRIAN | 508.90 TD | Interbedded dark purple silty mudstone and pale greenish grey siltstone, dip 30. |

---

UPWOOD (1965) 524.93 283.04 6.25

IGS Ann. Rpt. 1965 IGS 73/12

| | | |
|---|---|---|
| DRIFT | 1.22 | |
| OXFORD CLAY | 27.79 | |
| KELLAWAYS | 33.27 | |
| BLISWORTH LIMESTONE | 39.30 | |
| U & L ESTUARINES | 51.59 | |
| U LIAS | 75.06 | |
| M & L LIAS | 177.02 | |
| KEUPER MARL | 190.6 | |
| ? PRE CAMBRIAN | 213.9 TD | Volcanic agglomerate and tuff. |

---

WARBOYS (1965) 529.03 278.39 21.18

IGS Ann. Rpt. 1965 Le Bas 1972

| | | |
|---|---|---|
| DRIFT | 1.3 | |
| OXFORD CLAY | 64.41 | |
| KELLAWAYS | 70.33 | |
| GREAT OOLITE | 75.18 | |
| U & L ESTUARINE | 87.15 | |
| U LIAS | 96.11 | |
| M & L LIAS | 170.46 | |
| DIORITE | 217.17 TD | Presumed Caledonian, K-Ar 305 +- 10 M.Yr. |

---

WIGGENHALL (Texaco 1971) 559.41 315.37 3.84 (GL 2.44)

| | | |
|---|---|---|
| DRIFT | 13.11 | |
| KIM'IDGE & AMPTHILL CLAY | 125.27 | |
| OXFORD CLAY | 177.39 | |
| KELLAWAYS | 188.98 | |
| M JURASSIC | 198.12 | |
| LIAS | 344.42 | |
| TRIASSIC | 434.64 | Sandstone, clay and pebble beds. Fragments of basement and pink granite . |
| ?PRE CAMBRIAN | 561.75 TD | Slate or meta-tuff. |

---

WISBECH (Texaco 1971) 540.660 309.425 2.72 (GL 1.18)

| | | |
|---|---|---|
| DRIFT | 16.76 | |
| U JURASSIC | 114.91 | |
| M JURASSIC | 128.70 | |
| U LIAS | 159.11 | |
| M LIAS | 302.97 | |
| L LIAS | 306.02 | |
| RHAETIC | 307.24 | |
| TRIASSIC | 321.87 | |
| ? BASEMENT | 323.70 TD | Grey, very hard quartzite. |

---

WITTERING (Gas Council 1966) 504.920 301.845 62.91

| | | |
|---|---|---|
| INFERIOR OOLITE | 3.66 | |
| U LIAS | 58.22 | |
| M & L LIAS | 263.96 | |
| RHAETIC | 278.28 | |
| KEUPER | 294.74 | |
| ? PRE CAMBRIAN | 309.37 TD | Grey, fine grained tuff. |

WYBOSTON (1955) 516.1 257.5 15.5

Summ. Prog. Geol Surv. 1955

| | | |
|---|---|---|
| DRIFT | 6.1 | |
| OXFORD CLAY | 19.5 | |
| KELLAWAYS | 25.07 | |
| CORNBRASH | 27.4 | |
| GREAT OOLITE | 32.0 | |
| U ESTUARINES | 42.2 | |
| U LIAS | 53.6 | |
| L LIAS | 110.6 | |
| U ORS | 181.1 | |
| U DEVONIAN | 224.3 | |
| CAMBRIAN | 235.6 TD | Dips up to 40. |

---

GAS COUNCIL HUNTINGDON SERIES (1964)

---

G H 1 517.070 276.210 25.0

| | | |
|---|---|---|
| OXFORD CLAY | 36.9 | |
| KELLAWAYS | 40.8 | |
| CORNBRASH | 43.0 | |
| BLISWORTH CLAY | 43.9 | |
| BLISWORTH LIMESTONE | 49.7 | |
| U & L ESTUARINE | 61.9 | |
| U LIAS | 85.3 | |
| M LIAS | 96.9 | |
| L LIAS | 181.7 | |
| RHAETIC | 184.1 | |
| KEUPER MARL | 189.6 | |
| KEUPER SANDSTONE | 199.7 | |
| ? ORS | 251.5 TD | |

---

G H 2 518.090 273.290 26.8

| | | |
|---|---|---|
| OXFORD CLAY | 39.3 | |
| KELLAWAYS | 43.9 | |
| CORNBRASH | 45.4 | |
| BLISWORTH LIMESTONE | 53.3 | |
| U & L ESTUARINE | 61.0 | |
| U LIAS | 82.3 | |
| M LIAS | 92.1 | |
| L LIAS | 169.8 | |
| RHAETIC | 175.0 | |
| KEUPER | 184.1 | |
| ? PALAEOZOIC | 199.6 | |

---

G H 3 518.930 269.650 23.8

| | | |
|---|---|---|
| OXFORD CLAY | 39.3 | |
| KELLAWAYS | 43.0 | |
| CORNBRASH | 44.8 | |
| BLISWORTH LIMESTONE | 55.5 | |
| U & L ESTUARINE | 60.7 | |
| U LIAS | 77.1 | |
| M LIAS | 84.7 | |
| L LIAS | 151.2 | |
| PALAEOZOIC | 183.8 TD | Dark grey siltstone. |

G H 4 518.900 259.220 19.5

| | |
|---|---|
| OXFORD CLAY | 35.7 |
| KELLAWAYS | 39.6 |
| CORNBRASH | 41.5 |
| BLISWORTH CLAY | 43.0 |
| BLISWORTH LIMESTONE | 50.9 |
| U & L ESTUARINE | 55.8 |
| U LIAS | 67.7 |
| M LIAS | 73.8 |
| L LIAS | 124.4 |
| ? RHAETIC | 125.0 |
| DEVONIAN | 165.5 TD |

---

G H 5 520.900 263.090 23.8

| | |
|---|---|
| OXFORD CLAY | 43.6 |
| KELLAWAYS | 47.5 |
| CORNBRASH | 49.1 |
| BLISWORTH CLAY | 50.6 |
| BLISWORTH LIMESTONE | 59.7 |
| U & L ESTUARINE | 65.8 |
| U LIAS | 76.8 |
| M LIAS | 82.6 |
| L LIAS | 136.2 |
| ORDOVICIAN | 181.4 TD Grey silty mudstone, dip 45-50. |

---

G H 6 513.900 279.850 30.2

| | |
|---|---|
| OXFORD CLAY | 60.4 |
| KELLAWAYS | 64.6 |
| CORNBRASH | 66.8 |
| BLISWORTH CLAY | 68.6 |
| BLISWORTH LIMESTONE | 77.4 |
| U & L ESTUARINE | 84.4 |
| U LIAS | 117.7 |
| M LIAS | 132.9 |
| L LIAS | 234.4 |
| RHAETIC | 239.6 |
| KEUPER + ? ORS | 284.7 TD |

---

G H 8 509.300 284.610 64.9

| | |
|---|---|
| BOULDER CLAY | 4.3 |
| OXFORD CLAY | 43.9 |
| KELLAWAYS | 49.1 |
| CORNBRASH | 50.9 |
| BLISWORTH CLAY | 52.7 |
| BLISWORTH LIMESTONE | 59.1 |
| U & L ESTUARINE | 70.7 |
| U LIAS | 118.6 |
| M LIAS | 137.8 |
| L LIAS | 269.7 |
| RHAETIC | 275.5 |
| KEUPER + ? ORS | 275.5 TD |

---

G H 10 505.970 287.400 36.6

| | |
|---|---|
| CORNBRASH | 1.8 |
| BLISWORTH CLAY | 4.9 |
| BLISWORTH LIMESTONE | 11.0 |
| U & L ESTUARINE | 22.8 |
| U LIAS | 77.7 |
| M LIAS | 100.0 |
| L LIAS | 244.4 |
| RHAETIC | 260.0 |
| KEUPER MARL | 265.2 |
| KEUPER SANDSTONE | 275.5 |
| PALAEOZOIC/PRE CAMBRIAN | 288.0 TD |

G H 13 500.650 275.770 78.0

| | |
|---|---|
| BOULDER CLAY | 2.4 |
| OXFORD CLAY | 19.8 |
| KELLAWAYS | 24.1 |
| BLISWORTH CLAY | 29.9 |
| BLISWORTH LIMESTONE | 38.1 |
| U & L ESTUARINE | 44.2 |
| U LIAS | 94.8 |
| M LIAS | 111.3 |
| L LIAS | 232.0 |
| RHAETIC | 238.0 |
| KEUPER MARL + ? ORS | 265.2 TD |

---

GAS COUNCIL STAMFORD SERIES 1964-5

---

G St 2 506.740 296.730 19.5

| | |
|---|---|
| U LIAS | 43.9 |
| M LIAS | 73.1 |
| L LIAS | 232.0 |
| RHAETIC | 244.1 |
| KEUPER MARL | 247.5 |
| KEUPER SANDSTONE | 253.0 |
| PALAEOZOIC/PRE CAMBRIAN | 268.8 TD |

---

G St 3 507.120 299.220 21.9

| | |
|---|---|
| LINCS LIMESTONE | 0.9 |
| L ESTUARINE | 6.7 |
| U LIAS | 53.9 |
| M LIAS | 83.5 |
| L LIAS | 252.1 |
| RHAETIC | 264.0 |
| KEUPER MARL | 273.7 |
| KEUPER SANDSTONE | 287.7 |
| PALAEOZOIC/PRE CAMBRIAN | 289.6 TD |

---

G St 10 506.580 300.960 24.4

| | |
|---|---|
| HEAD | 1.8 |
| U LIAS | 34.1 |
| M LIAS | 63.1 |
| L LIAS | 232.3 |
| RHAETIC | 243.2 |
| KEUPER MARL | 252.4 |
| KEUPER SANDSTONE | 276.1 |
| PALAEOZOIC/PRE CAMBRIAN | 279.2 TD |

## APPENDIX 1.2

| | | | | |
|---|---|---|---|---|
| BILLESDON | | 470.8 | 302.2 | c.160 |
| Richardson 1926 | | | | |
| DRIFT | 5.8 | | | |
| L LIAS | 216.7 | | | |
| (L) RHAETIC | 218.2 | | | |
| KEUPER MARL | 295.4 TD | | | |
| BINGHAM 1 | | 472.52 | 339.35 | 26.59 |
| NAMURIAN | 873.86 | | | |
| DINANTIAN | 1814.7 TD | | | |
| BLETCHLEY (1887) | | 486.84 | 233.77 | 24.1 |
| Jukes-Brown 1889 | | | | |
| OXFORD CLAY | 45.1 | | | |
| ESTUARINE SERIES | 68.6 | | | |
| M LIAS | 125.0 TD | Granitic pebbles at base. | | |
| HANGINGHILL FARM (1970) | | 431.345 | 316.718 | 127.14 |
| IGS Ann. Rpt 1970 | | | | |
| U COAL MEASURES | 15.34 | | | |
| M COAL MEASURES | 155.75 TD | | | |
| HATHERN 1 (1970) | | 451.59 | 324.16 | 46.02 |
| KEUPER MARL | 106.7 | | | |
| COAL MEASURES | 137.2 | | | |
| MILLSTONE GRIT | 304.7 | | | |
| CARBONIFEROUS LIMESTONE | 631.6 TD | | | |
| HOTON HILLS (1974) | | 456.76 | 321.82 | 70.10 |
| Jones 1981 | | | | |
| TRIAS | 198. | | | |
| MILLSTONE GRIT | 260.4 TD | | | |
| KETTERING ROAD KINGSTHORPE | | 477. | 262.5 | 84.73 |
| Woodward and Thompson 1909 | | | | |
| NORTHAMPTON SAND | 5.5 | | | |
| U LIAS | 52.1 | | | |
| M LIAS | 82.6 | | | |
| L LIAS | 224.9 | | | |
| RHAETIC | 233.2 | | | |
| TRIAS | 245.5 | | | |
| L CARBONIFEROUS | 259.4 TD | | | |
| LONG CLAWSON (1943) | | - | - | 54.2 |
| Lees & Taitt 1946 | | | | |
| TRIASSIC | 417.6 | | | |
| ? PERMIAN | 426.7 | | | |
| COAL MEASURES | 854.4 | | | |
| MILLSTONE GRIT | 1332.0 | | | |
| CARBONIFEROUS LIMESTONE | 1434.1 TD | | | |

| | | | | |
|---|---|---|---|---|
| MELBOURNE A (IGS 1966) | | 438.2 | 323.74 | 89.15 |
| IGS Ann. Rpt 1966 | | | | |
| PERMO-TRIAS | 4.8 | | | |
| L COAL MEASURES | 7.0 | | | |
| MILLSTONE GRIT | 101.06 TD | | | |

---

| | | | | |
|---|---|---|---|---|
| MELBOURNE B (IGS 1966) | | 439.21 | 323.74 | 89.3 |
| IGS Ann. Rpt 1966 | | | | |
| MILLSTONE GRIT | 140.6 | | | |
| CARBONIFEROUS LIMESTONE | 169.25 TD | | | |
| PARSONS DROVE | | 537.93 | 310.52 | 1.85 |
| IGS 80/11 | | | | |
| DRIFT | 17.8 | | | |
| U JURASSIC | 29.2 | | | |
| OXFORD CLAY & KELLAWAYS | 92.02 | | | |
| GT OOLITE & U ESTUARINE | 107.75 | | | |
| LINCOLNSHIRE LIMESTONE | 133.10 | | | |
| U LIAS | 149.11 TD | | | |

---

| | | | | |
|---|---|---|---|---|
| RATCLIFFE COLLEGE | | 462.35 | 315.05 | 95. |
| Richardson 1926 | | | | |
| DRIFT | 27.0 | | | |
| KEUPER | 73.0 TD | | | |

---

| | | | | |
|---|---|---|---|---|
| SOUTHEREY | | 569.3 | 296.5 | 3.0 |
| Summ. Prog. Geol Surv. 1922 | | | | |
| CHALK | 12.2 | | | |
| KIMMERIDGE CLAY | 69.5 | | | |
| OXFORD CLAY | 146.0 | | | |
| L LIAS | 204.2 TD | | | |

---

| | | | | |
|---|---|---|---|---|
| THORNEY (1908) | | 525.3 | 305.6 | C.2.0 |
| Whitaker 1922 | | | | |
| DRIFT | 1.60 | | | |
| OXFORD CLAY | 46.71 | | | |
| GT OOLITE | 60.8 | | | |
| U ESTUARINE | 66.83 | | | |
| INFERIOR OOLITE | 82.24 TD | | | |

---

| | | | | |
|---|---|---|---|---|
| WESTFIELD LANE (NCB) | | 491.990 | 341.721 | ? |
| NAMURIAN | 643.00 | | | |
| DINANTIAN LIMESTONE | 679.60 TD | | | |

---

| | | | | |
|---|---|---|---|---|
| WIDMERPOOL (1945) | | 463.657 | 329.583 | 81.08 |
| Falcon and Kent 1960 | | | | |
| KEUPER MARL | 246.04 | | | |
| BUNTER | 310.8 | | | |
| COAL MEASURES | 592.5 | | | |
| MILLSTONE GRIT | 1325.88 | | | |
| CARBONIFEROUS LIMESTONE | 1891.0 TD | Lower Carboniferous Limestone Shales. | | |

212 MELTON SPINNEY (1976) 476.754 322.566 123.58

| | |
|---|---|
| BOULDER CLAY | 55. |
| L LIAS | 274.5 |
| RHAETIC | 277.5 |
| KEUPER MARL | 426. |
| KEUPER SANDSTONE | 465. |
| BUNTER | 527.9 |
| COAL MEASURES | 619.45 TD |

---

213 SCALFORD STATION 475.481 323.075 127.18

| | |
|---|---|
| M & L LIAS | 267.5 |
| RHAETIC | 276.2 |
| KEUPER MARL | 446.3 |
| KEUPER SANDSTONE | 497. |
| BUNTER | 538.7 |
| COAL MEASURES | 706.23 TD |

---

214 WYCOMB 477.730 324.884 131.

| | |
|---|---|
| TRIASSIC | 558. |
| COAL MEASURES | 709.75 TD |

---

215 BROUGHTON LODGE (1974) 470.323 325.302 68.46

| | |
|---|---|
| LIAS | 138.5 |
| RHAETIC | 148.2 |
| KEUPER MARL | 313.0 |
| KEUPER SANDSTONE | 354.8 |
| BUNTER | 422.3 |
| COAL MEASURES | 601.89 TD |

---

216 LONG CLAWSON WINDMILL (1974) 472.721 327.055 71.95

| | |
|---|---|
| LIAS | 141. |
| RHAETIC | 148. |
| KEUPER MARL | 315. |
| KEUPER SANDSTONE | 366.6 |
| BUNTER | 432. |
| COAL MEASURES | 610.05 TD |

---

217 WELBY CHURCH 472.260 320.836 108.03

| | |
|---|---|
| RHAETIC | 180.72 |
| BUNTER | 400.03 |
| PERMIAN | 413.27 |
| COAL MEASURES | to TD |

205 ASFORDBY FARM (1976) 471.75 320.21 107.19

| | |
|---|---|
| RHAETIC | 179.0 |
| KEUPER | 371.5 |
| BUNTER | 413. |
| COAL MEASURES | c.620. |
| MILLSTONE GRIT | 650.30 TD |

---

206 GLEBE FARM (1976) 470.850 321.400 132.6

| | |
|---|---|
| BOULDER CLAY | 40. |
| L LIAS | 195.7 |
| RHAETIC | 201.7 |
| KEUPER MARL | 365. |
| KEUPER SANDSTONE | 412. |
| BUNTER | 444.03 |
| COAL MEASURES | 650.00 TD |

---

207 GREAT FRAMLANDS (1976) 474.572 322.289 131.71

| | |
|---|---|
| BOULDER CLAY | 40.0 |
| L LIAS | 272.8 |
| RHAETIC | 275. |
| KEUPER MARL | 435. |
| KEUPER SANDSTONE | 480. |
| BUNTER | 519.99 |
| COAL MEASURES | 743. |
| MILLSTONE GRIT | 893.56 TD |

---

208 HOLWELL MOUTH 472.689 324.145 c.150.

| | |
|---|---|
| TRIAS | 516.5 |
| COAL MEASURES | 679.39 TD |

---

209 STONEPIT SPINNEY (1976) 470.874 323.526 153.09

| | |
|---|---|
| BOULDER CLAY | 5. |
| M LIAS | 20. |
| L LIAS | 242. |
| RHAETIC | 253. |
| KEUPER MARL | 428. |
| KEUPER SANDSTONE | 471.5 |
| BUNTER | 502. |
| COAL MEASURES | 654.52 TD |

---

210 WARTNABY (1976) 471.476 322.430 142.3

| | |
|---|---|
| BOULDER CLAY | 20. |
| L LIAS | 242. |
| RHAETIC | 245. |
| KEUPER MARL | 360. Approx 50 m. lost by faulting. |
| KEUPER SANDSTONE | 401. |
| BUNTER | 438. |
| COAL MEASURES | 642.83 TD |

---

211 WELBY (1975) 473.344 320.741 115.53

| | |
|---|---|
| L LIAS | 190. |
| RHAETIC | 214. |
| TRIASSIC | 433.15 |
| COAL MEASURES | 591.00 TD |

| | | | | |
|---|---|---|---|---|
| G St 15 | | 499.080 | 303.680 | 28.0 |
| DRIFT | 3.7 | | | |
| M LIAS | 27.4 | | | |
| L LIAS | 215.5 | | | |
| RHAETIC | 227.4 | | | |
| KEUPER MARL | 246.3 TD | | | |

---

| | | | | |
|---|---|---|---|---|
| G St 16 | | 506.300 | 303.280 | 38.4 |
| U LIAS | 59.4 | | | |
| M LIAS | 90.8 | | | |
| L LIAS | 270.1 | | | |
| RHAETIC | 282.9 | | | |
| KEUPER MARL | 290.5 TD | | | |

---

NATIONAL COAL BOARD NORTH EAST LEICESTERSHIRE PROSPECT

---

| | | | | |
|---|---|---|---|---|
| 200 GRIMSTON (1976) | | 468.522 | 320.895 | 96.15 |
| L LIAS | 138.0 | | | |
| RHAETIC | 144.5 | | | |
| KEUPER MARL | 318.8 | | | |
| KEUPER SANDSTONE | 356.0 | | | |
| BUNTER | 401.5 | | | |
| COAL MEASURES | 592.90 TD | | | |

---

| | | | | |
|---|---|---|---|---|
| 201 GREEN HILL (1976) | | 469.323 | 323.056 | 149.6 |
| BOULDER CLAY | 30.0 | | | |
| L LIAS | 247.4 | | | |
| RHAETIC | 252.0 | | | |
| KEUPER MARL | 410.6 | | | |
| KEUPER SANDSTONE | 453.5 | | | |
| BUNTER | 507.65 | | | |
| COAL MEASURES | 697.59 TD | | | |

---

| | | | | |
|---|---|---|---|---|
| 202 HATTON LODGE (1976) | | 469.320 | 324.597 | 80.57 |
| L LIAS | 181.5 | | | |
| RHAETIC | 184.8 | | | |
| KEUPER MARL | 330. | | | |
| KEUPER SANDSTONE | 377.5 | | | |
| BUNTER | 431.25 | | | |
| COAL MEASURES | 548.03 TD | | | |

---

| | | | | |
|---|---|---|---|---|
| 203 PERKINS LANE (1976) | | 468.080 | 322.438 | 155.27 |
| BOULDER CLAY | 3.0 | | | |
| M LIAS | 15.0 | | | |
| L LIAS | 251.0 | | | |
| RHAETIC | 256.5 | | | |
| KEUPER MARL | 374.5 | | | |
| KEUPER SANDSTONE | 420.0 | | | |
| BUNTER | 452.8 | | | |
| COAL MEASURES | 622.46 TD | | | |

---

| | | | | |
|---|---|---|---|---|
| 204 AB KETTLEBY (1976) | | 472.628 | 322.628 | 131.71 |
| BOULDER CLAY | 40.0 | | | |
| L LIAS | 262.5 | | | |
| RHAETIC | 266.4 | | | |
| KEUPER MARL | 428.0 | | | |
| KEUPER SANDSTONE | 475.5 | | | |
| BUNTER | 507.37 | | | |
| COAL MEASURES | 672.01 TD | | | |

G H 14 501.470 278.000 66.1

| | |
|---|---|
| BOULDER CLAY | 1.8 |
| OXFORD CLAY | 7.0 |
| KELLAWAYS | 12.5 |
| CORNBRASH | 14.0 |
| BLISWORTH CLAY | 16.8 |
| BLISWORTH LIMESTONE | 22.9 |
| U & L ESTUARINE | 31.4 |
| NORTHAMPTON SAND | 32.9 |
| U LIAS | 86.9 |
| M LIAS | 105.5 |
| L LIAS | 235.0 |
| RHAETIC | 241.7 |
| KEUPER MARL | 274.3 TD |

---

GAS COUNCIL St. NEOTS SERIES 1964-5

---

G Ne 1 496.630 270.080 47.6

| | |
|---|---|
| LIAS | 175.3 |
| KEUPER | 195.1 |
| CARBONIFEROUS LIMESTONE | 200.0 TD |

---

G Ne 2 499.500 272.330 44.8

| | |
|---|---|
| RHAETIC | 187.5 |
| KEUPER MARL | 193.6 TD |

---

GAS COUNCIL STAMFORD SERIES 1964-5

---

G St 1 504.770 293.010 19.5

| | |
|---|---|
| DRIFT | 5.8 |
| NORTHAMPTON SAND | 7.9 |
| U LIAS | 64.9 |
| M LIAS | 92.3 |
| L LIAS | 247.5 |
| RHAETIC | 264.0 |
| KEUPER | 292.0 |

---

G St 4 501.610 299.780 59.1

| | |
|---|---|
| LINCOLNSHIRE LIMESTONE | 6.1 |
| L ESTUARINE | 11.9 |
| NORTHAMPTON SAND | 15.8 |
| U LIAS | 76.8 |
| M LIAS | 107.9 |
| L LIAS | 278.9 |
| RHAETIC | 282.9 |

---

G St 8 499.200 301.760 63.1

| | |
|---|---|
| LINCOLNSHIRE LIMESTONE | 3.3 |
| L ESTUARINE | 4.6 |
| NORTHAMPTON SAND | 8.5 |
| U LIAS | 52.1 |
| M LIAS | 85.3 |
| L LIAS | 270.1 |
| RHAETIC | 279.2 |
| KEUPER | 290.5 TD |

| | | | | |
|---|---|---|---|---|
| WYSALL 2 | | 460.775 | 327.75 | 76.8 |
| KEUPER | 310. | | | |
| COAL MEASURES | 467.9 | | | |
| MILLSTONE GRIT | 502.3 TD | | | |

---

GAS COUNCIL HUNTINGDON SERIES (1964)

---

| | | | | |
|---|---|---|---|---|
| G H 7 | | 511.540 | 283.070 | 43.0 |
| OXFORD CLAY | 29.3 | | | |
| KELLAWAYS | 34.4 | | | |
| CORNBRASH | 35.7 | | | |
| BLISWORTH CLAY | 37.2 | | | |
| BLISWORTH LIMESTONE | 43.6 | | | |
| U & L ESTUARINE | 54.3 | | | |
| ? NORTHAMPTON SAND | 57.3 | | | |
| U LIAS | 97.8 | | | |
| M LIAS | 115.8 | | | |
| L LIAS | 228.6 | | | |
| RHAETIC | 237.4 | | | |
| KEUPER | 267.3 TD | | | |

---

| | | | | |
|---|---|---|---|---|
| G H 9 | | 508.420 | 285.500 | 69.8 |
| BOULDER CLAY | 6.1 | | | |
| OXFORD CLAY | 52.1 | | | |
| KELLAWAYS | 57.0 | | | |
| CORNBRASH | 58.8 | | | |
| BLISWORTH CLAY | 60.7 | | | |
| BLISWORTH LIMESTONE | 67.1 | | | |
| U & L ESTUARINE | 78.3 | | | |
| U LIAS | 124.4 | | | |
| M LIAS | 143.3 | | | |
| L LIAS | 266.1 | | | |
| RHAETIC | 271.6 | | | |
| KEUPER | 291.1 TD | | | |

---

| | | | | |
|---|---|---|---|---|
| G H 11 | | 504.460 | 285.740 | 36.0 |
| CORNBRASH | 0.9 | | | |
| BLISWORTH CLAY | 3.7 | | | |
| BLISWORTH LIMESTONE | 9.4 | | | |
| U & L ESTUARINE | 27.1 | | | |
| U LIAS | 79.6 | | | |
| M LIAS | 103.0 | | | |
| L LIAS | 244.4 | | | |
| RHAETIC | 265.2 | | | |
| KEUPER | 274.3 TD | | | |

---

| | | | | |
|---|---|---|---|---|
| G H 12 | | 504.980 | 280.170 | 45.7 |
| BOULDER CLAY | 1.2 | | | |
| OXFORD CLAY | 36.6 | | | |
| KELLAWAYS | 42.4 | | | |
| CORNBRASH | 44.2 | | | |
| BLISWORTH CLAY | 46.6 | | | |
| BLISWORTH LIMESTONE | 52.7 | | | |
| U & L ESTUARINE | 60.7 | | | |
| U LIAS | 111.9 | | | |
| M LIAS | 129.8 | | | |
| L LIAS | 255.1 | | | |
| RHAETIC | 262.1 | | | |
| KEUPER | 269.4 TD | | | |

# APPENDIX TWO

## GRIDDING AND CONTOURING ROUTINES

The way in which irregularly spaced data is contoured can affect the data and hence any models fitted to the data. The gravity and magnetic data used for the modelling in chapter 8 were from the GINOSURF graphics library and are described briefly here.

GINOSURF is an appendix to the GINO-F graphical system and contains a number of functions to grid and the contour irregularly spaced data.

### Gridding

The gridding is done by means of the RANGRD routine. The z value of each node on an x-y grid is determined from a least squares fit of a parabolic surface to the weighted data points. The weighting (W) is given by:

$W = (S-D)^2/D$ where S is the radius of the circular search area and D is the distance to the data point. A minimum of four points are required for a solution but in practice the value of S is increased until six points are found. The value of S is determined by the algorithm such that there is an average of 24 points in any circular search area. 24 is the preferred value since at the corners of the grid the quarter circle search area should still contain 6 points, this avoids the need for frequent changes of S. Increasing the number of points within the search area increases the degree of smoothing.

Contouring

Contours are drawn through the gridded data by the routine DRACON. The point at which the contour enters each grid rectangle is determined by linear interpolation along the side of the rectangle. The contour is then traced through the rectangle by interpolation on the diagonals and then out through another side. It is therefore important that the grid mesh is sufficiently small for linear interpolation to be valid and, in general, fine enough that a contour will not cross a mesh line more than once between adjacent grid points. Clearly the grid must be smaller than the dimensions of the smallest anomaly that is to be preserved in the contouring.

Full details of these routines can be found in the GINOSURF user manual, University of Salford Computer Centre.

# APPENDIX THREE

## EAST MIDLANDS XRF ANALYSES

Table A2.1 contains six analyses made on the Leicester XRF spectrometer of samples of granitic rocks from the East Midlands.

The analyses are not directly relevant to the work described in this thesis and are only included here for the reference of any future workers on the geochemistry of these rocks.

The samples were all pellets; the analyses were made on 27-11-81 (major elements), Ø5-12-81 (trace elements Nb-Zn) and Ø4-1Ø-82 (trace elements Cr-Ba).

The Warboys sample was from near the top of the intrusion and therefore one of the least altered (Le Bas 1972).

$Fe_2O_3$ is total.

| Pellet | Sample location |
|---|---|
| L825 | Buddon Wood Quarry, Mountsorrel. |
| L826 | Buddon Wood Quarry, Mountsorrel. |
| L827 | Kirby Lane borehole, (Leicester sample no. 71583). |
| L828 | Croft Quarry (tonalite). |
| L829 | Enderby Quarry (microtonalite). |
| L83Ø | Warboys borehole, 173 m below OD, (IGS BX 7294). |

| Wt% | L825 | L826 | L827 | L828 | L829 | L830 |
|---|---|---|---|---|---|---|
| $SiO_2$ | 69.3 | 69.5 | 67.9 | 62.6 | 59.2 | 50.8 |
| $TiO_2$ | 0.46 | 0.44 | 0.50 | 0.57 | 0.64 | 0.86 |
| $Al_2O_3$ | 14.5 | 13.9 | 15.4 | 16.2 | 15.4 | 13.5 |
| $Fe_2O_3$ | 2.64 | 2.52 | 3.46 | 4.24 | 5.29 | 9.76 |
| MnO | 0.058 | 0.059 | 0.019 | 0.076 | 0.084 | 0.136 |
| MgO | 1.7 | 1.8 | 1.4 | 3.1 | 4.8 | 9.4 |
| CaO | 2.88 | 1.80 | 1.06 | 3.73 | 4.14 | 8.97 |
| $Na_2O$ | 4.01 | 3.49 | 3.01 | 4.28 | 3.29 | 1.83 |
| $K_2O$ | 3.297 | 3.833 | 5.075 | 2.186 | 2.539 | 1.219 |
| $P_2O_5$ | 0.124 | 0.111 | 0.111 | 0.196 | 0.202 | 0.181 |
| TOTALS | 98.97 | 97.45 | 97.94 | 97.18 | 95.58 | 96.66 |
| PPM | | | | | | |
| Nb | 9.6 | 9.2 | 9.2 | 8.8 | 7.9 | 9.0 |
| Zr | 168. | 136. | 134. | 166. | 158. | 105. |
| Y | 29.6 | 25.0 | 24.5 | 22.0 | 17.6 | 19.7 |
| Sr | 272. | 192. | 136. | 540. | 472. | 214. |
| U | 3. | 3. | 2. | 3. | 3. | 3. |
| Rb | 120.5 | 120.5 | 165.5 | 62.0 | 43.7 | 25.3 |
| Th | 13. | 13. | 12. | 6. | 7. | 4. |
| Pb | 18. | 13. | 12. | 6. | 7. | 4. |
| Ga | 16.3 | 15.1 | 14.6 | 17.7 | 17.0 | 17.8 |
| Zn | 42. | 34. | 24. | 67. | 63. | 83. |
| Cr | 10. | 10. | 18. | 11. | 28. | 215. |
| V | 48. | 48. | 46. | 78. | 112. | 270. |
| La | 33. | 30. | 26. | 26. | 21. | 13. |
| Ce | 64. | 61. | 50. | 58. | 47. | 31. |
| Nd | 27. | 24. | 21. | 26. | 23. | 16. |
| Ba | 593. | 645. | 754. | 483. | 476. | 246. |

Table A2.1 : XRF analyses